






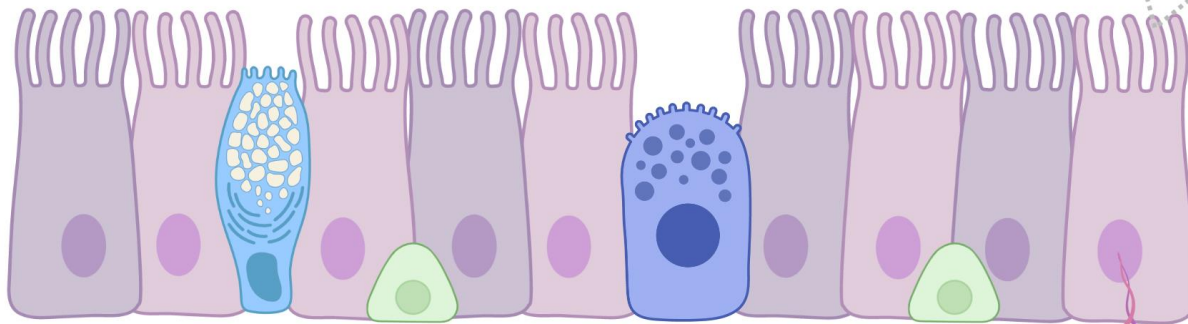
Universitat Autònoma de Barcelona

**ADVERTIMENT.** L'accés als continguts d'aquesta tesi queda condicionat a l'acceptació de les condicions d'ús establertes per la següent llicència Creative Commons:  [http://cat.creativecommons.org/?page\\_id=184](http://cat.creativecommons.org/?page_id=184)

**ADVERTENCIA.** El acceso a los contenidos de esta tesis queda condicionado a la aceptación de las condiciones de uso establecidas por la siguiente licencia Creative Commons:  <http://es.creativecommons.org/blog/licencias/>

**WARNING.** The access to the contents of this doctoral thesis it is limited to the acceptance of the use conditions set by the following Creative Commons license:  <https://creativecommons.org/licenses/?lang=en>

# MOLECULAR CHARACTERIZATION OF PRIMARY CILIARY DYSKINESIA



PhD thesis

Noelia Baz Redón

2022

Programa de Doctorado en Pediatria,  
Obstetricia y Ginecología

Universitat Autònoma de Barcelona









Universitat Autònoma  
de Barcelona

FACULTAD DE MEDICINA

DEPARTAMENTO DE PEDIATRÍA, DE OBSTETRICIA,  
GINECOLOGÍA, Y DE MEDICINA PREVENTIVA Y  
SALUD PÚBLICA

# **MOLECULAR CHARACTERIZATION OF PRIMARY CILIARY DYSKINESIA**

**Tesis doctoral**

Noelia Baz Redón

**Directores de tesis**

Antonio Moreno Galdó

Núria Camats Tarruella

Barcelona, junio de 2022





Universitat Autònoma  
de Barcelona

Facultad de Medicina

Departamento de Pediatría, de Obstetricia, Ginecología, y de  
Medicina Preventiva y Salud Pública

**Dr. Antonio Moreno Galdó**, Profesor Agregado de Pediatría de la *Universitat Autònoma de Barcelona* y Jefe de Servicio de Pediatría y sus áreas específicas, *Hospital Universitari Vall d'Hebron*, Barcelona.

Certifica:

Que **Noelia Baz Redón** ha realizado bajo mi dirección y tutorización la Tesis Doctoral titulada “**Molecular characterization of Primary Ciliary Dyskinesia**”, que reúne los requisitos para ser defendida ante el tribunal oportuno para la obtención del grado de Doctora por la *Universitat Autònoma de Barcelona*.

Y para que así conste, firmo el presente documento.

Barcelona, a 30 de junio de 2022

Antonio Moreno Galdó







Universitat Autònoma  
de Barcelona

Facultad de Medicina

Departamento de Pediatría, de Obstetricia, Ginecología, y de  
Medicina Preventiva y Salud Pública

**Dra. Núria Camats Tarruella**, Investigadora sénior del grupo de investigación Crecimiento y Desarrollo del *Vall d'Hebron Institut de Recerca (VHIR)*, Barcelona.

Certifica:

Que **Noelia Baz Redón** ha realizado bajo mi dirección la Tesis Doctoral titulada "**Molecular characterization of Primary Ciliary Dyskinesia**", que reúne los requisitos para ser defendida ante el tribunal oportuno para la obtención del grado de Doctora por la *Universitat Autònoma de Barcelona*.

Y para que así conste, firmo el presente documento.

Barcelona, a 30 de junio de 2022

Núria Camats Tarruella



*A mi familia*



# AGRADECIMIENTOS

En primer lugar me gustaría agradecer a Antonio Moreno, mi tutor y director, por ofrecerme la oportunidad de trabajar en su grupo y realizar la tesis doctoral en este proyecto. Gracias por la confianza ofrecida y el rigor en tu dirección.

A Núria Camats, mi directora de tesis y compañera de laboratorio, gracias por ser un referente en mis inicios en la investigación. Por dejarme participar en cada uno de los proyectos, enseñándome cada paso y escuchando mis ideas. De todo esto he aprendido que la ciencia es un camino difícil, lleno de obstáculos, pero con una gran satisfacción final al cumplir tus objetivos. Gracias también por el soporte en el proceso de escritura de la tesis y tus correcciones minuciosas.

Agradezco a todos mis compañeros del grupo de Crecimiento y Desarrollo. Especialmente a Mónica Fernández, gracias por ser una gran compañera de despacho y laboratorio, espero haberme llevado un cachito de tu experiencia en genética. A Sandra Rovira, gracias por ser una referente en esta enfermedad y transmitirme tu entusiasmo en su estudio, por enseñarme el análisis de videomicroscopía y tener tanta paciencia conmigo para recibir los resultados y discutir los casos.

Gracias a toda mi familia por el apoyo en estos años y teneros siempre cerca. A mis padres por ser el mejor ejemplo de esfuerzo y trabajo para conseguir lo que uno se propone. A Héctor, gracias por escucharme cuando te explico lo que hago, aunque siempre digas que no eres de ciencias. Por mostrarte siempre orgulloso de lo que hago, aunque mi mayor orgullo es tener el mejor hermano.

A Joan por su comprensión y paciencia en esta montaña rusa, por sus ánimos incondicionales en todo lo que hago y comprender el esfuerzo y dedicación que ha implicado este trabajo.

A mis amigos por sus ánimos y apoyo moral, por escucharme en los momentos difíciles y animarme a seguir adelante con el trabajo. A Pablo y Anna, que están pasando por lo mismo que yo, espero ayudaros tanto como me habéis ayudado vosotros animándome en el sprint final.

A todos, muchas gracias.



# RESUMEN

## Introducción:

El cilio móvil es un orgánulo celular con estructura compleja que se localiza en la superficie apical de las células epiteliales de distintos órganos humanos. Su estructura transversal consta del axonema de 9+2 microtúbulos un importante número de complejos multiproteicos que forman las siguientes subestructuras: los brazos de dineína, los puentes de nexina, la vaina central y los brazos radiales. La discinesia ciliar primaria (DCP) es una enfermedad minoritaria de herencia autosómica recesiva (1:15.000 recién nacidos) causada por la alteración de la estructura y función ciliar que impide el correcto aclaramiento de las secreciones mucosas. Las manifestaciones clínicas de esta enfermedad incluyen tos productiva, otitis medias supuradas prolongadas, rinosinusitis, bronquitis y/o neumonías de repetición, bronquiectasias, infertilidad masculina, subfertilidad femenina, y *situs inversus* (50%) o heterotaxia (6%). El diagnóstico de DCP es complejo y basado en la combinación de diferentes técnicas. La genética y la inmunofluorescencia se han propuesto recientemente como técnicas para mejorar el conocimiento de los genes causantes de la enfermedad e incrementar la tasa de diagnóstico en DCP.

## Objetivos:

Optimizar el análisis genético y de inmunofluorescencia para incrementar la tasa de diagnóstico en nuestra cohorte y mejorar el conocimiento de la relación entre el defecto genético específico y la estructura y función ciliar.

## Metodología:

Se trata de un estudio transversal multicéntrico de pacientes con alta sospecha de DCP según los criterios de la *European Respiratory Society*. Para caracterizar las alteraciones genéticas en nuestra cohorte, se diseñó un panel de secuenciación de alto rendimiento que incluía un total de 44 genes asociados a DCP usando la tecnología de captura *SeqCap EZ*. Se realizaron estudios de secuenciación de exoma completo en los pacientes sin resultado genético. Los estudios de inmunofluorescencia se realizaron aplicando un panel de cuatro anticuerpos comerciales marcados fluorescentemente (DNAH5, DNALI1, GAS8 y RSPH4A o RSPH9) para el estudio de la presencia y localización de estas proteínas en las células del epitelio respiratorio de muestras de cepillado nasal.



## Resultados:

Se incluyeron en el estudio genético 79 pacientes, 53 de los cuales fueron clasificados como DCP confirmada o muy probable. La sensibilidad del panel de 44 genes de DCP fue del 81,1% y la especificidad del 100%. Se encontraron variantes candidatas en alguno de los genes incluidos en 43 pacientes con DCP, 51,2% (22/43) fueron homocigotos y 48,8% (21/43) heterocigotos compuestos. Los genes más frecuentes en nuestra cohorte fueron *DNAH5* y *CCDC39*. Encontramos 52 variantes distintas, 36 de las cuales no habían sido descritas en la literatura. La variante más detectada fue en el gen *RSPH1* (c.85G>T/p.Glu39Ter). En nueve pacientes sin resultado genético positivo y en un paciente inicialmente considerado DCP poco probable, se realizaron estudios de secuenciación de exoma completo. Dos pacientes presentaron variantes candidatas en dos genes recientemente asociados con DCP: *CFAP300/C11orf70* and *DNAAF6/PIH1D3*. Cuatro pacientes presentaron variantes en genes candidatos relacionados con la estructura o función ciliar o flagelar o con la ciliogénesis que podrían explicar el fenotipo. Proponemos *GOLGA3* y *D2CD3* como posibles genes causantes de DCP. En relación al análisis de inmunofluorescencia, el panel de cuatro anticuerpos se testó en muestras de cepillado nasal de 74 pacientes con sospecha clínica de DCP. Sesenta y ocho (91,9%) se pudieron evaluar para todos los anticuerpos. Treinta y tres casos (44,6%) presentaron ausencia o localización aberrante de algunas de estas proteínas en el axonema ciliar (15 con ausencia en el axonema ciliar y 3 con localización proximal de *DNAH5*, 3 con ausencia de *DNAH5* y *DNALI1*, 7 con ausencia de *DNALI1* y localización citoplasmática de *GAS8*, 1 con ausencia de *GAS8*, 3 con ausencia de *RSPH9* y 1 con ausencia de *RSPH4A*). Quince pacientes tenían DCP confirmada o muy probable pero resultados de inmunofluorescencia normales (sensibilidad 68,8% y especificidad 100%), tres de ellos con variantes probablemente patogénicas en *DNAH11*. Considerando estos resultados de inmunofluorescencia proponemos un panel de anticuerpos de dos pasos: una primera ronda con los anticuerpos *DNAH5*, *DNALI1*, *GAS8* y *RSPH9*, y una segunda ronda, si fuera necesario, con *DNAH11* y *SPEF2*.

## Conclusiones:

El diseño e implementación de un panel de genes a medida tiene un alto rendimiento en el diagnóstico de la DCP. El análisis de secuenciación de exoma completo es una técnica útil en casos con alta sospecha de DCP sin variantes candidatas en los genes conocidos causantes de DCP. El análisis de inmunofluorescencia es una técnica rápida, con alta disponibilidad y de bajo coste para el estudio de la DCP, aunque no se puede utilizar como prueba independiente.

# ABSTRACT

## **Introduction:**

Motile cilia are highly complex hair-like organelles protruding from the apical surface of epithelia cells of various human organ systems. They contain a 9+2 tubulin-based axoneme core structure and an important number of multiprotein complexes comprising the sub-structures: the dynein arms, the nexin links, the central sheath and the radial spokes. Primary ciliary dyskinesia (PCD) is an autosomal recessive rare disease (1-15,000 live-born children) caused by an alteration of ciliary structure and function, which impairs the clearance of respiratory secretions. Its clinical manifestations include chronic wet cough, secretory otitis media, rhinosinusitis, repeated episodes of bronchitis and/or recurrent pneumonia, bronchiectasis, male infertility, female subfertility, and *situs inversus* (50%) or heterotaxia (6%). PCD diagnosis is complex and based on a combination of techniques. Genetics and immunofluorescence have been recently proposed as reliable techniques to improve understanding of disease-causing genes and diagnosis rate in PCD.

## **Objectives:**

Optimize genetic and immunofluorescence analysis to improve the diagnosis rate in our cohort and help understand the correlation between a specific genetic defect and ciliary structure and function.

## **Methods:**

This was a multicenter cross-sectional study of patients with a high suspicion of PCD according to the European Respiratory Society criteria. To characterize the genetic alterations in our cohort, we designed a gene panel for massive sequencing using *SeqCap EZ* capture technology that included 44 genes associated with PCD. Whole-exome sequencing was conducted on patients with a gene panel negative result. Immunofluorescence studies were carried out applying a four commercial fluorescently labeled antibody panel (DNAH5, DNALI1, GAS8 and RSPH4A or RSPH9) to study the presence and distribution of these ciliary proteins in nasal brushing respiratory cell samples.

## **Results:**

Seventy-nine patients, 53 of whom had a diagnosis of confirmed or highly probable PCD, were included in the genetic study. The sensitivity of the 44 PCD gene panel was 81.1%, with a

specificity of 100%. Candidate variants were found in some of the genes of the panel in 43 patients with PCD, 51.2% (22/43) of whom were homozygotes and 48.8% (21/43) compound heterozygotes. The most common causative genes were *DNAH5* and *CCDC39*. We found 52 different variants, 36 of which were not previously described in the literature and the most prevalent variant was detected in *RSPH1* (c.85G>T/p.Glu39Ter). In nine patients with gene panel negative result and in one patient firstly considered unlikely PCD, whole-exome sequencing was carried out. Two patients presented candidate variants in two recently genes associated with PCD: *CFAP300/C11orf70* and *DNAAF6/PIH1D3*. Four patients presented variants in candidate genes related with cilia or flagella structure and function or in ciliogenesis genes, which could explain their phenotype. We proposed *GOLGA3* and *C2CD3* as possible PCD causing genes. Regarding immunofluorescence analysis, the four antibody-panel was tested in nasal brushing samples of 74 patients with clinical suspicion of PCD. Sixty-eight (91.9%) patients were evaluable for all tested antibodies. Thirty-three cases (44.6%) presented an absence or mislocation of protein in ciliary axoneme (15 absent and 3 proximal distribution of *DNAH5* in the ciliary axoneme, 3 absent *DNAH5* and *DNALI1*, 7 absent *DNALI1* and cytoplasmatic localization of *GAS8*, 1 absent *GAS8*, 3 absent *RSPH9* and 1 absent *RSPH4A*). Fifteen patients had confirmed or highly likely PCD but normal immunofluorescence results (68.8% sensitivity and 100% specificity), three of them with confirmed likely pathogenic variants in *DNAH11*. Considering our immunofluorescence results we proposed a two-step antibody panel: a first round with *DNAH5*, *DNALI1*, *GAS8* and *RSPH9* antibodies, and a second round, if required, with *DNAH11* and *SPEF2* antibodies.

### **Conclusions:**

The design and implementation of a tailored gene panel produces a high yield in the genetic diagnosis of PCD. Whole-exome sequencing analysis is a useful technique in PCD suspected cases with non-genetic variants in known PCD causing genes. Immunofluorescence analysis is a quick, available, low-cost and reliable diagnostic test for PCD, although it cannot be used as a standalone test.

# ABBREVIATIONS

ACMG	American College of Medical Genetics and Genomics
ALI	Air-liquid interface
ATS	American Thoracic Society
BB	Basal body
CBF	Ciliary beat frequency
CBP	Ciliary beat pattern
CI	Confidence interval
CNV	Copy number variations
CP	Central pair
DNAAF	Dynein axonemal assembly factors
DRC	Dynein regulatory complex
ERS	European Respiratory Society
HC	Heavy chains
HGVS	Human Genome Variation Society
HSVM	High-speed video-microscopy
Hz	Hertz
IC	Intermediate chains
IDA	Inner dynein arm
IF	Immunofluorescence
IFT	Intraflagellar transport
LC	Light chains
MAF	Minor allele frequency
MIP	Microtubule inner protein
MTD	Microtubular disorganization
N-DRC	Nexin-dynein regulatory complex
nNO	Nasal nitric oxide
ODA	Outer dynein arm
ODA1	Outer dynein arm type 1
ODA2	Outer dynein arm type 2
ODA-DC	Outer dynein arm docking complex
PCD	Primary ciliary dyskinesia
PICADAR	Primary Ciliary Dyskinesia Rule
RS	Radial spoke
TEM	Transmission electron microscopy
TZ	Transition zone
VUS	Variants of uncertain significance
WES	Whole exome sequencing



# INDEX

1. INTRODUCTION.....	1
1.1. CILIA.....	3
1.1.1. CILIA SUBTYPES .....	3
1.1.2. CILIA STRUCTURE .....	3
1.1.2.1. Outer and inner dynein arms .....	5
1.1.2.2. Nexin-dynein regulatory complex.....	7
1.1.2.3. Radial spokes.....	8
1.1.2.4. Central pair complex and microtubule inner proteins.....	9
1.1.2.5. Ciliary base structure.....	10
1.1.3. AIRWAY EPITHELIA .....	12
1.1.4. CILIA ASSEMBLY.....	12
1.1.4.1. Ciliogenesis.....	12
1.1.4.2. Axonemal component assembly and intraflagellar transport .....	14
1.2. PRIMARY CILIARY DYSKINESIA.....	16
1.2.1. EPIDEMIOLOGY .....	16
1.2.2. CLINICAL FEATURES.....	16
1.2.3. MANAGEMENT .....	18
1.2.4. DIAGNOSIS.....	18
1.2.4.1. Nasal nitric oxide screening .....	21
1.2.4.2. High-speed video-microscopy .....	22
1.2.4.3. Transmission electron microscopy.....	25
1.2.4.4. Respiratory ciliated cell culture.....	28
1.2.4.5. Immunofluorescence microscopy analysis .....	30
1.2.4.6. Genetics.....	33
2. HYPOTHESIS AND OBJECTIVES .....	35
2.1. HYPOTHESIS.....	37
2.2. OBJECTIVES.....	37
3. METHODS.....	39

3.1. PATIENTS .....	41
3.2. PCD DIAGNOSTIC EVALUATION.....	41
3.3. NASAL NITRIC OXIDE SCREENING.....	41
3.4. HIGH-SPEED VIDEO-MICROSCOPY .....	41
3.5. GENETICS.....	42
3.5.1. PATIENTS .....	42
3.5.2. HIGH-THROUGHPUT PCD GENE PANEL AND DATA ANALYSIS .....	42
3.5.2.1. Library preparation and bioinformatics analysis.....	42
3.5.2.2. Statistical data analysis .....	45
3.5.3. WHOLE EXOME SEQUENCING .....	46
3.6. IMMUNOFLUORESCENCE TECHNIQUE AND ANALYSIS .....	46
3.6.1. PATIENTS .....	46
3.6.2. IMMUNOFLUORESCENCE TECHNIQUE AND ANALYSIS.....	47
3.6.3. DATA ANALYSIS .....	48
4. RESULTS.....	49
4.1. RESULTS I: IMPLEMENTATION OF A GENE PANEL FOR GENETIC DIAGNOSIS OF PRIMARY CILIARY DYSKINESIA.....	51
4.2. RESULTS II: IMMUNOFLUORESCENCE ANALYSIS AS A DIAGNOSTIC TOOL IN A SPANISH COHORT OF PATIENTS WITH SUSPECTED PRIMARY CILIARY DYSKINESIA .....	61
4.3. RESULTS III: WHOLE EXOME SEQUENCING IN HIGHLY LIKELY PCD PATIENTS WITH NEGATIVE GENE PANEL RESULTS .....	78
5. DISCUSSION .....	81
5.1. GENETICS: PCD-GENE PANEL.....	83
5.2. GENETICS: WHOLE EXOME SEQUENCING .....	85
5.3. IMMUNOFLUORESCENCE ANALYSIS .....	88
5.4. GENOTYPE-PHENOTYPE CORRELATION .....	91
6. CONCLUSIONS .....	93
7. REFERENCES .....	97
APPENDIX I .....	113
APPENDIX II .....	125

# **1. INTRODUCTION**





## 1.1. CILIA

Cilia and flagella are highly complex microtubule-based organelles that extend from the surface of some cell types. These evolutionary conserved organelles are present in unicellular organisms and different cells of multicellular organisms [1,2], so their function and structure have been thoroughly studied using various model organisms, such as *Chlamydomonas* spp., *Planaria* (flatworms), *Xenopus*, zebrafish and mouse [2].

Some cells exhibit only a monocilium, or primary cilium, whereas other cell types assemble apically a group of multiple motile cilia (200-300 cilia), which generate a direct fluid flow along their apical surface [1,2].

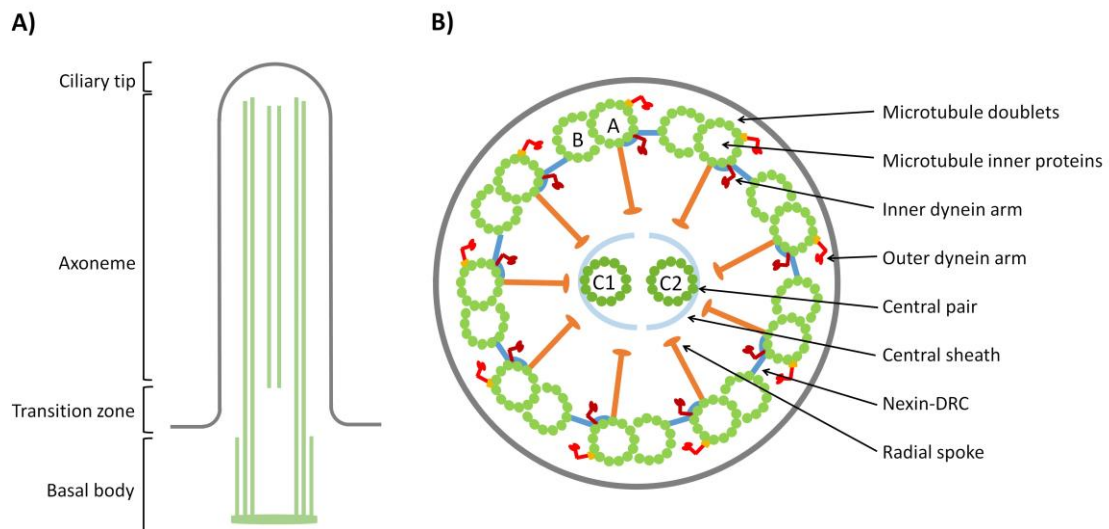
### 1.1.1. CILIA SUBTYPES

The ciliary axoneme is the longitudinal part of cilia, composed of a highly ordered structure of nine peripheral microtubule doublets with or without a central pair (CP) complex [2]. Cilia are classified according to their axoneme structure and movement capacity (motile and immotile) [1,2]. Four ciliary subtypes are described in humans: (a) motile 9+2 cilia, such as respiratory and ependymal cilia, and cilia in testis deferent ducts, uterus or fallopian tubes; (b) motile 9+0 cilia, for example, nodal cilia; (c) non-motile 9+2 cilia, such as inner ear kinocilia; and (d) non-motile 9+0 cilia, for instance, renal monocilia and photoreceptor-connecting cilia [1–3]. The sperm flagellum also has a 9+2 structure [3]. Non-motile cilia were previously designated as sensory cilia because of their function in sight, hearing and smell organs. However, more recent studies have reported that all cilia (motile and immotile) have sensory functions [4].

### 1.1.2. CILIA STRUCTURE

Cilia (5-7  $\mu\text{m}$  length and 0.2-0.3  $\mu\text{m}$  diameter) are longitudinally divided into the following subcomponents (from proximal to distal): basal body (BB), transition zone (TZ), axoneme and ciliary tip [1]. The basal body is formed by microtubule triplets (A, B and C) and connects the cilia to the cell. In the transition zone, this triplet structure becomes a doublet 9+2 axoneme structure. The ciliary tip is formed by microtubule plus (+) ends, from which axonemes grow, and a CP (Figure 1A) [1].

The ciliary axoneme is composed by 9 peripheral microtubule doublets (A- and B-tubules) and a CP based on two single microtubules (C1 and C2) (Figure 1B). The peripheral A-tubule is composed of 13 protofilaments in a complete circular shape, and the B-tubule is formed by 10 protofilaments attached to the A-tubule. The microtubule protofilaments are composed of  $\alpha$ -tubulin and  $\beta$ -tubulin heterodimers (Figure 1B) [5].



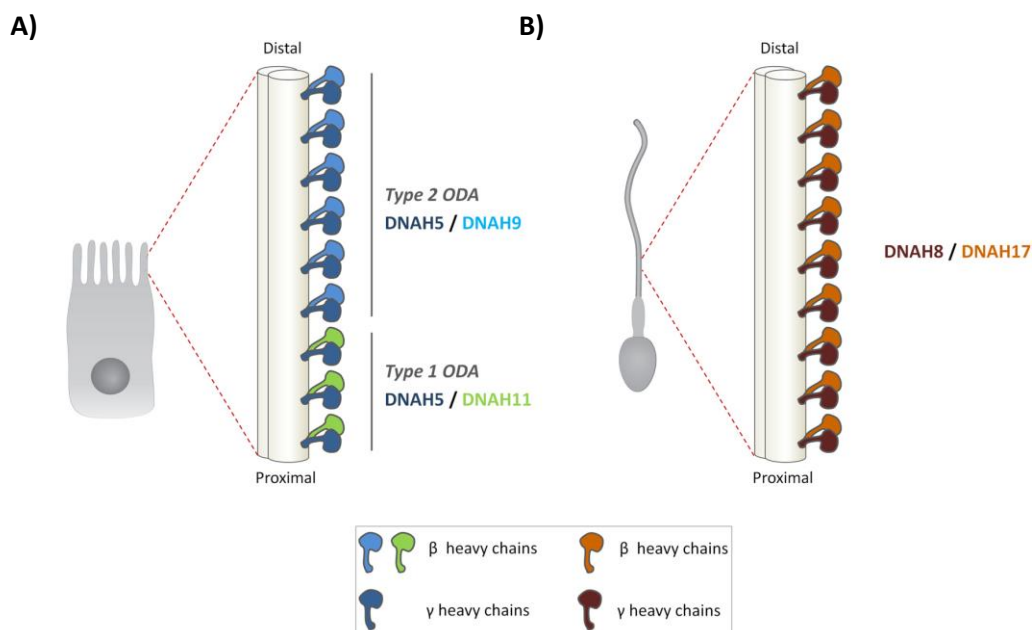
**Figure 1: Diagram of cilia structure. A)** Longitudinal section of a motile cilium with the microtubule structure (*green*) and its parts. **B)** Transverse section of the axoneme with the ultrastructure of a 9+2, consisting of nine peripheral microtubule doublets (A and B) and a central pair (C1 and C2). Labels indicate the ultrastructure components. DRC: dynein regulatory complex.

An important number of multiprotein complexes are distributed among the microtubule core of the ciliary axoneme: the dynein arms, the nexin links, the central sheath and the radial spokes (Figure 1B) [3]. The function of the outer dynein arms (ODAs), located more peripherally, is to generate the majority of the beating force and to control the speed of the ciliary beat, whereas the inner dynein arms (IDAs) are thought to regulate the beat amplitude or waveform [2]. The structures nexin-dynein regulatory complex (N-DRC), radial spokes (RSs) and CP complex are believed to serve as sensors that modulate the ciliary beating, especially the waveform, and regulate the activity of dynein arms in both motile cilia and flagella [2]. It has been described that >650 proteins comprise these structures, and defects in genes encoding those proteins have been associated with motile ciliopathies [2].

### 1.1.2.1. Outer and inner dynein arms

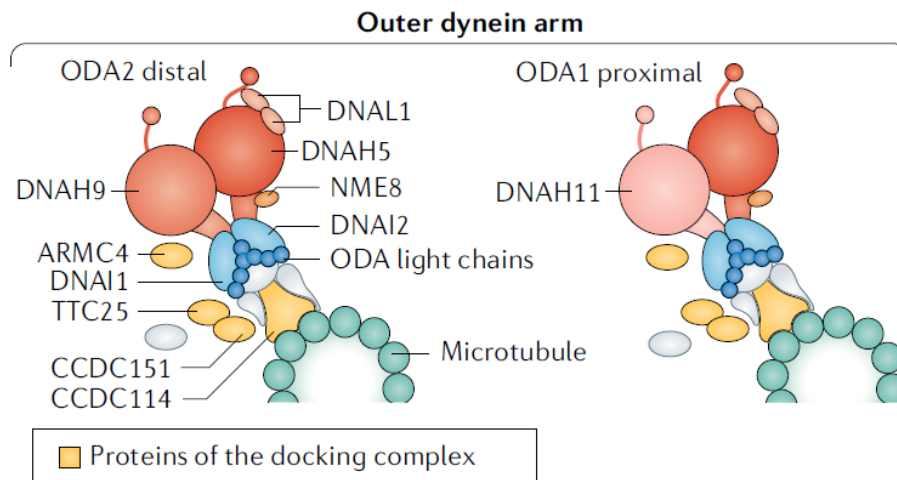
The dynein arms are motor complexes formed by the assembly of different polypeptides: dynein heavy chains (HC) of 400-500 kDa, intermediate chains (IC) of 45-110 kDa and light chains (LC) of 8-55 kDa. The dynein arms are attached to the peripheral A-tubule. The ATPase activity that resides in the HC molecules provides the necessary energy so that the A-tubule slides over the B-tubule of the next pair, resulting in the beating of cilium [3].

The composition of ODAs is homogeneous. Particularly, in human respiratory cells, ODAs contain two dynein HC, thus two ODA types have been described depending on the HC composition: ODA type 1 (ODA1) and type 2 (ODA2). Each ODA consists of a  $\gamma$ -HC and a  $\beta$ -HC. ODA1 is located in the proximal part of the ciliary axoneme and contains the  $\gamma$ -HC DNAH5 and the  $\beta$ -HC DNAH11, and ODA2 is present in distal axoneme and contains DNAH5 and  $\beta$ -HC DNAH9 (Figure 2A) [6]. A different type of ODA containing DNAH17 and DNAH8 has been described in sperm flagella (Figure 2B) [7]. Besides, the ODA IC proteins described in human respiratory cilia are DNAI1, DNAI2 and NME8, while DNAL1 is an ODA LC protein (Figure 3) [2,8]. The exact function and location of NME8 (encoded by *NME8/TXNDC3*) have yet to be determined.



**Figure 2: Schematic model of cilia and spermatozoa heavy chains (HC) of outer dynein arms (ODAs).** **A)** Longitudinal view of respiratory epithelial ciliated cells showing an axonemal proximal ODA with the  $\gamma$ -HC DNAH5 and  $\beta$ -HC DNAH11, and a distal ODA composed by the  $\gamma$ -HC DNAH5 and  $\beta$ -HC DNAH9. **B)** In

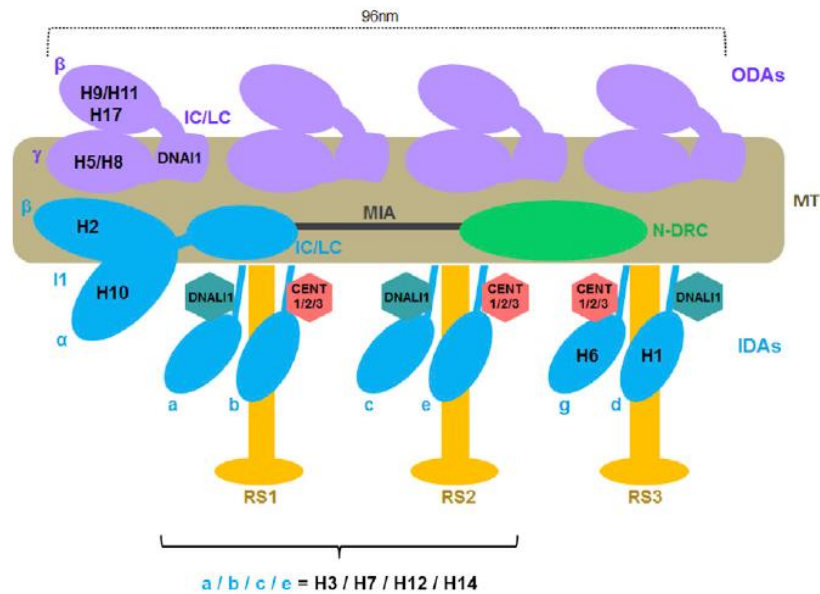
spermatozoa flagella, a unique ODA type, composed of  $\gamma$ -HC DNAH8 and  $\beta$ -HC DNAH17, was described. Figure from Legendre *et al.* 2021 [8].



**Figure 3: Diagram of the outer dynein arm (ODA) structure.** Structure and proteins comprising the distal ODA type 2 (ODA2) and proximal ODA type 1 (ODA1). ODA docking complex (ODA-DC) proteins are also represented (yellow). Figure adapted from Wallmeier *et al.* [2].

The ODAs are attached to the A-tubule by the ODA docking complex (ODA-DC) in 24-nm longitudinal repeats. This ODA-DC seems to stabilize the axonemal structure and regulate ciliary beat [2,9]. It is composed of proteins CCDC114 (encoded by *ODAD1/CCDC114*) [10], ARMC4 (*ODAD2/ARMC4*) [11], CCDC151 (*ODAD3/CCDC151*) [12] and TTC25 (*ODAD4/TTC25*) [13], (Figure 3). Additionally, the CCDC103 protein seems to be a core factor for ODA binding to the microtubule, but it acts independently to ODA-DC proteins, and further studies are necessary to reveal how this protein assembles with the other ODA components [14].

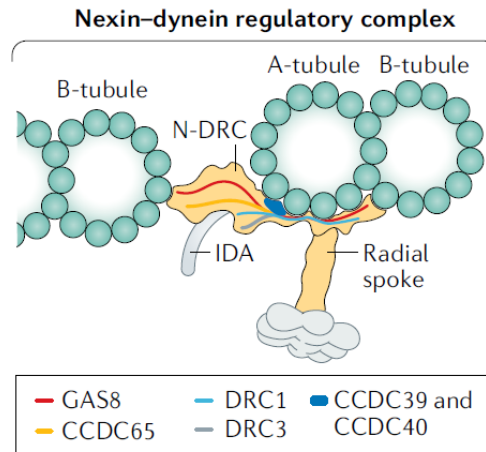
The IDAs are longitudinally repeated every 96nm and are more complex structures than ODAs. The knowledge of the seven different IDA subspecies and their exact composition and localization was provided by studies in the flagellated alga *Chlamydomonas reinhardtii*. The seven IDA subspecies include six single-headed IDAs (a, b, c, e, g, and d) and one double-headed IDA (IDA-I1) assembled by DNAH2 and DNAH10 (Figure 4). In humans and in *Chlamydomonas*, the single-headed IDA subspecies a, c, and d bind the LC DNALI1, whereas the HC of other subspecies (b, e, and g) bind the centrin protein. DNAH1 corresponds to IDA subspecies d, DNAH6 to subspecies g, and both DNAH12 and DNAH3 to other IDA subspecies (a, b, c, or e) (Figure 4) [15].



**Figure 4: Diagrammatic representation of a 96-nm-long axonemal unit.** Inner dynein arm (IDA) localization and composition representation based on data from *Chlamydomonas*. Seven subspecies have been described, including six single-headed IDAs (a, b, c, e, g, and d) and one double-headed IDA (IDA-I1). ODA: outer dynein arm, IDA: inner dynein arm, N-DRC: nexin-dynein regulatory complex, MIA: modifier of inner arms, IC/LC: intermediate chain/light chain, RS: radial spoke, and MT: microtubules. Figure adapted from Thomas *et al.* [15].

#### 1.1.2.2. Nexin-dynein regulatory complex

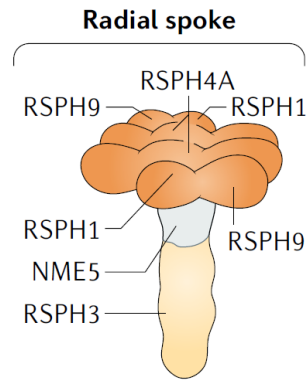
The N-DRC connects the peripheral microtubule doublets to each other. The proteins DRC1 (encoded by *DRC1/CCDC164*) [16], CCDC65 (*CCDC65/DRC2*) [17], DRC3 (*DRC3/LRRC48*) [18], and GAS8 (*GAS8/DRC4*) [19] encode this structure. Moreover, CCDC39 and CCDC40 are components of the axoneme ruler and create a structure that repeats every 96-nm. Mutations in these protein encoding genes, *CCDC39* [20] and *CCDC40* [21], cause a loss in DNALI1-containing IDA and N-DRC proteins, indicating that the CCDC39-CCDC40 complex is an attached site for these structures. That is why IDAs are also longitudinally repeated every 96nm (Figure 5) [2,22].



**Figure 5: Diagram of nexin-dynein regulatory complex (N-DRC).** Structure and proteins comprising the N-DRC, and localization of 96nm axoneme ruler proteins CCDC39 and CCDC40. Figure adapted from Wallmeier *et al.* [2].

### 1.1.2.3. Radial spokes

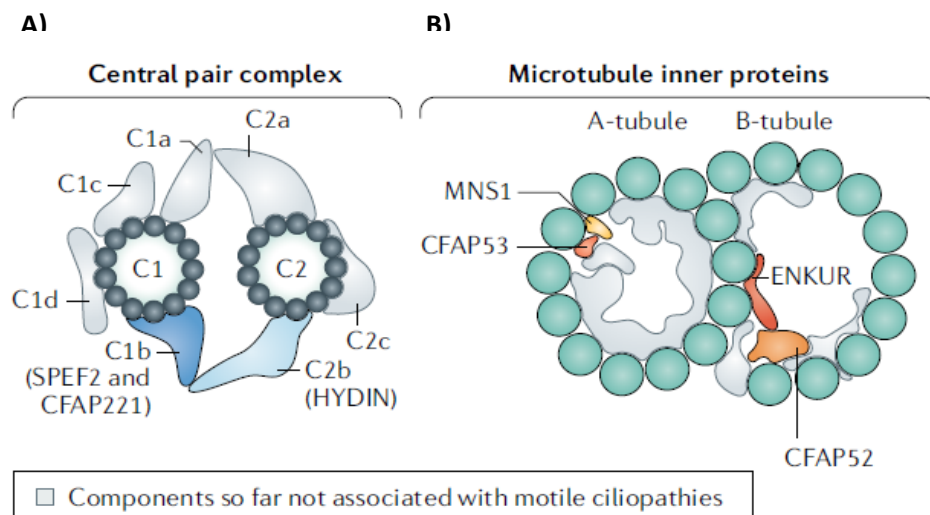
The RSs protrude from each A-tubule of the peripheral microtubules to the CP complex. They provide the structural cilia interface for transmitting regulatory signals to the arms [3]. According to studies in *Chlamydomonas reinhardtii* flagella, the RSs are T-shaped structures with a head of 5 proteins and a stalk of 18 proteins [23]. The head interacts with the central complex, and the spoke stalk contains domains associated with signal transduction, suggesting its role as a scaffold for signal proteins and a transducer of signals [24]. The RSs are partially pre-assembled in the cytoplasm from several smaller complexes and transported to the axoneme, where they unite with other RS proteins and are attached to microtubules, forming dimers [23]. The human RS head components are RSPH1 (encoded by *RSPH1*) [25], RSPH4A (*RSPH4A*) [26], RSPH9 (*RSPH9*) [26] and the RS stalk components NME5 (*NME5/RSPH23*) [27], RSPH3 (*RSPH3*) [28] and DNAJB13 (*DNAJB13*) [29] (Figure 6) [2,30].



**Figure 6: Model of the radial spoke (RS) head components.** Structure and location of RS head and stalk proteins. Figure adapted from Wallmeier *et al.* [2].

#### 1.1.2.4. Central pair complex and microtubule inner proteins

The CP complex is formed by two single microtubules (C1 and C2) and the proteins HYDIN (encoded by *HYDIN*) [31], SPEF2 (*SPEF2*) [32], STK36 (*STK36*) [33] and CFAP221 (*CFAP221*) [34] (Figure 7A). In the case of STK36, Edelbusch *et al.* [33] proposed that it might be located between the RS and CP, and play an important role in this connection, as an entire RS head is essential for the axonemal recruitment of STK36 [33].



**Figure 7: Diagram of central pair (CP) complex and microtubule inner proteins (MIPs).** **A)** Central single microtubules (C1 and C2) and proteins of the CP complex. **B)** Diagram of a peripheral microtubule doublet (A-tubule and B-tubule) indicating the MIPs. Components not associated with motile ciliopathies in light gray. Figure adapted from Wallmeier *et al.* [2].



The microtubule inner proteins (MIPs) are essential to establish the structure of microtubule doublets, maintain the microtubule periodicities along the axoneme, and stabilize the doublets against the mechanical stress of ciliary movement (Figure 7B) [9]. Recently, an important number of MIPs and their location have been described in *Chlamydomonas*. The orthologue protein studies suggest that FAP45 (ortholog of human protein encoded by *CFAP45/CCDC19*), with no mutations causing ciliopathies reported to date, and FAP52 (ortholog of human *CFAP52* encoded by *CFAP52/WDR16*) are luminal proteins in B-tubules necessary for the stability between the B-tubule protofilaments [35]. Moreover, FAP52 and FAP20, a previously known inner junction protein, are required for anchoring the B-tubule to the A-tubule, which is important for stabilizing the axonemal structure [35]. MNS1 is located in the luminal A-tubule and is a physical link between the lumen and the ODA-DC [9,36]. Other human MIPs related with ciliopathies are ENKURIN (encoded by *ENKUR*) [37], *CFAP53* (*CFAP53/CCDC11*) [38], and NME7 (*NME7/CFAP67*) [39] (Figure 7B).

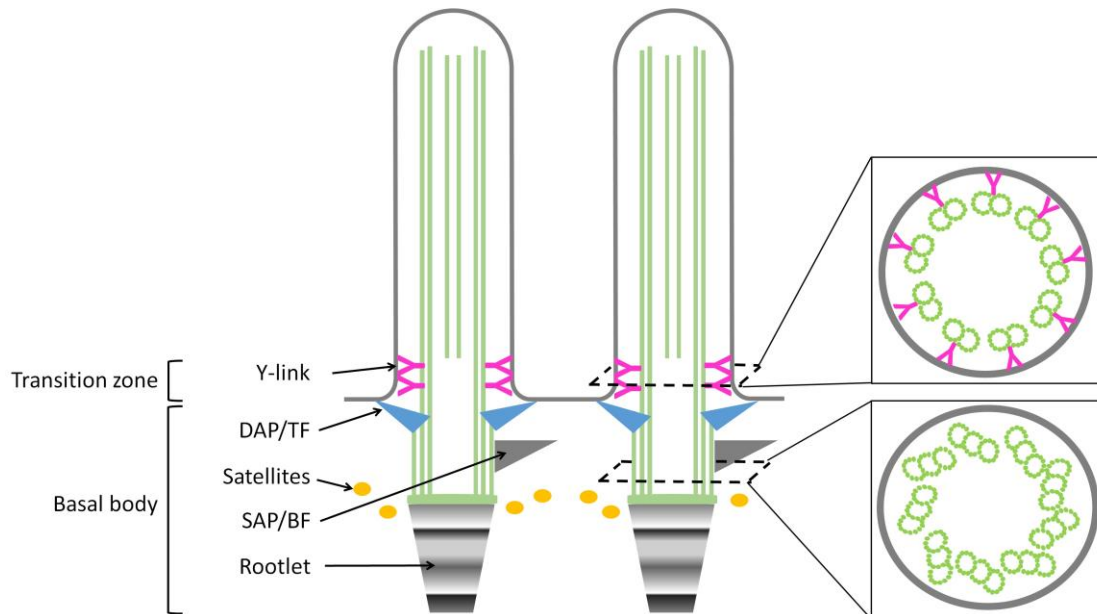
### **1.1.2.5. Ciliary base structure**

The TZ corresponds to the proximal portion of the ciliary axoneme distal to the BB, where the microtubule doublets convert to triplets (Figures 1 and 8). The TZ is required for the compartmentalization of the cilium, as it is the gate that controls the protein composition of ciliary axoneme. The Y-links are the microtubule-ciliary membrane connectors in this ciliary structure (Figure 8) [40].

Retinitis pigmentosa guanosine triphosphatase regulator protein (encoded by *RPGR*) is expressed in the connecting cilium localized between the inner and outer segments of photoreceptors (rods and cones), and in the TZ of respiratory cilia (Figure 8). It is suggested that RPGR protein may play a role establishing the proper respiratory cilia orientation [41].

The BB forms the base of the cilium and arises from the mother/older centriole of the centrosome. The centriole consists of 9 triplet microtubules on its proximal end, and 9 doublet microtubules on its distal end (Figure 8). Human basal bodies and centrosomes contain five types of tubulins:  $\alpha$ ,  $\beta$ ,  $\gamma$ ,  $\delta$ , and  $\epsilon$ . Distal ends of the BBs have two sets of appendages, namely distal and subdistal appendages (DAPs and SAPs, respectively). DAPs or ciliary transition fibers dock BBs at the plasma membrane and initiate ciliogenesis. CEP164 (encoded by *CEP164*) is a protein of the transition fibers indispensable for ciliary vesicle formation, BBs docking, and

ciliogenesis coordination. SAPs or basal feet in cilia are involved in microtubule anchoring. Pericentriolar satellites consist of dozens of proteins required for ciliogenesis modulation, although their precise role is unknown. During cilia assembly, the BB facilitates formation of ciliary rootlet (formed by oligomers of rootletin) at the base (proximal end) providing support for the cilium and interacting with actin filaments (Figure 8) [42].



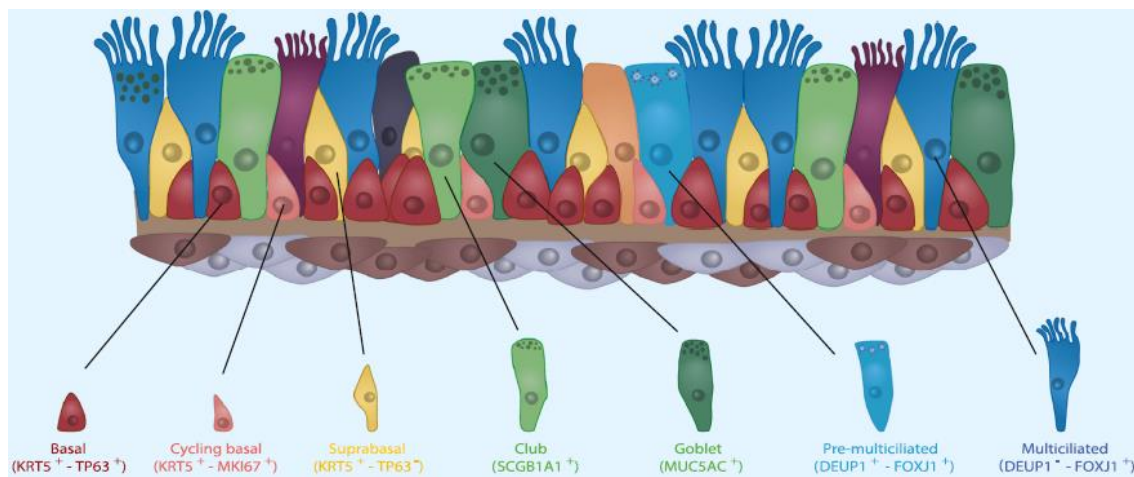
**Figure 8: Diagram of cilia, focused on ciliary base structure.** The transition zone is the most proximal axoneme structure, distal to basal bodies. In the transition zone, the Y-links connect the microtubules with the ciliary membrane. The basal bodies are composed by nine microtubule triplet structures and different sub-structures: DAPs/TF, SAP/BF, and ciliary rootlet. DAP: distal appendage; TF: transition fiber; SAP: subdistal appendage; BF: basal feet.

Growth arrest-specific protein 2-like 2 (encoded by *GAS2L2*) is abundant in the apical surface of the ciliated cells and it is localized in the basal bodies, basal feet, basal-body rootlets and actin filaments (Figure 8). It has been proposed that *GAS2L2* plays a role in the airways by inter-connecting the cytoskeletal elements and the basal body. Thus, *GAS2L2* helps maintain the correct orientation of basal bodies, so, pathogenic variants in this gene caused defects in ciliary orientation [43].

*OFD1* (encoded by *OFD1*) is localized at the basal feet and pericentriolar satellites of BBs (Figure 8) and mutations in the gene cause reduced number of cilia [2,44].

### 1.1.3. AIRWAY EPITHELIA

The cellular composition of the airways is now well characterized, as single-cell RNA sequencing studies have allowed to characterize different gene markers for each cell type [45]. The airway pseudostratified columnar ciliated epithelium is composed of five main cell types: basal, suprabasal, club, goblet and multiciliated cells (Figure 9). Basal cells are the progenitor cells attached to the basal lamina, and they differentiate into club cells, by going through an intermediate suprabasal state. Then, club cells mature into goblet cells or differentiate into multiciliated cells. Club cells are luminal cells that secrete anti-inflammatory and immunomodulating compounds. Goblet cells are luminal mucin secretory cells that form the airway mucus that should be expelled out the airways with the coordinated beating of cilia in the apical surface of multiciliated cells [8,45].



**Figure 9: Diagram of the airway epithelia with its different cell types.** Cellular composition of the trachea and large airways, well characterized with gene markers (in brackets) defined for each cell type. Figure adapted from Legendre *et al.* 2021 [8].

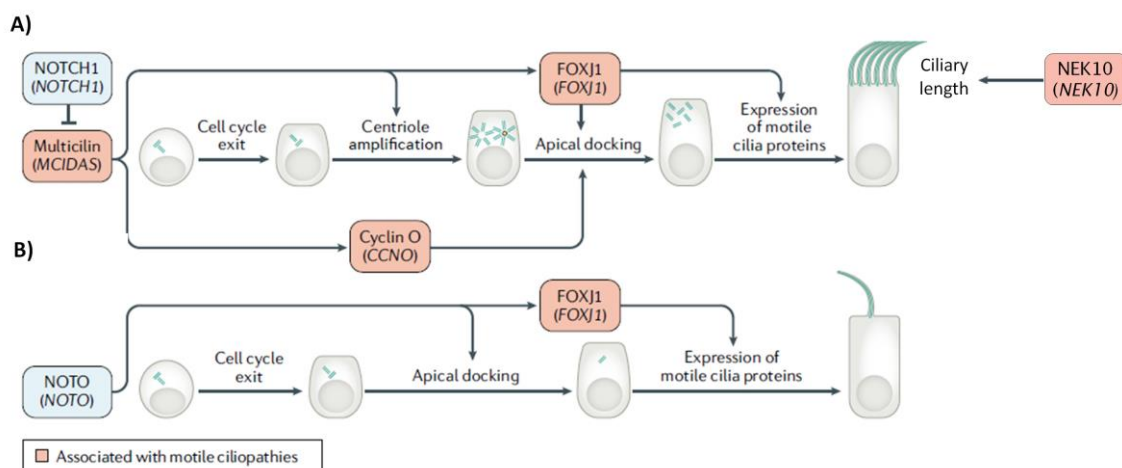
### 1.1.4. CILIA ASSEMBLY

#### 1.1.4.1. Ciliogenesis

Cilia are found in quiescent and proliferative cells in the G1 cell cycle phase. In dividing cells, cilia are resorbed before the S phase or during the G2 phase. Apparently, there seems to be a bidirectional crosstalk between cell division and ciliogenesis, as improper cell division can result in abnormal ciliogenesis [46]. In dividing cells, centrosomes (each with a mother and a daughter centriole) generate the mitotic spindle and perform other functions in cell cycle

progression [46]. Additionally, during the short period of differentiation in multiciliated cells, they generate hundreds of centrioles that act as nucleation points for cilia growth serving as basal bodies [2].

During multiciliogenesis, NOTCH1 acts as a repressor of multicilin (encoded by *MCIDAS*) that regulates cyclin O (encoded by *CCNO*) and the transcription factor FOXJ1 [2]. As a result of multicilin inhibition, cells exit the cell cycle and new centrioles are formed. Cyclin O mediates the amplification and the apical surface migration of centrioles, and FOXJ1 mediates their docking [47]. Each docked centriole is now called basal body, from which an axoneme structure emerges (Figure 10A) [2]. Due to their specific function, pathogenic variants in *MCIDAS* and *CCNO* result in centriole amplification defect, which leads to a decreasing number of cilia per cell. In contrast, pathogenic variants in *FOXJ1* do not affect the number of basal bodies, but those are mislocalized within the cytoplasm, so that the number of correct assembly cilia is reduced in most of the cells [2,47]. The transcription factor NOTO (encoded by *NOTO*) is expressed in the left/right organizer in mouse and other vertebrate embryos during embryogenesis. NOTO transcriptionally activates *FOXJ1* expression and thus, regulates ciliogenesis in the cells of the embryonic node (Figure 10B). That is why patients with *FOXJ1* defects also present right/left asymmetry defects [47].



**Figure 10: Scheme of ciliogenesis in multiciliated cells and ciliated cells of the embryonic node. A)** Illustration of ciliogenesis in multiciliated cells by NOTCH1 pathway and implicated factors. **B)** Illustration of ciliogenesis in nodal cilia following the NOTO pathway and action of factor FOXJ1. Figure adapted from Wallmeier *et al.* [2].

Recently, NEK10 (encoded by *NEK10*) was described as a specific serine/threonine-protein kinase that regulates the motile ciliary proteome promoting ciliary length and mucociliary transport (Figure 10). Patients with *NEK10* defects present shorter cilia but a normal number, radial structure and ciliary beat [48].

#### **1.1.4.2. Axonemal component assembly and intraflagellar transport**

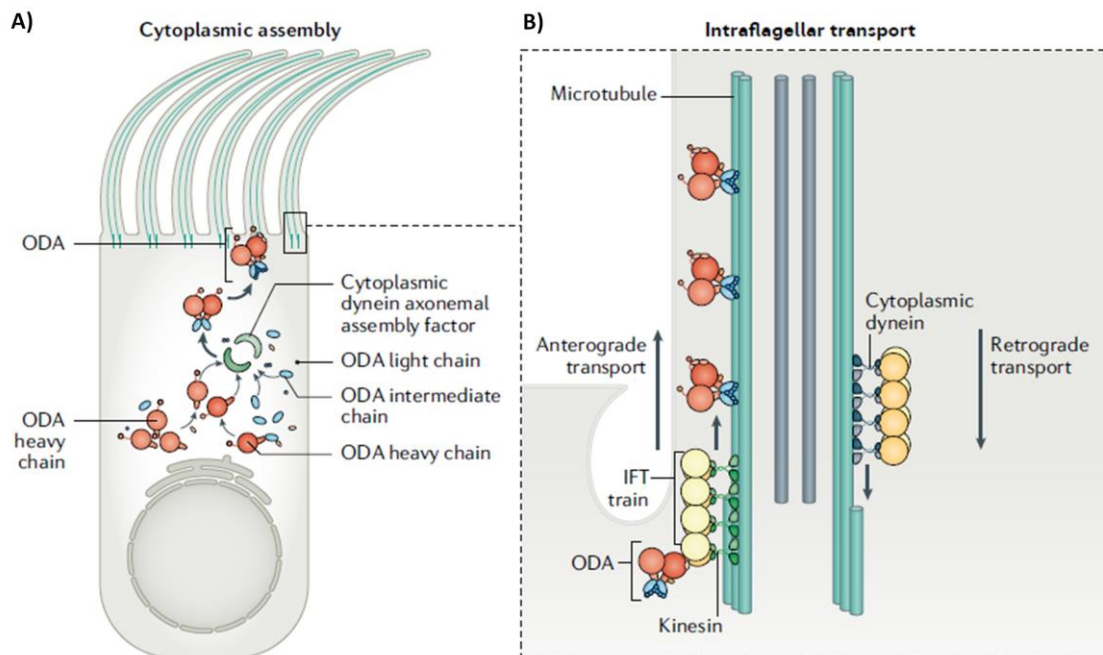
Axonemal dynein motors are pre-assembled in large multiprotein complexes within the cytoplasm by an array of cytoplasmic proteins collectively known as dynein axonemal assembly factors (DNAAFs). Proteomic experiments first described a relation between DNAAFs and heat shock family chaperones, and reported that DNAAFs, dynein subunits and chaperones co-localize in distinct cytosolic foci called dynein axonemal particles, where occur the pre-assembly of axonemal components [49]. These 1-3  $\mu\text{m}$  foci are irregularly shaped and are typically localized in the middle third of the apicobasal axis of multiciliated cells [49].

In humans, most DNAAFs are related to the assembly of ODA and IDA, so that pathogenic variants in those proteins cause a combined defect in both structures. Defects in *DNAAF1/LRRC50* [50], *DNAAF3/C19orf51* [51], *DNAAF5/HEATR2* [52], *DNAAF6/PIH1D3* [53,54], *CFAP298/C21orf59* [55], *SPAG1* [56], *LRRC6* [57], *ZMYND10* [58], *CFAP300/C11orf70* [59,60] (encoding different DNAAFs) result in the loss of both ODA types and the IDA light chain DNALI1, whereas defects in DNAAF coding genes *DNAAF2/KTU* [61] and *DNAAF4/DYX1C1* [62] lead to the loss of ODA2 and IDA (Figure 11A) [2]. CFAP57 (encoded by *CFAP57*) has been recently described to participate in the assembly of IDA components [63].

Recently, Thomas *et al.* described a different dynein arm assembly mechanism between human respiratory cilia and sperm flagella thanks to the study of *TTC12* (encoding the DNAAF protein TTC12). They observed that genetic variants in *TTC12* cause defects in IDA in respiratory epithelial cells, whereas they cause an absence of both ODA and IDA in sperm flagella [15].

The intraflagellar transport (IFT) mechanism associates with linear arrays, known as IFT trains, to transport cargo proteins and motor complexes in both directions along the microtubule. Anterograde transport occurs along the B-tubules heading towards the ciliary axoneme, whereas retrograde transport occurs along the A-tubules towards cytoplasm [9]. ODA-DC first

assemble in the cytoplasm, and then ODA and ODA-DC are transported independently by this IFT mechanism and attached along the ciliary axoneme (Figure 11B) [2].



**Figure 11: Diagram of outer dynein arms (ODAs) cytoplasmic assembly and transport. A)** ODAs are first pre-assembled within the cytoplasm by cytoplasmic dynein axonemal assembly factors (DNAAFs). **B)** Once assembled, ODAs are transported by the intraflagellar transport (IFT) machinery to the ciliary or flagellar axoneme. Figure adapted from Wallmeier *et al.* [2].

## **1.2. PRIMARY CILIARY DYSKINESIA**

Primary ciliary dyskinesia (PCD) is a rare respiratory disease caused by an alteration of ciliary structure, which impairs mucociliary clearance [2,8]. PCD is a genetically heterogeneous disorder that involves the majority of genes encoding the proteins described above. Most genetic defects associated with PCD are inherited in an autosomal recessive manner, except for three X-linked genes: PIH1D3 [53,54] that codes for a DNAAF; RPGR that causes retinitis pigmentosa [64]; and OFD1 that is associated with mental retardation and oral-facial-digital type 1 syndrome [44]. Recently, dominant pathogenic variants in FOXJ1 have been described in some PCD cases [47].

### **1.2.1. EPIDEMIOLOGY**

PCD epidemiologic data are scarcely available and based on estimates, as only a proportion of PCD cases are correctly diagnosed, and among these, only a few patients are included in national and international registries [2]. In 2010, Kuehni *et al.* conducted a survey study of pediatric PCD patients from specialized centers and estimated that the prevalence in Europe ranges from 1-10,000 to 20,000 live-born children [65]. In Europe, the median age of diagnosis is 5.3 years old (4.8 years old in the British Isles, 5 in Western Europe, 5.5 in Northern Europe, 6.5 in Southern Europe and 6.8 in Eastern Europe) [65]. The age of diagnosis is lower in patients with *situs inversus* (3.5 years old) and in those treated in tertiary referral centers (4.1 years old) [65].

National and international registries are essential to provide epidemiological data and clinical information of patients. An international PCD registry was launched in 2014 [66].

### **1.2.2. CLINICAL FEATURES**

PCD presents a broad clinical phenotype. The main PCD manifestations are recurrent upper and lower respiratory infections that can complicate with bronchiectasis. Many of the airway symptoms or signs of PCD also occur in healthy children, and that is why diagnosis is often delayed beyond childhood. Neonatal distress is a manifestation of PCD and patients require continuous supplemental oxygen for days to weeks. Also, pneumonia or atelectasis may

require a prolonged hospital stay in the neonatal unit. During childhood, the most common findings are chronic wet cough, secretory otitis media, rhinosinusitis and repeated episodes of bronchitis and/or recurrent pneumonia. The symptoms persist during adulthood, but the risk of bronchiectasis development increases with aging [67].

The most commonly detected pathogen in these patients' sputum cultures is *Haemophilus influenzae*. Other common pathogens are *Streptococcus pneumoniae*, *Moraxella catarrhalis*, and *Staphylococcus aureus* in early childhood. *Pseudomonas aeruginosa* and other Gram-positive pathogens are prevalent in older patients. *P. aeruginosa* frequently colonizes the lower respiratory tract, and the incidence of chronic infection is higher than previously reported [68].

An abnormal sperm structure can also cause a reduction or loss of the flagellum's ability to swing, causing male infertility in some PCD patients. Moreover, females with PCD may experience subfertility with an increased ectopic pregnancy rate, and decreased fertilization rate due to defects in ciliary function in the oviducts [67].

Motility of nodal monocilium is essential to generate the current flow necessary to initiate the signaling cascade for left-right body asymmetry. Therefore, defects in its function cause *situs inversus* in half of PCD patients [69]. Heterotaxy, defined as an abnormal arrangement across the left-right axis of internal thoracoabdominal organs, is described in 6-12% of cases and usually courses with congenital heart disease [69,70].

PCD respiratory symptoms have been described in association with sensory ciliopathies and mental retardation in cases with retinitis pigmentosa [64] and oral-facial-digital type 1 syndrome [44], respectively.

Regarding PCD classification in Spanish cohorts, Armengot-Carceller *et al.* designed a decision tree to classify new individuals of a Mediterranean cohort as PCD or PCD-like patients based on the most predictive PCD symptoms: pansinusitis, *situs inversus*, periodicity, rhinorrhea, bronchiectasis, and chronic wet cough [71].



### 1.2.3. MANAGEMENT

The currently used treatment strategies in PCD are mostly based on therapy notions and experiences in other diseases with defective mucociliary clearance, particularly cystic fibrosis [69,72]. However, as the underlying molecular defects of diseases are entirely different, the effectiveness of medications might differ among them. The currently available treatments are symptomatic treatments that aim to slow down disease progression [2]. PCD management includes: stimulation of the airway clearance, antibiotics to treat upper and lower respiratory tract infections, surveillance of pulmonary function, detection and early treatment of otitis and rhinosinusitis, and early referral to bronchiectasis centers [73].

To improve the outcomes, standardized care at specialized centers is recommended using a multidisciplinary approach, including pulmonologists, physiotherapists, otolaryngologists, nutritionists, specialized nurses and assisted reproduction specialists when needed [73].

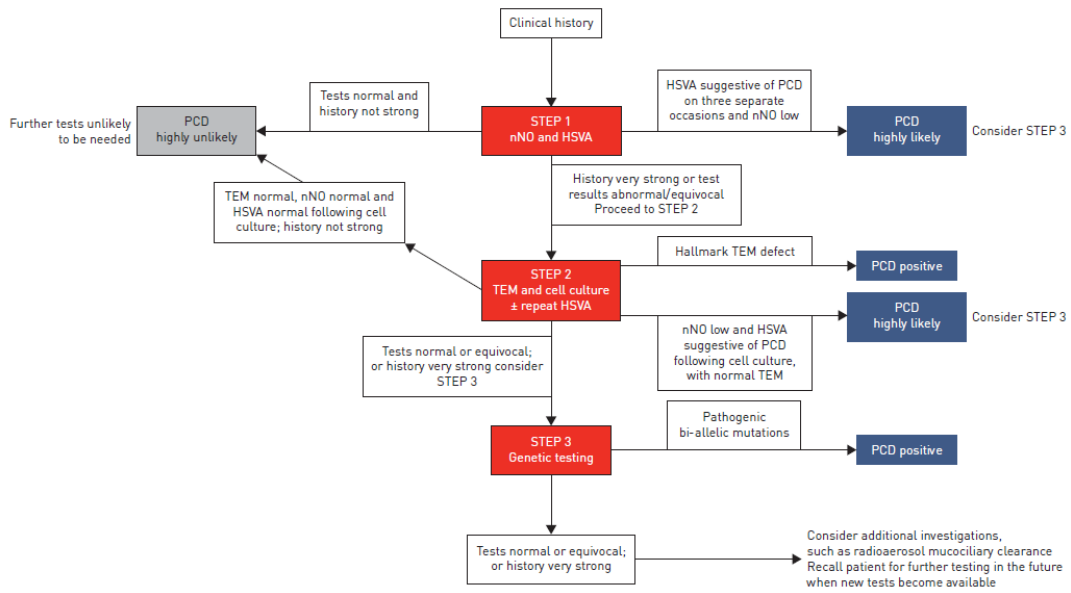
It is important to focus on the pulmonary exacerbations as they may affect lung function and are a risk factor for poor prognostic. The first clinical trial ever performed in PCD studied a long-term azithromycin therapy, and indicated that prophylactic antibiotic treatment could halve the number of respiratory exacerbations [2,72]. The first gene therapy studies using lentiviral vectors demonstrate the restoration of ciliary activity of PCD cells [74], and open up the possibility of a future transition from symptom-oriented therapies to personalized medicine [2].

### 1.2.4. DIAGNOSIS

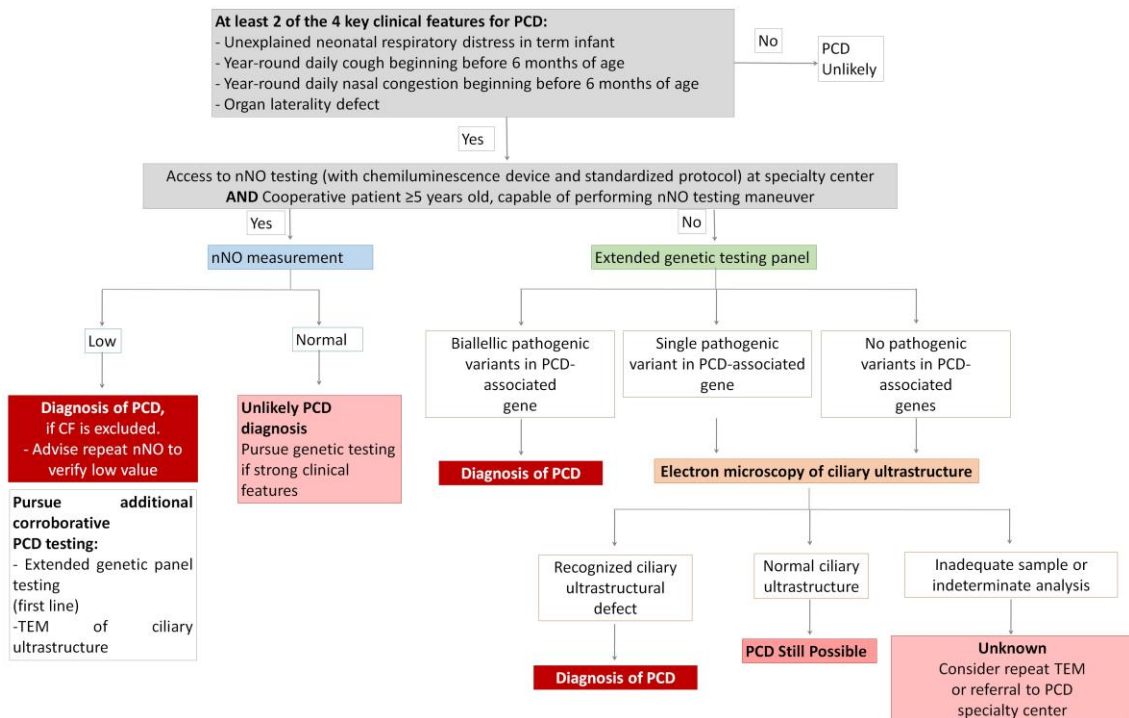
PCD patients often experience a long delay before a correct diagnosis is achieved, with the possibility of lung function impairment [75]. There are multiple reasons for this underdiagnosis. General clinicians and pulmonologists encounter few cases of PCD during their careers, so their experience with this disease is limited [2]. It has been described that 37% of positive PCD patients had more than 40 medical visits before being referred for diagnostic testing, and only 3% had been referred soon after birth [76]. PCD symptoms are non-specific, so diseases such as cystic fibrosis, allergies or immunodeficiencies should be ruled out first. PCD patients with *situs inversus totalis* are diagnosed earlier, at 3.5 years old, compared with 5.8 years of age in paediatric patients without this clinical sign [65].

There is no gold-standard diagnostic test for PCD, and there are limitations of the available techniques. The European Respiratory Society (ERS) [77] and the American Thoracic Society (ATS) [78] have recently proposed the combined use of different diagnostic techniques to improve the accuracy and diagnosis rate of PCD. Nowadays, PCD available diagnosis techniques include [2,77]: nasal nitric oxide (nNO) screening, high-speed video-microscopy (HSVM) analysis, transmission electron microscopy (TEM) analysis, immunofluorescence (IF) microscopy analysis and genetics.

Confirming or discarding PCD diagnosis is not always straightforward and easy, and guidelines of both ERS (Figure 12) and ATS (Figure 13) propose a combination of tests following different diagnostic algorithms. Diagnosis cannot be excluded nor confirmed on multiple occasions if clinical data are highly suggestive, but tests are not. Therefore, the ERS guidelines classify patients as "positive", "highly likely", or "highly unlikely" PCD [77]. There are important differences between the two guidelines, being the most important ones the role of nNO and genetics. nNO is the first step (if it is available) for ATS guidelines to continue or not the diagnostics tests, whereas it is only complementary for ERS guidelines. Besides, genetic studies are considered paramount to diagnose PCD in the American algorithm, but not in the European one, where it is only indicated in non-conclusive or positive cases, if available. Regarding HSVM functional study, it is not considered a routine test for the ATS guidelines, and it is only performed in specialized centers in non-conclusive cases. On the contrary, it is the first step for the European ones. Conversely, TEM analysis is considered in both guidelines and IF is not considered as a diagnostic test in any of them due to its lack of standardization. These days, there is an ongoing international consensus for IF analysis.



**Figure 12: European Respiratory Society (ERS) guidelines diagnostic algorithm for primary ciliary dyskinesia (PCD).** Diagnostic steps and outcome (positive, highly likely and highly unlikely PCD). nNO: nasal nitric oxide; HSVA: high-speed video-microscopy analysis; TEM: transmission electron microscopy. Figure from Lucas *et al.* [77].



**Figure 13: Suggested diagnostic algorithm in American Thoracic Society (ATS) guidelines for evaluating patients with suspected primary ciliary dyskinesia.** CF: cystic fibrosis; nNO: nasal nitric oxide; PCD: primary ciliary dyskinesia. Figure adapted from Shapiro *et al.* [78].

In 2016, Behan *et al.* [79] published a predictive clinical tool for patients with suspected PCD before referring them to PCD centers (PICADAR, Primary Ciliary Dyskinesia Rule). PICADAR score applies to patients with wet cough. It consists of seven questions or predictive parameters: full-term gestation, neonatal chest symptoms, neonatal intensive care admission, chronic rhinitis, ear symptoms, *situs inversus* and congenital cardiac defects. It has 0.90 sensitivity and 0.75 specificity for a cut-off value of 5 points (Figure 14) [79]. As well, low nNO values combined with a modified PICADAR score of  $\geq 2$  has been tested as a practical and cheap screening test for PCD in adults with bronchiectasis [80].

PICADAR		
Does the patient have a daily wet cough that started in early childhood?	<b>Yes</b> – complete PICADAR <b>No</b> – <b>STOP</b> . PICADAR is not designed for patients without a wet cough	
1. Was the patient born pre-term or full term?	Term	2
2. Did the patient experience chest symptoms in the neonatal period (e.g. tachypnoea, cough, pneumonia)?	Yes	2
3. Was the patient admitted to a neonatal unit?	Yes	2
4. Does the patient have a situs abnormality (situs inversus or heterotaxy)?	Yes	4
5. Does the patient have a congenital heart defect?	Yes	2
6. Does the patient have persistent perennial rhinitis?	Yes	1
7. Does the patient experience chronic ear or hearing symptoms (e.g. glue ear, serous otitis media, hearing loss, ear perforation)?	Yes	1
<b>Total score =</b>		

**Figure 14: PICADAR predictive score with seven questions to predict the probability of having primary ciliary dyskinesia (PCD).** This score can be used in patients with wet cough and symptoms starting in early childhood. The total score is calculated following the individual question's score. Table from Behan *et al.* [79].

#### **1.2.4.1. Nasal nitric oxide screening**

Nitric oxide (NO) is a small diffusible gas molecule involved in regulating ciliary motility and antimicrobial activity within the airways [2]. For unknown reasons, nasal NO (nNO) is lower in PCD compared with healthy subjects and individuals affected by other respiratory diseases [81]. Possible explanations could be: (1) increased breakdown of NO to metabolites; (2)

reduced nNO biosynthesis because of reduction of NO synthesizing activity; (3) NO being trapped in the obstructed paranasal sinuses; and (4) reduced production and storage capacity of NO in the sinuses [81]. Low nNO levels have been reported in patients with cystic fibrosis and patients with nasal polyps, thus these diseases should be discarded [2]. Furthermore, acute respiratory tract infections cause temporary reductions in nNO levels, so nNO measurements should be performed in periods without infection [82].

The nNO measurement is a non-invasive test based on measurements in aspirated nasal air directed to a NO analyzer, so it may be a useful diagnostic test. Nevertheless, more studies are necessary to standardize nNO measurement and define cut-off values to distinguish PCD patients from healthy controls [2]. The accuracy of nNO in PCD varies by type of analyzer, sampling method and age of the patient. In fact, nNO test is not well validated in children aged <6 years [77]. According to previously published studies, the ERS guidelines consider that nNO measurement is an accurate test when it is measured by a stationary chemiluminescence analyzer using velum closure technique (0.9-1 sensitivity and 0.7-0.97 specificity) [77]. Beydon *et al.* [83] recently carried out a retrospective study on a large population screened for PCD and described the routine practice and potential clinical impact of nNO in young children. They concluded that tidal breathing method was the only method feasible in children younger than 5 years old with a sensitivity of 77.4%, whereas, the breath holding (velum closure) method had a sensitivity and specificity in patients of 5 years of age or older [83]. nNO levels within the normal range have been recorded in some individuals with pathogenic variants in *DNAH9*, *GAS8*, *STK36*, *CCDC103*, *RSPH1*, *GAS2L2*, *NEK10* or *FOXJ1* genes [2].

Altogether, according to the ERS guidelines, facing a case of PCD-suggestive clinic, whether supported or not by nNO results, further diagnostic tests are recommended. Moreover, cut-off nNO levels are different in ERS and ATS guidelines, being 30 nL/min the cut-off value established in ERS for nNO [77], while ATS guidelines accept the use of nNO measurements alone when repeated low measurements (<77 nL/min) are observed [78,84].

### **1.2.4.2. High-speed video-microscopy**

PCD is caused by an abnormal ciliary function, which can be analyzed *ex vivo* by studying the ciliary activity in the respiratory epithelium from the nose or bronchus [77]. According to ERS guidelines, the first test to be carried out on suspicion of PCD (regardless of nNO rate) is the

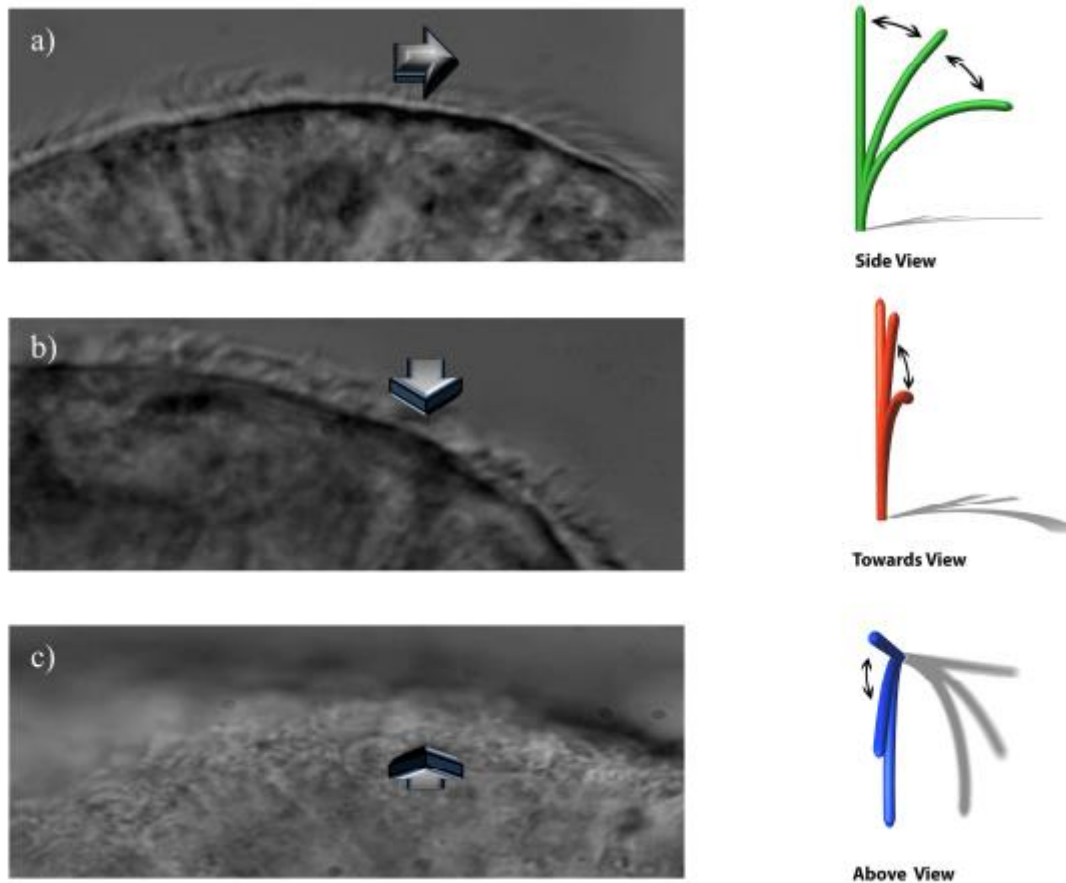
study of the ciliary beat frequency (CBF) and pattern (CBP) by high-speed video-microscopy (HSVM) [77].

The HSVM analysis must be performed in the first few hours after sample collection. Sommer *et al.* [85] found that the ciliary beat accelerates during the 3 first hours after the test with a plateau between 3 and 9 hours, and later, the speed decreases to half of the initial speed after 12 hours. For these reasons, it is recommended to analyze the sample in the first 9 hours after collection [85].

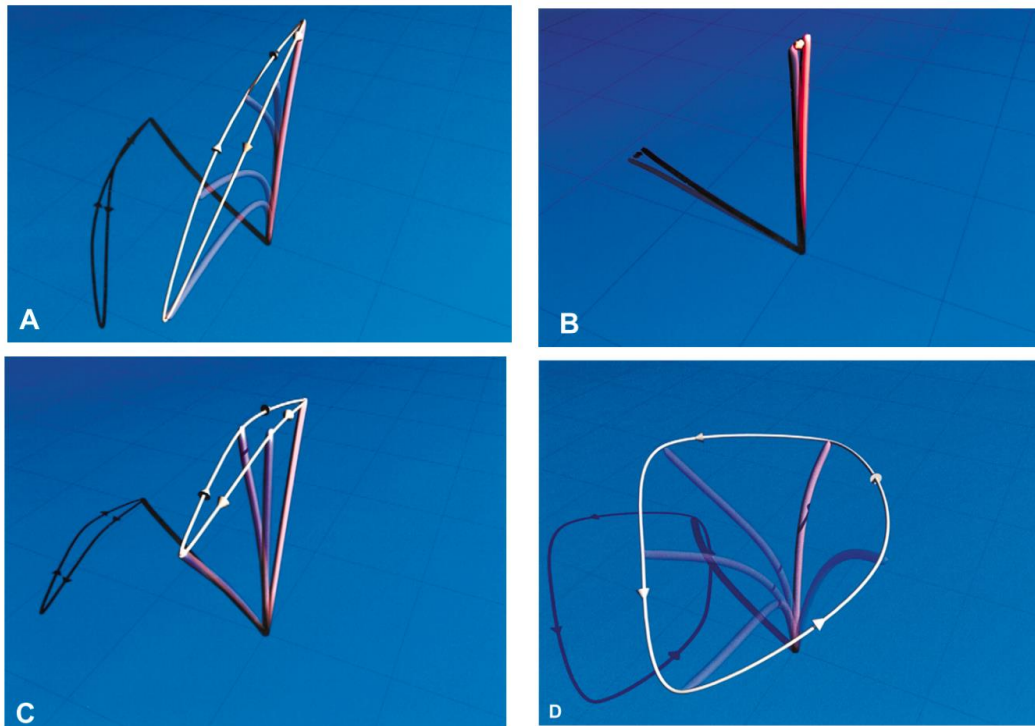
Movement of cilia is recorded with a high-speed camera at 400-500 images per second and then can be played back at reduced frames to its analysis. It is necessary to analyze CBF and CBP in different planes: lateral or side view, towards the observer and from above (Figure 15) [86,87]. Ciliary function varies on different conditions such as pH changes, bacterial contaminations and temperature, with some centers measuring HSVM at 37°C and others at lower temperatures [77]. The reference range for the CBF depends on the study (e.g. between 8.7-18.8 Hz) [86], so it is recommended that each center has its own reference values. At least 10 ciliated epithelial edges with 10 cells in each of them should be evaluated in each sample, in addition to analyzing the pattern with at least two overhead visions (from above vision/zenital plane). CBF should not be used without assessment of CBP because 10% of patients with PCD have normal CBF, but abnormal CBP [88]. Besides, sensitivity (0.97) and specificity (0.95) for the CBP is higher compared with the results of CBF (0.87 sensitivity and 0.77 specificity) [89]. Studies combining CBF and CBP presented a sensitivity of 0.96-1.00 and specificity 0.93-0.95 [77].

PCD patients present with abnormal or dyskinetic ciliary movement. The main different types of dyskinesia or ciliary beat patterns are immotile cilia, residual movement, stiff cilia, reduced ciliary amplitude, circular motion or disorganized ciliary beat (examples in Figure 16). Specific ciliary beat pattern defects have been associated with the different ultrastructure and genetic defects [90,91]. Cilia from patients with pathogenic variants in genes related to ODA show residual moment. Subjects with genetic defects in *DNAH11* cilia present with normal ultrastructure, but the CBF tends to increase, and abnormal hyperkinetic edges are observed [90]. When external and internal dynein arms and regulatory complex factors are affected, cilia are static (Figure 16B). Particularly, cases with defects in *CCDC39* and *CCDC40* have an extremely stiff beat pattern (Figure 16C). Furthermore, when the defects are in the radial

spoke head components, the CBF is normal or decreased but CBP shows a circular motion in some areas (Figure 16D). Pathogenic variants in *CCDC164* result in very subtle HSVM abnormalities with mild rigid pattern due to decreased amplitude. Some genetic defects, such as in *GAS8*, result in subtle defects that are hardly detectable by HSVM [90].



**Figure 15: Images of high-speed video-microscopy (left) and diagram (right) in three different beating planes.** The arrows indicate the ciliary movement according to the observer. **A)** Lateral or side view. **B)** View towards the observer. **C)** Above view. Figure from Kempeneers *et al.* [87].



**Figure 16: Diagram of different ciliary beat patterns. A)** Normal ciliary beat pattern. Cilia motion with a forward power stroke and a backward recovery stroke. **B)** Immotile cilia with occasional residual movement (slow, low amplitude, stiff flickering motion). **C)** Stiff cilia with markedly reduced amplitude. **D)** Circular motion about the base of the cilium. Figure from Chilvers *et al.* [91].

A recent study by Rubbo *et al.* [92] showed that HSVM studies have a high sensitivity (1.00) and specificity (0.93) for the diagnosis of PCD [92]. However, ATS guidelines and some centers still do not recommend HSVM for PCD suspected patients diagnosis because of its limitations: results can be altered by secondary infections and inflammation, lack of recognized reference standards and the fact that it is a subjective technique that needs expertise [78,93].

#### **1.2.4.3. Transmission electron microscopy**

Ciliary ultrastructure analysis by TEM is a complex technique that requires sophisticated equipment and considerable expertise. Respiratory epithelium is sampled by brush or curette biopsy, chemically fixed with glutaraldehyde, processed and embedded into blocks, which are sectioned with a microtome. Staining is performed with heavy metals (lead citrate and uranyl acetate or equivalent) and the ciliary ultrastructure parts (Figure 1B) are assessed under an electron microscope [77].

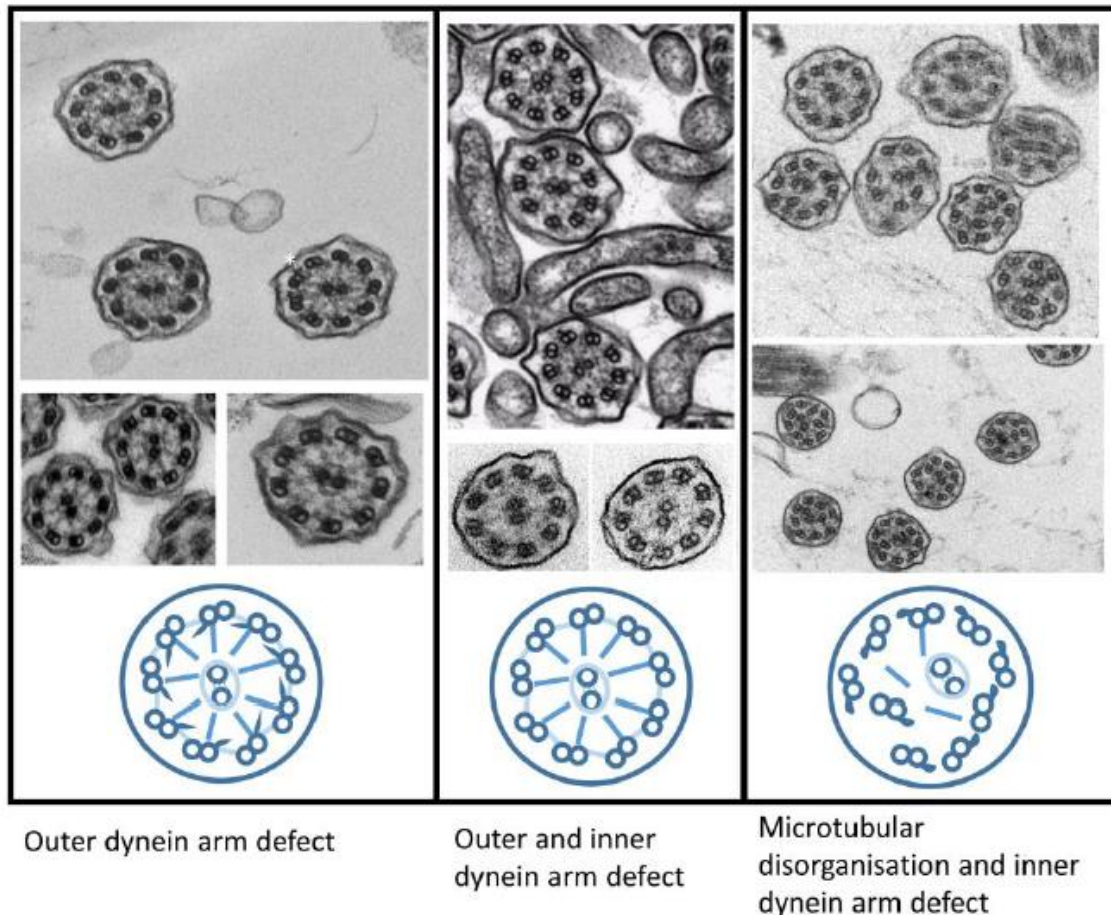


TEM analysis has been traditionally considered the gold standard diagnostic test for PCD. However, approximately 16-30% of all PCD cases have either normal or subtle ultrastructure defects, which are not easily detected by TEM. Thus, TEM cannot be considered a unique diagnostic test [77,94].

Recently, an international TEM consensus has been achieved [95]. The expert consensus identifies two classes of PCD TEM diagnostic defects (Figure 17): (1) class 1 defects which are hallmark defects that confirm the diagnosis (image examples in figure 18); and (2) class 2 defects that indicate PCD diagnosis in patients with clinical symptoms and consistent defects in different samples or after cell culture. Class 2 defects are more challenging to recognize and can occur because of secondary damage. This guideline clarifies the items to include in the reports and defines the adequacy of a diagnostic sample for PCD diagnosis by TEM [95].

<p><b>Class 1 defects: Hallmark diagnostic defects</b></p> <ul style="list-style-type: none"><li>• Outer dynein arm defect</li><li>• Outer and inner dynein arm defect</li><li>• Microtubular disorganisation and inner dynein arm defect</li></ul> <p><b>Class 2 defects: Indicate a PCD diagnosis with other supporting evidence</b></p> <ul style="list-style-type: none"><li>• Central complex defect</li><li>• Mislocalisation of basal bodies with few or no cilia</li><li>• Microtubular disorganisation defect with inner dynein arm present</li><li>• Outer dynein arm absence from 25%-50% cross sections</li><li>• Combined inner and outer dynein arm absence from 25-50% cross sections</li></ul>
--

**Figure 17: Summary table of class 1 and 2 ultrastructural defects for primary ciliary dyskinesia diagnosis.** Figure from Shoemark *et al.* [95].



**Figure 18: Ultrastructural images and axoneme diagrams of transmission electron microscopy class 1 defects.** Class 1 defects include outer dynein arm defects, outer and inner dynein arm defects, and microtubular disorganisation and inner dynein arm defects. Figure from Shoemark *et al.* [95].

Isolated ODA defects have been associated with numerous PCD genes encoding this structure. Combined ODA and IDA defects have been associated with multiple genes that encode cytoplasmic proteins involved in the pre-assembly of ciliary axonemes. Genetic pathogenic variants in nexin link and DRC genes lead to different ciliary ultrastructures. Pathogenic gene variants in *CCDC65*, *CCDC164*, and *GAS8* produce normal ciliary ultrastructure, while genetic defects in *CCDC39* and *CCDC40* are associated with IDA and microtubular disorganization (MTD) defects. Most cross-sections missing IDA and the accompanying MTD occur more sporadically in less than 50% of the axoneme cross-sections. The genetic causes of some IDA+MTD defects have not been discovered. Pathogenic variants in *DNAH11* and *HYDIN* produce normal ciliary ultrastructure, while mutations in genes encoding radial spoke head proteins result in some cross-sections with CP alterations intersperse with normal ones.

Defects in *CCNO* and *MCIDAS* cause near complete absence of respiratory cilia and defects in generation of basal bodies [94].

Besides, the recently developed TEM tomography enables tridimensional visualization of ciliary ultrastructure [2]. The absence of C2b projection of the CP apparatus in *HYDIN* loss-of-function mutant respiratory cells [31] and abnormalities in the ODA composition in *DNAH11* mutant cells were demonstrated by TEM tomography studies [96].

### **1.2.4.4. Respiratory ciliated cell culture**

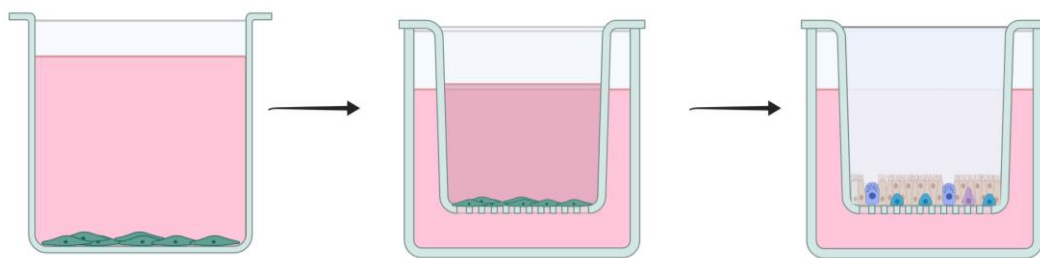
Secondary damage of ciliated nasal tissue is common in samples of PCD-candidate patients. This may be due to recurrent respiratory infections or to damaging tissue when taking biopsies. Secondary damage may give equivocal ultrastructure (TEM) lectures and/or cilia misfunction (HSVM) leading to false-positive results. Thus, it is necessary to distinguish acquired from inherited cilia abnormalities to give a proper PCD diagnosis. Besides, scarce samples or samples of low quality (with numerous red cells and/or mucus) may lead to mistaken results. In addition, TEM analysis needs a considerable amount of ciliated cells to be consistent, and a low amount of sampling may lead to false positives (21%) and false negatives [77]. Therefore, ERS guidelines recommend the study of ciliary abnormalities in three independent biopsy samples. Alternatively, as nasal biopsies would be uncomfortable for the patient and repeated biopsies could cause a delay in diagnosis, HSVM of cultured respiratory ciliated cells may contribute to improve the diagnosis accuracy [2,77]. Respiratory ciliated cell culture are directly derived from patients' nasal samples and show no secondary structural and functional abnormalities after ciliogenesis [97].

Two different approaches to cell culture in PCD have been developed: suspension cultures and air-liquid interface (ALI) cultures. Suspension cultures, so-called spheroids, consist of 3D-cell cultures in monolayer [98,99], whereas ALI cultures consist of 2D-cell cultures exposed to air [100,101].

The use of cell culture to improve the diagnosis of PCD was first led by Jorissen *et al.* [98]. CBF and ciliary coordination were assessed in 712 patients by using ciliated suspension culture (3D-cultures), so-called spheroids. Twenty percent of non-PCD patients presented an abnormal ciliary activity before culture, but after culture, 100% were normal. In contrast, 20% of PCD

patients had a normal CBF, and 10% had coordinated ciliary beat before culture. After culture, normal CBF was found in 7% of PCD patients. They concluded that, after culture, CBF analysis and, even more, coordinated ciliary activity (100% specific and sensitive) are highly reliable for PCD diagnosis [98]. Pifferi *et al.* [99] also assessed the results of CBF and CBP after a simplified method for spheroids. They investigated 9 doubtful cases and concluded that four patients had PCD and two presented secondary defects, yet three remained inconclusive [99].

However, the 3D-culture approach usually does not provide enough ciliated cells to perform a new TEM analysis [99]. Based on alternative methods of ciliated-cell cultures, widely used in research, Hirst *et al.* [100] first developed and evaluated an ALI culture from nasal epithelia to study PCD in 187 samples. ALI culture consisted of three phases (Figure 19): basal-cell proliferation, basal-cell proliferation in inserts, and airway culture. Cell suspensions were seeded on collagen-pre-coated culture plates for 2-7 days for basal cell (airway epithelia progenitors) proliferation. When confluent, basal cells were seeded on a collagen-coated transwell insert for 2 days, adding proliferation medium in both insert and plate. When confluent, proliferation medium was removed completely, and ALI medium was carefully basolaterally added (exclusively on the plate) to create an airway culture and induce differentiation of basal cells. According to Hirst *et al.* [100], ciliogenesis should appear after 2-3 weeks, and optimal ciliary growth, considered of more than 10% of culture surface, after 4-6 weeks since the exposure of cells to ALI [100]. From here, a small portion of the differentiated cultures may be used for HSVM (CBF and CBP), another portion for TEM [100], and the rest for other approaches (i.e. IF), or even frozen for further *in vitro* analyses.



**Figure 19: Air-liquid interface (ALI) cell culture steps (from left to right). (1) Basal-cell proliferation:** cell suspensions are seeded for basal cell proliferation. **(2) When confluent,** basal cells are seeded on a transwell insert for 2 days adding proliferation medium in both insert and plate. **(3) When confluent,** proliferation medium is removed, and ALI medium is basolaterally added on the plate (see arrow) to

create an airway culture and induce differentiation of basal cells. Ciliogenesis should occur after 2-3 weeks. BC: basal cells, TW: transwell insert. Created in BioRender.com.

The results of Hirst *et al.* [100] showed that more than half of the cultured biopsy-brushings (54%, 101/187) became ciliated and all allowed TEM and HSVM evaluations. ALI cultures helped to exclude PCD in eight suspected patients with high dyskinesia in original biopsies. Besides, six out of 25 biopsies without cilia could be re-evaluated thanks to ALI cultures: all showed normal function and ultrastructure [100]. In a second study, Hirst *et al.* [101] compared HSVM and TEM outcomes pre- and post-ALI cultures to assess the robustness of this technique after observing changes in post-culture ciliary phenotype in some of their patients. They observed that in all PCD cases, dyskinesia remained unchanged or increased, whereas in non-PCD subjects, secondary dyskinesia decreased. They concluded that this exacerbation in cilia phenotype did not affect the diagnosis of PCD and, in some cases, it may clarify it [101].

Ciliated-cell cultures are time-consuming and need special equipment and experienced personnel [98–100]. In addition, different factors can limit both ALI and spheroid outcomes. Inherent respiratory infections and relatively few cells obtained (in brushing or after dividing the sample for different tests) increase the chance of failed cultures [98–101]. Cultures started with few cells have a low potential of differentiation, and basal cells need more rounds to divide [100]. In practice, approximately only half of ALI cultures are successful (54%) and the rate of success is higher in biopsies with low dyskinesia [100]. This indicates that ciliogenesis in ALI cultures may also depend on the degree of damage [100]. On the contrary, spheroids have a higher percentage of success [99]. However, the advantages and possibilities of ciliated-cell cultures overcome their limitations. The use of cell culture from brush biopsy specimens may help avoid re-sampling, reduce false-positive diagnosis in patients with secondary ciliary dysfunction, reevaluate difficult samples, confirm the diagnosis of less common phenotypes and evaluate new PCD phenotypes.

### **1.2.4.5. Immunofluorescence microscopy analysis**

IF is a technique consisting in the use of fluorescently labelled antibodies for the detection of the presence and distribution of different ciliary proteins in human respiratory cells by fluorescence or confocal microscopy. It has been recently proposed as a tool to improve the diagnosis rate in PCD and to understand disease-causing genes [77,78]. Omran and Loges [102]

first described the methodology for IF staining of ciliated respiratory epithelial cells [102]. Nowadays, a significant number of antibodies against different cilia proteins are available, including antibodies against proteins in ODA, IDA, RS head and DRC [77].

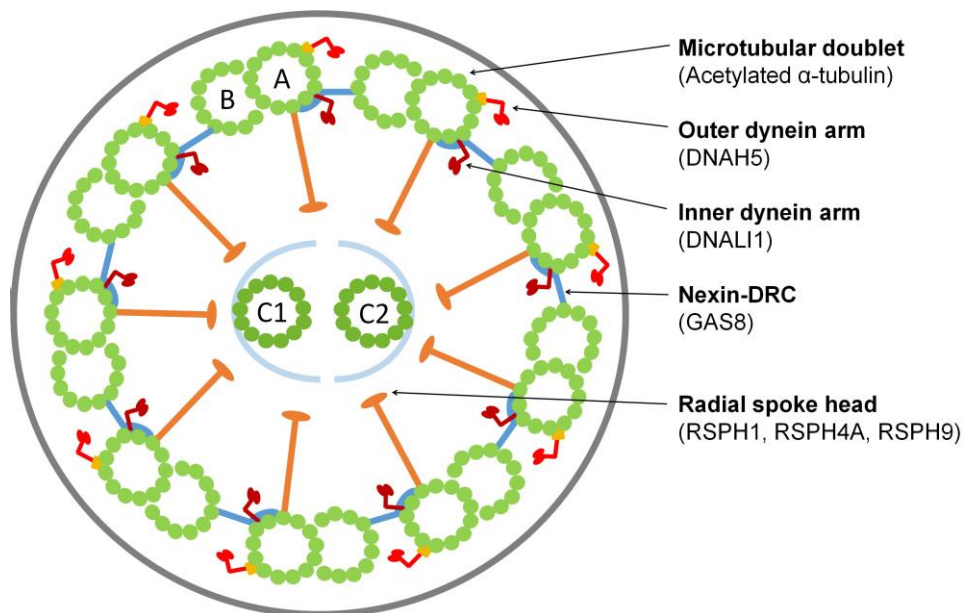
Different studies presented IF as a technique to understand the downstream effect of genetic variants in different PCD-related genes [77,103]. On this matter, Lucas *et al.* [77] published, in the ERS guidelines for the diagnosis of PCD, a review of the correlation between the PCD-causing genes and their associated findings by TEM and IF [77]. Therefore, IF has been used to study the defect in cilia proteins in cohorts of patients with a different range of genetic variants, providing information of the pathogenicity of these variants. For instance, this was described in a study of PCD patients with radial RS defects [30]. It is important to consider that IF analysis could detect abnormalities in cases without ultrastructural defects, and therefore not detected by TEM, as described in *DNAH11* defects [6].

IF is cheaper and easier than other techniques and the use of IF as a diagnostic test in PCD is likely to increase as more antibodies are becoming commercially available [77]. However, studies about using IF in diagnostic settings and IF validation studies are necessary to further consider IF as a diagnostic tool for PCD in diagnostic cohort studies [77]. The ATS considers IF as one of the emerging PCD diagnosis techniques, although it insists on the lack of consensus in a gold standard for diagnosis and the insufficient sensitivity and specificity when applied to the general population [78]. For these reasons, as mentioned, an international consensus for IF analysis is ongoing.

Several centers included in the international registry for PCD confirmed that they are using IF to aid diagnosis in PCD [66]. In this registry, a defect in cilia proteins studied by IF was one of the diagnosis criteria for the recruitment of patients [66]. In 2005, the first study using IF as a diagnostic tool was reported [104]. It was performed in a large cohort of patients suggestive of PCD and control subjects, and showed *DNAH5* mislocation in patients with an ODA defect previously described by TEM [104]. The same authors described a different cellular sublocation of *DNAH5* and *DNAH9* by IF, indicating two types of ODA [104].

A study by Shoemark *et al.* [105] studied the accuracy of IF in the diagnosis of PCD. The methodology applied in this study consists of a two-step incubation: one with acetylated  $\alpha$ -tubulin antibody, to visualize cilia, and another with six labeled antibodies against proteins in

cilia axoneme. Firstly, all samples were assessed with the primary antibodies: DNAH5 (an ODA component), DNALI1 (an IDA component) and RSPH4A (a RS component). Secondly, only selected cases were assessed with a second round of antibodies: RSPH9 (a RS component), RSPH1 (a RS component) and GAS8 (a component of the N-DRC). Target protein location is shown in Figure 20. Different results regarding the accuracy of IF as a diagnostic tool were then reported using the described panel of antibodies [105]. First, IF correctly identified mislocation or absence of target proteins in 35 patients with a confirmed ultrastructural defect by TEM. Second, IF diagnostic accuracy was studied in a cohort of 386 patients with symptoms suggestive of PCD. From these, the technique successfully identified an absence of target proteins in 22 of 25 patients with PCD, whereas the remaining three patients were demonstrated to have mutations in genes (*DNAH11* and *HYDIN*) already associated to normal ultrastructure. Normal staining was observed in 252 cases in which PCD was considered highly unlikely. Third, IF resulted in 39 of 71 cases with a previously inconclusive result in other diagnostic tests. Taking all these results into account, this study demonstrated that IF is a useful diagnostic technique and presents the same accuracy as well-performed TEM analysis, which is why the authors support IF as a routine diagnostic test for PCD, especially when TEM expertise or equipment is not available [105].



**Figure 20: Cilia axoneme in transverse section indicating the ultrastructure parts and the target proteins by immunofluorescence.** Proteins are indicated in parentheses. A and B: peripheral microtubule doublets; C1 and C2: central pair; DRC: dynein regulatory complex.

The use of IF as a diagnostic test in PCD is believed to increase with more antibodies becoming commercially available [77]. In a recent study, Liu *et al.* [106] presented a quantitative super-resolution imaging workflow to detect cilia defects thanks to the validation of 21 commercially available IF antibodies. Molecular defects using this super-resolution imaging toolbox were described in 31 clinical PCD cases, including patients with negative TEM results and/or with genetic variants of uncertain significance (VUS) [106].

The main advantage of IF is the reduction of costs and time compared to TEM analysis, so IF may improve accessibility and accuracy of PCD diagnosis to a wider population of patients [105,107]. Besides, IF also works on small samples [105], unlike TEM. Also, it is done in respiratory cells obtained by non-invasive brushings, and dried samples in slides, and therefore may be easily transported. Furthermore, it has been reported that secondary ciliary changes do not affect axonemal location of ODA components and this technique detects changes along the entire ciliary axoneme whereas TEM only studies a cross section of the cilia [102].

The major limitation of the IF analysis is that because of the use of primary antibodies targeting specific proteins, defects in unrelated proteins may be missed. Moreover, patients with partial defects or missense genetic variants have been shown to have normal IF results [105]. Furthermore, as new genes and proteins related to PCD are discovered, the antibody panels may need to be revised and expanded in the future for an accurate diagnosis [107].

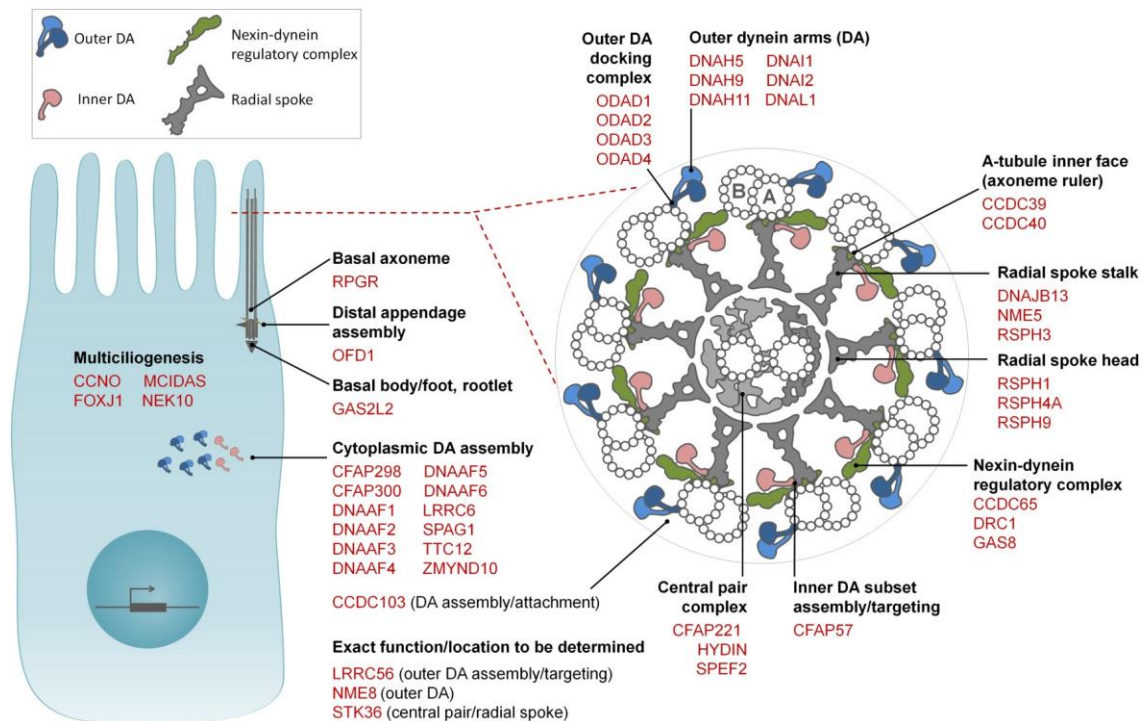
To summarize, IF seems to be a new reliable technique to study the molecular biology of cilia axoneme and improve the accuracy and diagnosis rate of PCD. However, validation studies are necessary to include this technique as part of the diagnostic algorithm in PCD diagnostic guidelines [77,78].

#### **1.2.4.6. Genetics**

Genetic analysis is usually an easy and quick diagnostic test and is specifically indicated when other PCD diagnosis techniques are unavailable or have equivocal results, such as normal ciliary ultrastructure described in patients with *DNAH11* variants. However, PCD is a genetically heterogeneous disorder and molecular testing is complicated. High-throughput sequencing enables the possibility of studying the different PCD-associated locus, and many centers offer this technology for PCD diagnosis [2,108–110].



Since the isolation of *DNAI1*, the first PCD gene, in 1999, more than 50 PCD-causing genes have been described, which allow the identification of a genetic cause in approximately 70-75% of patients with a highly probable PCD phenotype [2,8,111]. Likely pathogenic genetic variants causing impaired multiciliogenesis, ciliary structure and/or the function of axoneme have been described (Figure 21). Most of the variants (77%) are private, i.e. identified in a single family [112]. The distribution of PCD-causing genes may differ depending on ethnic origin being *DNAH5* and *DNAH11* the most prevalent defective genes in Caucasian European families, *CCDC39* and *CCDC40* in Arab families and *LRRC6* and *CCDC103* in South Asian families. Most of the described genetic variants predict a loss-of-function (nonsense, frameshift, splice site and a few large deletions) [112].



**Figure 21: Axonemal localization and function of the proteins encoded by PCD-causing genes.** Longitudinal view of an airway cell with cross-section of ciliary axoneme (dotted red lines). Location of encoded proteins (red). DA: dynein arm. Figure modified from Legendre *et al.* [8].

Genetic defects usually correlate with certain HSVM results, alterations in TEM and IF. Wallmeier *et al.* [2] recently reviewed the correlation between all known affected genes and related findings in other diagnostic tests [2].

## **2. HYPOTHESIS AND OBJECTIVES**



## **2.1. HYPOTHESIS**

The ERS [77] and the ATS [78] guidelines present genetic and IF analysis as new diagnostic techniques to improve the diagnosis rate in PCD. These techniques seem to have a great potential for a better understanding of PCD-causing genes and their cellular implications. Thus, optimizing these techniques will improve the diagnosis rate in our cohort and help understand the correlation between a specific genetic defect and ciliary structure and function.

## **2.2. OBJECTIVES**

1. Design, validate and apply a molecular panel of PCD-related genes, including all known genes causing PCD.
2. Verify the diagnostic usefulness of the gene panel in a cohort of patients with clinical suspicion of PCD.
3. Perform whole exome sequencing (WES) studies in unresolved genetic cases to discover new candidate genes.
4. Describe the genetic alterations associated with PCD in our cohort.
5. Optimize and apply an immunofluorescence commercial antibody panel to study ciliary structure in suspected PCD patients in a Spanish cohort.
6. Establish the utility and accuracy for PCD diagnosis of an immunofluorescence panel and characterize the ciliary structural defects of a Spanish cohort of patients with suspected PCD.
7. Study the correlation of clinical characteristics with the different diagnostic tools applied: genetics, immunofluorescence and high-speed video-microscopy.



## **3. METHODS**



### **3.1. PATIENTS**

This study belongs to a prospective multicentric study including patients with a clinical history suggestive of PCD from 2016 to 2020. This project was approved by the Clinical Research Ethics Committee (CEIC) of *Hospital Universitari Vall d'Hebron* (PR(AMI)148/2016). Written informed consents were obtained from  $\geq 18$ -year-old patients,  $\geq 12$ -year-old patients and their parents or guardians, and  $< 12$ -year-old patient's parents or guardians.

### **3.2. PCD DIAGNOSTIC EVALUATION**

Patients were evaluated for PCD with a clinical symptom questionnaire and PICADAR score [79], nNO determination, HSVM, IF analysis and genetic testing. In our setting, TEM analysis was available only in a few cases because of logistic difficulties.

ERS guidelines [77] were followed to classify patients as: (a) confirmed PCD (suggestive clinical history with hallmark ciliary ultrastructure defects assessed by TEM and/or presence of pathogenic bi-allelic variants in PCD-associated genes); (b) highly likely PCD (suggestive history with very low nNO and HSVM findings consistently suggestive of PCD after repeated analysis or cell culture); or (c) highly unlikely PCD (weak clinical history, normal nNO and normal HSVM).

### **3.3. NASAL NITRIC OXIDE SCREENING**

nNO measurements were performed using a CLD 88sp NO-analyzer (ECO MEDICS, AG, Duerten, Switzerland) according to ERS guidelines [113]. Transnasal nNO was measured following the ATS [78] and ERS [77] recommendations and standardizations.

### **3.4. HIGH-SPEED VIDEO-MICROSCOPY**

HSVM was performed to study CBF and CBP (local normal values: CBF 8.7–18.8 Hz; CBP  $\leq 20\%$  dyskinetic ciliated cells). Nasal respiratory epithelia were sampled by brushing the nasal mucosa at the inferior nasal meatus with a 2 mm diameter bronchoscopy brush submerged in HEPES-supplemented Medium 199 (pH 7.3) (Gibco, Thermo Fisher Scientific, Waltham, MA, USA), containing antibiotic and antifungal solutions (Gibco, Thermo Fisher Scientific). A



minimum of ten lateral strips with 10 cells each and two overhead (from above vision/zenital plane) axes, devoid of mucus if possible, were captured at 37°C with an optical microscope at X100 magnification coupled to a high-speed video camera (MotionPro® X4, IDT, CA, USA) using MotionPro® X4 software [114].

## **3.5. GENETICS**

### **3.5.1. PATIENTS**

In the period between January 2017 and November 2019, a total of 118 individuals, including 79 patients (74 index patients) and 39 relatives, were genetically studied using our high-throughput PCD gene panel. Out of the 79 patients, 53 were classified as confirmed or highly likely PCD and 26 as highly unlikely PCD. Being a reference center for the study of the disease, our Hospital recruited 41 patients (*Hospital Vall d'Hebron*). Samples were received and included from other hospitals all over the country: PCD group Valencia (n=14), *Hospital Sant Joan de Déu* (Esplugues de Llobregat, Barcelona) (n=14), *Hospital Miguel Servet* (Zaragoza) (n=4), *Hospital del Mar* (Barcelona) (n=2), *Hospital Parc Taulí* (Sabadell, Barcelona) (n=1), *Hospital Germans Trias i Pujol* (Badalona, Barcelona) (n=1), *Hospital Clínic* (Barcelona) (n=1) and *Hospital Son Llätzer* (Palma de Mallorca) (n=1).

### **3.5.2. HIGH-THROUGHPUT PCD GENE PANEL AND DATA ANALYSIS**

#### ***3.5.2.1. Library preparation and bioinformatics analysis***

Peripheral blood DNA was extracted by automated magnetic extraction (Chemagic, Perkin-Elmer, Waltham, MA, USA) or manual extraction using a Quick-DNA™ Midiprep Plus Kit (Zymo Research, Irvine, CA, USA). The DNA concentration was determined with a Qubit dsDNA BR Assay Kit in a Qubit 2.0 fluorimeter.

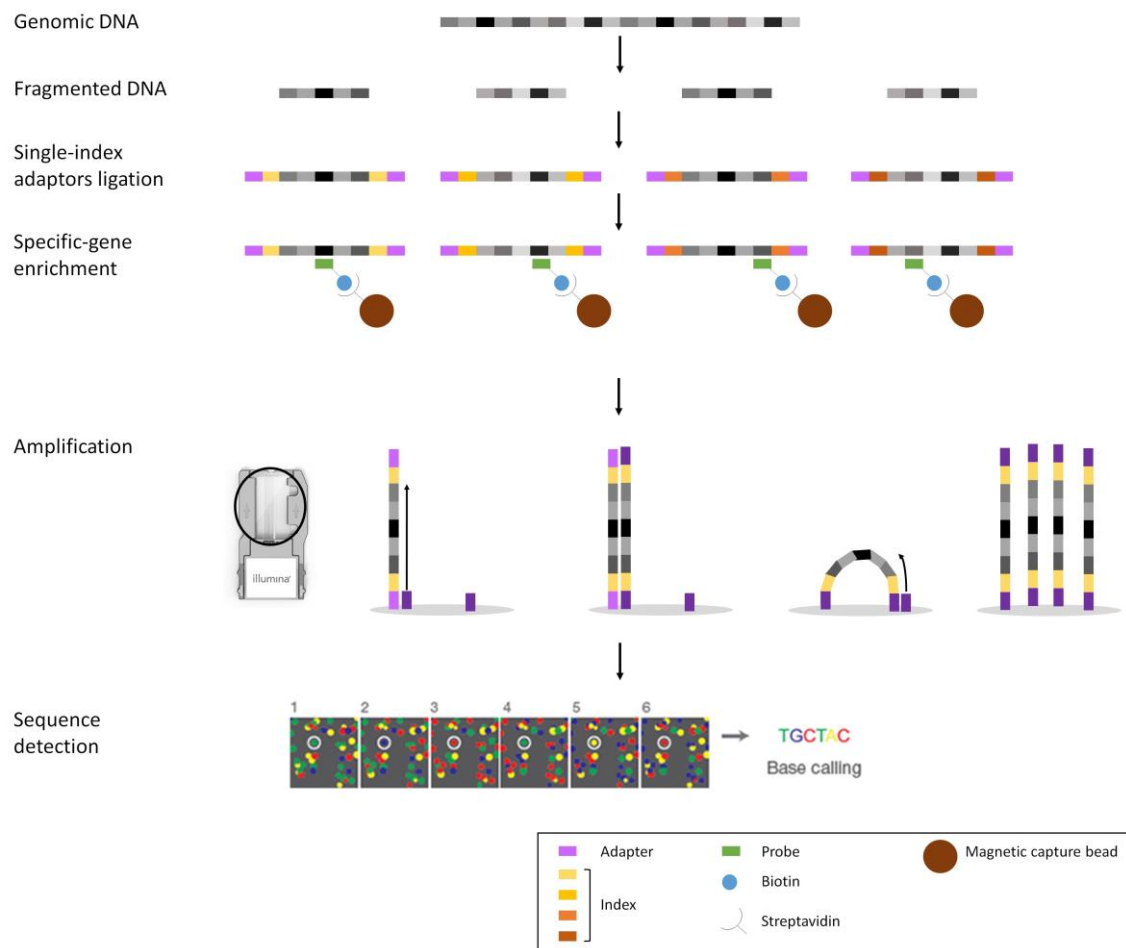
To carry out the genetic studies, a high-throughput gene panel was designed to allow exonic and flanking intronic region ( $\pm 20$  bp) sequencing using SeqCap EZ (Roche Nimblegen, Pleasanton, CA, USA) technology. This panel included 44 genes related to PCD, as described in the literature at time of design (Table 1).

**Table 1: Genes included in our high-throughput gene panel.**

Gene name	Gene ID	Transcript ID	Protein ID	Number of exons
<i>ARMC4/ODAD2</i>	NG_042820.1	NM_018076.3	NP_060546.2	29
<i>C21orf59/CFAP298</i>	NG_033839.2	NM_021254.2	NP_067077.1	7
<i>CCDC11/CFAP53</i>	NG_042815.1	NM_145020.3	NP_659457.2	8
<i>CCDC39</i>	NG_029581.1	NM_181426.1	NP_852091.1	20
<i>CCDC40</i>	NG_029761.1	NM_017950.3	NP_060420.2	26
<i>CCDC65</i>	NG_033837.1	NM_033124.4	NP_149115.2	8
<i>CCDC103</i>	NG_032792.1	NM_213607.2	NP_998772.1	4
<i>CCDC114</i>	NG_033251.1	NM_144577.3	NP_653178.3	19
<i>CCDC151</i>	NG_041777.1	NM_145045.4	NP_659482.3	14
<i>CCDC164/DRC1</i>	NG_042824.1	NM_145038.3	NP_659475.2	17
<i>CCNO</i>	NG_034201.1	NM_021147.4	NP_066970.3	3
<i>DNAAF1</i>	NG_021174.1	NM_178452.4	NP_848547.4	15
<i>DNAAF2</i>	NG_013070.1	NM_018139.2	NP_060609.2	3
<i>DNAAF3</i>	NG_032759.1	NM_001256714.1	NP_001243643.1	12
<i>DNAAF5</i>	NG_033137.1	NM_017802.3	NP_060272.3	13
<i>DNAH1</i>	NG_052911.1	NM_015512.4	NP_056327.4	81
<i>DNAH5</i>	NG_013081.1	NM_001369.2	NP_001360.1	86
<i>DNAH6</i>	NG_050957.1	NM_001370.1	NP_001361.1	81
<i>DNAH7</i>	NC_000002.12	NM_018897.2		69
<i>DNAH8</i>	NG_041805.1	NM_001206927.1	NP_001193856.1	97
<i>DNAH9</i>	NG_047047.1	NM_001372.3	NP_001363.2	73
<i>DNAH11</i>	NG_012886.2	NM_001277115.1	NP_001264044.1	82
<i>DNAI1</i>	NG_008127.1	NM_012144.3	NP_036276.1	24
<i>DNAI2</i>	NG_016865.1	NM_023036.4	NP_075462.3	17
<i>DNAL1</i>	NG_028083.1	NM_031427.3	NP_113615.2	10
<i>DNALI1</i>	NC_000001.11	NM_003462.3	NP_003453.3	6
<i>DYX1C1/DNAAF4</i>	NG_021213.1	NM_130810.3	NP_570722.2	11
<i>EPB41L4A</i>	NG_052950.1	NM_022140.3	NP_071423.4	26
<i>GAS8</i>	NG_046598.1	NM_001481.2	NP_001472.1	15
<i>HYDIN</i>	NG_033116.2	NM_001270974.1	NP_001257903.1	92
<i>LRRC6</i>	NG_033068.1	NM_012472.4	NP_036604.2	17
<i>MCIDAS</i>	NG_051620.1	NM_001190787.1	NP_001177716.1	7
<i>MNS1</i>	NC_000015.10	NM_018365.2	NP_060835.1	10
<i>NME8</i>	NG_015893.1	NM_016616.4	NP_057700.3	18
<i>OFD1</i>	NG_008872.1	NM_003611.2	NP_003602.1	27
<i>RPGR</i>	NG_009553.1	NM_000328.2	NP_000319.1	18
<i>RSPH1</i>	NG_034257.1	NM_080860.3	NP_543136.1	9
<i>RSPH3</i>	NG_051819.1	NM_031924.4	NP_114130.3	11
<i>RSPH4A</i>	NG_012934.1	NM_001010892.2	NP_001010892.1	7
<i>RSPH9</i>	NG_023436.1	NM_152732.4	NP_689945.2	7
<i>SPAG1</i>	NG_033834.1	NM_172218.2	NP_757367.1	21
<i>TEKT1</i>	NC_000017.11	NM_053285.1	NP_444515.1	8
<i>TTC25</i>	NG_053115.1	NM_031421.3	NP_113609.1	13
<i>ZMYND10</i>	NG_042828.1	NM_015896.2	NP_056980.2	12

ID: identification. ID data obtained from NCBI (National Center for Biotechnology Information, <https://www.ncbi.nlm.nih.gov/>) database.

DNA libraries with the regions of interest were prepared according to the manufacturer's instructions (SeqCap EZ, Roche Nimblegen). In Figure 22 is shown a diagram of this process. First, individual genomic DNA samples (from 12 to 14 patients) were quantified, and 100 ng of DNA were enzymatically fragmented for 21 min and tagged with a single-index adapter. Later then, fragments of a specific size were selected using magnetic beads and amplified by polymerase chain reaction (PCR) using index primers. At that point, an equal mass amount of each DNA library was mixed to obtain 1  $\mu$ g of the multiplex pool. This pool was subjected to an enrichment, hybridized with biotinylated gene-specific probes, captured with streptavidin-conjugated magnetic beads, stringently washed and eluted to obtain the enriched pool library. The pool library was amplified by PCR using the specific gene-panel oligos. Sequencing of 8 pM of the multiplex pool library was carried out using solid-bridge amplification technology (flow cell) and a massive next-generation sequencer MiSeq (Illumina, San Diego, CA, USA).



**Figure 22: Schematic diagram of gene-panel library preparation and sequence detection.** Part of the figure was taken from Illumina (<https://www.illumina.com/>).

The data analysis process included cutting sequences with Trimmomatic (Institute for Biology, Aachen, Germany) [115], an alignment of the sequences with the reference human genome GRCh (hg38) using BWA-MEM [116], variant detection with Genome Analysis Toolkit (GATK) Haplotype Caller (Broad Institute, Cambridge, MA, USA) [117] and variant annotation with ANNOVAR [118]. Only variants with a deep-coverage, i.e.  $\geq 20$  reads, were taken into account in the analysis. The list of the identified variants was compared with information from different databases to identify variants already described in association to a known phenotype: HGMD (Qiagen, Hilden, Germany), ClinVar (<https://www.ncbi.nlm.nih.gov/clinvar/>) [119]; and population frequency databases: GnomAD [120], ExAC (<http://exac.broadinstitute.org>) [121], 1000 genomes [122]. Remaining variants were then filtered to a minor allele frequency (MAF)  $< 1\%$ . In parallel, data analysis was also performed using VariantStudio v2.2.1 (Illumina, San Diego, CA, USA). The pathogenicity of the variants was evaluated using Alamut v2.11 software (Interactive Biosoftware, Rouen, France), which includes Mutation Taster, Polyphen, Aling GVG and SIFT, and Varsome (Saphetor, Lausanne, Switzerland), which includes DANN, GERP, and MutationTaster. The effect of variants identified in splicing regions was evaluated using SpliceSiteFinder, MaxEntScan, NNSPLICE, GeneSplicer and Human Splicing Finder, also included in Alamut v2.11. The sequencing data were reanalyzed using the bioinformatics software ExomeDepth19 [123] to detect copy number variations (CNVs). The nomenclature and classification of variants was based on the Human Genome Variation Society (HGVS) guidelines (<https://www.hgvs.org/>) [124] and the American College of Medical Genetics and Genomics (ACMG) (<https://www.acmg.net/>) [125].

The high-throughput likely pathogenic variants were confirmed by Sanger sequencing and, when possible, familial segregation analyses were performed.

### **3.5.2.2. Statistical data analysis**

The percentage, median and range, and mean and standard deviation (SD) were used for the description of the variables. To calculate the sensitivity and specificity of the gene panel, cases of confirmed or highly probable PCD were considered as cases diagnosed with PCD. The Chi-squared test was used for comparison between adult and child patients, with a p-value  $< 0.05$  being statistically significant. Analyses were conducted using Med-Calc Statistical Software version 19.1.3 (MedCalc Software bvba, Ostende, Belgium).

### 3.5.3. WHOLE EXOME SEQUENCING

In highly-likely PCD patients with a negative gene panel result, WES was carried out. Peripheral blood DNA was prepared according to required specifications and sent to the specialized genomic center CNAG-CRG (*Centro Nacional de Análisis Genómico*, Barcelona, Spain). WES was performed with ExomeCapture-Seq capture Nimblegen SeqCap EZ MedExome + mtDNA 47Mb (Roche, Nimblegen) technology.

The analysis methods included Illumina Sequencing Analysis Viewer (Illumina), Illumina run specifications (Illumina), and a quality control alignment INS-017 with human reference genome GRCh (hg37).

Identified variants with  $\geq 1\%$  allele frequency described in population frequency databases (GnomAD [120], ExAC [121], 1000 genomes [122]) were rejected. The genes corresponding to the remaining variants ( $MAF \leq 1\%$ ) were checked with different databases (OMIM <https://www.omim.org/> [126], ClinVar <https://www.ncbi.nlm.nih.gov/clinvar/> [119], and GeneCards <https://www.genecards.org/> [127]) to identify candidate genes according to published data. The pathogenicity of the variants was checked with Varsome (Saphetor, Lausanne, Switzerland), which is based on the ACMG criteria for pathogenic classification of variants. It also offers other relevant data, such a report of most of *in silico* prediction tests. The sequencing data were reanalyzed using the bioinformatics software ExomeDepth19 [123] to detect any copy number variations (CNVs). The nomenclature and classification of variants were based on the HGVS [124] and ACMG guidelines [125].

The candidate variants were confirmed by Sanger sequencing and, when possible, familial segregation analyses were performed.

## 3.6. IMMUNOFLUORESCENCE TECHNIQUE AND ANALYSIS

### 3.6.1. PATIENTS

This study belongs to a prospective multicentric study including 74 consecutive patients with a clinical history suggestive of PCD during the period from 2016 to 2020. The majority of patients attended *Hospital Universitari Vall d'Hebron* (HUVH), and patients and samples from other

hospitals from Spain were also analyzed: *Hospital Sant Joan de Déu* (Esplugues de Llobregat, Barcelona), *Hospital del Mar* (Barcelona), *Hospital Parc Taulí* (Sabadell, Barcelona), *Hospital Germans Trias i Pujol* (Badalona, Barcelona), *Hospital Clínic* (Barcelona), *Hospital Miguel Servet* (Zaragoza), *Hospital Josep Trueta* (Girona), *Hospital Universitari Sant Joan de Reus* (Reus, Tarragona), *Consorci Sanitari de Terrassa* (Terrasa, Barcelona) and PCD group Valencia (*Hospital Universitario y Politécnico la Fe*, *Hospital Clínico Universitario de Valencia* and INCLIVA).

### 3.6.2. IMMUNOFLUORESCENCE TECHNIQUE AND ANALYSIS

Nasal-brush respiratory epithelial samples from a total of 74 patients were spread or dropped, air-dried and stored at -80°C until use. Cells were fixed with 4% paraformaldehyde (PFA) for 15 min at room temperature (RT), washed 4 times with 1xPBS, permeabilized with 0.2% TritonX100 for 10 min at RT, and blocked with 1% fat-free skim milk in PBS overnight at +4°C to avoid nonspecific binding. Samples were incubated with primary antibodies (all Sigma Aldrich, St. Louis, MO, USA) for 4 hours at RT using the following dilutions in 1% skim milk: anti-DNAH5 antibody 1:200, anti-DNAL1 1:100, anti-GAS8 1:200, anti-RSPH4A 1:200 and anti-RSPH9 1:70. Slides were washed 5 times with 1xPBS at RT (2 washes of 10 min), and all slides were incubated for 45 min at RT with 1:2500 anti-acetylated tubulin antibody (Sigma Aldrich) for cilia localization. After 5 more washes with 1xPBS at RT (2 washes of 10 min), cells were incubated 30 min at RT with secondary monoclonal anti-rabbit Alexa Fluor 594 and anti-mouse Alexa Fluor 488 antibodies (Thermo Fisher, Waltham, MA, USA). Nuclei DNA was stained with Prolong antifade DAPI (Thermo Fisher). Finally, slides were sealed with coverslides and kept at +4°C.

Slides were analyzed using fluorescence microscopy at X100 magnification. A minimum of ten cells were analyzed for each target protein. The results were considered: (1) normal or present when the protein was present in 8 or more cells, (2) absent or aberrant when the protein was completely absent in the ciliary axoneme or had an abnormal distribution in 8 or more cells, (3) inconclusive when results differed from previously described ones, and (4) insufficient when less than ten cells were observed. In inconclusive or insufficient cases, IF was repeated when possible, following recommendations by Shoemark *et al.* [105].

Patients were analyzed using antibodies against component proteins for the different structures of the ciliary axoneme: DNAH5 (an ODA component), DNALI1 (an IDA component), GAS8 (an N-DRC component) and either RS head component RSPH4A (42 patients), or RS head component RSPH9 (31 patients) or both (one patient). When this analysis was designed, we specifically chose and optimized these commercial antibodies so as to detect most cilia defects, following Shoemark *et al.* [105] and expert recommendations (consultations to experts from Prof Omran's group and from University of Leicester). Anti-acetylated tubulin antibody was used to localize the microtubule doublet (protein location shown in Figure 20).

#### **3.6.3. DATA ANALYSIS**

Confirmed and highly likely PCD cases were considered as positive for calculation of sensitivity and specificity. Data were analyzed by using MedCalc Statistical Software version 19.5.3 (MedCalc Software bvba, Ostend, Belgium).

## **4. RESULTS**





## 4.1. RESULTS I

### IMPLEMENTATION OF A GENE PANEL FOR GENETIC DIAGNOSIS OF PRIMARY CILIARY DYSKINESIA

Baz-Redón, N.; Rovira-Amigo, S.; Paramonov, I.; Castillo-Corullón, S.; Cols Roig, M.; Antolín, M.; García Arumí, E.; Torrent-Vernetta, A.; de Mir Messa, I.; Gartner, S.; Iglesias-Serrano, I.; Caballero-Rabasco, M. A.; Asensio de la Cruz, O.; Vizmanos-Lamotte, G.; Martín de Vicente, C.; Martínez-Colls, M<sup>a</sup> del M.; Reula, A.; Escribano, A.; Dasí, F.; Armengot-Carceller, M.; Polverino, E.; Amengual Pieras, E.; Amaro-Rodríguez, R.; Garrido-Pontnou, M.; Tizzano, E.; Camats-Tarruella, N.; Fernández-Cancio, M.; Moreno-Galdó, A. Implementation of a Gene Panel for Genetic Diagnosis of Primary Ciliary Dyskinesia. *Arch. Bronconeumol.* **2021**, *57(3)*, 186-194, doi:10.1016/j.arbres.2020.02.010.

**(Appendix I)**

Between January 2017 and November 2019, 79 patients from 74 different families (74 proband cases) and 37 family members were genetically studied. Out of the 79 patients, 26 were classified as very unlikely PCD and, in all of them, the genetic study result was negative.

Out of the 53 patients with confirmed or highly likely PCD, 35 were children and 18 were adults. Forty-three patients were Caucasian, four (7.5%) Moroccan, four (7.5%) Pakistani, one was from the Middle East, and one from Latin America. Ten patients had a family history of consanguinity (Table 2 and Table 3). The most common clinical manifestations were chronic wet cough and chronic rhinitis, and half of the series had a history of neonatal distress and 32.7% had *situs inversus*. The frequency of bronchiectasis was statistically significantly higher in adult patients (94.1%) than in pediatric patients (51.4%) (Table 2 and Table 3), whereas the PICADAR score was equal to or greater than 5 in 31 patients (65.9%) (Table 3).

The value of nNO could be determined in 35 cases, with an average value of 25.9 (SD 29.1) nL/min. In 25 patients, it was less than 33 nL/min and only in two it was over 77 nL/min (Table 3). HSVM and TEM findings are listed in Table 3. In 15 cases, the ultrastructural defects observed by TEM directly provided a PCD diagnostic. HSVM was highly indicative of PCD in 52 patients (not available in patient 3), with the following alterations being found: immotile cilia (n=18), immotile cilia with residual movement (n=12), mainly stiff cilia and disorganized ciliary

beat (n=8), hyperkinetic cilia (n=5), circular motion (n=6), disorganized ciliary beat (n=2), and reduced distal movement (n=1).

**Table 2: Clinical characteristics of patients with primary ciliary dyskinesia included in the study.**

	Total (n = 53)	Adults (n = 18)	Children (n = 35)	P <sup>2</sup>
Age	15.0 (1 – 42)	23.0 (18 – 42)	10 (1 – 17)	
Sex (women)	41.5%	33.3%	45.7%	0.391
Body mass index <sup>1</sup>		21 (16–28)	–1 (–2, –6)	
Origin (Caucasian)	81.1%	100%	71.4%	0.012
Consanguinity	18.9%	0%	28.6%	0.012
<i>Situs inversus</i>	32.7%	17.6%	40.0%	0.103
Neonatal distress	50%	57.1%	47.0%	0.061
Chronic rhinitis	90.2%	87.5%	91.4%	0.121
Chronic cough	94.2%	94.1%	94.3%	0.371
Sinusitis	23.5%	56.2%	8.6%	<0.001
Recurrent otitis	52.9%	62.5%	48.6%	0.088
Recurrent bronchitis	47.1%	75%	34.3%	0.002
Recurrent pneumonia	25.0%	41.2%	17.1%	0.066
Bronchiectasis	65.4%	94.1%	51.4%	0.004

Data are expressed as median and range (in brackets) for quantitative variables (age, body mass index) and as a percentage for qualitative variables.

<sup>1</sup>Body mass index is expressed as kg/m<sup>2</sup> in adults and as Z-score in children.

<sup>2</sup>A p-value ≤0.05 is statistically significant.

DNA samples were sequenced using our gene panel, which covered 98.75% of the exons and flanking intronic areas of the 44 genes included (Table 1). The average coverage of the results was 600x with 80.7% reads on target.

Candidate gene variants were detected in 81.1% (43/53) of patients with suspected PCD, with 22 (51.2%) homozygous and 21 (48.8%) compound heterozygous variants. In 18.9% (10/53) of the patients, no variant that could explain the phenotype was detected (Table 4). The sensitivity of the technique was 81.1% (95% CI, 68.0%–90.6%) and specificity was 100% (95% CI, 86.8%–100%). The area under the ROC curve was 0.91 (95% CI, 0.82–0.96). A recent revision of PCD prevalence (confirmed or highly likely cases) of patients referred for clinical suspicion in the last 4 years was 27.4% (non-published data, data not shown). Considering this prevalence, genetic testing predictive value would be 100% and negative predictive value 93.3% (95% CI 88.9–96.1 %).

A total of 52 different variants were detected (1 in *ARMC4*, 1 in *CCDC114*, 1 in *CCDC151*, 8 in *CCDC39*, 3 in *CCDC40*, 14 in *DNAH5*, 2 in *DNAH9*, 8 in *DNAH11*, 4 in *DNAI2*, 1 in *RPGR*, 3 in *RSPH1*, 1 in *RSPH4A*, 1 in *RSPH9*, 2 in *SPAG1*, and 2 in *TTC25*) (Table 4). Sixteen of these had previously been associated with PCD [10,11,132,20,22,25,90,128–131] and 36 had not been

previously described in literature (Table 4). Besides, 14 (26.9%) were nonsense variants, 13 (25%) were frameshift, 13 (25%) splicing, 9 (17.3%) missense, and 3 (5.8%) CNVs. Overall, 51.9% (27/52) were classified as pathogenic (including the 3 CNVs), 21.2% (11/52) as likely pathogenic, and 26.9% (14/52) as VUS, according to the ACMG classification (Table 4). The most frequently described variant in our cohort belongs to *RSPH1*: c.85G>T/p.Glu39Ter detected in four patients (patients 33, 34, 35 and 36) out of five patients with variants in this gene. This *RSPH1* variant was detected in homozygosity, and in compound heterozygosity in patient 36 with the splicing variant c.275-2A>C.

**Table 3: Epidemiological and clinical data of the patients included in the genetic study.**

Patient	Consanguinity/ Family	Gender	Age (years-old)	PICADAR#	Neonatal distress	Rhinitis	Sinusitis	Wet cough	Repeated otitis	Repeated pneumonia	Repeated bronchitis	Bronchiectasis	<i>Situs inversus</i>	nNO (nl/min)	HSV1	TEM	Affected gene
1 <sup>a</sup>	N	M	25	7	Y	Y	N	Y	N	N	Y	Y	N	3.9	I	ODA+IDA	<i>ARMC4</i>
2 <sup>a</sup>	N	M	22	5	N	N	N	Y	Y	N	Y	N	N	-	I, RM	ODA+IDA	<i>CCDC114</i>
3 <sup>a</sup>	N	F	15	9	Y	N	N	N	N	N	N	N	Y	-	-	ODA	<i>CCDC151</i>
4 <sup>a</sup>	N	M	3	7	Y	Y	N	Y	N	N	N	N	N	-	I	-	<i>CCDC39</i>
5 <sup>a</sup>	N	M	18	6	Y	Y	Y	Y	N	N	N	Y	N	-	I	-	<i>CCDC39</i>
6 <sup>a</sup>	N	M	10	8	N	Y	N	Y	N	N	N	Y	Y	67.7	S, D	-	<i>CCDC39</i>
7 <sup>a</sup>	N	M	16	10	N	Y	N	Y	N	N	N	Y	Y	34.9	S, D	IDA	<i>CCDC39</i>
8 <sup>a</sup>	N	M	15	8	N	Y	N	Y	N	N	N	Y	Y	14.6	S, D, RM	-	<i>CCDC39</i>
9 <sup>a</sup>	N	F	21	5	Y	N	N	Y	N	N	Y	Y	N	-	I		<i>CCDC39</i>
10 <sup>a</sup>	N	M	19	10	Y	Y	N	Y	N	Y	Y	Y	Y	-	S, D, RM	IDA	<i>CCDC39</i>
11 <sup>a</sup>	Y	M	12	8	N	Y	N	Y	Y	N	Y	N	Y	1.65	S, D	IDA+MTD	<i>CCDC40</i>
12	Y/ sib. of 11	F	1	7	Y	Y	N	Y	N	N	N	N	N	-	S, D	IDA+MTD	<i>CCDC40</i>
13 <sup>a</sup>	N	F	16	8	N	Y	N	Y	N	N	N	N	Y	44.5	S, D, RM	ODA+IDA	<i>CCDC40</i>
14 <sup>a</sup>	N	F	14	4	Y	N	N	Y	Y	N	N	Y	N	17.2	I	ODA+IDA	<i>DNAH5</i>
15	N/ sib. of 14	F	17	4	N	Y	N	Y	Y	N	Y	Y	N	15.2	I, RM	-	<i>DNAH5</i>
16 <sup>a</sup>	N	F	10	4	N	Y	N	Y	Y	N	N	N	N	3.5	I	-	<i>DNAH5</i>
17 <sup>a</sup>	N	M	5	9	Y	N	N	N	Y	N	N	N	Y	-	I	-	<i>DNAH5</i>
18 <sup>a</sup>	N	M	17	8	N	Y	N	Y	N	N	N	Y	Y	6	I, RM	-	<i>DNAH5</i>
19 <sup>a</sup>	N	M	8	8	Y	Y	N	Y	N	N	Y	Y	Y	5.5	I, RM	-	<i>DNAH5</i>
20 <sup>a</sup>	N	M	20	4	N	Y	N	Y	Y	N	Y	Y	N	-	I	-	<i>DNAH5</i>
21 <sup>a</sup>	N	M	35	10	Y	Y	Y	Y	Y	Y	Y	Y	Y	4.7	I	-	<i>DNAH5</i>

Table 3 (continued)

22 <sup>a</sup>	Y	F	8	6	Y	Y	N	Y	Y	Y	Y	Y	N	-	I	-	<i>DNAH5</i>
23 <sup>a</sup>	N	F	15	4	N	Y	N	Y	N	N	N	N	N	-	Distal RM	-	<i>DNAH9</i>
24 <sup>a</sup>	N	M	3	11	Y	Y	N	Y	N	N	N	N	Y	15.01	HK	-	<i>DNAH11</i>
25 <sup>a</sup>	N	F	24	-	-	Y	Y	Y	Y	N	Y	Y	N	42.57	HK, S	-	<i>DNAH11</i>
26 <sup>a</sup>	Y	M	2	7	Y	Y	N	Y	N	N	Y	N	N	-	HK	-	<i>DNAH11</i>
27 <sup>a</sup>	N	M	19	4	N	Y	Y	Y	Y	N	Y	Y	N	4.3	HK	-	<i>DNAH11</i>
28 <sup>a</sup>	Y	F	6	4	N	Y	N	Y	N	Y	N	N	N	-	I	ODA	<i>DNAI2</i>
29	Y/ sib. of 28	M	10	6	Y	Y	N	Y	N	N	N	Y	N	14.2	I	ODA	<i>DNAI2</i>
30 <sup>a</sup>	N	M	17	8	N	Y	Y	Y	Y	N	Y	Y	Y	-	I	-	<i>DNAI2</i>
31 <sup>a</sup>	N	M	3	8	N	Y	N	Y	N	N	Y	N	Y	-	I	-	<i>DNAI2</i>
32 <sup>a</sup>	N	M	15	6	Y	Y	N	Y	Y	Y	Y	Y	N	52.6	HK	-	<i>RPGR</i>
33 <sup>a</sup>	N	F	42	4	N	Y	Y	N	Y	N	N	Y	N	67.3	C	CP	<i>RSPH1</i>
34 <sup>a</sup>	N	M	17	4	N	Y	N	Y	Y	N	N	Y	N	15.9	C	-	<i>RSPH1</i>
35	N/ sib. of 34	M	12	6	Y	Y	N	Y	N	N	N	N	N	47.8	C	-	<i>RSPH1</i>
36 <sup>a</sup>	N	F	27	5	Y	Y	N	Y	N	Y	N	Y	N	10	I, RM	-	<i>RSPH1</i>
37 <sup>a</sup>	N	M	21	4	Y	Y	Y	Y	N	Y	Y	Y	N	100	I, RM	-	<i>RSPH1</i>
38 <sup>a</sup>	Y	M	4	3	N	Y	N	Y	N	N	N	N	N	-	C	-	<i>RSPH4A</i>
39	Y/ sib. of 38	F	7	8	Y	Y	N	Y	Y	N	N	N	N	-	C	-	<i>RSPH4A</i>
40 <sup>a</sup>	Y	F	9	4	N	Y	N	Y	Y	N	N	Y	N	5.4	C	-	<i>RSPH9</i>
41 <sup>a</sup>	N	M	20	-	-	-	-	-	-	-	-	-	-	14.3	S, I, RM	-	<i>SPAG1</i>
42 <sup>a</sup>	N	M	16	10	Y	Y	N	Y	Y	N	N	N	Y	-	I, RM	ODA+IDA	<i>TTC25</i>
43 <sup>a</sup>	N	F	10	-	N	Y	N	Y	N	N	N	Y	Y	2.3	I	-	<i>TTC25</i>
44 <sup>a</sup>	N	F	12	6	Y	Y	N	Y	Y	N	Y	Y	N	128.7	D	-	-
45 <sup>a</sup>	N	F	9	4	N	Y	N	Y	Y	N	N	Y	N	15.8	S, D	-	-
46 <sup>a</sup>	N	M	25	4	N	Y	Y	Y	Y	Y	Y	Y	N	14.8	I, RM	Normal	-
47 <sup>a</sup>	N	F	15	-	-	Y	Y	Y	Y	Y	Y	Y	N	50.2	I, RM	-	-
48 <sup>a</sup>	N	F	18	4	N	Y	Y	Y	Y	Y	N	Y	N	3.5	I	-	-

Table 3 (continued)

49 <sup>a</sup>	N	F	32	-	-	Y	Y	Y	Y	N	Y	Y	Y	11.4	I, RM	-	-
50 <sup>a</sup>	N	M	32	-	-	-	-	Y	-	Y	-	Y	N	24.3	I, RM	-	-
51 <sup>a</sup>	N	F	8	4	N	Y	N	Y	Y	Y	Y	N	N	25.8	D	ODA+IDA	-
52 <sup>a</sup>	N	M	28	6	Y	Y	N	Y	Y	Y	Y	Y	N	14.6	I	-	-
53 <sup>a</sup>	N	M	17	6	Y	Y	Y	Y	Y	Y	Y	Y	N	5.1	I	-	-

<sup>a</sup>: proband patients; -: missing data; nNO: nasal nitric oxide; HSVM: high-speed video-microscopy; TEM: transmission electron microscopy; sib.: sibling; M: Male; F: female; Y: yes; N: no; #: PICADAR score following Behan *et al.* 2016 [79]; I: immotile cilia; RM: residual movement; S: stiff cilia; D: disorganized ciliary beat; HK: hyperkinetic cilia; C: circular movement of cilia; ODA: absence of outer dynein arm; IDA: absence of inner dynein arm; MTD: microtubular disorganization.

**Table 4: Results of the genetic study of patients with described variants that correlate with their phenotype.**

Patient	Origin	Consanguinity/ family	Gene	Zygoty	cDNA change	Protein change	Mutation type	ACMG classification	Familial cosegregation	Other family members affected	References
1 <sup>a</sup>	Caucasian	N	<i>ARMC4</i>	hom	c.1669G>T	p.Glu557Ter	nonsense	P	NA	-	Hjeij [11]
2 <sup>a</sup>	Caucasian	N	<i>CCDC114</i>	hom	c.1391+5G>A	-	splicing	VUS	Mo(+), Fa(+)	-	Knowles [10]
3 <sup>a</sup>	Caucasian	NA	<i>CCDC151</i>	hom	c.410G>A	p.Trp137Ter	nonsense	LP	Mo(+), Fa(+)	-	ND
4 <sup>a</sup>	Caucasian	N	<i>CCDC39</i>	comp. het	c.357+1G>C	-	splicing	P	Fa(+)	-	Merveille [20]
					c.2505_2506delCA	p.His835GlnfsTer4	frameshift	LP	Mo(+)	ND	
5 <sup>a</sup>	Caucasian	N	<i>CCDC39</i>	hom	c.2250delT	p.Gln751LysfsTer11	frameshift	LP	Mo(+), Fa(+)	-	ND
6 <sup>a</sup>	Caucasian	N	<i>CCDC39</i>	hom	c.610-2A>G	-	splicing	P	NA	-	Merveille [20]
7 <sup>a</sup>	Caucasian	N	<i>CCDC39</i>	comp. het	c.547_548delTT	p.Leu183GlyfsTer3	frameshift	LP	NA	-	ND
					c.1528-2A>G	-	splicing	P	ND		
8 <sup>a</sup>	Caucasian	N	<i>CCDC39</i>	comp. het	c.216_217delTT	p.Cys73GlnfsTer6	frameshift	LP	Fa(+)	-	Merveille [20]
					c.357+1G>C	-	splicing	P	Fa(-)	Merveille [20]	
9 <sup>a</sup>	Caucasian	N	<i>CCDC39</i>	hom	c.357+1G>C	-	splicing	P	Fa(+)	-	Merveille [20]
10 <sup>a</sup>	Caucasian	N	<i>CCDC39</i>	comp. het	c.547_548delTT	p.Leu183GlyfsTer3	frameshift	LP	NA	-	ND
					c.2596G>T	p.Glu866Ter	nonsense	P	Antony [22]		
11 <sup>a</sup>	Pakistani	Y	<i>CCDC40</i>	hom	c.1416delG	p.Ile473PhefsTer2	frameshift	P	Mo(+), Fa(+)	Affected sister/ brother (+)	Antony [22]
12	Pakistani	Y/ sib. of 11	<i>CCDC40</i>	hom	c.1416delG	p.Ile473PhefsTer2	frameshift	P	Mo(+), Fa(+)	Affected brother/ Brother (+)	Antony [22]
13 <sup>a</sup>	Caucasian	N	<i>CCDC40</i>	comp. het	c.2T>G	p.Met1Arg	missense	LP	Fa(+)	-	ND
					526-pb del inc. ex.8 and ex.9	-	CNV	P	Mo(+)	ND	
14 <sup>a</sup>	Caucasian	N	<i>DNAH5</i>	comp. het	c.12706-2A>T	-	splicing	P	Fa(+)	Affected sister	Baz-Redón [128]
					c.4625_4628delGAGA	p.Arg1542ThrfsTer6	frameshift	LP	Mo(+)	Baz-Redón [128]	



Table 4 (continued)

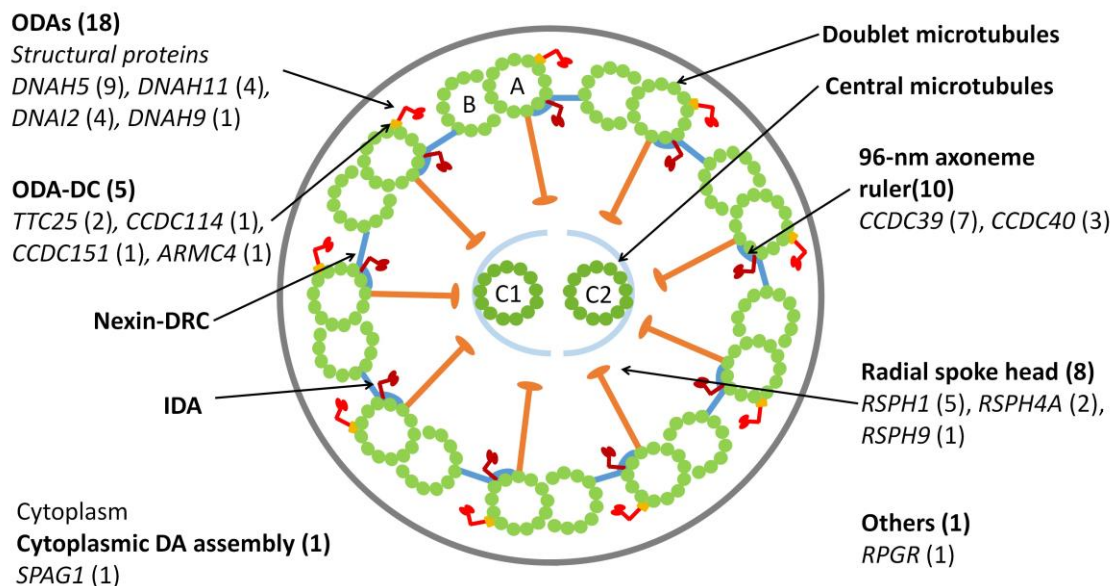
15	Caucasian	N/ sib. of 14	<i>DNAH5</i>	comp. het	c.12706-2A>T	-	splicing	P	Fa(+)	Affected sister	Baz-Redón [128]
					c.4625_4628delGAGA	p.Arg1542ThrfsTer6	frameshift	LP	Mo(+)		Baz-Redón [128]
16 <sup>a</sup>	Caucasian	N	<i>DNAH5</i>	comp. het	c.11761G>C	p.Gly3921Arg	missense	VUS	NA	-	ND
					c.13060delG	p.Ala4354ArgfsTer23	frameshift	P			Olm [131]
17 <sup>a</sup>	Caucasian	N	<i>DNAH5</i>	comp. het	c.2283_2284delAG	p.Arg761SerfsTer10	frameshift	P	Fa(+)	-	ND
					c.3861T>G	p.Tyr1287Ter	nonsense	P	Mo(+)		ND
18 <sup>a</sup>	Caucasian	N	<i>DNAH5</i>	comp. het	c.8311C>T	p.Arg2771Cys	missense	VUS	Mo(+)	-	ND
					c.10615C>T	p.Arg3539Cys	missense	VUS	Mo(-)		Faily [132]
19 <sup>a</sup>	Caucasian	N	<i>DNAH5</i>	comp. het	c.10813G>A	p.Asp3605Asn	missense	VUS	Fa(-)	-	Raidt [90]
					3.2-kb del inc. ex.2 and ex.3	-	CNV	P	Fa(+)		ND
20 <sup>a</sup>	Caucasian	N	<i>DNAH5</i>	hom	c.13486C>T	p.Arg4496Ter	nonsense	P	Mo(+)	-	Hornef [129]
21 <sup>a</sup>	Caucasian	N	<i>DNAH5</i>	comp. het	c.2575A>T	p.Lys859Ter	nonsense	P	NA	Son(+)	ND
					c.9730G>T	p.Glu3244Ter	nonsense	P			ND
22 <sup>a</sup>	Caucasian	Y	<i>DNAH5</i>	hom	3.3-kb del inc. ex.29 and ex.30	-	CNV	P	NA	-	ND
23 <sup>a</sup>	Caucasian	N	<i>DNAH9</i>	comp. het	c.7822-1G>A	-	splicing	P	NA	-	ND
					c.8992C>T	p.Gln2998Ter	nonsense	P			ND
24 <sup>a</sup>	Caucasian	N	<i>DNAH11</i>	comp. het	c.12507+1G>C	-	splicing	P	Paternal grandmother (+)	-	ND
					c.13412_13415dupAAAC	p.Lys4473AsnfsTer11	frameshift	LP	Maternal grandmother (+)		ND
25 <sup>a</sup>	Caucasian	N	<i>DNAH11</i>	comp. het	c.927_931delTAAAC	p.Ser312LeufsTer66	frameshift	LP	NA	-	ND
					c.7645+5G>A	-	splicing	VUS			ND
26 <sup>a</sup>	Arab	Y	<i>DNAH11</i>	comp. het	c.983-1G>T	-	splicing	P	NA	-	ND
					c.3439C>T	p.Gln1147Ter	nonsense	P			ND

Table 4 (continued)

27 <sup>a</sup>	Caucasian	N	<i>DNAH11</i>	comp. het	c.3898C>T c.6983+1G>A	p.Gln1300Ter -	nonsense splicing	P P	NA	-	ND ND
28 <sup>a</sup>	Pakistani	Y	<i>DNAI2</i>	hom	c.546C>A	p.Tyr182Ter	nonsense	P	Mo(+), Fa(+)	Affected brother	Rudilla [133]
29	Pakistani	Y/ sib. of 28	<i>DNAI2</i>	hom	c.546C>A	p.Tyr182Ter	nonsense	P	Mo(+), Fa(+)	Affected sister	Rudilla [133]
30 <sup>a</sup>	Caucasian	N	<i>DNAI2</i>	hom	c.346-3T>G	-	splicing	VUS	NA	-	Loges [130]
31 <sup>a</sup>	Caucasian	N	<i>DNAI2</i>	comp. het	c.184-14G>A c.740G>A	- p.Arg247Gln	splicing missense	VUS VUS	Fa(+) Mo(+)	-	ND ND
32 <sup>a</sup>	Caucasian	N	<i>RPGR</i>	hom	c.920C>A	p.Thr307Lys	missense	VUS	NA	-	ND
33 <sup>a</sup>	Caucasian	N	<i>RSPH1</i>	hom	c.85G>T	p.Glu29Ter	nonsense	P	NA	-	Kott [25]
34 <sup>a</sup>	Caucasian	N	<i>RSPH1</i>	hom	c.85G>T	p.Glu29Ter	nonsense	P	NA	Affected brother	Kott [25]
35	Caucasian	N / sib. of 34	<i>RPSH1</i>	hom	c.85G>T	p.Glu29Ter	nonsense	P	NA	Affected brother	Kott [25]
36 <sup>a</sup>	Caucasian	N	<i>RSPH1</i>	comp. het	c.85G>T c.275-2A>C	p.Glu29Ter -	nonsense splicing	P P	NA	-	Kott [25] Kott [25]
37 <sup>a</sup>	Caucasian	N	<i>RSPH1</i>	comp. het	c.70C>T c.275-2A>C	p.Arg24Trp -	missense splicing	VUS P	NA	-	ND Kott [25]
38 <sup>a</sup>	Moroccan	Y	<i>RSPH4A</i>	hom	c.1453C>T	p.Arg485Ter	nonsense	P	NA	Affected sister	ND
39	Moroccan	Y/ sib. of 38	<i>RSPH4A</i>	hom	c.1453C>T	p.Arg485Ter	nonsense	P	NA	Affected brother	ND
40 <sup>a</sup>	Moroccan	Y	<i>RSPH9</i>	hom	c.293_294delTG	p.Val98GlyfsTer14	frameshift	LP	NA	-	ND
41 <sup>a</sup>	Caucasian	N	<i>SPAG1</i>	comp. het	c.583delA c.1855G>C	p.Ile195Ter p.Asp619His	nonsense missense	LP VUS	Mo(+) Mo(-)	-	ND ND
42 <sup>a</sup>	Caucasian	N	<i>TTC25</i>	hom	c.244delA	p.Lys82ArgfsTer29	frameshift	VUS	Mo(+), Fa(+)	Sister (+)	ND
43 <sup>a</sup>	Moroccan	N	<i>TTC25</i>	hom	c.655_659delCTGAC	p.Leu219CysfsTer62	frameshift	VUS	Mo(+), Fa(+)	-	ND

<sup>a</sup>:Proband patients; -: missing or no data; ACMG: American College of Medical Genetics; Y: yes; N: no; sib.: sibling; comp.:compound; het: heterozygous; hom: homozygous; del: deletion; inc.: including; ex.: exon; bp: base pairs; kb: kilobases; NA: no data available; Fa: father; Mo:mother; (+):carrier; (-): non carrier; P: pathogenic; LP: likely pathogenic; CNV: copy number variation; VUS: variant of uncertain significance; ND: non-described variant.

Eighteen patients presented variants in genes related to structural proteins of the ODA (*DNAH5* [n=9], *DNAH11* [n=4], *DNAI2* [n=4], *DNAH9* [n=1]), five related to the ODA docking complex (*TTC25* [n=2], *CCDC114* [n=1], *CCDC151* [n=1], *ARMC4* [n=1]) and eight showed variants in genes encoding RS proteins (*RSPH1* [n=5], *RSPH4A* [n=2], *RSPH9* [n=1]) (Figure 23, Table 4). Besides, ten patients carried variants in genes encoding axoneme regulatory complex proteins (*CCDC39* [n=7], *CCDC40* [n=3]); one patient presented variants in *SPAG1*, which encodes a protein probably related to the transport or cytoplasmic DNAAF, and one had variants in *RPGR*, a gene associated with retinitis pigmentosa (Figure 23, Table 4). The variants in the three most frequent genes (*DNAH5*, *CCDC39* and *RSPH1*) occurred only in patients of Caucasian origin. In patients of non-Caucasian origin, the most common causative genes were *CCDC40*, *DNAI2* and *RSPH4A*, with two cases each.



**Figure 23: Cross-sectional diagram of a respiratory cilium showing its structural components and genes in which variants have been found.** The number of patients with variants in each gene is shown in parentheses. ODA: outer dynein arm; DC: docking complex; DRC: dynein regulator complex; IDA: inner dynein arm; DA: dynein arm.

Thirty-seven family members from 22 different families have been tested using the gene panel. All analyzed parents (18 different families) were carriers of some of the variants detected in their children. DNA from the paternal grandparents and the maternal grandmother of patient 24 was analyzed and the variant c.12507+1G>C was determined to be of paternal origin, while the variant c.13412\_13415dupAAAC was of maternal origin (Table 4).

## 4.2. RESULTS II

### IMMUNOFLUORESCENCE ANALYSIS AS A DIAGNOSTIC TOOL IN A SPANISH COHORT OF PATIENTS WITH SUSPECTED PRIMARY CILIARY DYSKINESIA

Baz-Redón, N.; Rovira-Amigo, S.; Fernández-Cancio, M.; Castillo-Corullón, S.; Cols, M.; Caballero-Rabasco, M.A.; Asensio, Ó.; Martín de Vicente, C.; Martínez-Colls, M<sup>a</sup> del M.; Torrent-Vernetta, A.; de Mir-Messa, I.; Gartner, S.; Iglesias-Serrano, I.; Díez-Izquierdo, A.; Polverino, E.; Amengual-Pieras, E.; Amaro-Rodríguez, R.; Vendrell, M.; Mumany, M.; Pascual-Sánchez, M<sup>a</sup> T.; Pérez-Dueñas, B.; Reula, A.; Escribano, A.; Dasí, F.; Armengot-Carceller, M.; Garrido-Pontnou, M.; Camats-Tarruella, N.; Moreno-Galdó, A. Immunofluorescence Analysis as a Diagnostic Tool in a Spanish Cohort of Patients with Suspected Primary Ciliary Dyskinesia. *J. Clin. Med.* **2020**, *9*, 3603, doi:10.3390/jcm9113603.

#### (Appendix II)

An immunofluorescence analysis was performed in a cohort of 74 PCD-suspected patients. Sixty-six percent of patients included in this study were <18 years old (49/74) and the mean age at study was 17.9 years (range 1–63) (Table 5).

**Table 5: Immunofluorescence results from 74 PCD-suspected patients related to the results of the PCD diagnostic evaluation.**

Immunofluorescence test outcome (n=74)	PCD diagnostic evaluation			
	Confirmed (n=25)	Highly likely (n=25)	Highly unlikely (n=24)	
Evaluable/Closed	68 (91.9%)	24	24	20
Normal results (all markers present)	35 (47.3%)	3	12	20
Absent/aberrant results	33 (44.6%)	21	12	0
DNAH5 (-) (ODA)	15			
Proximal DNAH5 (ODA)	3			
DNAH5 (-), DNALI1 (-) (ODA+IDA)	3			
DNALI1 (-), GAS8 (-) (IDA+Nexin-DRC)	7			
GAS8 (-) (Nexin-DRC)	1			
RSPH9 (-) (Radial spoke)	3			
RSPH4A (-) (Radial spoke)	1			
Inconclusive/insufficient results	6 (8.1%)	1	1	4

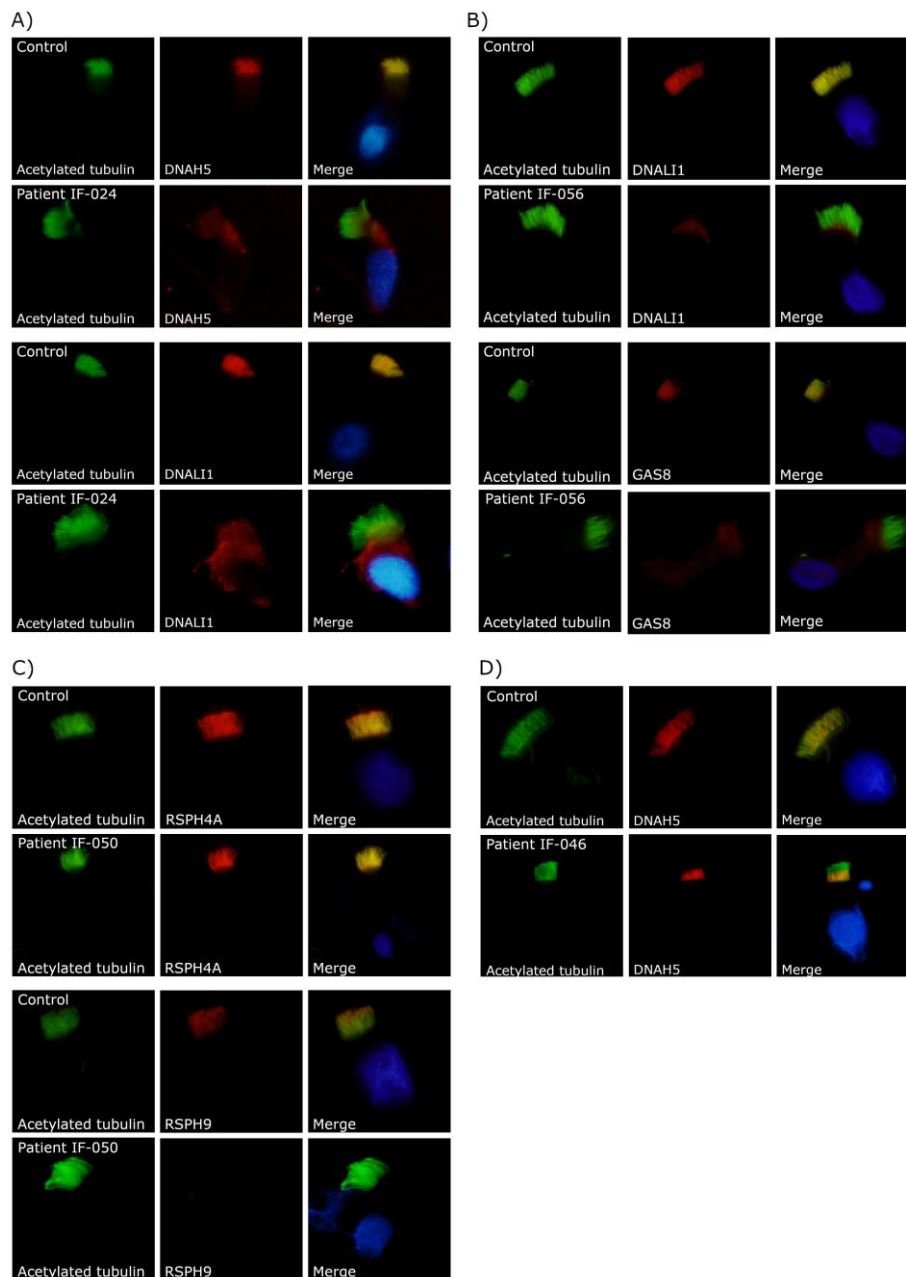
(-): absent in ciliary axoneme; ODA: outer dynein arm; IDA: inner dynein arm; DRC: dynein regulatory complex

After PCD diagnostic evaluation of these patients, 25 of them were considered as confirmed PCD, 25 as highly likely and 24 as highly unlikely PCD (Table 5).

IF was technically evaluable for all tested antibodies in 68 patients (91.9%), whereas in six, the results were inconclusive/insufficient (8.1%) (Table 5). IF analysis demonstrated an absence or aberrant location of one or more proteins in the ciliary axoneme in 33 cases: 15 patients presented absent DNAH5; 3 a proximal localization of DNAH5 in ciliary axoneme; 3 patients exhibited absent DNAH5 and DNALI1; 7 showed absent DNALI1 and a cytoplasmic localization of GAS8; 1 patient presented absent GAS8; 3 showed absent RSPH9; and 1 had absent RSPH4A (Table 5). Figure 24 shows examples of absence/aberrant location of IF markers in four patients with confirmed PCD.

To evaluate the usefulness of IF analysis as a tool for PCD diagnosis, IF results were compared with those obtained from our PCD gene panel and HSVM analyses (Table 6). The 33 patients with aberrant/absent ciliary-axoneme proteins had been diagnosed with confirmed or highly likely PCD. All of them presented a concordant abnormal HSVM and 21 of them presented likely pathogenic variants in PCD-related genes (Table 6). The relation of these abnormal IF results with clinical characteristics and other PCD diagnostic tests for each patient is shown in Table 7.

Thirty-five patients had normal distribution or presence of all IF antibodies. The clinical characteristics and results of PCD diagnostic tests for each patient with normal IF are presented in Table 8. We confirmed PCD in three of these patients because they presented likely pathogenic variants in *DNAH11* and hyperkinetic stiff cilia by HSVM (Tables 6 and 8). Another patient presented two variants in *SPAG1*, but there was no concordance with HSVM and IF results (Table 8). Other 11 patients presented normal IF, but abnormal HSVM results together with typical PCD symptoms, so they were considered highly likely PCD (Table 8). Thus far, we have not detected any likely pathogenic genetic variant in these patients. Finally, 20 out of the 33 patients with normal IF were considered highly unlikely to have PCD because of weak clinical history, normal or mild HSVM results and/or negative genetics (Table 8).



**Figure 24: Example results of immunofluorescence technique in control subjects and patients with primary ciliary dyskinesia.** The first column shows cilia stained with anti-acetylated  $\alpha$ -tubulin (green); the second column shows the protein of interest (red); and the third column shows the final merged image with the nuclei stained with DAPI (blue). **A)** Patient IF-024 exhibited absent DNAH5 and DNALI1. **B)** Patient IF-056 had absent DNALI1 and cytoplasmic localization of GAS8. **C)** Patient IF-050 showed a normal axonemal localization of RSPH4A and absent RSPH9. **D)** Patient IF-046 presented a proximal localization of DNAH5.

It should be mentioned that six (8.1%) samples were not technically evaluable by our IF panel: two cases lacked enough cells to analyze and were considered insufficient; two cases remained inconclusive for one or more antibodies; and two cases resulted in being insufficient for some markers and inconclusive for others (Table 9). Only one patient with insufficient and inconclusive IF sample was diagnosed with PCD because of presenting stiff cilia by HSVM and concurring likely pathogenic variants in *CCDC39*. Among the other cases, four were finally regarded as not having PCD or unlikely to have PCD because of normal or mild HSVM results (Table 9).

Based on all previous results, IF analysis as a diagnostic test for PCD had a sensitivity of 68.8% (95% CI 53.7–81.3%) and a specificity of 100% (95% CI 83.2–100%). In our laboratory, the PCD prevalence (confirmed or highly likely cases) of patients referred for clinical suspicion in the last 4 years was 27.4% (non-published data, data not shown). Considering this prevalence, IF positive predictive value would be 100% and negative predictive value 89.4% (95% CI 84.8–92.8%).

**Table 6: Relation among immunofluorescence analysis, high-speed video-microscopy, genetics, and clinical characteristics in our PCD patients.**

IF affected markers (ultrastructural part)	#	HSVM	Genetics (#)	PCD symptoms					
				Neonatal distress	Upper respiratory tract	Lower respiratory tract	Bronchiectasis	Chronic ear or hearing	<i>Situs</i> abnormality
DNAH5 (ODA)	15	Completely immotile cilia or residual motility	<i>CCDC151</i> (1), <i>DNAH5</i> (5), <i>DNAI2</i> (4), <i>TTC25</i> (1)	+/-	+/-	+/-	+/-	+/-	+/-
Proximal DNAH5 (ODA)	3	Subtle defects (stiff and disorganized ciliary beat)	<i>DNAH9</i> (1)	-	+	+/-	+/-	+/-	+/-
DNAH5+DNALI1 (ODA+IDA)	3	Completely immotile cilia	NA	+	+	+/-	+	+	+/-
DNALI1+GAS8 (IDA+Nexin-DRC)	7	Mainly stiff cilia and immotile cilia	<i>CCDC39</i> (3), <i>CCDC40</i> (3)	+/-	+	+/-	+/-	+/-	+/-
GAS8 (Nexin-DRC)	1	Hyperkinetic stiff cilia	NA	+	+	-	+	+	-
RSPH4A or RSPH9 (radial spoke)	4	Stiff and circular motion	<i>RSPH1</i> (1), <i>RSPH4A</i> (1), <i>RSPH9</i> (1)	+/-	+	+/-	+/-	+/-	-
All markers present (normal result)	3	Hyperkinetic stiff cilia	<i>DNAH11</i> (3)	+/-	+	+/-	+/-	+/-	+/-

IF: immunofluorescence; #: number of patients; HSVM: high-speed video-microscopy; ODA: outer dynein arm; IDA: inner dynein arm; DRC: dynein regulatory complex; NA: no genetic data available; +: symptoms present in all patients; -: symptoms absent in all patients; +/-: symptoms present in some patients.



**Table 7: Patients with absence or aberrant distribution of target proteins by immunofluorescence and correlation with other PCD-analysis techniques.**

Patient #	YOB/Gender/Origin/ Consanguinity/Family	PICADAR score [79]/PCD symptoms	nNO (nl/min)	Affected IF markers	HSVM	TEM	Genetics	Diagnosis [77] - Next step	Patient# in Baz-Redón <i>et al.</i> 2021 [134]
IF-009	2002/M/Caucasian/N	6/Neonatal distress. Chronic rhinitis and wet cough. Sinusitis. Recurrent otitis and hearing loss. Recurrent bronchitis and pneumonia. Bronchiectasis. Persistent atelectasis.	5.1	DNAH5-, DNALI1-	Completely immotile	NA	Negative	Highly likely PCD - WES	53
IF-013	2016/M/Caucasian/N	8/Chronic rhinitis and wet cough. Recurrent bronchitis. <i>Situs inversus</i> .	NA	DNAH5-	Completely immotile	NA	<i>DNAI2</i> (c.184-14G>A het. + c.740G>A/p.Arg247Gln het.)	Confirmed PCD <i>DNAI2</i>	31
IF-015	2006/M/Caucasian/N	8/Chronic rhinitis and wet cough. Bronchiectasis. <i>Situs inversus</i> .	67.7	DNALI1-, GAS8-	Mainly stiff	NA	<i>CCDC39</i> (c.610-2A>G hom.)	Confirmed PCD <i>CCDC39</i>	6
IF-021	2007/M/Pakistan/Y/sib. of IF-056, IF-057	8/Chronic rhinitis and wet cough. Recurrent otitis. Hearing loss. Recurrent bronchitis and pneumonia. Heterotaxy.	6.4	DNALI1-, GAS8-	Mainly stiff	NA	<i>CCDC40</i> (c.1416delG/p.Ile473PhefsTer2 hom.)	Confirmed PCD <i>CCDC40</i>	11
IF-024	1991/M/Caucasian/N	6/Neonatal distress. Chronic rhinitis and wet cough. Recurrent otitis and hearing loss. Recurrent bronchitis. Bronchiectasis.	14.6	DNAH5-, DNALI1-	Completely immotile	Loss 30% ODA and 70% IDA	Negative	Highly likely PCD - WES	52

Table 7 (continued)

IF-025	1964/M/Caucasian/NA	?/Wet cough. Bronchiectasis. Infertility.	112.8	RSPH9-	Stiff	NA	NA	Highly likely PCD - Genetics	
IF-031	1992/F/Caucasian/N	5/Neonatal distress. Chronic rhinitis and wet cough. Recurrent pneumonia. Bronchiectasis.	10	RSPH9-	Stiff	Loss 40% ODA and 80% IDA	<i>RSPH1</i> (c.85G>T/p.Glu29Ter het. + c.275-2A>C het.)	Confirmed PCD <i>RSPH1</i>	36
IF-040	2006/F/Moroccan/N	?/Chronic rhinitis and wet cough. Bronchiectasis. <i>Situs inversus</i> .	2.3	DNAH5-	Completely immotile	NA	<i>TTC25</i> (c.655_659delCTGAC/p.Leu219CysfsTer62 hom.)	Confirmed PCD <i>TTC25</i>	43
IF-041	2015/M/Moroccan/Y	3/Chronic rhinitis and wet cough.	NA	RSPH4A-	Circular	NA	<i>RSPH4A</i> (c.1453C>T/p.Arg486STer hom.)	Confirmed PCD <i>RSPH4A</i>	38
IF-043	2013/F/Pakistani/Y/sib. of IF-044	4/Chronic rhinitis and wet cough. Recurrent pneumonia. Persistent atelectasis.	NA	DNAH5-	Completely immotile	ODA defect	<i>DNAI2</i> (c.546C>A/p.Tyr182Ter hom.)	Confirmed PCD <i>DNAI2</i>	28
IF-044	2006/M/Pakistani/Y/sib. of IF-043	6/Neonatal distress. Chronic rhinitis and cough. Bronchiectasis.	14.2	DNAH5-	Completely immotile	Partial ODA defect	<i>DNAI2</i> (c.546C>A/p.Tyr182Ter hom.)	Confirmed PCD <i>DNAI2</i>	29
IF-045	2005/F/Caucasian/N	4/Chronic rhinitis and cough. Bronchiectasis. Recurrent otitis. Hearing loss.	17.2	DNAH5-	Completely immotile	Loss 30% ODA and 70% IDA	<i>DNAH5</i> (c.4625_4628delGAGA/p.Arg1542ThrfsTer6 het. + c.12706-2A>T het.)	Confirmed PCD <i>DNAH5</i>	14

Table 7 (continued)

IF-046	2004/F/Caucasian/N	4/Chronic rhinitis and wet cough.	NA	Proximal DNAH5	Subtle defects (disorganized ciliary beat)	NA	DNAH9 (c.7822-1G>A het. + c.8992C>T/p.Gln2998Ter het.)	Confirmed PCD DNAH9	23
IF-047	1970/M/Caucasian/N	?/Chronic rhinitis and wet cough. Sinusitis. Recurrent otitis and hearing loss. <i>Situs inversus</i> .	188.1	Proximal DNAH5	Subtle defects (stiff and disorganized ciliary beat)	NA	Negative	Highly likely PCD - WES	
IF-050	2010/F/Moroccan/Y	4/Chronic rhinitis and cough. Bronchiectasis. Recurrent otitis. Lobectomy.	5.4	RSPH4A+, RSPH9-	Stiff and circular	NA	RSPH9 (c.293_294delTG/p.Val98GlyfsTer14 hom.)	Confirmed PCD RSPH9	40
IF-053	1984/M/Caucasian/N/father of IF-067	10/Neonatal distress. Chronic rhinitis and wet cough. Sinusitis. Recurrent otitis and hearing loss. Repeated bronchitis and pneumonia. Bronchiectasis. <i>Situs inversus</i> .	4.7	DNAH5-	Completely immotile	NA	DNAH5 (c.2575A>T/p.Lys859Ter het. + c.9730G>T/p.Glu3244Ter het.)	Confirmed PCD DNAH5	21
IF-055	2011/F/Caucasian/Y	6/Neonatal distress. Chronic rhinitis and wet cough. Recurrent otitis and hearing loss. Recurrent bronchitis and pneumoniae. Bronchiectasis.	NA	DNAH5-	Completely immotile	NA	DNAH5 (3.3kb inc. ex.29 and ex.30 del het.)	Confirmed PCD DNAH5	22

Table 7 (continued)

IF-056	2018/F/Pakistan/Y/sib. of IF-021, IF-057	7/Neonatal distress. Chronic rhinitis and cough. Recurrent atelectasis.	NA	DNALI1-, GAS8-	Stiff and immotile	NA	<i>CCDC40</i> (c.1416delG/ p.Ile473PhefsTer2 hom.)	Confirmed PCD <i>CCDC40</i>	12
IF-060	2003/F/Caucasian/N	8/Chronic rhinitis and wet cough. <i>Situs inversus</i> .	44.5	DNALI1-, GAS8-	Mainly stiff	ODA and IDA defects	<i>CCDC40</i> (c.2T>G/p.Met1Arg het. + 526pb inc. ex.8 and ex.9 del het.)	Confirmed PCD <i>CCDC40</i>	13
IF-061	2011/M/Caucasian/N	8/Neonatal distress. Chronic rhinitis and wet cough. Bronchiectasis. <i>Situs inversus</i> .	5.5	DNAH5-	Immotile, residual motility	NA	<i>DNAH5</i> (3.2kb inc. ex.2 and ex.3 del het. + c.10813G>A/p.Asp3605Asn het.)	Confirmed PCD <i>DNAH5</i>	19
IF-062	2002/M/Caucasian/N	8/Chronic rhinitis and wet cough. Sinusitis. Recurrent otitis and hearing loss. Recurrent bronchitis. Bronchiectasis. <i>Situs inversus</i> .	NA	DNAH5-	Completely immotile	NA	<i>DNAI2</i> (c.346-3T>G hom.)	Confirmed PCD <i>DNAI2</i>	30
IF-071	1957/F/Caucasian/N	6/Neonatal distress. Chronic rhinitis and sinusitis. Hearing loss. Bronchiectasis.	5.6	GAS8-	Hyperkinetic stiff cilia	NA	NA	Highly likely PCD	
IF-072	2001/M/Caucasian/N	6/Neonatal distress. Chronic rhinosinusitis and wet cough. Bronchiectasis.	NA	DNALI1-, GAS8-	Immotile	NA	<i>CCDC39</i> (c.2250delT/ p.Gln751LysfsTer11 hom.)	Confirmed PCD <i>CCDC39</i>	5
IF-073	2014/M/Caucasian/N	9/Neonatal distress. Wet cough. Recurrent otitis. <i>Situs inversus</i> .	NA	DNAH5-	Immotile	NA	<i>DNAH5</i> (c.2283_2284del/ p.Arg761SerfsTer10 het. + c.3861T>G/p.Tyr1287Ter het.)	Confirmed PCD <i>DNAH5</i>	17

Table 7 (continued)

IF-076	2004/M/Caucasian/N	3/Chronic rhinitis. Recurrent bronchitis. Bronchiectasis.	193.3	Proximal DNAH5	Subtle defects (stiff and immotile)	NA	Negative	Highly likely PCD - WES	
IF-089	2004/M/Caucasian/N	8/Chronic rhinitis. Recurrent otitis. Recurrent bronchitis. Bronchiectasis. <i>Situs inversus</i> .	27.4	DNAH5-	Completely immotile	NA	NA	Highly likely PCD - Genetics	
IF-091	2016/F/NA/NA	?/Neonatal distress. Chronic rhinitis and wet cough. Recurrent pneumonia. <i>Situs inversus</i> .	NA	DNAH5-	Immotile, residual motility	NA	NA	Highly likely PCD - Genetics	
IF-092	2016/M/Caucasian/N	7/Neonatal distress. Chronic rhinitis and wet cough.	NA	DNALI1-, GAS8-	Immotile	NA	<i>CCDC39</i> (c.357+1G>C het. + c.2505_2506delCA/p.His835GlnfsTer4 het.)	Confirmed PCD <i>CCDC39</i>	4
IF-093	2002/M/NA/NA	?/Neonatal distress. Chronic rhinitis and wet cough. Rhinosinusitis. Recurrent otitis. Recurrent pneumonia. Bronchiectasis.	NA	DNAH5-	Immotile, residual motility	NA	NA	Highly likely PCD - Genetics	
IF-094	2011/F/NA/NA	?/Neonatal distress. Chronic rhinitis and wet cough. Recurrent otitis. Bronchiectasis. Persistent atelectasis. <i>Situs inversus</i> .	NA	DNAH5-, DNALI1-	Completely immotile	NA	NA	Highly likely PCD - Genetics	
IF-095	2004/F/Caucasian/NA	9/Neonatal distress. Hearing loss. Recurrent pneumonia. <i>Situs inversus</i> .	NA	DNAH5-	NA	ODA hypoplasia	<i>CCDC151</i> (c.410G>A/p.Trp137Ter hom.)	Confirmed PCD <i>CCDC151</i>	3

Table 7 (continued)

IF-096	1972/M/NA/NA	?/Neonatal distress. Chronic rhinitis and wet cough. Rhinosinusitis. Recurrent otitis. Recurrent pneumonia. Fertility problems.	NA	DNAH5-	Immotile	NA	NA	Highly likely PCD - Genetics
IF-098	2014/M/NA/NA	?/Neonatal distress. Chronic rhinitis and wet cough. <i>Situs inversus</i> .	NA	DNALI1-, GAS8-	Immotile and stiff	NA	NA	Highly likely PCD - Genetics

Patient#: patient identification number; YOB: year of birth; PCD: primary ciliary dyskinesia; nNO: nasal nitric oxide; IF: immunofluorescence; HSVM: high-speed video-microscopy; TEM: transmission electron microscopy; M: male; F: female; N: no; Y: yes; Sib.: sibling; NA: not available data; ?: PICADAR was not calculated due to missing data; +: present in ciliary axoneme; -: absent in ciliary axoneme; ODA: outer dynein arms; IDA: inner dynein arms; het.: heterozygous variant; hom.: homozygous variant; inc.: including; ex.: exon; WES: whole-exome sequencing

**Table 8: Patients with normal localization of target proteins by immunofluorescence and correlation with other PCD-analysis techniques.**

Patient#	YOB/Gender/Origin/ Consanguinity/Family	PICADAR score [79] /PCD symptoms	nNO (nl/min)	Affected IF markers	HSVM	TEM	Genetics	Diagnosis [77] - Next step	Patient# in Baz- Redón <i>et al.</i> 2021 [134]
IF-002	2016/M/Caucasian/N	11/Neonatal distress. Chronic rhinitis and cough. <i>Situs inversus totalis</i> .	15.01	All markers +	Hyperkinetic stiff cilia	NA	<i>DNAH11</i> (c.12507+1G>C het. + c.13415_13416insCAAA/ p.Thr4472fs het.)	Confirmed PCD <i>DNAH11</i>	24
IF-003	2001/F/Caucasian/N	4/Chronic rhinitis and wet cough. Sinusitis. Recurrent otitis and hearing loss. Recurrent pneumonia. Bronchiectasis.	3.5	All markers +	Immotile	NA	Negative	Highly likely PCD - WES	48
IF-005	2004/F/South- American/N	?/Chronic rhinitis and wet cough. Sinusitis. Recurrent otitis and hearing loss. Recurrent bronchitis and pneumonia. Bronchiectasis.	50.2	All markers +	Disorganized ciliary beat	NA	Negative	Highly likely PCD - WES	47
IF-010	2002/M/Moroccan/NA	?/Chronic rhinitis and wet cough. Recurrent otitis and hearing loss. Bronchiectasis.	13.8	All markers +	Normal	NA	Negative	Highly unlikely PCD	
IF-011	1999/M/Caucasian/N	?/Chronic rhinitis and wet cough. Recurrent otitis and hearing loss. <i>Situs inversus</i> .	14.3	All markers +	Stiff	NA	<i>SPAG1</i> (c.583delA/ p.Ile195Ter het. + c.1855G>C/p.Asp619His het.)	Highly likely PCD – Re-evaluation of variants and/or IF with new sample.	41
IF-016	2013/M/Caucasian/N	2/Chronic wet cough. Bronchiectasis.	NA	All markers +	Normal	NA	Negative	Highly unlikely PCD	

Table 8 (continued)

IF-017	2016/M/Moroccan/N	8/Neonatal distress. <i>Situs inversus</i> .	NA	All markers +	Normal	NA	Negative	Highly unlikely PCD	
IF-018	1994/M/Caucasian/N	4/Chronic rhinitis and wet cough. Nasal polyps. Sinusitis. Recurrent otitis and hearing loss. Recurrent bronchitis and pneumoniae. Bronchiectasis.	14.8	All markers +	Immotile and disorganized ciliary beat	Loss 10% ODA and 40% IDA	Negative	Highly likely PCD - WES	46
IF-022	2003/F/Caucasian/N	2/Chronic rhinitis. Recurrent otitis.	100	All markers +	Normal	NA	Negative	Highly unlikely PCD	
IF-023	2013/F/Caucasian/N	?/Wet cough	NA	All markers +	Normal	NA	Negative	Highly unlikely PCD	
IF-028	2010/F/Caucasian/N	2/Bronchiectasis	NA	All markers +	Normal	NA	Negative	Highly unlikely PCD	
IF-029	2012/F/Caucasian/N	4/Neonatal distress. Recurrent bronchitis and pneumonia.	NA	All markers +	Normal	NA	Negative	Highly unlikely PCD	
IF-030	2006/M/Caucasian/N	?/Chronic rhinitis and wet cough. Bronchiectasis.	196.8	All markers +	Normal	NA	Negative	Highly unlikely PCD	
IF-032	1985/M/Caucasian/NA	?/Wet cough. Recurrent pneumonia. Bronchiectasis. Infertility.	103.2	All markers +	Reduced CBF	NA	NA	Highly likely PCD - Genetics	
IF-034	2007/F/Caucasian/N	6/Neonatal distress. Chronic rhinitis and wet cough. Recurrent otitis and hearing loss. Recurrent bronchitis. Bronchiectasis.	128.7	All markers +	Completely immotile	NA	Negative	Highly likely PCD - WES	44



Table 8 (continued)

IF-035	2007/M/Caucasian/NA	?/Wet cough. Bronchiectasis.	NA	All markers +	Normal	NA	Negative	Highly unlikely PCD	
IF-036	2004/M/Caucasian/N	2/Bronchiectasis. Recurrent bronchitis and pneumonia.	NA	All markers +	Normal	NA	Negative	Highly unlikely PCD	
IF-037	1987/M/Caucasian/N	?/Chronic rhinitis and wet cough. Nasal polyps. Sinusitis. Repeated pneumonia. Bronchiectasis. Lobectomy.	24.3	All markers +	Immotile	NA	Negative	Highly likely PCD - WES	50
IF-039	2010/F/Caucasian/N	4/Chronic rhinitis and wet cough. Nasal polyps. Recurrent otitis and hearing loss. Bronchiectasis.	15.8	All markers +	Stiff and disorganized ciliary beat	NA	Negative	Highly likely PCD - WES	45
IF-042	2011/F/Caucasian/NA	3/Chronic rhinitis. Bronchiectasis.	NA	All markers +	Normal	NA	NA	Highly unlikely PCD	
IF-048	2005/F/Caucasian/N	7/Neonatal distress. Chronic rhinitis and cough. Recurrent atelectasis.	44.5	All markers +	Normal	NA	Negative	Highly unlikely PCD	
IF-049	2017/M/Arabian/Y	7/Neonatal distress. Chronic rhinitis and wet cough. Recurrent bronchitis. Cardiopathy.	NA	All markers +	Hyperkinetic stiff cilia	NA	<i>DNAH11</i> (c.983-1G>T het. + c.3439C>T/p.Gln1147Ter het.)	Confirmed PCD <i>DNAH11</i>	26
IF-051	2004/M/Caucasian/N	4/Chronic rhinitis and cough. Bronchiectasis. Recurrent otitis. Hearing loss.	NA	All markers +	Normal	NA	NA	Highly unlikely PCD	
IF-052	1963/M/Caucasian/N	3/Chronic rhinitis and cough. Bronchiectasis. Infertility	12.8	All markers +	Mainly stiff	NA	NA	Highly likely PCD - Genetics	

Table 8 (continued)

IF-057	2016/M/Pakistani/Y/ sib. of IF-021, IF-056	2/Recurrent bronchitis and pneumonias.	NA	All markers +	Normal	NA	Negative	Highly unlikely PCD	
IF-058	1964/F/Caucasian/N	2/Bronchiectasis. Recurrent pneumonias.	218.7	All markers +	Normal	NA	Negative	Highly unlikely PCD	
IF-059	2002/F/Caucasian/N	2/Recurrent pneumonias	300	All markers +	Normal	NA	Negative	Highly unlikely PCD	
IF-063	1967/F/Caucasian/NA	?/Chronic rhinitis and wet cough. Sinusitis. Recurrent otitis and hearing loss. Recurrent bronchitis. Bronchiectasis. <i>Situs inversus.</i>	11.4	All markers +	Stiff and immotile	NA	Negative	Highly likely PCD - WES	49
IF-064	2016/F/Caucasian/N	3/Chronic rhinitis. Persistent atelectasis.	NA	All markers +	Normal	NA	NA	Highly unlikely PCD	
IF-066	1983/F/Caucasian/N	8/Chronic rhinitis and cough. Recurrent otitis. Hearing loss. Neonatal distres and intensive care	154.7	All markers +	Normal	NA	NA	Highly unlikely PCD	
IF-067	2018/M/Caucasian/N/s on of IF-053	2/Recurrent bronchitis	NA	All markers +	Normal	NA	Negative	Highly unlikely PCD	
IF-068	2000/M/Caucasian/N	4/Chronic rhinitis and wet cough. Sinusitis. Recurrent otitis and hearing loss. Recurrent bronchitis. Bronchiectasis.	4.3	All markers +	Hyperkinetic stiff cilia	NA	<i>DNAH11</i> (c.3898C>T/p.Gln1300Ter het. + c.6983+1G>A het.)	Confirmed PCD <i>DNAH11</i>	27

Table 8 (continued)

IF-077	2011/F/Moroccan/NA	2/Bronchiectasis	145	All markers +	Normal	NA	NA	Highly unlikely PCD
IF-097	1973/F/NA/NA	?/Chronic rhinitis and wet cough. Recurrent otitis and hearing loss. Bronchiectasis. Fertility problems.	NA	All markers +	Immotile and stiff	NA	NA	Highly likely PCD - Genetics
IF-102	2016/M/Pakistani/Y	2/Recurrent bronchitis	44.2	All markers +	Disorganized ciliary beat and stiff	NA	NA	Highly likely PCD - Genetics

Patient#: patient identification number; YOB: year of birth; PCD: primary ciliary dyskinesia; nNO: nasal nitric oxide; IF: immunofluorescence; HSVM: high-speed video-microscopy; TEM: transmission electron microscopy; M: male; F: female; N: no; Y: yes; Sib.: sibling; NA: not available data; ?: PICADAR was not calculated due to missing data; +: present in ciliary axoneme; -: absent in ciliary axoneme; CBF: ciliary beat frequency; ODA: outer dynein arms; IDA: inner dynein arms; het.: heterozygous variant; WES: whole-exome sequencing

**Table 9: Patients with inconclusive and/or insufficient immunofluorescence results and correlation with other PCD-analysis techniques.**

Patient#	YOB/Gender/Origin/ Consanguinity/Family	PICADAR score [79]/PCD symptoms	nNO (nl/min)	Affected IF markers	HSVM	TEM	Genetics	Diagnosis [77] - Next step	Patient# in Baz- Redón <i>et</i> <i>al.</i> 2021 [134]
IF-006	2004/M/Caucasian/N	8/Chronic rhinitis and wet cough. Bronchiectasis. <i>Situs</i> <i>inversus</i> .	14.6	Insufficient and inconclusive	Stiff and immotile	NA	<i>CCDC39</i> (c.216_217delTT/p.Cys73GlnfsTer6 het. + c.357+1G>C het.)	Confirmed PCD <i>CCDC39</i>	8
IF-012	1977/F/Caucasian/NA	?/Chronic rhinitis and wet cough. Sinusitis. Recurrent otitis. Bronchiectasis.	155.9	Insufficient	Normal	NA	NA	Highly unlikely PCD	
IF-014	2008/M/Caucasian/N	8/Neonatal distress. Recurrent bronchitis. <i>Situs</i> <i>inversus</i> .	115.8	Inconclusive	Normal	NA	NA	Highly unlikely PCD	
IF-019	2006/M/Caucasian/NA	2/Chronic wet cough. Nasal polyps.	NA	Insufficient and inconclusive	Normal	NA	NA	Highly unlikely PCD	
IF-074	2019/F/Pakistani/Y	9/Neonatal distress. Chronic rhinitis. <i>Situs inversus</i> .	9	Inconclusive	Completely immotile	NA	NA	Highly likely PCD - Genetics	
IF-100	2004/M/Caucasian/N	?/Recurrent bronchitis.	NA	Insufficient	Normal	NA	NA	Highly unlikely PCD	

Patient#: patient identification number; YOB: year of birth; PCD: primary ciliary dyskinesia; nNO: nasal nitric oxide; IF: immunofluorescence; HSVM: high-speed video-microscopy; TEM: transmission electron microscopy; M: male; F: female; N: no; Y: yes; NA: not available data; ?: PICADAR was not calculated due to missing data; het.: heterozygous variant

### 4.3. RESULTS III

#### **WHOLE EXOME SEQUENCING IN HIGHLY LIKELY PCD PATIENTS WITH NEGATIVE GENE PANEL RESULTS**

*(Data not published)*

The high-throughput gene panel approach allowed the study of point variants, small indels and CNVs in analyzed PCD causing genes. Candidate variants were found in 81.1% (43/53) of patients with PCD. However, 18.9% (10/53) of highly likely PCD patients were left without a genetic diagnosis with our PCD gene panel design, which includes 44 previously described genes (Table 1). Therefore, a WES analysis was carried out in nine of those patients without diagnosis [134], and also in a patient (IF-047) first considered unlikely PCD because of nearly normal HSVM but consistent PCD symptoms and aberrant IF.

WES analysis of two of these patients showed two likely pathogenic variants in two recently described genes associated with PCD, thus not included in our gene panel approach. Patient 52/IF-024 (Table 3 [134] and Table 7 [135], respectively) was homozygous for the VUS variant c.758A>C/p.(His253Pro) in *CFAP300/C11orf70*. Patient 53/IF-009 (Table 3 [134] and Table 7 [135], respectively) was hemizygous for the splicing pathogenic variant c.430-1G>A in *DNAAF6/PIH1D3*.

Regarding the rest of the patients, we described variants in four of them (patients 45/IF-039 48/IF-003, 49/IF-063 and 50/IF-037) in candidate genes related to cilia and/or flagella structure or ciliogenesis, which could explain their phenotype (Table 3 [134] and Table 8 [135]). Patient 45/IF-039 presented two heterozygous variants in the Golgin subfamily A member 3 (*GOLGA3*) (c.4435C>G/p.Pro1479Ala and c.4427\_4438delACGCCGCCAC/p.His1476\_Pro1479del), classified as VUS according to ACMG classification. In patient 48/IF-003 two variants in *DNAH5* (c.6731A>T/p.Lys2244Met and c.9943C>A/p.Pro3315Thr) were detected in the high-throughput gene panel analysis, but were discarded as there was no concordance with other diagnostic results. In WES analysis, we detected two missense variants in *DNAH2* (c.5986G>A/p.Asp1996Asn and c.890A>G/p.Lys297Arg), both classified as benign. Furthermore, patient 49/IF-063 presented variants in two cilia or flagella related genes, which were considered candidate genes: *MAPK15* and *TTC12*. In *MAPK15*, the patient presented two variants: a VUS frameshift variant (c.298\_299delAG/p.Ser100ProfsTer15) and a splicing variant

(c.287-54dupC) in a repetitive cytosine region, which was classified also as VUS. In *TTC12*, the patient presented a missense VUS variant (c.1911C>G/p.Asn637Lys) and an intronic variant located upstream the codifying region (c.-15-189G>A), classified as benign. Finally, patient 50/IF-037 presented different variants in the candidate gene *C2CD3*: two frameshift pathogenic variants (c.6137\_6156del/p.Arg2046AsnfsTer2 and c.6094\_6128del/p.Arg2032HisfsTer8), two frameshift variants classified as likely pathogenic (c.6133delA/p.Thr2045GlnfsTer30 and c.6130delA/p.Ile2044LeufsTer31), a VUS variant (c.6169\_6177delCCAGCCTAC/p.Pro2057\_Tyr2059del), and a missense likely benign variant (c.6166G>T/p.Gly2056Cys).

In the remaining three patients previously analyzed with our gene panel approach (44/IF-034, 46/IF-018 and 47/IF-005; Table 3 [134] and Table 8 [135]) and in the patient IF-047 (Table 7 [135]) no candidate genes related to their phenotype were detected by the WES data analysis.



## **5. DISCUSSION**





## 5.1. GENETICS: PCD-GENE PANEL

In a cohort of 53 patients with confirmed or highly likely PCD, positive genetic results were obtained in 81.1% of cases using a high-throughput sequencing panel of 44 genes. In other 26 patients referred for suspicious respiratory symptoms, but with a diagnosis of unlikely PCD after initial tests, the genetic study was negative. This is the first study, to our knowledge, to describe the genes that cause PCD in a large cohort of patients in Spain.

Our results have confirmed that, in our population, this gene panel correctly identified patients with PCD (sensitivity of 81.1%) and ruled out those with a low suspicion of PCD (specificity of 100%). It has been described that the accuracy of gene panels increases as newly discovered genes are added. According to previous publications, sensitivity of PCD gene panels ranges between 43% and 70% [108–110], and more recently it has been described to be even higher (82%) [112].

When using the PCD diagnostic tools available to date, diagnostic is complex and may generate uncertainties and doubts among doctors and patients concerning the prognosis and course of the disease. The nNO determination with a cut-off point of 77 nL/min has a high sensitivity (93.6%), but a specificity of 78.9% [136]. TEM is specific (100%) but fails to identify 21% of cases. Furthermore, it must be interpreted by highly expert technicians, and suitable samples are not always obtained [77,94]. HSVM combining CBF and CBP has excellent sensitivity and specificity (0.96-1.00 and 0.93-0.95, respectively) [77]; however, it also needs expert technicians and often has to be repeated several times [105]. Although genetic studies may fail to identify 20% of cases, they correctly identify the genetic cause of the disease and provide clearer guidance for treatment and genetic counseling. They also help to understand the genetic background of the disease for future specific treatment research, such as gene or protein therapies [111].

The distribution of genes that cause PCD differs depending on ethnicity [112]. In our cohort, *DNAH5* and *CCDC39* were the most prevalent genes, and both were found only in patients of Caucasian origin (Table 4). *DNAH5* has been described as the most frequent gene in Caucasian patients, explaining 15%-37% of cases [108,109,112,132], but it is rarer in other populations, such as in Arabs [110,112]. The *CCDC39* gene has previously been described in patients of

European origin [22] but, together with *CCDC40*, are the most frequently mutated genes in Arab origin population [110,112].

Gene panel high-throughput sequencing can be used to identify point variants, small insertions and deletions (indels), and copy number variants (CNVs) of PCD-causing genes described to date. The majority of the variants described in our patients (82.7%) caused loss of protein function (nonsense, frameshift, CNV and splicing), similar to results described in other studies [112]. Nine patients (17.3%) presented missense variants, which were catalogued as VUS according to the ACMG [125] classification, with the exception of the c.2T>G/p.Met1Arg variant in *CCDC40* (patient 13), that affected the first amino acid and was classified as likely pathogenic (Table 4). These missense variants were considered as possible causes of protein alterations as were *in silico* predicted to be deleterious. Ideally, these missense defects should be tested *in vitro* in patient nasal respiratory epithelium cell cultures or animal models.

A total of 36 novel variants were identified and 16 were previously described in literature [10,11,132,20,22,25,90,128–131]. The most frequently described variant in our cohort belongs to *RSPH1*: c.85G>T/p.Glu39Ter. This nonsense variant was detected in four (3 probands) out of five patients with *RSPH1* defects in homozygosity or compound heterozygosity with the splicing variant c.275-2A>C, both previously described [25]. The remaining *RSPH1* patient was heterozygous for the splicing variant and the novel variant c.70C>T/p.Arg24Trp. Strikingly, two of these *RSPH1* variants are very close. Considering the nearness of the most frequently described *RSPH1* variant in our cohort (c.85G>T/p.Glu39Ter) and the novel one (c.70C>T/p.Arg24Trp), we consider this genetic area a possible hotspot.

Given the large number of variants that can be identified with high-throughput sequencing, many of which are classified as benign, it is useful to correlate TEM and HSVM findings with these genetic results to interpret them correctly. In our cohort, a good correlation between ultrastructure and genetic findings was obtained in only 6 cases, due to difficulties of TEM interpretation and its limitations (false positive results caused by respiratory infections or processing artifacts) [94,128] (Table 3). In contrast, HSVM analyses showed a good correlation with genetic findings in all cases (Table 3).

Patients 13 and 19, who initially had a single heterozygous variant in genes *CCDC40* and *DNAH5*, respectively, were resolved with a bioinformatics analysis of CNVs. In those patients,

the familial segregation study confirmed that the deletions were carried in the non-variant carrying allele, with the mother of patient 13 and the father of patient 19 being identified as the carriers of these deletions (Table 4). In patient 22, a homozygous deletion was detected in the *DNAH5* gene using the same CNV analysis (Table 4). Then, we detected a 5.77% (3/52 variants) of CNVs, close to previously published studies using the same bioinformatics analysis approach [110,112]. These results may confirm that bioinformatics analysis of CNVs is a useful tool for resolving some cases, especially those with monoallelic variants in a candidate gene that correlates with the phenotype.

It should be noted that all cases of consanguinity in our cohort had a positive molecular result and were homozygous for the detected variants, all of which were classified as pathogenic or likely pathogenic (Table 4).

The limitations of our PCD gene panel strategy are mainly related to the number of patients studied, which, although significant for a rare disease, must be expanded to better understand the frequency of the different variants in our population, both Caucasian and non-Caucasian. High-throughput sequencing cannot detect all deletions/duplications in genes, but this has been solved by analyzing CNVs with bioinformatics tools. This must be considered only as an approximation, so confirmation of findings by using other methods is highly recommended. Other limitations are those inherent to gene panel studies, since neither the entire exome nor the genome are analyzed. However, this facilitates the interpretation of results since the analysis of the whole exome or genome may contain a very high number of variants that lack pathogenic significance in healthy population. Moreover, gene panels' coverage is optimized in comparison to exome sequencing. Even though our 44 PCD custom gene panel has been designed to genetically characterize our cohort, new PCD genes are described every year [32,47,59], so this gene panel has already been expanded with recently discovered data.

## **5.2. GENETICS: WHOLE EXOME SEQUENCING**

Using our 44 PCD gene panel approach, a total of 18.9% (10/53) of highly likely PCD patients were left without a genetic diagnosis. A WES analysis was carried out in nine of those patients without genetic diagnosis [134] and also in a patient (IF-047) firstly considered unlikely PCD because of nearly normal HSVM, but consistent PCD symptoms and aberrant IF.

WES analysis was conclusive in two of the analyzed patients with likely pathogenic variants in *CFAP300/C11orf70* (patient 52/IF-024, Table 3 [134] and Table 7 [135]) and *DNAAF6/PIH1D3* (patient 53/IF-009, Table 3 [134] and Table 7 [135]). These genes were recently described as cytoplasmic ODA and IDA assembly factors [53,54,59,60], so our WES results were concordant with immotile cilia by HSVM and absence of ODA (DNAH5) and IDA (DNALI1) proteins by IF (Table 7) [134,135].

In patient 45/IF-039, two variants (missense and deletion) in close genetic position (c.4435C>G/p.Pro1479Ala and c.4427\_4438delACGCCGCCCCAC/p.His1476\_Pro1479del) were detected in *GOLGA3*. When analyzing by Sanger sequencing, the deletion was observed in homozygosity. Shamseldin *et al.* [137] already proposed *GOLGA3* as a novel PCD gene candidate, as a biallelic likely pathogenic variant was encountered in two siblings by WES analysis [137]. In male germ cells, interactions of SPEF2 with the dynein 1 complex and *GOLGA3* have been confirmed, which further supports the role of *GOLGA3* in Golgi-derived vesicular transport during spermiogenesis [138]. A new IF analysis of SPEF2 in patient 45/IF-039, showed that this protein was absent in ciliary axoneme. This is concordant to *GOLGA3* being the PCD causing gene and supports that a possible interaction between SPEF2 and *GOLGA3* may also occur in airway ciliated cells.

In patient 48/IF-003, *DNAH2* was firstly considered a candidate gene. This gene was previously described as essential for ciliary beating, as its depletion caused paralyzed multicilia [139]. This result is concordant with immotile cilia in our patient sample, although the percentage of affected cells is about half, which could be explained by the fact that the described variants (c.5986G>A/p.Asp1996Asn and c.890A>G/p.Lys297Arg) are missense, as previously observed in *TTC12* defects [15]. In *Chlamydomonas* spp. studies, *DNAH2* was described as a component of double-headed IDA. In the IF analysis of patient 48/IF-003, DNALI1 was present in the ciliary axoneme, but as this protein is a component of single-headed IDA it may not be affected in *DNAH2* mutants [15,140]. Recently, *DNAH2* variants detected in our patient were classified as benign according to ACMG criteria, so it must be taken into consideration that *DNAH2* variants might not be the cause of our patient's phenotype. That is why we reconsidered the *DNAH5* variants (c.6731A>T/p.Lys2244Met and c.9943C>A/p.Pro3315Thr) previously detected in this patient with our gene panel approach, as a possible cause of the phenotype. HSVM and IF analyses in this patient do not correlate with *DNAH5* defects, which could be explained by

more subtle defects in cases with missense variants, as previously described [15]. Thus, this patient is under further investigation.

In patient 49/IF-063, *MAPK15* and *TTC12* were considered candidate genes. *MAPK15* is a gene related to ciliogenesis regulation, as its depletion in human epithelial cells abrogated ciliogenesis and reduced ciliary length [141]. Miyatake *et al.* [142] described that the knockdown of *Xenopus MAPK15* orthologue affected both the number and length of cilia in multiciliated cells and inhibits the apical migration of basal bodies [142]. In our patient, the number and length of cilia do not seem to be affected when observed by HSVM. Furthermore, we observed a correct apical migration of basal bodies thanks to anti-GAS8 antibody by IF. As little evidence of *MAPK15* function and effect on human basal bodies have been described, it cannot be discarded as a candidate gene. However, it has to be taken into consideration that the splicing variant (c.287-54dupC) detected in patient 49/IF-063 was recently described as VUS-benign and it is located in a cytosine-rich region, so a Sanger sequencing analysis is necessary. Regarding *TTC12* gene, it was recently described to encode the DNAAF protein involved in the assembly of IDA in respiratory epithelial cells [15]. Individuals with *TTC12* genetic defects presented with variable proportions of immotile cilia, normal beat frequency and moderate beating defects by HSVM, and DNALI1 strongly reduced but partially present in the proximal part of ciliary axoneme by IF [15]. Considering that one of the *TTC12* genetic variants described in patient 49/IF-063 was recently described as benign, and DNALI1 was observed to be present in ciliary axoneme by IF, *TTC12* is unlikely to be the cause of this patient's phenotype.

In patient 50/IF-037, *C2CD3* was considered a candidate gene. The centriole protein *C2CD3* has been predicted to be an essential regulator for cilia formation, and genetic variants in human *C2CD3* are associated with the human ciliopathy oral-facial-digital type 14 syndrome (OFD14) as it is required for craniofacial development [143]. Chang *et al.* [143] also observed several tissue-specific isoforms of *C2cd3* in mice and suggest that the genetic background may contribute to phenotypic variation [143]. Further studies are necessary to describe the expression of *C2CD3* in human airway epithelia and understand its role. In patient 50/IF-037 different variants were found in *C2CD3*, but as they are in a nearby region, it is necessary to study them by classical Sanger sequencing. This patient is still under further investigation.

Three of the analyzed patients still remain without a genetic diagnosis (44/IF-034, 46/IF-018, 47/IF-005, and IF-047) and a WES data reanalysis is ongoing.

### **5.3. IMMUNOFLUORESCENCE ANALYSIS**

We have explored the diagnostic utility of an IF panel of commercial antibodies in 74 patients with clinical suspicion of PCD. A technically evaluable result was possible in 91.9% of cases (Table 5). IF evidenced a protein defect in 44.6% of analyzed patients, all with confirmed or highly likely PCD (Table 5). A normal IF result (47.3% of cases) was seen not only in all non-PCD patients, but also in some patients with confirmed or highly likely PCD. This means that IF detected ciliary structural defects in 68.8% of confirmed or highly likely PCD patients. In our population, IF has shown a positive predictive value (when a positive value is consistent with a PCD diagnosis) of 100% and a negative predictive value (when a normal result may be seen not only in non-PCD patients but also in PCD patients) of 89.4%. Considering our low availability of TEM results, IF was a useful PCD diagnostic test, because it showed a sensitivity (68.8%) close to TEM studies, where 30% of all affected individuals had normal ciliary ultrastructure [144].

To our knowledge, only one previous study by Shoemark *et al.* [105] evaluated the accuracy of IF in PCD, concluding that IF and TEM have a similar diagnostic rate. Therefore, they proposed IF as a useful diagnostic tool when TEM equipment or expertise is not available, as IF is cheaper, easier to perform, requires more basic equipment and improves the turnaround time [105]. As TEM analysis was not available in most of our cases, we have confirmed that, under these circumstances, IF is a reliable test to study cilia structure. Furthermore, IF may be useful to confirm the results of other diagnostic tests like HSVM and genetics and guide new tests in those cases with absent or aberrant protein/s localization. In Shoemark's study, IF failed to identify 12% of PCD cases [105], which is lower than the 31.3% of normal IF results that we found in our confirmed or highly likely PCD cases. This difference could be related to genetic differences between both series.

Our IF panel could not detect defects caused by *DNAH11* genetic variants in our patients, consistent with previously reported data [6]. For this reason, an anti-DNAH11 commercial antibody has been optimized in order to include it in the IF panel. As it happens with DNAH11, other ciliary proteins have been described to cause none or subtle ultrastructural defects: HYDIN [31], STK36 [33] and, most recently, SPEF2 [32]. STK36 has been described as a protein

involved in the interaction between the central pair and the radial spoke [33]. HYDIN and SPEF2 have been functionally described to cause central pair defects in humans, and mutants of both proteins can be detected using anti-SPEF2 antibody [32], which has been also recently optimized in our laboratory. These ultrastructural defects could explain some of our normal IF results in highly likely PCD patients.

Some patients' diagnosis could not be resolved by IF as analysis was inconclusive and/or insufficient for some of the target proteins, requiring reevaluation of new brushing samples. Blood and mucus in the IF samples were found to be confounding factors in the analysis in a previous publication [105]. From our experience, we considered the slides with nasal brush sample prepared by dropping a better option than those by spreading. Slides with a dropped sample allowed a faster analysis because they have more cells in a smaller area. In addition, when the sample contained mucus, analysis was more complicated in spread samples, and usually there were not enough viable cells to complete the analysis.

The major limitation of the IF analysis is that, because of the use of primary antibodies directed to specific proteins, defects in unrelated proteins may be missed [105]. Moreover, patients with partial defects or missense mutations have been reported to have normal IF results [105], although we do not have any of these cases. As new genes and proteins related to PCD are discovered, the IF antibody panels may need to be revised and expanded in the future for an accurate diagnosis [107]. In fact, antibodies against a high number of ciliary proteins are already commercially available, although most of them have not been tested and/or validated for IF or in human respiratory tissue yet [106]. For this reason, the optimization of antibodies in nasal brushing samples is difficult and time-consuming. Furthermore, from our experience, we have not even been able to properly optimize some commercially available antibodies, i.e., anti-CCDC39 and anti-DNAH9. Further antibody optimization is necessary, and Liu *et al.*'s extensive IF technical protocols may help with this [106]. Another pitfall is the lack of consensus regarding the performance of the IF technique and, more importantly, the agreement in its analysis. Currently, a consensus statement on IF, initiated during the European BEAT-PCD 2019, is on the way.

One important limitation of measuring the accuracy of IF for PCD diagnosis is the lack of a gold standard reference against which to measure it. In our study, we use the ERS task force criteria



[77] assuming as a standard for comparison confirmed and highly likely PCD cases, with the added limitation of low availability of TEM analysis.

The positive rate of our series was quite high (25 confirmed and 25 highly likely of 74 cases). This is related to a previous pre-screening for IF study of cases with more suggestive clinical symptoms.

In our IF approach, radial spoke defects were first studied with the RSPH4A antibody and later with RSPH9. We decided to switch to RSPH9 because it is more informative for detecting all radial spoke head defects, and it has been recommended due to its reported absence from ciliary axonemes in radial spoke mutant cells [30,105]. In fact, one of our patients had normal RSPH4A, but absent RSPH9 (Figure 24C).

Taking everything into account, we propose a two-step IF analysis: a first panel with DNAH5, DNALI1, GAS8 and RSPH9 and, in cases with normal IF and consistent PCD suspicion (clinical symptoms and other techniques), a second IF round with antibodies against ciliary components associated with none or subtle ultrastructural defects: DNAH11 [6], STK36 [33] and SPEF2 [32]. At the moment, DNAH11 and SPEF2 commercial antibodies have been optimized in our laboratory for nasal brushing samples IF. Shoemark *et al.* [105] also recommended a first antibody panel with DNAH5, GAS8 and RSPH9 and omitted DNALI1 because its absence always coexists with an absence of DNAH5 or GAS8 [105]. This recommendation is supported by our cohort results, but as TEM is mostly unavailable and we are using IF results to clarify the genetics, we considered to maintain anti-DNALI1 antibody in our IF studies. Therefore, our proposed two-step IF analysis may be used in cases with non-available TEM. Alternatively, centers with available TEM analysis might use a first step IF panel with DNAH11, SPEF2, GAS8 and RSPH9 antibodies, omitting DNAH5 and DNALI1. For the translation to clinical diagnosis, Liu *et al.* [106] also proposed a restricted 10-antibody panel (instead of 21) based on proteins which are non-detectable by TEM or those indirectly detecting mislocation of other proteins (DNAH5, DNAH11, DNALI1, GAS8, CCDC65, RSPH4A, RSPH9, RPGR, OFD1 and SPEF2) [106]. Although a quantitative super-resolution imaging tool, such as the one proposed by Liu *et al.* [106], gives much more information and may solve so-called difficult or unsolved cases, it would be hard to implement in our clinical setting due to its high costs in time and personnel.

## 5.4. GENOTYPE-PHENOTYPE CORRELATION

Considering the results of all the available techniques in our laboratory, a genotype-phenotype correlation, including cellular phenotype (ciliary motility) and clinical symptoms, could be described in our cohort, which also confirms published data.

Different ODA defects have been observed in our cohort. DNAH5 absence in ciliary axoneme correlated with immotile cilia by HSVM and variants in genes related to ODA defects concurring with other studies: *DNAH5* [128,145], *DNAI2* [130], *TTC25* [13] and *CCDC151* [12] (Tables 6 and 7). Moreover, we found proximal axonemal DNAH5 IF staining in three unrelated patients of our cohort (Figure 24D) with mild clinical symptoms and subtle HSVM defects (mainly stiff and disorganized ciliary beat). One of them presented likely pathogenic variants in *DNAH9*, in concordance with recently published data [146,147] (Tables 6 and 7). Three patients have likely pathogenic variants in *DNAH11* with hyperkinetic stiff cilia by HSVM, with all four first-step IF panel antibodies present in ciliary axoneme, and clinical presentation of respiratory disease, including bronchiectasis and *situs* abnormalities (Tables 6 and 8). These results were concordant with previously reported data regarding *DNAH11* defects [6].

Some of the patients showed absence of both DNAH5 and DNALI1 (Figure 24A) and completely immotile cilia by immunofluorescence. We could not find any candidate variant in these patients using the high-throughput 44 PCD gene panel (Tables 6 and 7). However, WES analysis confirmed likely pathogenic variants in *CFAP300/C11orf70* and *DNAAF6/PIH1D3*, both genes recently described to encode cytoplasmic ODA and IDA assembly factors [53,54,59,60].

The patients with absent DNALI1 and abnormal localization (cytoplasmatic) of GAS8 (Figure 24B) had mainly stiff (reduced amplitude) and immotile cilia, and likely pathogenic variants in *CCDC39* and *CCDC40* (Tables 6 and 7). These results are consistent with previous description of *CCDC39* [20] and *CCDC40* [21] as assembling factors of the IDA and the nexin–dynein regulatory complex structures [20–22].

Only one patient of our IF results presented an absence of GAS8 in ciliary axoneme. This patient had hyperkinetic stiff cilia and respiratory symptoms beginning at neonatal age without *situs* abnormalities (Tables 6 and 7). These results could be explained by defects in the nexin–dynein regulatory complex (DRC) subunits, as previously described [16,17,19].

Genetic defects in radial spoke proteins in our patients were detected with RSPH4 or RSPH9 antibodies and were related to *situs solitus* and two different HSVM patterns: circular motion and stiff cilia, consistent with previously reported data (Tables 6 and 7) [25,26,30].

## **6. CONCLUSIONS**



1. The designed high-throughput sequencing panel of 44 primary ciliary dyskinesia (PCD) causing genes has been a reliable tool for improving the diagnosis of this disease (81.1% sensitivity and 100% specificity). However, it is necessary to extensively revise and update this gene panel to increase its accuracy, due to the constant description of new PCD causing or candidate genes.
2. *DNAH5* and *CCDC39* have been described as the most frequently affected genes in the Spanish PCD population.
3. We have detected 36 novel PCD gene variants (pathogenic, likely pathogenic and VUS) in our PCD patients. Most of these PCD gene variants cause loss of protein function (nonsense, frameshift, CNVs and splicing).
4. We have characterized a *RSPH1* gene hotspot thanks to the observation of the prevalence of the most frequent occurring variant (c.85G>T/p.Glu39Ter) together with a close novel variant (c.70C>T/p.Arg24Trp).
5. Bioinformatics analysis of CNVs has been a useful tool to resolve cases with monoallelic variants in a candidate gene correlating with the phenotype.
6. Whole-exome sequencing analysis is useful in PCD suspected cases without genetic candidate variants. It has allowed to describe the genetic PCD cause in two patients with variants in two genes recently associated with PCD (*CFAP300/C11orf70* and *DNAAF6/PIH1D3*). It has also highlighted two genes newly related to PCD: *GOLGA3* and *C2CD3*.
7. Immunofluorescence is a cheap, easy and widely available test to include in PCD diagnosis, which can substitute TEM ciliary ultrastructure analysis when this is unavailable.
8. Our immunofluorescence commercial antibody panel is a useful and reliable technique for PCD diagnosis (with a sensitivity of 68.8% and a specificity of 100%), and also for understanding ciliary structure. Ciliary structure defects observed by immunofluorescence have confirmed the genetic results in our patients.

9. We propose an immunofluorescence strategy consisting in a two-step commercial antibody panel: a first round with DNAH5, DNALI1, GAS8 and RSPH9, and a second round, if required, with DNAH11 and SPEF2.
  
10. We have observed a genotype-phenotype correlation in our PCD patients. Specific genetic defects correlated with the phenotype of patients, in terms of ciliary structure and function (ciliary beat frequency and pattern) and clinical symptoms. These results were concordant with previous studies.

## **7. REFERENCES**





1. Fliegauf, M.; Benzing, T.; Omran, H. When cilia go bad: Cilia defects and ciliopathies. *Nat. Rev. Mol. Cell Biol.* **2007**, *8*, 880–893, doi:10.1038/nrm2278.
2. Wallmeier, J.; Nielsen, K.G.; Kuehni, C.E.; Lucas, J.S.; Leigh, M.W.; Zariwala, M.A.; Omran, H. Motile ciliopathies. *Nat. Rev. Dis. Prim.* **2020**, *6*, 1–29, doi:10.1038/s41572-020-0209-6.
3. Ibañez-Tallon, I.; Heintz, N.; Omran, H. To beat or not to beat : roles of cilia in development and disease. *Hum. Mol. Genet.* **2003**, *12*, 27–35, doi:10.1093/hmg/ddg061.
4. Shah, A.S.; Ben-Shahar, Y.; Moninger, T.O.; Kline, J.N.; Welsh, M.J. Motile Cilia of Human Airway Epithelia Are Chemosensory. *Science* (80-. ). **2009**, *235*, 1131–1134, doi:10.1126/science.1173869.
5. Mizuno, N.; Taschner, M.; Engel, B.D.; Lorentzen, E. Structural studies of ciliary components. *J. Mol. Biol.* **2012**, *422*, 163–180, doi:10.1016/j.jmb.2012.05.040.
6. Dougherty, G.W.; Loges, N.T.; Klinkenbusch, J.A.; Olbrich, H.; Pennekamp, P.; Menchen, T.; Raidt, J.; Wallmeier, J.; Werner, C.; Westermann, C.; *et al.* DNAH11 Localization in the Proximal Region of Respiratory Cilia Defines Distinct Outer Dynein Arm Complexes. *Am. J. Respir. Cell Mol. Biol.* **2016**, *55*, 213–224, doi:10.1165/rcmb.2015-0353OC.
7. Whitfield, M.; Thomas, L.; Bequignon, E.; Schmitt, A.; Stouvenel, L.; Montantin, G.; Tissier, S.; Duquesnoy, P.; Copin, B.; Chantot, S.; *et al.* Mutations in DNAH17, Encoding a Sperm-Specific Axonemal Outer Dynein Arm Heavy Chain, Cause Isolated Male Infertility Due to Asthenozoospermia. *Am. J. Hum. Genet.* **2019**, *105*, 198–212, doi:10.1016/j.ajhg.2019.04.015.
8. Legendre, M.; Zaragosi, L.E.; Mitchison, H.M. Motile cilia and airway disease. *Semin. Cell Dev. Biol.* **2021**, *110*, 19–33, doi:10.1016/j.semcdb.2020.11.007.
9. Ma, M.; Stoyanova, M.; Rademacher, G.; Dutcher, S.K.; Brown, A.; Zhang, R. Structure of the Decorated Ciliary Doublet Microtubule. *Cell* **2019**, *179*, 909–922.e12, doi:10.1016/j.cell.2019.09.030.
10. Knowles, M.R.; Leigh, M.W.; Ostrowski, L.E.; Huang, L.; Carson, J.L.; Hazucha, M.J.; Yin, W.; Berg, J.S.; Davis, S.D.; Dell, S.D.; *et al.* Exome sequencing identifies mutations in CCDC114 as a cause of primary ciliary dyskinesia. *Am. J. Hum. Genet.* **2013**, *92*, 99–106, doi:10.1016/j.ajhg.2012.11.003.
11. Hjeij, R.; Lindstrand, A.; Francis, R.; Zariwala, M.A.; Liu, X.; Li, Y.; Damerla, R.; Dougherty, G.W.; Abouhamed, M.; Olbrich, H.; *et al.* ARMC4 mutations cause primary ciliary dyskinesia with randomization of left/right body asymmetry. *Am. J. Hum. Genet.* **2013**, *93*, 357–367, doi:10.1016/j.ajhg.2013.06.009.
12. Hjeij, R.; Onoufriadis, A.; Watson, C.M.; Slagle, C.E.; Klena, N.T.; Dougherty, G.W.; Kurkowiak, M.; Loges, N.T.; Diggle, C.P.; Morante, N.F.C.; *et al.* CCDC151 mutations cause primary ciliary dyskinesia by disruption of the outer dynein arm docking complex formation. *Am. J. Hum. Genet.* **2014**, *95*, 257–274, doi:10.1016/j.ajhg.2014.08.005.
13. Wallmeier, J.; Shiratori, H.; Dougherty, G.W.; Edelbusch, C.; Hjeij, R.; Loges, N.T.; Menchen, T.; Olbrich, H.; Pennekamp, P.; Raidt, J.; *et al.* TTC25 Deficiency Results in Defects of the Outer Dynein Arm Docking Machinery and Primary Ciliary Dyskinesia with Left-Right Body Asymmetry

- Randomization. *Am. J. Hum. Genet.* **2016**, *99*, 460–469, doi:10.1016/j.ajhg.2016.06.014.
14. Panizzi, J.R.; Becker-heck, A.; Castleman, V.H.; Al-mutairi, D.; Liu, Y.; Loges, N.T.; Pathak, N.; Austin-tse, C.; Sheridan, E.; Schmidts, M.; *et al.* CCDC103 mutations cause primary ciliary dyskinesia by disrupting assembly of ciliary dynein arms. *Nat. Genet.* **2012**, *44*, 714–719, doi:10.1038/ng.2277.
  15. Thomas, L.; Bouhouche, K.; Whitfield, M.; Thouvenin, G.; Coste, A.; Louis, B.; Szymanski, C.; Bequignon, E.; Papon, J.F.; Castelli, M.; *et al.* TTC12 Loss-of-Function Mutations Cause Primary Ciliary Dyskinesia and Unveil Distinct Dynein Assembly Mechanisms in Motile Cilia Versus Flagella. *Am. J. Hum. Genet.* **2020**, *106*, 153–169, doi:10.1016/j.ajhg.2019.12.010.
  16. Wirschel, M.; Olbrich, H.; Werner, C.; Tritschler, D.; Bower, R.; Sale, W.; Loges, N.T.; Pennekamp, P.; Lindberg, S.; Stenram, U.; *et al.* The nexin-dynein regulatory complex subunit DRC 1 is essential for motile cilia function in algae and humans. *Nat. Genet.* **2013**, *45*, 1–18, doi:10.1038/ng.2533.
  17. Horani, A.; Brody, S.L.; Ferkol, T.W.; Shoseyov, D.; Wasserman, M.G.; Ta-shma, A.; Wilson, K.S.; Bayly, P. V.; Amirav, I.; Cohen-cyberknoh, M.; *et al.* CCDC65 Mutation Causes Primary Ciliary Dyskinesia with Normal Ultrastructure and Hyperkinetic Cilia. *PLoS One* **2013**, *8*, e72299, doi:10.1371/journal.pone.0072299.
  18. Ha, S.; Lindsay, A.M.; Timms, A.E.; Beier, D.R. Mutations in Dnaaf1 and Lrrc48 cause hydrocephalus, laterality defects, and sinusitis in mice. *G3 Genes, Genomes, Genet.* **2016**, *6*, 2479–2487, doi:10.1534/g3.116.030791.
  19. Olbrich, H.; Cremers, C.; Loges, N.T.; Werner, C.; Nielsen, K.G.; Marthin, J.K.; Philipsen, M.; Wallmeier, J.; Pennekamp, P.; Menchen, T.; *et al.* Loss-of-Function GAS8 Mutations Cause Primary Ciliary Dyskinesia and Disrupt the Nexin-Dynein Regulatory Complex. *Am. J. Hum. Genet.* **2015**, *97*, 546–554, doi:10.1016/j.ajhg.2015.08.012.
  20. Merveille, A.C.; Davis, E.E.; Becker-Heck, A.; Legendre, M.; Amirav, I.; Bataille, G.; Belmont, J.; Beydon, N.; Billen, F.; Clément, A.; *et al.* CCDC39 is required for assembly of inner dynein arms and the dynein regulatory complex and for normal ciliary motility in humans and dogs. *Nat. Genet.* **2011**, *43*, 72–78, doi:10.1038/ng.726.
  21. Becker-Heck, A.; Zohn, I.; Okabe, N.; Pollock, A.; Baker, K.; Sullivan-Brown, J.; McSheene, J.; Loges, N.T.; Olbrich, H.; Haeffner, K.; *et al.* The coiled-coil domain containing protein CCDC40 is essential for motile cilia function and left-right axis formation. *Nat. Genet.* **2011**, *43*, 79–84, doi:10.1038/ng.727.The.
  22. Antony, D.; Becker-Heck, A.; Zariwala, M.A.; Schmidts, M.; Onoufriadis, A.; Forouhan, M.; Wilson, R.; Taylor-Cox, T.; Dewar, A.; Jackson, C.; *et al.* Mutations in CCDC39 and CCDC40 are the major cause of primary ciliary dyskinesia with axonemal disorganisation and absent inner dynein arms. *Hum. Mutat.* **2013**, *34*, 462–472, doi:10.1002/humu.22261.
  23. Diener, D.R.; Yang, P.; Geimer, S.; Cole, D.G.; Sale, W.S.; Rosenbaum, J.L. Sequential assembly of flagellar radial spokes. *Cytoskeleton* **2011**, *68*, 389–400, doi:10.1002/cm.20520.
  24. Yang, P.; Diener, D.R.; Yang, C.; Kohno, T.; Pazour, G.J.; Dienes, J.M.; Agrin, N.S.; King, S.M.; Sale,

- W.S.; Kamiya, R.; *et al.* Radial spoke proteins of *Chlamydomonas* flagella. *J. Cell Sci.* **2006**, *119*, 1165–1174, doi:10.1242/jcs.02811.
25. Kott, E.; Legendre, M.; Copin, B.; Moal, F.D.; Montantin, G.; Duquesnoy, P.; Piterboth, W.; Amram, D.; Bassinet, L.; Beucher, J.; *et al.* Loss-of-Function Mutations in RSPH1 Cause Primary Ciliary Dyskinesia with Central-Complex and Radial-Spoke Defects. *Am. J. Hum. Genet.* **2013**, *93*, 561–570, doi:10.1016/j.ajhg.2013.07.013.
26. Castleman, V.H.; Romio, L.; Chodhari, R.; Hirst, R.A.; Castro, S.C.P. De; Parker, K.A.; Ybot-gonzalez, P.; Emes, R.D.; Wilson, S.W.; Wallis, C.; *et al.* Mutations in Radial Spoke Head Protein Genes RSPH9 and RSPH4A Cause Primary Ciliary Dyskinesia with Central-Microtubular-Pair Abnormalities. *Am. J. Hum. Genet.* **2009**, *84*, 197–209, doi:10.1016/j.ajhg.2009.01.011.
27. Cho, E.H.; Huh, H.J.; Jeong, I.; Lee, N.Y.; Koh, W.J.; Park, H.C.; Ki, C.S. A nonsense variant in NME5 causes human primary ciliary dyskinesia with radial spoke defects. *Clin. Genet.* **2020**, *98*, 64–68, doi:10.1111/cge.13742.
28. Jeanson, L.; Copin, B.; Papon, J.F.; Dastot-Le Moal, F.; Duquesnoy, P.; Montantin, G.; Cadranel, J.; Corvol, H.; Coste, A.; Désir, J.; *et al.* RSPH3 Mutations Cause Primary Ciliary Dyskinesia with Central-Complex Defects and a Near Absence of Radial Spokes. *Am. J. Hum. Genet.* **2015**, *97*, 153–162, doi:10.1016/j.ajhg.2015.05.004.
29. El Khouri, E.; Thomas, L.; Jeanson, L.; Bequignon, E.; Vallette, B.; Duquesnoy, P.; Montantin, G.; Copin, B.; Dastot-Le Moal, F.; Blanchon, S.; *et al.* Mutations in DNAJB13, Encoding an HSP40 Family Member, Cause Primary Ciliary Dyskinesia and Male Infertility. *Am. J. Hum. Genet.* **2016**, *99*, 489–500, doi:10.1016/j.ajhg.2016.06.022.
30. Frommer, A.; Hjeij, R.; Loges, N.T.; Edelbusch, C.; Jahnke, C.; Raidt, J.; Werner, C.; Wallmeier, J.; Olbrich, H.; Cindri, S.; *et al.* Immunofluorescence Analysis and Diagnosis of Primary Ciliary Dyskinesia with Radial Spoke Defects. *Am. J. Respir. Cell Mol. Biol.* **2015**, *53*, 563–573, doi:10.1165/rcmb.2014-0483OC.
31. Olbrich, H.; Schmidts, M.; Werner, C.; Onoufriadis, A.; Loges, N.T.; Raidt, J.; Banki, N.F.; Shoemark, A.; Burgoyne, T.; Al Turki, S.; *et al.* Recessive HYDIN mutations cause primary ciliary dyskinesia without randomization of left-right body asymmetry. *Am. J. Hum. Genet.* **2012**, *91*, 672–684, doi:10.1016/j.ajhg.2012.08.016.
32. Cindrić, S.; Dougherty, G.W.; Olbrich, H.; Hjeij, R.; Loges, N.T.; Amirav, I.; Philipsen, M.C.; Marthin, J.K.; Nielsen, K.G.; Sutharsan, S.; *et al.* SPEF2 - and HYDIN -mutant Cilia Lack the Central Pair Associated Protein SPEF2 Aiding PCD Diagnostics. *Am. J. Respir. Cell Mol. Biol.* **2019**, *23*, 1–59, doi:10.1165/rcmb.2019-0086oc.
33. Edelbusch, C.; Cindri, S.; Dougherty, G.W.; Loges, N.T.; Rivlin, J.; Wallmeier, J.; Pennekamp, P.; Amirav, I. Mutation of Serine/Threonine Protein Kinase 36 (STK36) Causes Primary Ciliary Dyskinesia with a Central Pair Defect. *Hum. Mutat.* **2017**, *38*, 964–969, doi:10.1002/humu.23261.
34. Bustamante-Marin, X.M.; Shapiro, A.; Sears, P.; Charng, W.-L.; Conrad, D.F.; Leigh, M.W.; Knowles, M.R.; Ostrowski, L.E.; Zariwala, M.A. Identification of Genetic Variants in CFAP221 as a Cause of Primary Ciliary Dyskinesia. *J. Hu* **2020**, *65*, 175–180, doi:10.1038/s10038-019-0686-1.

35. Owa, M.; Uchihashi, T.; Yanagisawa, H. aki; Yamano, T.; Iguchi, H.; Fukuzawa, H.; Wakabayashi, K. ichi; Ando, T.; Kikkawa, M. Inner lumen proteins stabilize doublet microtubules in cilia and flagella. *Nat. Commun.* **2019**, *10*, 1–10, doi:10.1038/s41467-019-09051-x.
36. Ta-Shma, A.; Hjeij, R.; Perles, Z.; Dougherty, G.W.; Abu Zahira, I.; Letteboer, S.J.F.; Antony, D.; Darwish, A.; Mans, D.A.; Spittler, S.; *et al.* Homozygous loss-of-function mutations in MNS1 cause laterality defects and likely male infertility. *PLoS Genet.* **2018**, *14*, 1–23, doi:10.1371/journal.pgen.1007602.
37. Sigg, M.A.; Menchen, T.; Lee, C.; Johnson, J.; Melissa, K.; Choksi, S.P.; Garcia, G.; Busengdal, H.; Dougherty, G.; Pennekamp, P.; *et al.* Evolutionary proteomics uncovers ancient associations of cilia with signaling pathways. *Dev. Cell* **2017**, *43*, 744–762.e11, doi:10.1016/j.devcel.2017.11.014.
38. Narasimhan, V.; Hjeij, R.; Vij, S.; Loges, N.T.; Wallmeier, J.; Koerner-Rettberg, C.; Werner, C.; Thamilselvam, S.K.; Boey, A.; Choksi, S.; *et al.* Mutations in CCDC11, which encodes a coiled-coil containing ciliary protein, causes situs inversus due to dysmotility of monocilia in the left-right organizer. *Hum. Mutat.* **2015**, *36*, 307–318, doi:10.1002/humu.22738.
39. Reish, O.; Aspit, L.; Zouella, A.; Roth, Y.; Polak-Charcon, S.; Baboushkin, T.; Benyamini, L.; Scheetz, T.E.; Mussaffi, H.; Sheffield, V.C.; *et al.* A Homozygous Nme7 Mutation Is Associated with Situs Inversus Totalis. *Hum. Mutat.* **2016**, *37*, 727–731, doi:doi:10.1002/humu.22998.
40. Gonçalves, J.; Pelletier, L. The ciliary transition zone: Finding the pieces and assembling the gate. *Mol. Cells* **2017**, *40*, 243–253, doi:10.14348/molcells.2017.0054.
41. Bukowy-Bieryłło, Z.; Ziętkiewicz, E.; Loges, N.T.; Wittmer, M.; Geremek, M.; Olbrich, H.; Fliegau, M.; Voelkel, K.; Rutkiewicz, E.; Rutland, J.; *et al.* RPGR mutations might cause reduced orientation of respiratory cilia. *Pediatr. Pulmonol.* **2013**, *48*, 352–363, doi:10.1002/ppul.22632.
42. Vertii, A.; Hung, H.F.; Hehnly, H.; Doxsey, S. Human basal body basics. *Cilia* **2016**, *5*, 1–7, doi:10.1186/s13630-016-0030-8.
43. Bustamante-Marin, X.M.; Yin, W.N.; Sears, P.R.; Werner, M.E.; Brotslaw, E.J.; Mitchell, B.J.; Jania, C.M.; Zeman, K.L.; Rogers, T.D.; Herring, L.E.; *et al.* Lack of GAS2L2 Causes PCD by Impairing Cilia Orientation and Mucociliary Clearance. *Am. J. Hum. Genet.* **2019**, *104*, 229–245, doi:10.1016/j.ajhg.2018.12.009.
44. Budny, B.; Chen, W.; Omran, H.; Fliegau, M.; Tzschach, A.; Wisniewska, M.; Jensen, L.R.; Raynaud, M.; Shoichet, S.A.; Badura, M.; *et al.* A novel X-linked recessive mental retardation syndrome comprising macrocephaly and ciliary dysfunction is allelic to oral-facial-digital type I syndrome. *Hum. Genet.* **2006**, *120*, 171–178, doi:10.1007/s00439-006-0210-5.
45. Deprez, M.; Zaragosi, L.E.; Truchi, M.; Becavin, C.; García, S.R.; Arguel, M.J.; Plaisant, M.; Magnone, V.; Lebrigand, K.; Abelanet, S.; *et al.* A single-cell atlas of the human healthy airways. *Am. J. Respir. Crit. Care Med.* **2020**, *202*, 1636–1645, doi:10.1164/rccm.201911-2199OC.
46. Avasthi, P.; Marshall, W.F. Stages of Ciliogenesis and Regulation of Ciliary Length. *Differentiation* **2012**, *83*, S30–S42, doi:10.1016/j.diff.2011.11.015.
47. Wallmeier, J.; Frank, D.; Shoemark, A.; Nöthe-Menchen, T.; Cindric, S.; Olbrich, H.; Loges, N.T.;

- Apra, I.; Dougherty, G.W.; Pennekamp, P.; *et al.* De Novo Mutations in FOXJ1 Result in a Motile Ciliopathy with Hydrocephalus and Randomization of Left/Right Body Asymmetry. *Am. J. Hum. Genet.* **2019**, *105*, 1030–1039, doi:10.1016/j.ajhg.2019.09.022.
48. Chivukula, R.R.; Montoro, D.T.; Leung, H.M.; Yang, J.; Shamseldin, H.E.; Taylor, M.S.; Dougherty, G.W.; Maimoona, A.; Carson, J.; Daniels, L.A.; *et al.* A human ciliopathy reveals essential functions for NEK10 in airway mucociliary clearance. *Nat. Med.* **2020**, *26*, 244–251, doi:10.1038/s41591-019-0730-x.
49. Huizar, R.L.; Lee, C.; Boulgakov, A.A.; Horani, A.; Tu, F.; Marcotte, E.M.; Brody, S.L.; Wallingford, J.B. A liquid-like organelle at the root of motile ciliopathy. *Elife* **2018**, *7*, 1–24, doi:10.7554/eLife.38497.
50. Loges, N.T.; Olbrich, H.; Becker-Heck, A.; Häffner, K.; Heer, A.; Reinhard, C.; Schmidts, M.; Kispert, A.; Zariwala, M.A.; Leigh, M.W.; *et al.* Deletions and Point Mutations of LRRC50 Cause Primary Ciliary Dyskinesia Due to Dynein Arm Defects. *Am. J. Hum. Genet.* **2009**, *85*, 883–889, doi:10.1016/j.ajhg.2009.10.018.
51. Mitchison, H.M.; Schmidts, M.; Loges, N.T.; Freshour, J.; Dritsoula, A.; Hirst, R.A.; O’Callaghan, C.; Blau, H.; Al Dabbagh, M.; Olbrich, H.; *et al.* Mutations in axonemal dynein assembly factor DNAAF3 cause primary ciliary dyskinesia Hannah. *Nat. Ge* **2012**, *44*, 381–S2, doi:10.1038/ng.1106.
52. Horani, A.; Druley, T.E.; Zariwala, M.A.; Patel, A.C.; Levinson, B.T.; Van Arendonk, L.G.; Thornton, K.C.; Giacalone, J.C.; Albee, A.J.; Wilson, K.S.; *et al.* Whole-exome capture and sequencing identifies HEATR2 mutation as a cause of primary ciliary dyskinesia. *Am. J. Hum. Genet.* **2012**, *91*, 685–693, doi:10.1016/j.ajhg.2012.08.022.
53. Olcese, C.; Patel, M.P.; Shoemark, A.; Kiviluoto, S.; Legendre, M.; Williams, H.J.; Vaughan, C.K.; Hayward, J.; Goldenberg, A.; Emes, R.D.; *et al.* X-linked primary ciliary dyskinesia due to mutations in the cytoplasmic axonemal dynein assembly factor PIH1D3. *Nat. Commun.* **2017**, *8*, 1–15, doi:10.1038/ncomms14279.
54. Paff, T.; Loges, N.T.; Apra, I.; Wu, K.; Bakey, Z.; Haarman, E.G.; Daniels, J.M.A.; Siermans, E.A.; Bogunovic, N.; Dougherty, G.W.; *et al.* Mutations in PIH1D3 Cause X-Linked Primary Ciliary Dyskinesia with Outer and Inner Dynein Arm Defects. *Am. J. Hum. Genet.* **2017**, *100*, 160–168, doi:10.1016/j.ajhg.2016.11.019.
55. Austin-Tse, C.; Halbritter, J.; Zariwala, M.A.; Gilberti, R.M.; Gee, H.Y.; Hellman, N.; Pathak, N.; Liu, Y.; Panizzi, J.R.; Patel-King, R.S.; *et al.* Zebrafish ciliopathy screen plus human mutational analysis identifies C21orf59 and CCDC65 defects as causing primary ciliary dyskinesia. *Am. J. Hum. Genet.* **2013**, *93*, 672–686, doi:10.1016/j.ajhg.2013.08.015.
56. Knowles, M.R.; Ostrowski, L.E.; Loges, N.T.; Hurd, T.; Leigh, M.W.; Huang, L.; Wolf, W.E.; Carson, J.L.; Hazucha, M.J.; Yin, W.; *et al.* Mutations in SPAG1 cause primary ciliary dyskinesia associated with defective outer and inner dynein arms. *Am. J. Hum. Genet.* **2013**, *93*, 711–720, doi:10.1016/j.ajhg.2013.07.025.
57. Kott, E.; Duquesnoy, P.; Copin, B.; Legendre, M.; Dastot-Le Moal, F.; Montantin, G.; Jeanson, L.; Tamalet, A.; Papon, J.F.; Siffroi, J.P.; *et al.* Loss-of-function mutations in LRRC6, a gene essential for proper axonemal assembly of inner and outer dynein arms, cause primary ciliary dyskinesia.

- Am. J. Hum. Genet.* **2012**, *91*, 958–964, doi:10.1016/j.ajhg.2012.10.003.
58. Zariwala, M.A.; Gee, H.Y.; Kurkowiak, M.; Al-Mutairi, D.A.; Leigh, M.W.; Hurd, T.W.; Hjeij, R.; Dell, S.D.; Chaki, M.; Dougherty, G.W.; *et al.* ZMYND10 is mutated in primary ciliary dyskinesia and interacts with LRRC6. *Am. J. Hum. Genet.* **2013**, *93*, 336–345, doi:10.1016/j.ajhg.2013.06.007.
59. Höben, I.M.; Hjeij, R.; Olbrich, H.; Dougherty, G.W.; Nöthe-Menzen, T.; Aprea, I.; Frank, D.; Pennekamp, P.; Dworniczak, B.; Wallmeier, J.; *et al.* Mutations in C11orf70 Cause Primary Ciliary Dyskinesia with Randomization of Left/Right Body Asymmetry Due to Defects of Outer and Inner Dynein Arms. *Am. J. Hum. Genet.* **2018**, *102*, 973–984, doi:10.1016/j.ajhg.2018.03.025.
60. Fassad, M.R.; Shoemark, A.; le Borgne, P.; Koll, F.; Patel, M.; Dixon, M.; Hayward, J.; Richardson, C.; Frost, E.; Jenkins, L.; *et al.* C11orf70 Mutations Disrupting the Intraflagellar Transport-Dependent Assembly of Multiple Axonemal Dyneins Cause Primary Ciliary Dyskinesia. *Am. J. Hum. Genet.* **2018**, *102*, 956–972, doi:10.1016/j.ajhg.2018.03.024.
61. Omran, H.; Kobayashi, D.; Olbrich, H.; Tsukahara, T.; Loges, T.; Hagiwara, H.; Zhang, Q.; Leblond, G.; O’Toole, E.; Hara, C.; *et al.* Ktu/PF13 is required for cytoplasmic pre-assembly of axonemal dyneins. *Nature* **208AD**, *456*, 611–616, doi:10.1038/nature07471.
62. Tarkar, A.; Loges, N.T.; Slagle, C.E.; Francis, R.; Gerard, W.; Tamayo, J. V; Shook, B.; Cantino, M.; Schwartz, D.; Jahnke, C.; *et al.* DYX1C1 is required for axonemal dynein assembly and ciliary motility. *Nat. Genet.* **2013**, *45*, 995–1003, doi:10.1038/ng.2707.
63. Bustamante-Marin, X.M.; Horani, A.; Stoyanova, M.; Charng, W.L.; Bottier, M.; Sears, P.R.; Yin, W.N.; Daniels, L.A.; Bowen, H.; Conrad, D.F.; *et al.* Mutation of CFAP57, a protein required for the asymmetric targeting of a subset of inner dynein arms in *Chlamydomonas*, causes primary ciliary dyskinesia. *PLoS Genet.* **2020**, *16*, 1–27, doi:10.1371/JOURNAL.PGEN.1008691.
64. Moore, A.; Escudier, E.; Roger, G.; Tamalet, A.; Pelosse, B.; Marlin, S.; Clément, A.; Geremek, M.; Delaisi, B.; Bridoux, A.M.; *et al.* RPGR is mutated in patients with a complex X linked phenotype combining primary ciliary dyskinesia and retinitis pigmentosa. *J. Med. Genet.* **2006**, *43*, 326–333, doi:10.1136/jmg.2005.034868.
65. Kuehni, C.E.; Frischer, T.; Strippoli, M.P.F.; Maurer, E.; Bush, A.; Nielsen, K.G.; Escribano, A.; Lucase, J.S.A.; Yiallourous, P.; Omran, H.; *et al.* Factors influencing age at diagnosis of primary ciliary dyskinesia in European children. *Eur. Respir. J.* **2010**, *36*, 1248–1258, doi:10.1183/09031936.00001010.
66. Werner, C.; Lablans, M.; Ataian, M.; Raidt, J.; Wallmeier, J.; Große-onnebrink, J.; Kuehni, C.E.; Haarman, E.G.; Leigh, M.W.; Quittner, A.L.; *et al.* An international registry for primary ciliary dyskinesia. *Eur. Respir. J.* **2016**, *47*, 849–859, doi:10.1183/13993003.00776-2015.
67. Mirra, V.; Werner, C.; Santamaria, F. Primary ciliary dyskinesia: An update on clinical aspects, genetics, diagnosis, and future treatment strategies. *Front. Pediatr.* **2017**, *5*, 1–13, doi:10.3389/fped.2017.00135.
68. Alanin, M.C.; Nielsen, K.G.; von Buchwald, C.; Skov, M.; Aanaes, K.; Høiby, N.; Johansen, H.K. A longitudinal study of lung bacterial pathogens in patients with primary ciliary dyskinesia. *Clin. Microbiol. Infect.* **2015**, *21*, 1093.e1–1093.e7, doi:10.1016/j.cmi.2015.08.020.

69. Lucas, J.S.; Burgess, A.; Mitchison, H.M.; Moya, E.; Williamson, M.; Hogg, C. Diagnosis and management of primary ciliary dyskinesia. *Arch. Dis. Child.* **2014**, *99*, 850–856, doi:10.1136/archdischild-2013-304831.
70. Shapiro, A.J.; Davis, S.D.; Ferkol, T.; Dell, S.D.; Rosenfeld, M.; Olivier, K.N.; Sagel, S.D.; Milla, C.; Zariwala, M.A.; Wolf, W.; *et al.* Laterality defects other than situs inversus totalis in primary ciliary dyskinesia: Insights into situs ambiguus and heterotaxy. *Chest* **2014**, *146*, 1176–1186, doi:10.1378/chest.13-1704.
71. Armengot-Carceller, M.; Reula, A.; Mata-Roig, M.; Pérez-Panadés, J.; Milian-Medina, L.; Carda-Batalla, C. Understanding Primary Ciliary Dyskinesia: Experience From a Mediterranean Diagnostic Reference Centre. *J. Clin. Med.* **2020**, *9*, 810, doi:10.3390/jcm9030810.
72. Werner, C.; Onnebrink, J.G.; Omran, H. Diagnosis and management of primary ciliary dyskinesia. *Cilia* **2015**, *4*, 1–9, doi:10.1186/s13630-014-0011-8.
73. Lobo, J.; Zariwala, M.A.; Noone, P.G. Primary Ciliary Dyskinesia. *Semin. Respir. Crit. Care Med.* **2015**, *36*, 169–179, doi:10.1055/s-0035-1546748.
74. Ostrowski, L.E.; Yin, W.; Patel, M.; Sechelski, J.; Rogers, T.; Burns, K.; Grubb, B.R.; Olsen, J.C. Restoring ciliary function to differentiated Primary Ciliary Dyskinesia cells with a lentiviral vector. *Gene Ther.* **2014**, *21*, 253–261, doi:10.1038/gt.2013.79.
75. Lucas, J.S.; Leigh, M.W. Diagnosis of primary ciliary dyskinesia: Searching for a gold standard. *Eur. Respir. J.* **2014**, *44*, 1418–1422, doi:10.1183/09031936.00175614.
76. Behan, L.; Galvin, A.D.; Rubbo, B.; Masefield, S.; Copeland, F.; Manion, M.; Rindlisbacher, B.; Redfern, B.; Lucas, J.S. Diagnosing primary ciliary dyskinesia: An international patient perspective. *Eur. Respir. J.* **2016**, *48*, 1096–1107, doi:10.1183/13993003.02018-2015.
77. Lucas, J.S.; Barbato, A.; Collins, S.A.; Goutaki, M.; Behan, L.; Caudri, D.; Dell, S.; Eber, E.; Escudier, E.; Hirst, R.A.; *et al.* European Respiratory Society guidelines for the diagnosis of primary ciliary dyskinesia. *Eur. Respir. J.* **2017**, *49*, doi:10.1183/13993003.01090-2016.
78. Shapiro, A.J.; Davis, S.D.; Polineni, D.; Manion, M.; Rosenfeld, M.; Dell, S.D.; Chilvers, M.A.; Ferkol, T.W.; Zariwala, M.A.; Sagel, S.D.; *et al.* Diagnosis of Primary Ciliary Dyskinesia An Official American Thoracic Society Clinical Practice Guideline. *Am. J. Respir. Crit. Care Med.* **2018**, *197*, e24-39, doi:10.1164/rccm.201805-0819ST.
79. Behan, L.; Dimitrov, B.D.; Kuehni, C.E.; Hogg, C.; Carroll, M.; Evans, H.J.; Goutaki, M.; Harris, A.; Packham, S.; Walker, W.T.; *et al.* PICADAR: a diagnostic predictive tool for primary ciliary dyskinesia. *Eur. Respir. J.* **2016**, *47*, 1103–1112, doi:10.1183/13993003.01551-2015.
80. Rademacher, J.; Buck, A.; Schwerk, N.; Price, M.; Fuge, J.; Welte, T.; Ringshausen, F.C. Nasal Nitric Oxide Measurement and a Modified PICADAR Score for the Screening of Primary Ciliary Dyskinesia in Adults with Bronchiectasis. *Pneumologie* **2017**, *71*, 543–548, doi:10.1055/s-0043-111909.
81. Walker, W.T.; Jackson, C.L.; Lackie, P.M.; Hogg, C.; Lucas, J.S. Nitric oxide in primary ciliary dyskinesia. *Eur. Respir. J.* **2012**, *40*, 1024–1032, doi:10.1183/09031936.00176111.



82. Marthin, J.K.; Philipsen, M.C.; Rosthøj, S.; Nielsen, K.G. Infant nasal nitric oxide over time: Natural evolution and impact of respiratory tract infection. *Eur. Respir. J.* **2018**, *51*, 1702503, doi:10.1183/13993003.02503-2017.
83. Beydon, N.; Tamalet, A.; Escudier, E.; Legendre, M.; Thouvenin, G. Breath-holding and tidal breathing nasal NO to screen children for Primary Ciliary Dyskinesia. *Pediatr. Pulmonol.* **2021**, *56*, 2242–2249, doi:10.1002/ppul.25432.
84. Leigh, M.W.; Hazucha, M.J.; Chawla, K.K.; Baker, B.R.; Shapiro, A.J.; Brown, D.E.; Lavange, L.M.; Horton, B.J.; Qaqish, B.; Carson, J.L.; *et al.* Standardizing nasal nitric oxide measurement as a test for primary ciliary dyskinesia. *Ann. Am. Thorac. Soc.* **2013**, *10*, 574–581, doi:10.1513/AnnalsATS.201305-110OC.
85. Sommer, J.U.; Gross, S.; Hörmann, K.; Stuck, B.A. Time-dependent changes in nasal ciliary beat frequency. *Eur. Arch. Oto-Rhino-Laryngology* **2010**, *267*, 1383–1387, doi:10.1007/s00405-010-1211-5.
86. Chilvers, M.A.; Rutman, A.; O’Callaghan, C. Functional analysis of cilia and ciliated epithelial ultrastructure in healthy children and young adults. *Thorax* **2003**, *58*, 333–338, doi:10.1136/thorax.58.4.333.
87. Kempeneers, C.; Seaton, C.; Chilvers, M.A. Variation of Ciliary Beat Pattern in Three Different Beating Planes in Healthy Subjects. *Chest* **2017**, *151*, 993–1001, doi:10.1016/j.chest.2016.09.015.
88. Hogg, C. Primary ciliary dyskinesia: when to suspect the diagnosis and how to confirm it. *Paediatr. Respir. Rev.* **2009**, *10*, 44–50, doi:10.1016/j.prrv.2008.10.001.
89. Stannard, W.A.; Chilvers, M.A.; Rutman, A.R.; Williams, C.D.; O’Callaghan, C. Diagnostic testing of patients suspected of primary ciliary dyskinesia. *Am. J. Respir. Crit. Care Med.* **2010**, *181*, 307–314, doi:10.1164/rccm.200903-0459OC.
90. Raidt, J.; Wallmeier, J.; Hjej, R.; Onnebrink, J.G.; Pennekamp, P.; Loges, N.T.; Olbrich, H.; Häffner, K.; Dougherty, G.W.; Omran, H.; *et al.* Ciliary beat pattern and frequency in genetic variants of primary ciliary dyskinesia. *Eur. Respir. J.* **2014**, *44*, 1579–1588, doi:10.1183/09031936.00052014.
91. Chilvers, M.A.; Rutman, A.; O’Callaghan, C. Ciliary beat pattern is associated with specific ultrastructural defects in primary ciliary dyskinesia. *J. Allergy Clin. Immunol.* **2003**, *112*, 518–524, doi:10.1067/mai.2003.1701.
92. Rubbo, B.; Shoemark, A.; Jackson, C.L.; Hirst, R.; Thompson, J.; Hayes, J.; Frost, E.; Copeland, F.; Hogg, C.; O’Callaghan, C.; *et al.* Accuracy of High-Speed Video Analysis to Diagnose Primary Ciliary Dyskinesia. *Chest* **2019**, *155*, 1008–1017, doi:10.1016/j.chest.2019.01.036.
93. Shapiro, A.J.; Leigh, M.W.; Omran, H.; Lavergne, V.; Knowles, M.R. Errors in Methodology Affect Diagnostic Accuracy of High-Speed Videomicroscopy Analysis in Primary Ciliary Dyskinesia. *Chest* **2019**, *156*, 1032–1033, doi:10.1016/j.chest.2019.06.021.
94. Shapiro, A.J.; Leigh, M.W. Value of transmission electron microscopy for primary ciliary dyskinesia diagnosis in the era of molecular medicine: Genetic defects with normal and non-

- diagnostic ciliary ultrastructure. *Ultrastruct. Pathol.* **2017**, *41*, 373–385, doi:10.1080/01913123.2017.1362088.
95. Shoemark, A.; Boon, M.; Brochhausen, C.; Bukowy-Bieryllo, Z.; de Santi, M.M.; Goggin, P.; Griffin, P.; Hegele, R.G.; Hirst, R.A.; Leigh, M.W.; *et al.* International consensus guideline for reporting transmission electron microscopy results in the diagnosis of Primary Ciliary Dyskinesia (BEAT PCD TEM Criteria). *Eur. Respir. J.* **2020**, *55*, 1900725, doi:10.1183/13993003.00725-2019.
96. Shoemark, A.; Burgoyne, T.; Kwan, R.; Dixon, M.; Patel, M.P.; Rogers, A. V.; Onoufriadis, A.; Scully, J.; Daudvohra, F.; Cullup, T.; *et al.* Primary ciliary dyskinesia with normal ultrastructure: Three-dimensional tomography detects absence of DNAH11. *Eur. Respir. J.* **2018**, *51*, 1701809, doi:10.1183/13993003.01809-2017.
97. Jorissen, M.; Bessems, A. Normal ciliary beat frequency after ciliogenesis in nasal epithelial cells cultured sequentially as monolayer and in suspension. *Acta Otolaryngol.* **1995**, *115*, 66–70, doi:10.3109/00016489509133349.
98. Jorissen, M.; Willems, T.; Van Der Schueren, B. Ciliary function analysis for the diagnosis of primary ciliary dyskinesia: Advantages of ciliogenesis in culture. *Acta Otolaryngol.* **2000**, *120*, 291–295, doi:10.1080/000164800750001116.
99. Pifferi, M.; Bush, A.; Montemurro, F.; Pioggia, G.; Piras, M.; Tartarisco, G.; Cicco, M. Di; Chinellato, I.; Cangiottie, A.M.; Boner, A.L. Rapid diagnosis of primary ciliary dyskinesia: Cell culture and soft computing analysis. *Eur. Respir. J.* **2013**, *41*, 960–965, doi:10.1183/09031936.00039412.
100. Hirst, R.A.; Rutman, A.; Williams, G.; O’Callaghan, C. Ciliated air-liquid cultures as an aid to diagnostic testing of primary ciliary dyskinesia. *Chest* **2010**, *138*, 1441–1447, doi:10.1378/chest.10-0175.
101. Hirst, R.A.; Jackson, C.L.; Coles, J.L.; Williams, G.; Rutman, A.; Goggin, P.M.; Adam, E.C.; Page, A.; Evans, H.J.; Lackie, P.M.; *et al.* Culture of primary ciliary dyskinesia epithelial cells at air-liquid interface can alter ciliary phenotype but remains a robust and informative diagnostic aid. *PLoS One* **2014**, *9*, 1–7, doi:10.1371/journal.pone.0089675.
102. Omran, H.; Loges, N.T. Immunofluorescence Staining of Ciliated Respiratory Epithelial Cells. *Methods Cell Biol.* **2009**, *91*, 123–133, doi:10.1016/S0091-679X(08)91007-4.
103. Damseh, N.; Quercia, N.; Rumman, N.; Dell, S.D.; Kim, R.H. Primary ciliary dyskinesia : mechanisms and management. *Appl. Clin. Genet.* **2017**, *10*, 67–74, doi:10.2147/TACG.S127129.
104. Fliegau, M.; Olbrich, H.; Horvath, J.; Wildhaber, J.H.; Zariwala, M.A.; Kennedy, M.; Knowles, M.R.; Omran, H. Mislocalization of DNAH5 and DNAH9 in respiratory cells from patients with primary ciliary dyskinesia. *Am. J. Respir. Crit. Care Med.* **2005**, *171*, 1343–1349, doi:10.1164/rccm.200411-1583OC.
105. Shoemark, A.; Frost, E.; Dixon, M.; Ollosson, S.; Kilpin, K.; Patel, M.; Scully, J.; Rogers, A. V; Mitchison, H.M.; Bush, A.; *et al.* Accuracy of Immunofluorescence in the Diagnosis of Primary Ciliary Dyskinesia. *Am. J. Respir. Crit. Care Med.* **2017**, *196*, 94–101, doi:10.1164/rccm.201607-1351OC.

106. Liu, Z.; Nguyen, Q.P.H.; Guan, Q.; Albulescu, A.; Erdman, L.; Mahdaviyeh, Y.; Kang, J.; Ouyang, H.; Hegele, R.G.; Moraes, T.; *et al.* A quantitative super-resolution imaging toolbox for diagnosis of motile ciliopathies. *Sci. Transl. Med.* **2020**, *12*, 1–13, doi:10.1126/scitranslmed.aay0071.
107. Knowles, M.R.; Leigh, M.W. Primary Ciliary Dyskinesia Diagnosis Is Color Better Than Black and White? *Am. J. Respir. Crit. Care Med.* **2017**, *196*, 9–10, doi:10.1164/rccm.201702-0426ED.
108. Djakow, J.; Kramna, L.; Dusatkova, L.; Uhlik, J.; Pursiheimo, J.-P.; Svobodova, T.; Pohunek, P.; Cinek, O. An Effective Combination of Sanger and Next Generation Sequencing in Diagnostics of Primary Ciliary Dyskinesia. *Pediatr. Pulmonol.* **2016**, *51*, 498–509, doi:10.1002/ppul.23261.
109. Boaretto, F.; Snijders, D.; Salvorio, C.; Spalletta, A.; Mostacciolo, M.L.; Collura, M.; Cazzato, S.; Gironi, D.; Silvestri, M.; Rossi, G.A.; *et al.* Diagnosis of Primary Ciliary Dyskinesia by a Targeted Next-Generation Sequencing Panel Molecular and Clinical Findings in Italian Patients. *J. Mol. Diagnostics* **2016**, *18*, 912–922, doi:10.1016/j.jmoldx.2016.07.002.
110. Fassad, M.R.; Shoman, W.I.; Morsy, H.; Patel, M.P.; Radwan, N.; Jenkins, L.; Cullup, T.; Fouda, E.; Mitchison, H.M. Clinical and genetic spectrum in 33 Egyptian families with suspected primary ciliary dyskinesia. *Clin. Genet.* **2020**, *97*, 509–515, doi:10.1111/cge.13661.
111. Lucas, J.S.; Davis, S.D.; Omran, H.; Shoemark, A. Primary ciliary dyskinesia in the genomics age. *Lancet Respir. Med.* **2020**, *8*, 202–216, doi:10.1016/S2213-2600(19)30374-1.
112. Fassad, M.R.; Patel, M.P.; Shoemark, A.; Cullup, T.; Hayward, J.; Dixon, M.; Rogers, A. V.; Olsson, S.; Jackson, C.; Goggin, P.; *et al.* Clinical utility of NGS diagnosis and disease stratification in a multiethnic primary ciliary dyskinesia cohort. *J. Med. Genet.* **2020**, *57*, 322–330, doi:10.1136/jmedgenet-2019-106501.
113. Horváth, I.; Barnes, P.J.; Högman, M.; Olin, A.; Amann, A.; Antus, B.; Baraldi, E.; Bikov, A.; Boots, A.W.; Bos, L.D.; *et al.* A European Respiratory Society technical standard : exhaled biomarkers in lung disease. *Eur. Respir. J.* **2017**, *49*, 1600965, doi:10.1183/13993003.00965-2016.
114. Kempeneers, C.; Seaton, C.; Garcia Espinosa, B.; Chilvers, M.A. Ciliary functional analysis : Beating a path towards standardization. *Pediatr. Pulmonol.* **2019**, *54*, 1–12, doi:10.1002/ppul.24439.
115. Bolger, A.M.; Lohse, M.; Usadel, B. Trimmomatic: A flexible trimmer for Illumina sequence data. *Bioinformatics* **2014**, *30*, 2114–2120, doi:10.1093/bioinformatics/btu170.
116. Li, H. Aligning sequence reads, clone sequences and assembly contigs with BWA-MEM. *Oxford University Press* **2013**, *00*, 1–3.
117. McKenna, A.; Hanna, M.; Banks, E.; Sivachenko, A.; Cibulskis, K.; Kernytzky, A.; Garimella, K.; Altshuler, D.; Stacey, G.; Daly, M.; *et al.* The Genome Analysis Toolkit: A MapReduce framework for analyzing next-generation DNA sequencing data. *Genome Res.* **2010**, *20*, 1297–1303, doi:10.1101/gr.107524.110.
118. Wang, K.; Li, M.; Hakonarson, H. ANNOVAR: Functional annotation of genetic variants from high-throughput sequencing data. *Nucleic Acids Res.* **2010**, *38*, 1–7, doi:10.1093/nar/gkq603.

119. Landrum, M.J.; Lee, J.M.; Benson, M.; Brown, G.R.; Chao, C.; Chitipiralla, S.; Gu, B.; Hart, J.; Hoffman, D.; Jang, W.; *et al.* ClinVar: Improving access to variant interpretations and supporting evidence. *Nucleic Acids Res.* **2018**, *46*, D1062–D1067, doi:10.1093/nar/gkx1153.
120. Karczewski, K.J.; Francioli, L.C.; Tiao, G.; Cummings, B.B.; Alfoldi, J.; Wang, Q.; Collins, R.L.; Laricchia, K.M.; Ganna, A.; Birnbaum, D.P.; *et al.* The mutational constraint spectrum quantified from variation in 141,456 humans. *Nature* **2020**, *581*, 434–443, doi:10.1038/s41586-020-2308-7.
121. Karczewski, K.J.; Weisburd, B.; Thomas, B.; Solomonson, M.; Ruderfer, D.M.; Kavanagh, D.; Hamamsy, T.; Lek, M.; Samocha, K.E.; Cummings, B.B.; *et al.* The ExAC browser: Displaying reference data information from over 60 000 exomes. *Nucleic Acids Res.* **2017**, *45*, D840–D845, doi:10.1093/nar/gkw971.
122. Auton, A.; Abecasis, G.R.; Altshuler, D.M.; Durbin, R.M.; Bentley, D.R.; Chakravarti, A.; Clark, A.G.; Donnelly, P.; Eichler, E.E.; Flicek, P.; *et al.* A global reference for human genetic variation. *Nature* **2015**, *526*, 68–74, doi:10.1038/nature15393.
123. Plagnol, V.; Curtis, J.; Epstein, M.; Mok, K.Y.; Stebbings, E.; Grigoriadou, S.; Wood, N.W.; Hambleton, S.; Burns, S.O.; Thrasher, A.J.; *et al.* A robust model for read count data in exome sequencing experiments and implications for copy number variant calling. *Bioinformatics* **2012**, *28*, 2747–2754, doi:10.1093/bioinformatics/bts526.
124. den Dunnen, J.T.; Dalgleish, R.; Maglott, D.R.; Hart, R.K.; Greenblatt, M.S.; McGowan-Jordan, J.; Roux, A.F.; Smith, T.; Antonarakis, S.E.; Taschner, P.E.M. HGVS Recommendations for the Description of Sequence Variants: 2016 Update. *Hum. Mutat.* **2016**, *37*, 564–569, doi:10.1002/humu.22981.
125. Richards, S.; Aziz, N.; Bale, S.; Bick, D.; Das, S.; Gastier-Foster, J.; Grody, W.W.; Hegde, M.; Lyon, E.; Spector, E.; *et al.* Standards and guidelines for the interpretation of sequence variants: A joint consensus recommendation of the American College of Medical Genetics and Genomics and the Association for Molecular Pathology. *Genet. Med.* **2015**, *17*, 405–424, doi:10.1038/gim.2015.30.
126. McKusick, V.A. Mendelian Inheritance in Man and its online version, OMIM. *Am. J. Hum. Genet.* **2007**, *80*, 588–604, doi:10.1086/514346.
127. Stelzer, G.; Rosen, N.; Plaschkes, I.; Zimmerman, S.; Twik, M.; Fishilevich, S.; Iny Stein, T.; Nudel, R.; Lieder, I.; Mazor, Y.; *et al.* The GeneCards suite: From gene data mining to disease genome sequence analyses. *Curr. Protoc. Bioinforma.* **2016**, *54*, 1.30.1-1.30.33, doi:10.1002/cpbi.5.
128. Baz-Redón, N.; Rovira-Amigo, S.; Camats-Tarruella, N.; Fernández-Cancio, M.; Garrido-Pontnou, M.; Antolín, M.; Reula, A.; Armengot-Carceller, M.; Carrascosa, A.; Moreno-Galdó, A. Role of Immunofluorescence and Molecular Diagnosis in the Characterization of Primary Ciliary Dyskinesia. *Arch. Bronconeumol.* **2019**, *55*, 439–441, doi:10.1016/j.arbr.2019.01.007.
129. Hornef, N.; Olbrich, H.; Horvath, J.; Zariwala, M.A.; Fliegauf, M.; Loges, N.T.; Wildhaber, J.; Noone, P.G.; Kennedy, M.; Antonarakis, S.E.; *et al.* DNAH5 mutations are a common cause of primary ciliary dyskinesia with outer dynein arm defects. *Am. J. Respir. Crit. Care Med.* **2006**, *174*, 120–126, doi:10.1164/rccm.200601-084OC.
130. Loges, N.T.; Olbrich, H.; Fenske, L.; Mussaffi, H.; Horvath, J.; Fliegauf, M.; Kuhl, H.; Baktai, G.;

- Peterffy, E.; Chodhari, R.; *et al.* DNAI2 Mutations Cause Primary Ciliary Dyskinesia with Defects in the Outer Dynein Arm. *Am. J. Hum. Genet.* **2008**, *83*, 547–558, doi:10.1016/j.ajhg.2008.10.001.
131. Olm, M.A.K.; Marson, F.A.L.; Athanazio, R.A.; Nakagawa, N.K.; Macchione, M.; Loges, N.T.; Omran, H.; Rached, S.Z.; Bertuzzo, C.S.; Stelmach, R.; *et al.* Severe pulmonary disease in an adult primary ciliary dyskinesia population in Brazil. *Sci. Rep.* **2019**, *9*, 1–11, doi:10.1038/s41598-019-45017-1.
132. Faily, M.; Bartoloni, L.; Letourneau, A.; Munoz, A.; Falconnet, E.; Rossier, C.; De Santi, M.; Santamaria, F.; Sacco, O.; Delozier-Blanchet, C.D.; *et al.* Mutations in DNAH5 account for only 15% of a nonpreselected cohort of patients with primary ciliary dyskinesia. *J. Med. Genet.* **2009**, *46*, 281–286, doi:10.1136/jmg.2008.061176.
133. Rudilla, F.; Franco-Jarava, C.; Martínez-Gallo, M.; Garcia-Prat, M.; Martín-Nalda, A.; Rivière, J.; Aguiló-Cucurull, A.; Mongay, L.; Vidal, F.; Solanich, X.; *et al.* Expanding the Clinical and Genetic Spectra of Primary Immunodeficiency-Related Disorders With Clinical Exome Sequencing: Expected and Unexpected Findings. *Front. Immunol.* **2019**, *10*, 2325, doi:10.3389/fimmu.2019.02325.
134. Baz-Redón, N.; Rovira-Amigo, S.; Paramonov, I.; Castillo-Corullón, S.; Cols-Roig, M.; Antolín, M.; García-Arumí, E.; Torrent-Vernetta, A.; de Mir Messa, I.; Gartner, S.; *et al.* Implementation of a gene panel for genetic diagnosis of primary ciliary dyskinesia. *Arch. Bronconeumol.* **2021**, *57*, 186–194, doi:10.1016/j.arbr.2021.01.003.
135. Baz-Redón, N.; Rovira-Amigo, S.; Fernández-Cancio, M.; Castillo-Corullón, S.; Cols, M.; Caballero-Rabasco, M.A.; Asensio, Ó.; Martín de Vicente, C.; Martínez-Colls, M. del M.; Torrent-Vernetta, A.; *et al.* Immunofluorescence Analysis as a Diagnostic Tool in a Spanish Cohort of Patients with Suspected Primary Ciliary Dyskinesia. *J. Clin. Med.* **2020**, *9*, 3603, doi:10.3390/jcm9113603.
136. Collins, S.A.; Behan, L.; Harris, A.; Gove, K.; Lucas, J.S. The dangers of widespread nitric oxide screening for primary ciliary dyskinesia. *Thorax* **2016**, *71*, 560–561, doi:10.1136/thoraxjnl-2015-208056.
137. Shamseldin, H.E.; Al Mogarri, I.; Alqwaiee, M.M.; Alharbi, A.S.; Baqais, K.; AlSaadi, M.; AlAnzi, T.; Alhashem, A.; Saghier, A.; Ameen, W.; *et al.* An exome-first approach to aid in the diagnosis of primary ciliary dyskinesia. *Hum. Genet.* **2020**, *139*, 1273–1283, doi:10.1007/s00439-020-02170-2.
138. Lehti, M.S.; Zhang, F.P.; Kotaja, N.; Sironen, A. SPEF2 functions in microtubule-mediated transport in elongating spermatids to ensure proper male germ cell differentiation. *Development* **2017**, *144*, 2683–2693, doi:10.1242/dev.152108.
139. Zhang, Y.; Chen, Y.; Zheng, J.; Wang, J.; Duan, S.; Zhang, W.; Yan, X.; Zhu, X. Vertebrate dynein-f depends on Wdr78 for axonemal localization and is essential for ciliary beat. *J. Mol. Cell Biol.* **2019**, *11*, 383–394, doi:10.1093/jmcb/mjy043.
140. Pazour, G.J.; Agrin, N.; Walker, B.L.; Witman, G.B. Identification of predicted human outer dynein arm genes: Candidates for primary ciliary dyskinesia genes. *J. Med. Genet.* **2006**, *43*, 62–73, doi:10.1136/jmg.2005.033001.

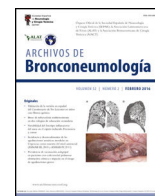
141. Kazatskaya, A.; Kuhns, S.; Lambacher, N.J.; Kennedy, J.E.; Brear, A.G.; McManus, G.J.; Sengupta, P.; Blacque, O.E. Primary Cilium Formation and Ciliary Protein Trafficking Is Regulated by the Atypical MAP Kinase MAPK15 in *Caenorhabditis elegans* and Human Cells. *Genetics* **2017**, *207*, 1423–1440, doi:10.1534/genetics.117.300383/-/DC1.1.
142. Miyatake, K.; Kusakabe, M.; Takahashi, C.; Nishida, E. ERK7 regulates ciliogenesis by phosphorylating the actin regulator CapZIP in cooperation with Dishevelled. *Nat. Commun.* **2015**, *6*, doi:10.1038/ncomms7666.
143. Chang, C.F.; Brown, K.M.; Yang, Y.; Brugmann, S.A. Centriolar Protein C2cd3 Is Required for Craniofacial Development. *Front. Cell Dev. Biol.* **2021**, *9*, 647391, doi:10.3389/fcell.2021.647391.
144. Kouis, P.; Yiallourous, P.K.; Middleton, N.; Evans, J.S.; Kyriacou, K.; Papatheodorou, S.I. Prevalence of primary ciliary dyskinesia in consecutive referrals of suspect cases and the transmission electron microscopy detection rate: a systematic review and meta-analysis. *Pediatr. Res.* **2017**, *81*, 398–405, doi:10.1038/pr.2016.263.
145. Fliegauf, M.; Olbrich, H.; Horvath, J.; Wildhaber, J.H.; Zariwala, M.A.; Kennedy, M.; Knowles, M.R.; Omran, H. Mislocalization of DNAH5 and DNAH9 in Respiratory Cells from Patients with Primary Ciliary Dyskinesia. *Am. J. Respir. Crit. Care Med.* **2005**, *171*, 1343–1349, doi:10.1164/rccm.200411-1583OC.
146. Loges, N.T.; Antony, D.; Maver, A.; Deardorff, M.A.; Güleç, E.Y.; Gezirici, A. Recessive DNAH9 Loss-of-Function Mutations Cause Laterality Defects and Subtle Respiratory Ciliary-Beating Defects. *Am. Journ* **2018**, *103*, 995–1008, doi:10.1016/j.ajhg.2018.10.020.
147. Fassad, M.R.; Shoemark, A.; Legendre, M.; Hirst, R.A.; Koll, F.; Borgne, P.; Louis, B.; Daudvohra, F.; Patel, M.P.; Thomas, L.; *et al.* Mutations in Outer Dynein Arm Heavy Chain DNAH9 Cause Motile Cilia Defects and Situs Inversus. *Am. J. Hum. Genet.* **2018**, *103*, 1–11, doi:10.1016/j.ajhg.2018.10.016.



# **APPENDIX I**







## Original Article

# Implementation of a gene panel for genetic diagnosis of primary ciliary dyskinesia<sup>☆</sup>



Noelia Baz-Redón,<sup>a,b,1</sup> Sandra Rovira-Amigo,<sup>a,b,c,1</sup> Ida Paramonov,<sup>a,d</sup> Silvia Castillo-Corullón,<sup>e</sup> María Cols-Roig,<sup>f</sup> María Antolín,<sup>a,d</sup> Elena García-Arumí,<sup>a,d,g</sup> Alba Torrent-Vernetta,<sup>a,b,c</sup> Inés de Mir Messa,<sup>a,c</sup> Silvia Gartner,<sup>a,c</sup> Ignacio Iglesias-Serrano,<sup>a,c</sup> M. Araceli Caballero-Rabasco,<sup>h</sup> Óscar Asensio de la Cruz,<sup>i</sup> Gerardo Vizmanos-Lamotte,<sup>j</sup> Carlos Martín de Vicente,<sup>k</sup> María del Mar Martínez-Colls,<sup>l</sup> Ana Reula,<sup>m</sup> Amparo Escribano,<sup>e,n</sup> Francisco Dasí,<sup>n,o</sup> Miguel Armengot-Carceller,<sup>m,p,q</sup> Eva Polverino,<sup>a,r</sup> Esther Amengual Pieras,<sup>s</sup> Rosanel Amaro-Rodríguez,<sup>t</sup> Marta Garrido-Pontnou,<sup>u</sup> Eduardo Tizzano,<sup>a,d</sup> Núria Camats-Tarruella,<sup>a,g,2</sup> Mónica Fernández-Cancio,<sup>a,g,2</sup> Antonio Moreno-Galdó<sup>a,b,c,g,\*,2</sup>

<sup>a</sup> Vall d'Hebron Institut de Recerca (VHIR), Hospital Universitari Vall d'Hebron, Barcelona, Spain

<sup>b</sup> Departamento de Pediatría, Obstetricia, Ginecología, Medicina Preventiva y Salud Pública, Universitat Autònoma de Barcelona, Barcelona, Spain

<sup>c</sup> Sección de Alergología Pediátrica, Neumología Pediátrica y Fibrosis Quística, Hospital Universitari Vall d'Hebron, Barcelona, Spain

<sup>d</sup> Área de Genética Clínica y Molecular, Hospital Universitari Vall d'Hebron, Barcelona, Spain

<sup>e</sup> Unidad de Neumología Pediátrica, Hospital Clínico Universitario de Valencia, Universidad de Valencia, Valencia, Spain

<sup>f</sup> Sección de Neumología Infantil y Unidad de Fibrosis Quística, Hospital Sant Joan de Déu, Barcelona, Spain

<sup>g</sup> CIBER de Enfermedades raras, CIBERER, Instituto de Salud Carlos III (ISCIII), Madrid, Spain

<sup>h</sup> Unidad de Neumología Pediátrica, Hospital del Mar, Barcelona, Spain

<sup>i</sup> Unidad de Neumología Pediátrica, Hospital Parc Taulí, Sabadell, Barcelona, Spain

<sup>j</sup> Servicio de Pediatría, Pôle Pédiatrique de Cerdagne - ALEPPA, Osséja, France

<sup>k</sup> Unidad de Neumología Pediátrica, Hospital Miguel Servet, Zaragoza, Spain

<sup>l</sup> Unidad de Neumología Pediátrica, Hospital Germans Trias i Pujol, Badalona, Barcelona, Spain

<sup>m</sup> Grupo de Biomedicina Molecular, Celular y Genómica, IIS La Fe, Universidad de Valencia, Valencia, Spain

<sup>n</sup> Departamento de Fisiología, Universidad de Valencia, Valencia, Spain

<sup>o</sup> UCIM, Instituto de Investigación Sanitaria INCLIVA, Valencia, Spain

<sup>p</sup> Servicio de Otorrinolaringología, Hospital Universitario y Politécnico La Fe, Valencia, Spain

<sup>q</sup> CIBER de Enfermedades Respiratorias, CIBERES, Instituto de Salud Carlos III (ISCIII), Madrid, Spain

<sup>r</sup> Servicio de Neumología, Hospital Universitari Vall d'Hebron, Barcelona, Spain

<sup>s</sup> Hospital de Son Llàtzer, Palma de Mallorca, Balears, Spain

<sup>t</sup> Servicio de Neumología, Hospital Clínic, Barcelona, Spain

<sup>u</sup> Servicio de Anatomía Patológica, Hospital Universitari Vall d'Hebron, Barcelona, Spain

## ARTICLE INFO

## Article history:

Received 12 January 2020

Accepted 18 February 2020

Available online 22 January 2021

## Keywords:

Primary ciliary dyskinesia

Massive sequencing

Gene panel

High-speed optical videomicroscopy

Electron microscopy

## ABSTRACT

**Introduction:** Primary ciliary dyskinesia (PCD) is characterized by an alteration in the ciliary structure causing difficulty in the clearance of respiratory secretions. Diagnosis is complex and based on a combination of techniques. The objective of this study was to design a gene panel including all known causative genes, and to corroborate their diagnostic utility in a cohort of Spanish patients.

**Methods:** This was a multicenter cross-sectional study of patients with a high suspicion of PCD according to European Respiratory Society criteria. We designed a gene panel for massive sequencing using SeqCap EZ capture technology that included 44 genes associated with PCD.

**Results:** We included 79 patients, 53 of whom had a diagnosis of confirmed or highly probable PCD. The sensitivity of the gene panel was 81.1%, with a specificity of 100%. Candidate variants were found in some of the genes of the panel in 43 patients with PCD, 51.2% (22/43) of whom were homozygotes

<sup>☆</sup> Please cite this article as: Baz-Redón N, Rovira-Amigo S, Paramonov I, Castillo-Corullón S, Cols-Roig M, Antolín M, et al. Implementación de un panel de genes para el diagnóstico genético de la discinesia ciliar primaria. Arch Bronconeumol. 2021;57:186–194.

\* Corresponding author.

E-mail address: [amoreno@vhebron.net](mailto:amoreno@vhebron.net) (A. Moreno-Galdó).

<sup>1</sup> These authors should be considered as first co-authors.

<sup>2</sup> These authors should be considered as senior co-authors.

and 48.8% (21/43) compound heterozygotes. The most common causative genes were *DNAH5* and *CCDC39*. We found 52 different variants, 36 of which were not previously described in the literature.

**Conclusions:** The design and implementation of a tailored gene panel produces a high yield in the genetic diagnosis of PCD. This panel provides a better understanding of the causative factors involved in these patients and lays down the groundwork for future therapeutic approaches.

© 2020 SEPAR. Published by Elsevier España, S.L.U. All rights reserved.

## Implementación de un panel de genes para el diagnóstico genético de la discinesia ciliar primaria

### R E S U M E N

#### Palabras clave:

Discinesia ciliar primaria  
Secuenciación masiva  
Panel de genes  
Videomicroscopía óptica de alta velocidad  
Microscopía electrónica

**Introducción:** La discinesia ciliar primaria (DCP) es una enfermedad caracterizada por una alteración en la estructura ciliar que impide el correcto aclaramiento de las secreciones respiratorias. Su diagnóstico es complejo y se basa en una combinación de técnicas. El objetivo de este estudio fue diseñar un panel de genes incluyendo todos los genes causantes conocidos y comprobar su utilidad diagnóstica en una cohorte de pacientes españoles.

**Métodos:** Estudio transversal multicéntrico de pacientes con sospecha elevada de DCP, aplicando los criterios de la European Respiratory Society. Diseño de un panel de genes para secuenciación masiva con la tecnología de captura SeqCap EZ technology, incluyendo 44 genes relacionados con la DCP.

**Resultados:** Se incluyó a 79 pacientes de los que 53 presentaron un diagnóstico de DCP confirmado o muy probable. La sensibilidad del panel de genes fue del 81,1% con una especificidad del 100%. Se encontraron variantes candidatas en alguno de los genes del panel en 43 de los pacientes con DCP, siendo 51,2% (22/43) homocigotos y 48,8% (21/43) heterocigotos compuestos. Los genes causales más frecuentes fueron *DNAH5* y *CCDC39*. Encontramos 52 variantes distintas, 36 no descritas previamente en la literatura.

**Conclusiones:** El diseño y la implementación de un panel de genes a medida tiene un alto rendimiento diagnóstico genético de la DCP, lo que permite conocer mejor la afectación causal de estos pacientes y sentar las bases para futuros abordajes terapéuticos.

© 2020 SEPAR. Publicado por Elsevier España, S.L.U. Todos los derechos reservados.

## Introduction

Primary ciliary dyskinesia (PCD) is a rare disease, occurring in 1/15,000 newborns. It is characterized by an alteration in ciliary structure and function that prevents the correct clearance of respiratory secretions.<sup>1,2</sup> Clinical manifestations include productive cough, chronic rhinitis, recurrent otitis, recurrent bronchitis, bronchiectasis,<sup>3</sup> male infertility, female subfertility, *situs inversus* (50%),<sup>1,2</sup> and heterotaxy (6–12%).<sup>4</sup>

It presents with characteristic symptoms, but some are similar to those of other respiratory diseases: PCD is therefore difficult to diagnose and the process is based on a combination of different tests. The European Respiratory Society (ERS)<sup>5</sup> and the American Thoracic Society (ATS)<sup>6</sup> have made diagnostic recommendations using different approaches and algorithms. In the ERS recommendations, for example, low nasal nitric oxide (nNO) is considered a screening test, while according to the ATS this result can be diagnostic if it is measured with a chemiluminescence analyzer in patients at least 5 years of age, after ruling out cystic fibrosis.<sup>6</sup>

High-speed videomicroscopy (HSVM), which analyzes ciliary beat pattern and beat frequency, is highly sensitive and specific for diagnosis, although its interpretation has a subjective component and results can be altered by respiratory infections.<sup>7</sup> In the opinion of the ERS, an anomalous result on this test is highly suggestive of a diagnosis of PCD,<sup>5</sup> but the ATS does not include it in its algorithm other than as supplementary test.<sup>6</sup> Immunofluorescence study of ciliary proteins is a promising technique,<sup>8,9</sup> although it has not yet been included in the diagnostic recommendations.<sup>5,6</sup>

Currently, the presence of alterations on electron microscopy (EM) (outer dynein arm defects, inner and outer dynein arm defects, inner dynein arm defects with microtubular disorganization, and central pair absence) and the finding of pathogenic variants in the genetic study are considered indicators that confirm PCD.<sup>5,6</sup> While EM is a complex technique that gives numerous false positives and

negatives,<sup>5</sup> genetic studies using massive sequencing technology are opening up new approaches that offer greater diagnostic yield.

PCD is a disease caused by variants in different genes encoding ciliary axoneme proteins. Most genes associated with PCD are autosomal recessive, with the exception of the recently described *PIH1D3* that is linked to the X chromosome,<sup>10</sup> and 2 genes that cause syndromic PCD: *RPGR*, linked to the X chromosome, whose mutations give rise to PCD and retinitis pigmentosa,<sup>11</sup> and *OFD1*, whose mutations cause PCD and intellectual impairment.<sup>12</sup> At present, just over 40 genes associated with PCD that define the molecular diagnosis of approximately 70% of patients have been described.<sup>13</sup>

The aim of this study was to design a massive sequencing panel that includes all known genes causing PCD and to verify their diagnostic usefulness in a cohort of patients with clinical suspicion of PCD.

## Methods

### Patients

We performed a multicenter, cross-sectional study of a cohort of patients with a clinical history indicative of PCD referred for assessment to the PCD diagnostic center of the Hospital Universitari Vall d'Hebron (Barcelona) and the PCD group in Valencia.

The project was approved by the Ethics Committee of the participating hospitals and authorization for inclusion was requested from parents or legal guardians of children under the age of 12; from the parents or guardians and patients aged between 12 and 18; and from patients over 18 years of age.

Patients were included from the Vall d'Hebron Hospital (n = 41), the PCD group in Valencia (n = 14), Hospital Sant Joan de Déu (Esplugues, Barcelona) (n = 14), Hospital Miguel Servet (Zaragoza) (n = 4), Hospital del Mar (Barcelona) (n = 2), Hospital Parc Taulí (Sabadell, Barcelona) (n = 1), Germans Trias i Pujol Hospital

**Table 1**  
List of genes included in the primary ciliary dyskinesia panel.

Gene name	Gene ID	Transcript ID	Protein ID	Number of exons
ARMC4	NG.042820.1	NM.018076.3	NP.060546.2	29
C21orf59/CFAP298	NG.033839.2	NM.021254.2	NP.067077.1	7
CCDC11/CFAP53	NG.042815.1	NM.145020.3	NP.659457.2	8
CCDC39	NG.029581.1	NM.181426.1	NP.852091.1	20
CCDC40	NG.029761.1	NM.017950.3	NP.060420.2	26
CCDC65	NG.033837.1	NM.033124.4	NP.149115.2	8
CCDC103	NG.032792.1	NM.213607.2	NP.998772.1	4
CCDC114	NG.033251.1	NM.144577.3	NP.653178.3	19
CCDC151	NG.041777.1	NM.145045.4	NP.659482.3	14
CCDC164/DRC1	NG.042824.1	NM.145038.3	NP.659475.2	17
CCNO	NG.034201.1	NM.021147.4	NP.066970.3	3
DNAAF1	NG.021174.1	NM.178452.4	NP.848547.4	15
DNAAF2	NG.013070.1	NM.018139.2	NP.060609.2	3
DNAAF3	NG.032759.1	NM.001256714.1	NP.001243643.1	12
DNAAF5	NG.033137.1	NM.017802.3	NP.060272.3	13
DNAH1	NG.052911.1	NM.015512.4	NP.056327.4	81
DNAH5	NG.013081.1	NM.001369.2	NP.001360.1	86
DNAH6	NG.050957.1	NM.001370.1	NP.001361.1	81
DNAH7	NC.000002.12	NM.018897.2		69
DNAH8	NG.041805.1	NM.001206927.1	NP.001193856.1	97
DNAH9	NG.047047.1	NM.001372.3	NP.001363.2	73
DNAH11	NG.012886.2	NM.001277115.1	NP.001264044.1	82
DNAI1	NG.008127.1	NM.012144.3	NP.036276.1	24
DNAI2	NG.016865.1	NM.023036.4	NP.075462.3	17
DNAL1	NG.028083.1	NM.031427.3	NP.113615.2	10
DNAL1	NC.000001.11	NM.003462.3	NP.003453.3	6
DYX1C1/DNAAF4	NG.021213.1	NM.130810.3	NP.570722.2	11
EPB41L4A	NG.052950.1	NM.022140.3	NP.071423.4	26
GAS8	NG.046598.1	NM.001481.2	NP.001472.1	15
HYDIN	NG.033116.2	NM.001270974.1	NP.001257903.1	92
LRRC6	NG.033068.1	NM.012472.4	NP.036604.2	17
MCIDAS	NG.051620.1	NM.001190787.1	NP.001177716.1	17
MNS1	NC.000015.10	NM.018365.2	NP.060835.1	10
NME8	NG.015893.1	NM.016616.4	NP.057700.3	18
OFD1	NG.008872.1	NM.003611.2	NP.003602.1	27
RPGR	NG.009553.1	NM.000328.2	NP.000319.1	18
RSPH1	NG.034257.1	NM.080860.3	NP.543136.1	9
RSPH3	NG.051819.1	NM.031924.4	NP.114130.3	11
RSPH4A	NG.012934.1	NM.001010892.2	NP.001010892.1	7
RSPH9	NG.023436.1	NM.152732.4	NP.689945.2	7
SPAG1	NG.033834.1	NM.172218.2	NP.757367.1	21
TEKT1	NC.000017.11	NM.053285.1	NP.444515.1	8
TTC25	NG.053115.1	NM.031421.3	NP.113609.1	13
ZMYND10	NG.042828.1	NM.015896.2	NP.056980.2	12

ID data were obtained from the National Center for Biotechnology Information (NCBI; <https://www.ncbi.nlm.nih.gov/>) database.  
ID: identification.

(Badalona, Barcelona) (n = 1), Hospital Clínic (Barcelona) (n = 1), and Hospital Son Llàtzer (Palma de Mallorca) (n = 1).

ERS recommendations<sup>5</sup> were followed to classify patients as confirmed (indicative history, diagnostic alterations on EM) or very likely PCD (suggestive history, low nNO, changes on HSVM), or as highly unlikely PCD, based on the evaluation of clinical data and the PICADAR score,<sup>14</sup> nNO, HSVM or EM.

A chemiluminescent nitric oxide analyzer (CLD 88sp NO-analysis, ECO MEDICS AG, Duerten, Switzerland) was used to determine nNO. Ciliary beat pattern and frequency were analyzed with a high-speed digital camera (MotionPro<sup>®</sup> X4, IDT, CA, USA) connected to an optical microscope.

Some data from patients 14 and 15 (Appendix B Table 1S, supplemental material) have been previously published.<sup>9</sup>

#### Massive sequencing and data analysis

DNA was extracted from peripheral blood by magnetic extraction (Chemagic, Perkin-Elmer, Waltham, MA, USA) or by manual extraction using the Quick-DNA<sup>™</sup> Midiprep Plus Kit (Zymo Research, Irvine, CA, USA). DNA concentration was determined with the Qubit dsDNA BR Assay Kit reagent on the Qubit 2.0 fluorometer.

For the genetic study, a panel was designed for the sequencing of exons and their flanking intronic regions ( $\pm 20$  bp) using SeqCap EZ capture technology (Roche NimbleGen, Pleasanton, CA, USA). This panel included 44 genes related to PCD, described in the literature at the time of design (Table 1).

Regions of interest were captured following the commercial protocol (SeqCap EZ [Roche NimbleGen, Pleasanton, CA, USA]), with 21 min enzymatic fragmentation. The library was sequenced using a next-generation MiSeq benchtop sequencer (Illumina, San Diego, CA, USA). The data analysis process included trimming the sequences with Trimmomatic (Institute for Biology, Aachen, Germany),<sup>15</sup> aligning the sequences with the reference human genome GRCh (hg38) using BWA-MEM,<sup>16</sup> detecting variants with the Genome Analysis Toolkit (GATK) Haplotype Caller (Broad Institute, Cambridge, MA, USA),<sup>17</sup> and annotating variants with ANNOVAR.<sup>18</sup> Variants with a coverage less than 20 were not considered in the analysis. The list of identified variants was compared with information from specific databases to identify variants already found to be associated with a known phenotype (HGMD, ClinVar) and population frequency databases (GnomAD, ExAC, 1000 genomes) to rule out variants that are present in the general population at a rate higher than 1%. In parallel, data were also analyzed using VariantStudio v2.2.1 (Illumina<sup>®</sup>, San

**Table 2**  
Clinical characteristics of patients with primary ciliary dyskinesia included in the study.

	Total (n = 53)	Adults (n = 18)	Children (n = 35)	p
Age	15.0 (1–42)	23.0 (18–42)	10 (1–17)	
Sex (women)	41.5%	33.3%	45.7%	0.391
Body mass index <sup>a</sup>		21 (16–28)	-1 (-2, -6)	
Origin (Caucasian)	81.1%	100%	71.4%	0.012
Consanguinity	18.9%	0%	28.6%	0.012
<i>Situs inversus</i>	32.7%	17.6%	40.0%	0.103
Neonatal distress	50%	57.1%	47.0%	0.061
Chronic rhinitis	90.2%	87.5%	91.4%	0.121
Chronic cough	94.2%	94.1%	94.3%	0.371
Sinusitis	23.5%	56.2%	8.6%	< 0.001
Recurrent otitis	52.9%	62.5%	48.6%	0.088
Recurrent bronchitis	47.1%	75%	34.3%	0.002
Recurrent pneumonia	25.0%	41.2%	17.1%	0.066
Bronchiectasis	65.4%	94.1%	51.4%	0.004

The data are expressed as median and range (in brackets) for quantitative variables (age, body mass index) and as a percentage for qualitative variables.

<sup>a</sup> Body mass index is expressed as kg/m<sup>2</sup> in adults and as Z-score in children.

Diego, CA, USA). The pathogenicity of the variants was evaluated using Alamut v2.11 software (Interactive Biosoftware, Rouen, France) which includes Mutation Taster, Polyphen, Aling GVDG and SIFT, and Varsome (Saphetor, Lausanne, Switzerland) which includes DANN, Gerp and MutationTaster. The effect of mutations identified in splicing regions was evaluated by SpliceSiteFinder, MaxEntScan, NNSPLICE, GeneSplicant, and Human Splicing Finder, also included in Alamut v2.11. Massive sequencing data were reanalyzed on ExomeDepth,<sup>19</sup> a bioinformatic platform used to detect copy number variations (CNV). Nomenclature and classification of variants are based on guidelines from the Human Genome Variation Society (HGVS) (<https://www.hgvs.org/>)<sup>20</sup> and the American College of Medical Genetics and Genomics (ACMGG) (<https://www.acmg.net/>).<sup>21</sup>

Probable pathogenic variants were confirmed in patients using Sanger sequencing and, where possible, familial cosegregation was analyzed.

### Statistical analysis

The percentage, median and range, and mean and standard deviation (SD) were used for the description of the variables. To calculate the sensitivity and specificity of the gene panel, cases of confirmed or highly probable PCD were considered as cases diagnosed with PCD. The Chi-squared test was used for comparison between adult and child patients, with a p value < 0.05 being statistically significant. Analyses were conducted using MedCalc Statistical Software version 19.1.3 (MedCalc Software bvba, Ostende, Belgium).

### Results

Between January 2017 and November 2019, 79 patients from 74 different families (74 index cases) and 39 family members were studied. Of the 79 patients, 26 were classified as very unlikely PCD and in all of them the genetic study was negative.

Of the 53 patients with confirmed or highly probable diagnosis of PCD, 35 were children and 18 were adults. Forty-three patients were Caucasian, 4 (7.5%) Moroccan, 4 (7.5%) Pakistani, 1 was from the Middle East, and 1 from Latin America. Ten patients had a family history of consanguinity (Table 2 and Appendix B Table 1S, supplementary material). The most common clinical manifestations were chronic cough and chronic rhinitis. Half of the series had a history of neonatal distress and 32.7% had *situs inversus*. The frequency of bronchiectasis was higher in adult patients (94.1%) than in pediatric patients (51.4%) (Table 2 and Appendix B Table 1S, supplementary material). The PICADAR score was equal to or greater than 5 in 31

patients (65.9%). The value of nNO could be determined in 35 cases, with an average value of 25.9 (SD 29.1) nl/min. In 25 patients, it was less than 33 nl/min and in only 2 was it more than 77 nl/min (Appendix B Table 1S, supplementary material). HSVM and EM findings are listed in Appendix B Table 1S, supplementary material. In 15 cases, the alteration observed on EM was considered diagnostic. HSVM was highly indicative of PCD in 52 patients (not available in patient 3), with the following alterations being found: static pattern (n = 18), static pattern with residual motion (n = 12), stiff, disorganized pattern (n = 8), hyperkinetic pattern (n = 5), rotating pattern (n = 6), dyskinesia (n = 2), and reduced distal movement (n = 1).

DNA samples were sequenced using our gene panel, which covered 98.75% of the exons and flanking intronic areas of the 44 genes included (Table 1). The average coverage of the results was 600x with 80.7% reads on target.

Candidate variants were found in 81.1% (43/53) of patients with PCD in some of the panel genes, with 22 (51.2%) homozygous and 21 (48.8%) compound heterozygous. In 18.9% (10/53) of the patients, no variant was found that could explain the phenotype (Table 3). The sensitivity of the technique was 81.1% (95% CI, 68.0%–90.6%) and specificity was 100% (95% CI, 86.8%–100%). The area under the ROC curve was 0.91 (95% CI, 0.82–0.96). The positive predictive value of the gene panel in our study population, where the prevalence of PCD cases was 67.1%, was 100% and the negative predictive value was 72.2% (95% CI, 59.8%–82.0%). A total of 52 different variants were found (1 in *ARMC4*, 1 in *CCDC114*, 1 in *CCDC151*, 8 in *CCDC39*, 3 in *CCDC40*, 14 in *DNAH5*, 2 in *DNAH9*, 8 in *DNAH11*, 4 in *DNAI2*, 1 in *RPGR*, 3 in *RSPH1*, 1 in *RSPH4A*, 1 in *RSPH9*, 2 in *SPAG1*, and 2 in *TTC25*), 16 of which had previously been associated with PCD<sup>9,22–31</sup> and 36 that had not been previously described in the literature (Table 3). Of the 52 variants found, 14 (26.9%) were non-sense variants, 13 (25%) were frameshift, 13 (25%) splicing, 9 (17.3%) missense, and 3 (5.8%) CNVs. Overall, 51.9% (27/52) were classified as pathogenic (including the 3 CNVs), 21.2% (11/52) as probably pathogenic, and 26.9% (14/52) as variants of uncertain significance (VUS), according to the ACMG classification (Table 3).

Eighteen patients presented variants in genes related to structural proteins of the outer dynein arms (*DNAH5* [n = 9], *DNAH11* [n = 4], *DNAI2* [n = 4], *DNAH9* [n = 1]) and 5 related to the outer dynein arm docking complex (*TTC25* [n = 2], *ARMC4* [n = 1], *CCDC114* [n = 1], *CCDC151* [n = 1]); 8 showed variants in genes encoding radial spoke proteins (*RSPH1* [n = 5], *RSPH4A* [n = 2], *RSPH9* [n = 1]); in 10, variants were detected in genes encoding axoneme regulatory complex proteins (*CCDC39* [n = 7], *CCDC40* [n = 3]); 1 patient presented variants in *SPAG1*, which encodes a protein probably related to the transport or cytoplasmic assembly of dynein complexes, and 1 with variants in *RPGR*, a gene associated with retinitis pigmentosa

**Table 3**  
Results of the genetic study of patients with described variants that correlate with their phenotype.

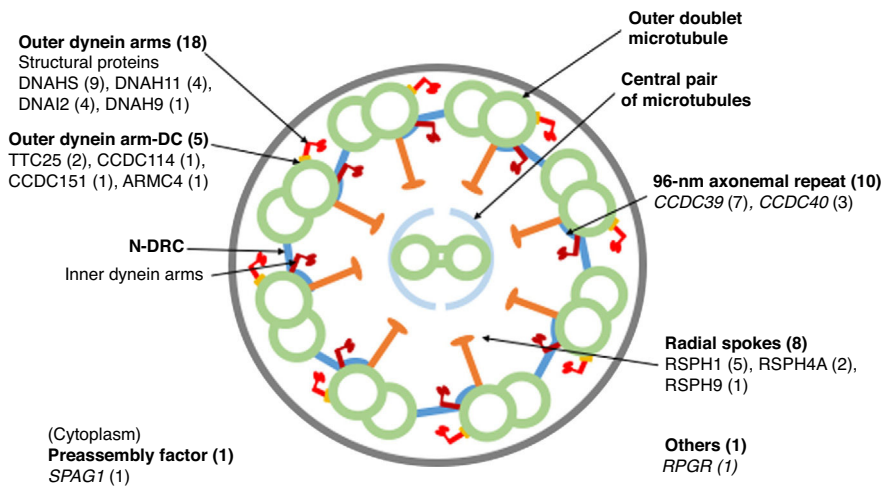
Patient	Origin	Consanguinity/ family	Gene	Zygoty	cDNA change	Protein change	Mutation type	ACMG classification	Familial cosegregation	Other family members	References
1 <sup>a</sup>	Caucasian	N	<i>ARMC4</i>	Hom	c.1669 G>T	p.Glu557Ter	<i>Nonsense</i>	Pathogenic	ND	–	Hjeij et al. <sup>22</sup>
2 <sup>a</sup>	Caucasian	N	<i>CCDC114</i>	Hom	c.1391 +5G>A	–	<i>Splicing</i>	VUS	Parents carriers	–	Knowles et al. <sup>23</sup>
3 <sup>a</sup>	Caucasian	ND	<i>CCDC151</i>	Hom	c.410 G>A	p.Trp137Ter	<i>Nonsense</i>	Prob. pathogenic	Parents carriers	–	Not described
4 <sup>a</sup>	Caucasian	N	<i>CCDC39</i>	Comp het.	c.357 +1G>C c.2505_2506delCA	– p.His835GlnfsTer4	<i>Splicing</i> <i>Frameshift</i>	Pathogenic Prob. pathogenic	Father carrier Mother carrier	–	Merveille et al. <sup>24</sup> Not described
5 <sup>a</sup>	Caucasian	N	<i>CCDC39</i>	Hom	c.2250delT	p.Gln751LysfsTer11	<i>Frameshift</i>	Prob. pathogenic	Parents carriers	–	Not described
6 <sup>a</sup>	Caucasian	N	<i>CCDC39</i>	Hom	c.610-2A>G	–	<i>Splicing</i>	Pathogenic	ND	–	Merveille et al. <sup>24</sup>
7 <sup>a</sup>	Caucasian	N	<i>CCDC39</i>	Comp het.	c.547_548delTT c.1528-2A>G	p.Leu183GlyfsTer3 –	<i>Frameshift</i> <i>Splicing</i>	Prob. pathogenic Pathogenic	ND	–	Not described Not described
8 <sup>a</sup>	Caucasian	N	<i>CCDC39</i>	Comp het.	c.216_217delTT c.357 +1G>C	p.Cys73GlnfsTer6 –	<i>Frameshift</i> <i>Splicing</i>	Prob. pathogenic Pathogenic	Father carrier Father carrier	–	Merveille et al. <sup>24</sup> Merveille et al. <sup>24</sup>
9 <sup>a</sup>	Caucasian	N	<i>CCDC39</i>	Hom	c.357 +1G>C	–	<i>Splicing</i>	Pathogenic	Father carrier	–	Merveille et al. <sup>24</sup>
10 <sup>a</sup>	Caucasian	N	<i>CCDC39</i>	Comp het.	c.547_548delTT c.2596 G>T	p.Leu183GlyfsTer3 p.Glu866Ter	<i>Frameshift</i> <i>Nonsense</i>	Prob. pathogenic Pathogenic	ND	–	Not described Antony et al. <sup>25</sup>
11 <sup>a</sup>	Pakistani	Y	<i>CCDC40</i>	Hom	c.1416delG	p.Ile473PhefsTer2	<i>Frameshift</i>	Pathogenic	Parents carriers	Affected sister/brother carrier	Antony et al. <sup>25</sup>
12	Pakistani	Y / sib 11 y	<i>CCDC40</i>	Hom	c.1416delG	p.Ile473PhefsTer2	<i>Frameshift</i>	Pathogenic	Parents carriers	Affected sister/brother carrier	Antony et al. <sup>25</sup>
13 <sup>a</sup>	Caucasian	N	<i>CCDC40</i>	Comp het.	c.2 T>G 526bp inc. ex.8 and ex.9 del	p.Met1Arg –	<i>Missense</i> <b>CNV</b>	Prob. pathogenic Pathogenic	Father carrier Mother carrier	–	Not described Not described
14 <sup>a</sup>	Caucasian	N	<i>DNAH5</i>	Comp het.	c.12706-2A>T c.4625_4628delGAGA	– p.Arg1542 ThrfsTer6	<i>Splicing</i> <i>Frameshift</i>	Pathogenic Prob. pathogenic	Father carrier Mother carrier	Affected sister	Baz-Redón et al. <sup>9</sup> Baz-Redón et al. <sup>9</sup>
15	Caucasian	N / sib 14 y	<i>DNAH5</i>	Comp het.	c.12706-2A>T c.4625_4628delGAGA	– p.Arg1542 ThrfsTer6	<i>Splicing</i> <i>Frameshift</i>	Pathogenic Prob. pathogenic	Father carrier Mother carrier	Affected sister	Baz-Redón et al. <sup>9</sup> Baz-Redón et al. <sup>9</sup>
16 <sup>a</sup>	Caucasian	N	<i>DNAH5</i>	Comp het.	c.11761 G>C c.13060delG	p.Gly3921Arg p.Ala4354ArgfsTer23	<i>Missense</i> <i>Frameshift</i>	VUS Pathogenic	ND	–	Not described Olm et al. <sup>26</sup>
17 <sup>a</sup>	Caucasian	N	<i>DNAH5</i>	Comp het.	c.2283_2284delAG c.3861 T>G	p.Arg761SerfsTer10 p.Tyr1287Ter	<i>Frameshift</i> <i>Nonsense</i>	Pathogenic Pathogenic	Father carrier Mother carrier	–	Not described Not described
18 <sup>a</sup>	Caucasian	N	<i>DNAH5</i>	Comp het.	c.8311C>T c.10615C>T	p.Arg2771Cys p.Arg3539Cys	<i>Missense</i> <i>Missense</i>	VUS VUS	Mother carrier Mother not carrier	–	Not described Faily et al. <sup>27</sup>
19 <sup>a</sup>	Caucasian	N	<i>DNAH5</i>	Comp het.	c.10813 G>A 3,2 kb inc. ex.2 and ex.3 del	p.Asp3605Asn –	<i>Missense</i> <b>CNV</b>	VUS Pathogenic	Father carrier	–	Raidt et al. <sup>28</sup> Not described
20 <sup>a</sup>	Caucasian	N	<i>DNAH5</i>	Hom	c.13486C>T	p.Arg4496Ter	<i>Nonsense</i>	Pathogenic	Mother carrier	–	Hornef et al. <sup>29</sup>
21 <sup>a</sup>	Caucasian	N	<i>DNAH5</i>	Comp het.	c.2575A>T c.9730 G>T	p.Lys859Ter p.Glu3244Ter	<i>Nonsense</i> <i>Nonsense</i>	Pathogenic Pathogenic	ND	Child carrier	Not described Not described
22 <sup>a</sup>	Caucasian	Y	<i>DNAH5</i>	Hom	3.3 kb inc. ex.29 and ex.30 del	–	<b>CNV</b>	Pathogenic	ND	–	Not described

Table 3 (Continued)

Patient	Origin	Consanguinity/ family	Gene	Zygoty	cDNA change	Protein change	Mutation type	ACMG classification	Familial cosegregation	Other family members	References
23 <sup>a</sup>	Caucasian	N	<i>DNAH9</i>	Comp het.	c.7822-1G>A c.8992C>T	– p.Gln2998Ter	<i>Splicing</i> <i>Nonsense</i>	Pathogenic Pathogenic	ND	–	Not described Not described
24 <sup>a</sup>	Caucasian	N	<i>DNAH11</i>	Comp het.	c.12507+1G>C  c.13412..13415dupAAAC	–  p.Lys4473AsnfsTer11	<i>Splicing</i>  <i>Frameshift</i>	Pathogenic  Prob. pathogenic	Paternal grandmother carrier Paternal grandmother carrier	–	Not described Not described
25 <sup>a</sup>	Caucasian	N	<i>DNAH11</i>	Comp het.	c.927..931delTAAAC c.7645+5G>A	p.Ser312LeufsTer66 –	<i>Frameshift</i> <i>Splicing</i>	Prob. pathogenic VUS	ND	–	Not described Not described
26 <sup>a</sup>	Arab	Y	<i>DNAH11</i>	Comp het.	c.983-1G>T c.3439C>T	– p.Gln1147Ter	<i>Splicing</i> <i>Nonsense</i>	Pathogenic Pathogenic	ND	–	Not described Not described
27 <sup>a</sup>	Caucasian	N	<i>DNAH11</i>	Comp het.	c.3898C>T c.6983+1G>A	p.Gln1300Ter –	<i>Nonsense</i> <i>Splicing</i>	Pathogenic Pathogenic	ND	–	Not described Not described
28 <sup>a</sup>	Pakistani	Y	<i>DNAI2</i>	Hom	c.546C>A	p.Tyr182Ter	<i>Nonsense</i>	Pathogenic	Parents carriers	Affected sister	Not described
29	Pakistani	Y / sib 26 y	<i>DNAI2</i>	Hom	c.546C>A	p.Tyr182Ter	<i>Nonsense</i>	Pathogenic	Parents carriers	Affected sister	Not described
30 <sup>a</sup>	Caucasian	N	<i>DNAI2</i>	Hom	c.346-3T>G	–	<i>Splicing</i>	VUS	ND	–	Loges et al. <sup>30</sup>
31 <sup>a</sup>	Caucasian	N	<i>DNAI2</i>	Comp het.	c.184-14G>A c.740 G>A	– p.Arg247Gln	<i>Splicing</i> <i>Missense</i>	VUS VUS	Father carrier Mother carrier	–	Not described Not described
32 <sup>a</sup>	Caucasian	N	<i>RPGR</i>	Hom	c.920C>A	p.Thr307Lys	<i>Missense</i>	VUS	ND	–	Not described
33 <sup>a</sup>	Caucasian	N	<i>RSPH1</i>	Hom	c.85 G>T	p.Glu29Ter	<i>Nonsense</i>	Pathogenic	ND	–	Kott et al. <sup>31</sup>
34 <sup>a</sup>	Caucasian	N	<i>RSPH1</i>	Hom	c.85 G>T	p.Glu29Ter	<i>Nonsense</i>	Pathogenic	ND	Affected brother	Kott et al. <sup>31</sup>
35	Caucasian	N / sib 32 y	<i>RPSH1</i>	Hom	c.85 G>T	p.Glu29Ter	<i>Nonsense</i>	Pathogenic	ND	Affected brother	Kott et al. <sup>31</sup>
36 <sup>a</sup>	Caucasian	N	<i>RSPH1</i>	Comp het.	c.85 G>T c.275-2A>C	p.Glu29Ter –	<i>Nonsense</i> <i>Splicing</i>	Pathogenic Pathogenic	ND	–	Kott et al. <sup>31</sup> Kott et al. <sup>31</sup>
37 <sup>a</sup>	Caucasian	N	<i>RSPH1</i>	Comp het.	c.70C>T c.275-2A>C	p.Arg24Trp –	<i>Missense</i> <i>Splicing</i>	VUS Pathogenic	ND	–	Not described Kott et al. <sup>31</sup>
38 <sup>a</sup>	Moroccan	Y	<i>RSPH4A</i>	Hom	c.1453C>T	p.Arg485Ter	<i>Nonsense</i>	Pathogenic	ND	Affected sister	Not described
39	Moroccan	Y / sib 36 y	<i>RSPH4A</i>	Hom	c.1453C>T	p.Arg485Ter	<i>Nonsense</i>	Pathogenic	ND	Affected brother	Not described
40 <sup>a</sup>	Moroccan	Y	<i>RSPH9</i>	Hom	c.293..294delITG	p.Val98GlyfsTer14	<i>Frameshift</i>	Prob. pathogenic	ND	–	Not described
41 <sup>a</sup>	Caucasian	N	<i>SPAG1</i>	Comp het.	c.583delA c.1855 G>C	p.Ile195Ter p.Asp619His	<i>Nonsense</i> <i>Missense</i>	Prob. pathogenic VUS	Mother carrier Mother not carrier	–	Not described Not described
42 <sup>a</sup>	Caucasian	N	<i>TTC25</i>	Hom	c.244delA	p.Lys82ArgfsTer29	<i>Frameshift</i>	VUS	Parents carriers	Sister carrier	Not described
43 <sup>a</sup>	Moroccan	N	<i>TTC25</i>	Hom	c.655..659delCTGAC	p.Leu219CysfsTer62	<i>Frameshift</i>	VUS	Parents carriers	–	Not described

–: data missing; ACMG: American College of Medical Genetics; bp: base pairs; Comp het.: compound heterozygote; Ex.: exon; Het: heterozygote; Hom: homozygote; kb: kilobases; ND: no data; Prob. pathogenic: probably pathogenic; sib: sibling; VUS: variant of uncertain significance; y: years of age.

<sup>a</sup> Index patients.



**Fig. 1.** Cross-sectional diagram of a respiratory cilium showing its structural components and genes in which variants have been found. The number of patients with variants in each gene is shown in parentheses. N-DRC: nexin-dynein regulator complex; Outer dynein arm-DC: outer dynein arm docking complex.

(Fig. 1, Table 3). The variants in the 3 most common genes (*DNAH5*, *CCDC39* and *RSPH1*) occurred only in patients of Caucasian origin. In patients of non-Caucasian origin, the most common causative genes were *CCDC40*, *DNAI2* and *RSPH4A*, with 2 cases each.

Thirty-seven family members from 22 different families have been tested using the gene panel. All parents analyzed (18 different families) were carriers of some of the variants found in their children. DNA from the maternal grandparents and the maternal grandmother of patient 24 was analyzed and the variant c.12507+1G>C was determined to be of paternal origin, while the variant c.13412\_13415dupAAAC was of maternal origin (Table 3).

## Discussion

In a cohort of 53 patients with confirmed or highly probable PCD, positive genetic results were obtained in 81.1% of cases using a massive sequencing panel of 44 genes, allowing us to identify the gene causing the ciliary structure defect. In another 26 patients referred for suspicious respiratory symptoms, but with a diagnosis of very unlikely PCD after initial tests, the genetic study was negative. This is the first study, to our knowledge, to describe the genes that cause ciliary dyskinesia in a large cohort of patients in Spain.

Our results have confirmed that, in our population, this gene panel has a high diagnostic yield (sensitivity of 81.1%) and that it was able to rule out all patients with a low suspicion of PCD (specificity of 100%). The yield of gene panels applied to other populations has increased as new genes are discovered and incorporated into panels, and now ranges between 43% and 70%<sup>32–34</sup> and more recently 82%.<sup>35</sup>

The diagnosis of PCD using the techniques available to date is complex and generates many diagnostic uncertainties and doubts among doctors and patients concerning the prognosis and course of the disease. The determination of nNO with a cut-off point 77 nl/min has high sensitivity (93.6%), but a specificity of 78.9%.<sup>36</sup> Electron microscopy is specific (100%), but fails to identify 21% of cases. Furthermore, it must be interpreted by highly skilled operators, and suitable samples are not always obtained.<sup>5,37</sup> HSVM has excellent sensitivity and specificity; however, it also needs expert technicians and often has to be repeated several times.<sup>8</sup> Although genetic studies may fail to identify 20% of cases, they yield a definitive diagnosis and provide clearer guidance for treatment and genetic counselling, and a better groundwork for research into specific treatments, such as gene therapy or protein therapies.<sup>13</sup>

Massive sequencing with the gene panel can be used to study specific variants and small deletions or insertions (*indels*) and copy number variants (CNVs) of genes described to date as causing PCD. With this technique, a proportion of patients with confirmed or highly probable PCD, 18.9% in our series, is left without a genetic diagnosis. In these patients, analysis of the entire exome may help identify new genes that cause PCD.

The majority of the variants described in our patients (82.7%) caused loss of protein function (*nonsense*, *frameshift*, CNV and *splicing*), similar to results described in other studies.<sup>35</sup> In 9 (17.3%) patients, we found missense variants involving the change of a single amino acid that were catalogued as VUS according to the ACMG 21 classification, with the exception of the c.2T>G/p.Met1Arg variant (patient 13) that affected the first amino acid and was classified as probably pathogenic (Table 3). These missense variants were taken into account as a possible cause of protein alteration according to *in silico* predictions. Ideally, these missense defects should be tested *in vitro* in patient nasal respiratory epithelium cell cultures or animal models.

Given the large number of variants that can be identified with massive sequencing, many of which are benign, results can only be interpreted correctly if variants identified correlate with EM and HSVM findings. In our series, a good correlation between ultrastructure and genetic findings was obtained in only 6 cases, given the difficulties of EM interpretation and the possibilities of changes due to respiratory infections or processing artifacts,<sup>9,37</sup> while the HSVM study showed a good correlation with genetic findings in all cases.

Patients 13 and 19, who initially had a single heterozygous variant in genes *CCDC40* and *DNAH5*, respectively, were resolved with a bioinformatics analysis of CNV, as was the case in patient 22. In patients 13 and 19, deletions were described in the other allele that also agreed with the familial segregation study, with the mother of patient 13 and the father of patient 19 being identified as the carriers of these deletions (Table 3). In patient 22, a homozygous deletion was detected in the *DNAH5* gene. Bioinformatics analysis of CNV is a useful tool for resolving some cases, especially those with monoallelic variants in a candidate gene that fits the phenotype.

It should be noted that all cases of consanguinity in our cohort had a positive molecular result and were homozygous for the variants found, all of which were classified as pathogenic or probably pathogenic (Table 3).

The distribution of genes that cause PCD differs depending on ethnicity.<sup>35</sup> In our series, *DNAH5* and *CCDC39* were the most prevalent genes and both were found only in patients of Caucasian origin



(Table 3). *DNAH5* has been described as the most frequent gene in Caucasian studies, explaining 15%–37% of cases,<sup>27,32,33,35</sup> but it is rare in other populations, such as Arabs.<sup>34,35</sup> The *CCDC39* gene has previously been described in patients of European origin<sup>25</sup> and is one of the predominant genes in the population of Arab origin.<sup>34,35</sup>

The limitations of our study are mainly related to the number of patients studied which, although significant for a rare disease, must be expanded to better understand the frequency of the different variants in our population, both Caucasian and non-Caucasian. Massive sequencing cannot detect all deletions/duplications in genes, but this issue has been solved by bioinformatics processing with CNV analysis, although this is only an approximation and it is advisable to confirm findings with other methods. Other limitations are those inherent to gene panel studies, since neither the entire exome and nor the genome are analyzed. However, this facilitates the interpretation of results, since the analysis of the whole exome or genome may contain a very high number of variants that lack pathogenic significance in the healthy population. In gene panels, moreover, coverage is optimized with respect to exome sequencing. Although our custom gene panel has made it possible to determine the specific defect of patients diagnosed using molecular techniques, new PCD genes are described every year,<sup>38–40</sup> so this panel must be expanded with recently discovered data.

In conclusion, the results of this study show the utility of designing and implementing genetic analysis using custom gene panels, which is a useful tool for improving the diagnosis of PCD.

## Funding

This study was funded by a Strategic Action in Health grant from the Instituto de Salud Carlos III (ISCIII) (PI16/O1233), co-funded by the European Regional Development Fund, Operational Program Smart Growth 2014–2020, a grant from the Spanish Society of Pediatric Pulmonology (2016), and a scholarship from the Catalan Pulmonology Foundation (FUCAF) (2016). NCT received support for a Short Term Scientific Mission from COST Action BM1407.

## Conflict of interests

The authors state that they have no conflict of interests.

## Acknowledgements

The authors participate in COST Action BM1407 *Translational research in primary ciliary dyskinesia: bench, bedside, and population perspectives* (BEAT PCD). AMG and SRA participate in ERN-LUNG. This study was part of the Pediatrics, Obstetrics and Gynecology doctoral program at the Universitat Autònoma de Barcelona. We thank Dr. Josep Quer and Damir García-Cehic (Vall d'Hebron Institut de Recerca [VHIR], Barcelona) for their valuable collaboration and for their excellent assistance in massive sequencing techniques.

## Appendix A. Supplementary data

Supplementary material related to this article can be found, in the online version, at doi:<https://doi.org/10.1016/j.arbres.2020.02.010>.

## References

- Lucas JS, Burgess A, Mitchison HM, Moya E, Williamson M, Hogg C. Diagnosis and management of primary ciliary dyskinesia. *Arch Dis Child*. 2014;99:850–6, <http://dx.doi.org/10.1136/archdischild.2013-304831>.
- Reula A, Lucas J, Moreno-Galdó A, Romero T, Milara X, Carda C, et al. New insights in primary ciliary dyskinesia. *Expert Opin Orphan Drugs*. 2017;5:537–48, <http://dx.doi.org/10.1080/21678707.2017.1324780>.
- Martínez-García MA, Máz L, Oliveira C, Girón RM, de la Rosa D, Blanco M, et al. Spanish guidelines on the evaluation and diagnosis of bronchiectasis in adults. *Arch Bronconeumol*. 2018;54:79–87, <http://dx.doi.org/10.1016/j.arbres.2017.07.015>.
- Shapiro AJ, Davis SD, Ferkol T, Dell SD, Rosenfeld M, Olivier KN, et al. Genetic Disorders of Mucociliary Clearance Consortium. Laterality defects other than situs inversus totalis in primary ciliary dyskinesia: insights into situs ambiguus and heterotaxy. *Chest*. 2014;146:1176–86, <http://dx.doi.org/10.1378/chest.13-1704>.
- Lucas JS, Barbato A, Collins SA, Goutaki M, Behan L, Caudri D, et al. European Respiratory Society guidelines for the diagnosis of primary ciliary dyskinesia. *Eur Respir J*. 2017;49, <http://dx.doi.org/10.1183/13993003.01090-2016>.
- Shapiro AJ, Davis SD, Polineni D, Manion M, Rosenfeld M, Dell SD, et al. American Thoracic Society Diagnosis of Primary Ciliary Dyskinesia An official American Thoracic Society Clinical Practice Guideline. *Am J Respir Crit Care Med*. 2018;197:e24–39, <http://dx.doi.org/10.1164/rccm.201805-0819ST>.
- Rubbo B, Shoemark A, Jackson CL, Hirst R, Thompson J, Hayes J, et al. National PCD Service, UK. Accuracy of high-speed video analysis to diagnose primary ciliary dyskinesia. *Chest*. 2019;155:1008–17, <http://dx.doi.org/10.1016/j.chest.2019.01.036>.
- Shoemark A, Frost E, Dixon M, Olsson S, Kilpin K, Patel M, et al. Accuracy of immunofluorescence in the diagnosis of primary ciliary dyskinesia. *Am J Respir Crit Care Med*. 2017;196:94–101, <http://dx.doi.org/10.1164/rccm.201607-1351OC>.
- Baz-Redón N, Rovira-Amigo S, Camats-Tarruella N, Fernández-Cancio M, Garrido-Pontnou M, Antolín M, et al. Role of immunofluorescence and molecular diagnosis in the characterization of primary ciliary dyskinesia. *Arch Bronconeumol*. 2019;55:439–41, <http://dx.doi.org/10.1016/j.arbres.2019.01.021>.
- Olcese C, Patel MP, Shoemark A, Kiviluoto S, Legendre M, Williams HJ, et al. X-linked primary ciliary dyskinesia due to mutations in the cytoplasmic axonemal dynein assembly factor PIH1D3. *Nat Commun*. 2017;8:14279, <http://dx.doi.org/10.1038/ncomms14279>.
- Moore A, Escudier E, Roger G, Tamalet A, Pelosse B, Marlin S, et al. RPGR is mutated in patients with a complex X linked phenotype combining primary ciliary dyskinesia and retinitis pigmentosa. *J Med Genet*. 2006;43:326–33, <http://dx.doi.org/10.1136/jmg.2005.034868>.
- Budny B, Chen W, Omran H, Fliegau M, Tzschach A, Wisniewska M, et al. A novel X-linked recessive mental retardation syndrome comprising macrocephaly and ciliary dysfunction is allelic to oral – facial – digital type I syndrome. *Hum Genet*. 2006;120:171–8, <http://dx.doi.org/10.1007/s00439-006-0210-5>.
- Lucas JS, Davis SD, Omran H, Shoemark A. Primary ciliary dyskinesia in the genomics age. *Lancet Respir Med*. 2019, [http://dx.doi.org/10.1016/S2213-2600\(19\)30374-1](http://dx.doi.org/10.1016/S2213-2600(19)30374-1), pii: S2213-2600(19)30374-1.
- Behan L, Dimitrov BD, Kuehni CE, Hogg C, Carroll M, Evans HJ, et al. PICADAR : a diagnostic predictive tool for primary ciliary dyskinesia. *Eur Respir J*. 2016;47:1103–12, <http://dx.doi.org/10.1183/13993003.01551-2015>.
- Bolger AM, Lohse M, Usadel B. Genome analysis Trimmomatic: a flexible trimmer for Illumina sequence data. *Bioinformatics*. 2014;30:2114–20, <http://dx.doi.org/10.1093/bioinformatics/btu170>.
- Li H. Aligning sequence reads, clone sequences and assembly contigs with BWA-MEM. *arXiv:1303.3997v2 [q-bio.GN]*. 2013;00:1–3.
- Mckenna A, Hanna M, Banks E, Sivachenko A, Cibulskis K, Kernysky A, et al. The Genome Analysis Toolkit: a MapReduce framework for analyzing next-generation DNA sequencing data. *Genome Res*. 2010;1297–303, <http://dx.doi.org/10.1101/gr.107524.110>.
- Wang K, Li M, Hakonarson H. ANNOVAR: functional annotation of genetic variants from high-throughput sequencing data. *Nucleic Acids Res*. 2010;38:e164, <http://dx.doi.org/10.1093/nar/gkq603>.
- Plagnol V, Curtis J, Epstein M, Mok KY, Stebbings E, Grigoriadou S, et al. A robust model for read count data in exome sequencing experiments and implications for copy number variant calling. *Bioinformatics*. 2012;28:2747–54, <http://dx.doi.org/10.1093/bioinformatics/bts526>.
- Den Dunnen JT, Dalgleish R, Maglott DR, Hart RK, Greenblatt MS, et al. HGVS recommendations for the description of sequence variants: 2016 update. *Hum Mutat*. 2016;37:564–9, <http://dx.doi.org/10.1002/humu.22981>.
- Richards S, Aziz N, Bale S, Bick D, Das S. ACMG Standards and Guidelines Standards and guidelines for the interpretation of sequence variants: a joint consensus recommendation of the American College of Medical Genetics and Genomics and the Association for Molecular Pathology. *Genet Med*. 2015;17:405–24, <http://dx.doi.org/10.1038/gim.2015.30>.
- Hjej R, Lindstrand A, Francis R, Zariwala MA, Liu X, Li Y, et al. ARMC4 mutations cause primary ciliary dyskinesia with randomization of left / right body asymmetry. *Am J Hum Genet*. 2013;93:357–67, <http://dx.doi.org/10.1016/j.ajhg.2013.06.009>.
- Knowles MR, Leigh MW, Ostrowski LE, Huang L, Carson JL, Hazucha MJ, et al. Exome sequencing identifies mutations in *CCDC114* as a cause of primary ciliary dyskinesia. *Am J Hum Genet*. 2013;92:99–106, <http://dx.doi.org/10.1016/j.ajhg.2012.11.003>.
- Merveille AC, Davis EE, Becker-Heck A, Legendre M, Amirav I, Bataille G, et al. *CCDC39* is required for assembly of inner dynein arms and the dynein regulatory complex and for normal ciliary motility in humans and dogs. *Nat Genet*. 2011;43:72–8, <http://dx.doi.org/10.1038/ng.726>.
- Antony D, Becker-Heck A, Zariwala MA, Schmidts M, Onoufriadis A, Forouhan M, et al. Mutations in *CCDC39* and *CCDC40* are the major cause of primary ciliary dyskinesia with axonemal disorganization and absent inner dynein arms. *Hum Mutat*. 2013;34:462–72, <http://dx.doi.org/10.1002/humu.22261>.

26. Olm MAK, Marson FAL, Athanzio RA, Nakagawa NK, Macchione M, Loges NT, et al. Severe pulmonary disease in an adult primary ciliary dyskinesia population in Brazil. *Sci Rep*. 2019;9:8693, <http://dx.doi.org/10.1038/s41598-019-45017-1>.
27. Faily M, Bartoloni L, Letourneau A, Munoz A, Falconnet E, Rossier C, et al. Mutations in DNAH5 account for only 15 % of a non- preselected cohort of patients with primary ciliary dyskinesia. *J Med Genet*. 2009;281–6, <http://dx.doi.org/10.1136/jmg.2008.061176>.
28. Raidt J, Wallmeier J, Hjej R, Onnebrink JG, Pennekamp P, Loges NT, et al. Ciliary beat pattern and frequency in genetic variants of primary ciliary dyskinesia. *Eur Respir J*. 2014;44:1579–88, <http://dx.doi.org/10.1183/09031936.00052014>.
29. Hornef N, Olbrich H, Horvath J, Zariwala MA, Fliegauf M, Loges NT, et al. DNAH5 mutations are a common cause of primary ciliary dyskinesia with outer dynein arm defects. *Am J Respir Crit Care Med*. 2006;174:120–6, <http://dx.doi.org/10.1164/rccm.200601-0840C>.
30. Loges NT, Olbrich H, Fenske L, Mussaffi H, Horvath J, Fliegauf M, et al. DNAI2 mutations cause primary ciliary dyskinesia with defects in the outer dynein arm. *Am J Hum Genet*. 2008;83:547–58, <http://dx.doi.org/10.1016/j.ajhg.2008.10.001>.
31. Kott E, Legendre M, Copin B, Moal FD, Montant G, Duquesnoy P, et al. Loss-of-function mutations in RSPH1 cause primary ciliary dyskinesia with central-complex and radial-spoke defects. *Am J Hum Genet*. 2013;93:561–70, <http://dx.doi.org/10.1016/j.ajhg.2013.07.013>.
32. Djakow J, Kramn L, Dusátková L, Uhlík J, Pursiheimo J-P, Svobodová T, et al. An effective combination of sanger and next generation sequencing in diagnostics of primary ciliary dyskinesia. *Pediatr Pulmonol*. 2016;509:498–509, <http://dx.doi.org/10.1002/ppul.23261>.
33. Boaretto F, Snijders D, Salvo C, Spalletta A, Mostacciuolo ML, Collura M, et al. Diagnosis of primary ciliary dyskinesia by a targeted next-generation sequencing panel molecular and clinical findings in Italian patients. *J Mol Diagn*. 2016;18:912–22, <http://dx.doi.org/10.1016/j.jmoldx.2016.07.002>.
34. Fassad MR, Shoman WI, Morsy H, Patel MP, Radwan N, Jenkins L, et al. Clinical and genetic spectrum in 33 Egyptian families with suspected primary ciliary dyskinesia. *Clin Genet*. 2019, <http://dx.doi.org/10.1111/cge.13661>.
35. Fassad MR, Patel MP, Shoemark A, Cullup T, Hayward J, Dixon M, et al. Clinical utility of NGS diagnosis and disease stratification in a multiethnic primary ciliary dyskinesia cohort. *J Med Genet*. 2019, <http://dx.doi.org/10.1136/jmedgenet-2019-106501>, pii:jmedgenet-2019-106501.
36. Collins SA, Behan L, Harris A, Gove K, Lucas JS. The dangers of widespread nitric oxide screening for primary ciliary dyskinesia. *Thorax*. 2016;71:560–1, <http://dx.doi.org/10.1136/thoraxjnl-2015-208056>.
37. Shapiro AJ, Leigh MW. Value of transmission electron microscopy for primary ciliary dyskinesia diagnosis in the era of molecular medicine: genetic defects with normal and non-diagnostic ciliary ultrastructure. *Ultrastruct Pathol*. 2017;41:373–85, <http://dx.doi.org/10.1080/01913123.2017.1362088>.
38. Höben IM, Hjej R, Olbrich H, Dougherty GW, Nöthe-Menchen T, Aprea I, et al. Mutations in C11orf70 cause primary ciliary dyskinesia with randomization of left/right body asymmetry due to defects of outer and inner dynein arms. *Am J Hum Genet*. 2018;102:973–84, <http://dx.doi.org/10.1016/j.ajhg.2018.03.025>.
39. Cindrić S, Dougherty GW, Olbrich H, Hjej R, Loges NT, Amirav I, et al. SPEF2- and HYDIN-mutant cilia lack the central pair associated protein SPEF2 aiding PCD diagnostics. *Am J Respir Cell Mol Biol*. 2019, <http://dx.doi.org/10.1165/rcmb.2019-0086OC>.
40. Wallmeier J, Frank D, Shoemark A, Nöthe-Menchen T, Cindrić S, Olbrich H, et al. De novo mutations in FOXJ1 result in a motile ciliopathy with hydrocephalus and randomization of left/right body asymmetry. *Am J Hum Genet*. 2019;105:1030–9, <http://dx.doi.org/10.1016/j.ajhg.2019.09.022>.



## **APPENDIX II**





Article

# Immunofluorescence Analysis as a Diagnostic Tool in a Spanish Cohort of Patients with Suspected Primary Ciliary Dyskinesia

Noelia Baz-Redón <sup>1,2,†</sup>, Sandra Rovira-Amigo <sup>1,2,3,4,†</sup>, Mónica Fernández-Cancio <sup>1,4</sup>,  
Silvia Castillo-Corullón <sup>5</sup>, Maria Cols <sup>6</sup>, M. Araceli Caballero-Rabasco <sup>7</sup>, Óscar Asensio <sup>8</sup>,  
Carlos Martín de Vicente <sup>9</sup>, Maria del Mar Martínez-Colls <sup>10</sup>, Alba Torrent-Vernetta <sup>1,2,3,4</sup>,  
Inés de Mir-Messa <sup>1,3</sup>, Silvia Gartner <sup>1,3</sup>, Ignacio Iglesias-Serrano <sup>1,3</sup>, Ana Díez-Izquierdo <sup>1,3</sup>,  
Eva Polverino <sup>1,11</sup>, Esther Amengual-Pieras <sup>12</sup>, Rosanel Amaro-Rodríguez <sup>13</sup>,  
Montserrat Vendrell <sup>14,15,16</sup>, Marta Mumany <sup>17</sup>, María Teresa Pascual-Sánchez <sup>18</sup>,  
Belén Pérez-Dueñas <sup>1,3</sup>, Ana Reula <sup>19,20</sup>, Amparo Escribano <sup>5,20,21</sup>, Francisco Dasi <sup>20,21</sup>,  
Miguel Armengot-Carceller <sup>16,19,20,22</sup>, Marta Garrido-Pontnou <sup>23</sup>, Núria Camats-Tarruella <sup>1,4,‡</sup>  
and Antonio Moreno-Galdó <sup>1,2,3,4,\*,‡</sup>

- <sup>1</sup> Vall d'Hebron Institut de Recerca (VHIR), Vall d'Hebron Hospital Universitari, Vall d'Hebron Barcelona Hospital Campus, 08035 Barcelona, Spain; noelia.baz@vhir.org (N.B.-R.); srovi@yahoo.es (S.R.-A.); mfcancio75@gmail.com (M.F.-C.); atorrentvernetta@gmail.com (A.T.-V.); idemir@vhebron.net (I.d.M.-M.); silviagartner@gmail.com (S.G.); nachotela@gmail.com (I.I.-S.); anadiezizquierdo@gmail.com (A.D.-I.); evapo74@gmail.com (E.P.); belen.perez@vhir.org (B.P.-D.); nuria.camats@vhir.org (N.C.-T.)
- <sup>2</sup> Department of Pediatrics, Obstetrics, Gynecology, Preventative Medicine and Public Health. Universitat Autònoma de Barcelona, 08193 Barcelona, Spain
- <sup>3</sup> Department of Pediatrics, Vall d'Hebron Hospital Universitari, Vall d'Hebron Barcelona Hospital Campus, 08035 Barcelona, Spain
- <sup>4</sup> CIBER of Rare Diseases (CIBERER), Instituto de Salud Carlos III (ISCIII), 28029 Madrid, Spain
- <sup>5</sup> Pediatric Pulmonology Unit, Hospital Clínico Universitario de Valencia, 46010 Valencia, Spain; castillo\_sil@gva.es (S.C.-C.); aescribano@separ.es (A.E.)
- <sup>6</sup> Pediatric Pulmonology Department and Cystic Fibrosis Unit, Hospital Sant Joan de Déu, 08950 Barcelona, Spain; MCols@sjdhospitalbarcelona.org
- <sup>7</sup> Pediatric Pulmonology Unit, Department of Pediatrics, Hospital del Mar, 08003 Barcelona, Spain; MACaballeroRabasco@parcdesalutmar.cat
- <sup>8</sup> Pediatric Pulmonology Unit, Hospital Parc Taulí de Sabadell, 08208 Sabadell, Spain; oasensio58@gmail.com
- <sup>9</sup> Pediatric Pulmonology Unit, Hospital Miguel Servet, 50009 Zaragoza, Spain; carl\_zaragoza@yahoo.es
- <sup>10</sup> Pediatric Pulmonology Unit, Hospital Germans Trias i Pujol, 08916 Badalona, Spain; mimarmartinez@gmail.com
- <sup>11</sup> Pneumology Department, Vall d'Hebron Hospital Universitari, Vall d'Hebron Barcelona Hospital Campus, 08035 Barcelona, Spain
- <sup>12</sup> Department of Pediatrics, Hospital Universitario Son Llàtzer, 07198 Palma de Mallorca, Spain; eamengua@hsl.es
- <sup>13</sup> Pneumology Department, Hospital Clínic, 08036 Barcelona, Spain; ramaro@clinic.cat
- <sup>14</sup> Pneumology Department, Hospital Josep Trueta, 17007 Girona, Spain; mvendrell.girona.ics@gencat.cat
- <sup>15</sup> Girona Biomedical Research Institute (IDIBGI), Universitat de Girona, 17190 Girona, Spain
- <sup>16</sup> CIBER of Respiratory Diseases (CIBERES), Instituto de Salud Carlos III (ISCIII), 28029 Madrid, Spain; miguel.armengot@gmail.com
- <sup>17</sup> Pediatric Pulmonology Unit, Consorci Sanitari de Terrassa, 08191 Terrassa, Spain; 39769mme@comb.cat
- <sup>18</sup> Pediatric Pulmonology Unit, Hospital Universitari Sant Joan de Reus, 43204 Tarragona, Spain; maitepasc@gmail.com
- <sup>19</sup> Grupo de Biomedicina Molecular, Celular y Genómica, IIS La Fe, 46026 Valencia, Spain; areumar91@gmail.com
- <sup>20</sup> Department of Paediatrics, Obstetrics and Gynecology, Universitat de Valencia, 46010 Valencia, Spain; Dasi@uv.es
- <sup>21</sup> UCIM, Rare Respiratory Diseases Research Group, Instituto de Investigación Sanitaria INCLIVA, 46010 Valencia, Spain

<sup>22</sup> Otorhinolaryngology Department, Hospital Universitario y Politécnico La Fe, 46026 Valencia, Spain

<sup>23</sup> Department of Pathology, Vall d'Hebron Hospital Universitari, Vall d'Hebron Barcelona Hospital Campus, 08035 Barcelona, Spain; magarrido@vhebron.net

\* Correspondence: amoreno@vhebron.net

† These authors contributed equally to this work.

‡ Co-last authors.

Received: 20 October 2020; Accepted: 6 November 2020; Published: 9 November 2020



**Abstract:** Primary ciliary dyskinesia (PCD) is an autosomal recessive rare disease caused by an alteration of ciliary structure. Immunofluorescence, consisting in the detection of the presence and distribution of cilia proteins in human respiratory cells by fluorescence, has been recently proposed as a technique to improve understanding of disease-causing genes and diagnosis rate in PCD. The objective of this study is to determine the accuracy of a panel of four fluorescently labeled antibodies (DNAH5, DNALI1, GAS8 and RSPH4A or RSPH9) as a PCD diagnostic tool in the absence of transmission electron microscopy analysis. The panel was tested in nasal brushing samples of 74 patients with clinical suspicion of PCD. Sixty-eight (91.9%) patients were evaluable for all tested antibodies. Thirty-three cases (44.6%) presented an absence or mislocation of protein in the ciliary axoneme (15 absent and 3 proximal distribution of DNAH5 in the ciliary axoneme, 3 absent DNAH5 and DNALI1, 7 absent DNALI1 and cytoplasmatic localization of GAS8, 1 absent GAS8, 3 absent RSPH9 and 1 absent RSPH4A). Fifteen patients had confirmed or highly likely PCD but normal immunofluorescence results (68.8% sensitivity and 100% specificity). In conclusion, immunofluorescence analysis is a quick, available, low-cost and reliable diagnostic test for PCD, although it cannot be used as a standalone test.

**Keywords:** cilia; primary ciliary dyskinesia; PCD; immunofluorescence; antibody

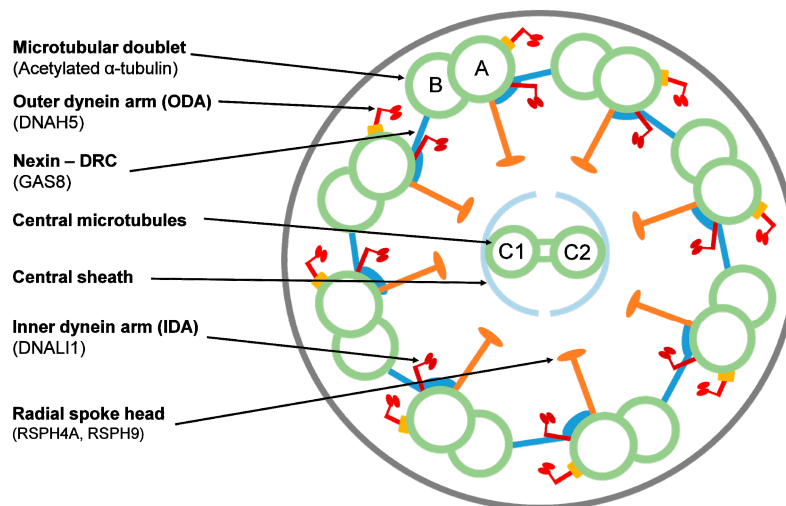
## 1. Introduction

Primary ciliary dyskinesia (PCD) is an autosomal recessive rare disease (1/15,000) caused by an alteration of ciliary structure, which impairs mucociliary clearance [1,2]. Symptoms of PCD may include persistent wet cough from early infancy, recurrent respiratory infections, bronchiectasis, chronic rhinosinusitis, persistent otitis media with effusion and associated conductive hearing loss, male infertility, female subfertility, situs inversus in half of PCD patients [1–3] and heterotaxic defects in 6–12% of cases [4].

Diagnosis is often delayed, with the possibility of an impairment of lung function [1], because of non-specificity of PCD symptoms and limitations of the available techniques [5]. According to the European Respiratory Society (ERS), PCD diagnosis is commonly based on studying the ciliary function by high-speed video-microscopy (HSVM) and ciliary ultrastructure by transmission electron microscopy (TEM) [6]. As there is not a unique gold standard diagnostic test, the ERS [6] and the American Thoracic Society (ATS) [7] have recently proposed the use of different diagnostic techniques to improve the accuracy and diagnosis rate of PCD.

Immunofluorescence (IF) is a technique consisting in the use of fluorescently labeled antibodies for the detection of the presence and distribution of different ciliary proteins in human respiratory cells by fluorescence or confocal microscopy, and it has been recently proposed as a tool to improve the diagnosis rate in PCD and facilitate a better understanding of disease-causing genes [6,7]. Motile respiratory cilia (9 + 2 cilia) are composed of nine peripheral microtubular doublets (composed of A and B tubules) and a central pair (C1 and C2) surrounded by a protein central sheath. An important number of protein complexes are distributed among these microtubule structures: the outer (ODA) and inner dynein arms (IDA), the nexin links, the central sheath and the radial spokes [8,9] (Figure 1).

The methodology for IF staining of ciliated respiratory epithelial cells was first described by Omran and Loges [10]. Nowadays, an important number of antibodies against different cilia proteins are available, including antibodies against proteins in ODA, IDA, radial spoke head and dynein regulatory complex [6]. IF is cheaper and easier than other techniques and the use of IF as a diagnostic test in PCD is likely to increase as more antibodies become available [6]. However, studies on the use of IF in diagnostic settings and IF validation studies are necessary to consider IF as a diagnostic tool for PCD in diagnostic cohort studies [6]. The ATS considers the IF as one of the emerging PCD diagnosis techniques, although it has emphasized the lack of consensus on a gold standard for diagnosis and the insufficient sensitivity and specificity when applied to the general population [7].



**Figure 1.** Ciliary axoneme in transverse section indicating the ultrastructural parts and the target proteins by immunofluorescence. Proteins are indicated in parentheses. DRC = dynein regulatory complex. A and B: outer microtubule doublets; C1 and C2: central pair.

A study by Shoemark et al. demonstrated that IF is a useful diagnostic technique and presents the same accuracy as well-performed TEM analysis, which is why the authors support IF as a routine diagnostic test for PCD, especially when TEM expertise or equipment is not available [5]. To our knowledge, this is the only study evaluating the accuracy of conventional IF for the diagnosis of PCD. In a recent study, Liu et al. presented a quantitative super-resolution imaging workflow for the detection of cilia defects thanks to the validation of 21 commercially available IF antibodies. Molecular defects using this super-resolution imaging toolbox were described in 31 clinical PCD cases, including patients with negative TEM results and/or with genetic variants of uncertain significance (VUS) [11].

We hypothesized that an IF panel would be a useful technique to study the cilia structure and improve PCD diagnosis, especially in settings with low availability of TEM results. Our aim was to establish the utility and accuracy for PCD diagnosis of an IF panel in a Spanish cohort of patients with suspected PCD in relation to clinical characteristics, genetics and/or HSVM.

## 2. Experimental Section

### 2.1. Patients

This study belongs to a prospective multicentric study including all 74 consecutive patients with a clinical history suggestive of PCD during the period from 2016 to 2020.

This project was approved by the Clinical Research Ethics Committee (CEIC) of Hospital Universitari Vall d'Hebron (PR(AMI)148/2016). Written informed consent was obtained from  $\geq 18$ -year-old patients, from  $\geq 12$ -year-old patients and their parents or guardians and from  $< 12$ -year-old patients' parents or guardians.



The majority of patients attended the Hospital Universitari Vall d'Hebron (HUVH), and patients and samples from other hospitals from Spain were also analyzed: Hospital Sant Joan de Déu (Esplugues de Llobregat, Barcelona), Hospital del Mar (Barcelona), Hospital Parc Taulí (Sabadell, Barcelona), Hospital Germans Trias i Pujol (Badalona, Barcelona), Hospital Clínic (Barcelona), Hospital Miguel Servet (Zaragoza), Hospital Josep Trueta (Girona), Hospital Universitari Sant Joan de Reus (Reus, Tarragona), Consorci Sanitari de Terrassa (Terrasa, Barcelona) and PCD group Valencia (Hospital Universitario y Politécnico la Fe, Hospital Clínico Universitario de Valencia and INCLIVA).

## 2.2. PCD Diagnostic Evaluation

Patients were evaluated for PCD with a clinical symptoms questionnaire and PICADAR (PrImary CiliARy DyskinesiA Rule) score [12], nasal nitric oxide (nNO), high-speed video-microscopy analysis (HSVM) and genetic testing. In our setting, TEM analysis was available only in a few cases because of logistic difficulties.

ERS guidelines [6] were followed to classify patients as: confirmed PCD (suggestive clinical history with hallmark ciliary ultrastructure defects assessed by TEM and/or presence of pathogenic bi-allelic variants in PCD-associated genes); highly likely PCD (suggestive history with very low nNO and HSVM findings consistently suggestive of PCD after repeated analysis or cell culture); or highly unlikely PCD (weak clinical history, normal nNO and normal HSVM).

Nasal nitric oxide (nNO) measurements were performed using CLD 88sp NO-analyzer (ECO MEDICS, AG, Duerten, Switzerland) according to ERS guidelines [13].

Genetic testing was performed with a high-throughput 44 PCD gene panel using the SeqCap EZ Technology (Roche Nimblegen, Pleasanton, CA, USA) as previously described [14]. Genetic results for most of the patients included in this study have been previously published [14].

HSVM was performed to study ciliary beat frequency (CBF) and ciliary beat pattern (CBP) (local normal values: CBF 8.7–18.8 Hz; CBP  $\leq$ 20% dyskinetic ciliated cells). Nasal respiratory epithelia were sampled at the inferior nasal meatus with a 2 mm diameter brush submerged in HEPES-supplemented Medium199. A minimum of ten lateral strips with 10 cells each and two overhead axes were captured at 37 °C with an optical microscope coupled to a high-speed video camera (MotionPro<sup>®</sup> X4, IDT, CA, USA) using MotionPro<sup>®</sup> X4 software [15].

## 2.3. Immunofluorescence Technique and Analysis

Nasal-brush respiratory epithelial samples were spread or dropped, air dried and stored at  $-80$  °C until use. Cells were fixed with 4% PFA for 15 min at room temperature (RT), washed 4 times with 1xPBS, permeabilized with 0.2% TritonX100 for 10 min at RT and blocked with 1% fat-free skim milk in PBS overnight at  $+4$  °C to avoid nonspecific binding. Samples were incubated with primary antibodies (all Sigma Aldrich, St. Louis, MO, USA) for 4 h at RT using the following dilutions in 1% skim milk: anti-DNAH5 antibody 1:200, anti-DNALI1 1:100, anti-GAS8 1:200, anti-RSPH4A 1:200 and anti-RSPH9 1:70.

We washed 5 times with 1xPBS at RT (2 washes of 10 min), and all slides were incubated for 45 min at RT with 1:2500 anti-acetylated tubulin antibody (Sigma Aldrich) for cilia localization. After 5 more washes with 1xPBS at RT (2 washes of 10 min), cells were incubated for 30 min at RT with secondary monoclonal anti-rabbit Alexa Fluor 594 and anti-mouse Alexa Fluor 488 antibodies (Thermo Fisher, Waltham, MA, USA). Nuclei DNA was stained with Prolong antifade DAPI (Thermo Fisher).

Slides were analyzed using a fluorescence microscope at X100 magnification. A minimum of ten cells were analyzed for each target protein. The results were considered: (1) normal or present when the protein was present in 8 or more cells, (2) absent or aberrant when the protein was completely absent in the ciliary axoneme or had an abnormal distribution in 8 or more cells, (3) inconclusive when results differed from previously described ones, and (4) insufficient when less than ten cells were observed. In inconclusive or insufficient cases, IF was repeated when possible, following recommendations by Shoemark et al. [5].

Patients were analyzed using antibodies against component proteins for the different structures of the ciliary axoneme: DNAH5 (an ODA component), DNALI1 (an IDA component), GAS8 (a nexin-dynein regulatory complex component) and radial spoke head components RSPH4A (42 patients), RSPH9 (31 patients) or both (1 patient). When this analysis was designed, we specifically chose and optimized these commercial antibodies to detect most cilia defects, following Shoemark et al. [5] and expert recommendations. Anti-acetylated tubulin antibody was used to localize the microtubular doublet (protein location shown in Figure 1).

#### 2.4. Data Analysis

Confirmed and highly likely PCD cases were considered as positive for calculation of sensitivity and specificity. Data were analyzed by using MedCalc Statistical Software version 19.5.3 (MedCalc Software bvba, Ostend, Belgium).

### 3. Results

Immunofluorescence analysis was performed in a cohort of 74 PCD-suspected patients. Sixty-six percent of patients included in this study were <18 years old (49/74) and the mean age at study was 17.9 years (range 1–63).

After PCD diagnostic evaluation, 25 patients were considered as confirmed PCD, 25 as highly likely and 24 as highly unlikely PCD (Table 1).

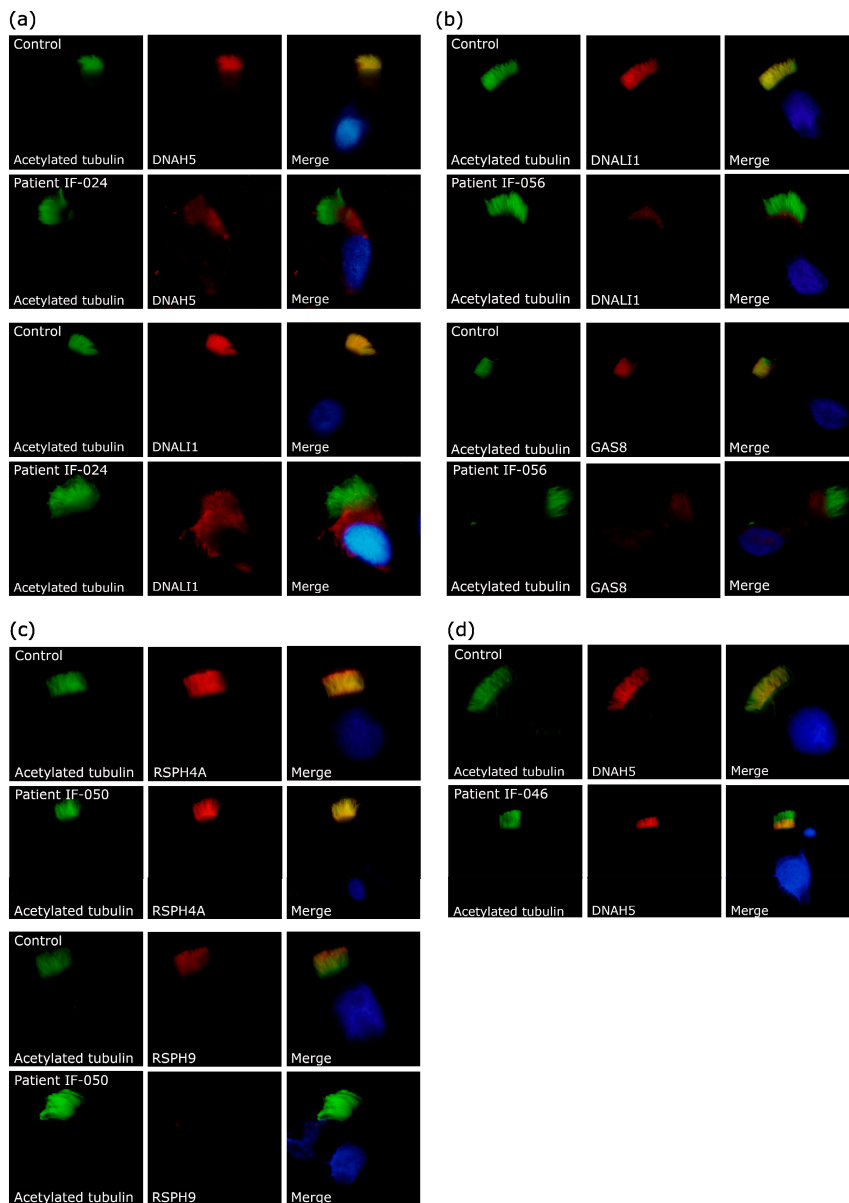
**Table 1.** Immunofluorescence results from 74 primary ciliary dyskinesia (PCD) suspected patients related to the results of the PCD diagnostic evaluation.

Immunofluorescence Test Outcome (n = 74)	PCD Diagnostic Evaluation			
	Confirmed (n = 25)	Highly Likely (n = 25)	Highly Unlikely (n = 24)	
Evaluable/Closed	68 (91.9%)	24	24	20
Normal results (all markers presents)	35 (47.3%)	3	12	20
Absent/aberrant results	33 (44.6%)	21	12	0
DNAH5 (-) (ODA)	15			
Proximal DNAH5 (ODA)	3			
DNAH5 (-), DNALI1 (-) (ODA+IDA)	3			
DNALI1 (-), GAS8 (-) (IDA+Nexin-DRC)	7			
GAS8 (-) (Nexin-DRC)	1			
RSPH9 (-) (Radial spoke)	3			
RSPH4A (-) (Radial spoke)	1			
Inconclusive/insufficient results	6 (8.1%)	1	1	4

(-): absent in ciliary axoneme; ODA: outer dynein arm; IDA: inner dynein arm; DRC: dynein regulatory complex.

IF was technically evaluable for all tested antibodies in 68 patients (91.9%), whereas in six, the results were inconclusive/insufficient (8.1%) (Table 1). IF analysis demonstrated an absence or aberrant localization of one or more proteins in the ciliary axoneme in 33 cases: 15 patients presented absent DNAH5; 3 a proximal localization of DNAH5 in ciliary axoneme; 3 patients exhibited absent DNAH5 and DNALI1; 7 showed absent DNALI1 and a cytoplasmatic localization of GAS8; 1 patient presented absent GAS8; 3 showed absent RSPH9; and 1 had absent RSPH4A (Table 1). Figure 2 shows examples of absence/aberrant localization of IF markers in four patients with confirmed PCD.

To evaluate the usefulness of IF analysis as a tool for PCD diagnosis, IF results were compared with those obtained from our PCD gene panel and HSVM analyses (Table 2). The 33 patients with aberrant/absent ciliary axoneme proteins had been diagnosed with confirmed or highly likely PCD. All of them presented a concordant abnormal HSVM and 21 of them presented likely pathogenic variants in PCD-related genes (Table 2). The relation of these abnormal IF results with clinical characteristics and other PCD diagnostic tests for each patient is shown in Table S1.



**Figure 2.** Example results of immunofluorescence technique in control subjects and patients with primary ciliary dyskinesia. The first column shows cilia by acetylated  $\alpha$ -tubulin (green); the second column shows the protein of interest (red); and the third column shows the final merged image with the nuclei stained with DAPI (blue). (a) Patient IF-024 exhibited absent DNAH5 and DNALI1. (b) Patient IF-056 had absent DNALI1 and cytoplasmic localization of GAS8. (c) Patient IF-050 showed a normal axonemal localization of RSPH4A and absent RSPH9. (d) Patient IF-046 presented a proximal localization of DNAH5.

**Table 2.** Correlation among immunofluorescence analysis, high-speed video-microscopy, genetics and clinical characteristics in our PCD patients.

IF Affected Markers (Ultrastructural Part)	#	HSVM	Genetics (#)	PCD Symptoms					
				Neonatal Distress	Upper Respiratory Tract	Lower Respiratory Tract	Bronchiectasis	Chronic Otitis or Hearing loss	Situs Abnormality
DNAH5 (ODA)	15	Completely immotile cilia or residual motility	<i>CCDC151</i> (1), <i>DNAH5</i> (5), <i>DNAI2</i> (4), <i>TTC25</i> (1), NA (4)	+/-	+	+	+/-	+/-	+/-
Proximal DNAH5 (ODA)	3	Subtle defects (stiff and disorganized ciliary beat)	<i>DNAH9</i> (1), Neg. (2)	-	+	+/-	+/-	+/-	+/-
DNAH5+DNALI1 (ODA+IDA)	3	Completely immotile cilia	Neg. (2), NA (1)	+	+	+	+	+	+/-
DNALI1+GAS8 (IDA+Nexin-DRC)	7	Mainly stiff cilia and immotile cilia	<i>CCDC39</i> (3), <i>CCDC40</i> (3), NA (1)	+/-	+	+/-	+/-	+/-	+/-
GAS8 (Nexin-DRC)	1	Hyperkinetic stiff cilia	NA (1)	+	+	+	+	+	-
RSPH4A or RSPH9 (Radial spoke)	4	Stiff and circular motion	<i>RSPH1</i> (1), <i>RSPH4A</i> (1), <i>RSPH9</i> (1), NA (1)	+/-	+	+/-	+/-	+/-	-
All markers present (normal result)	3	Hyperkinetic stiff cilia	<i>DNAH11</i> (3)	+/-	+	+/-	+/-	+/-	+/-

IF: immunofluorescence; #: number of patients; HSVM: high-speed video-microscopy; ODA: outer dynein arm; IDA: inner dynein arm; DRC: dynein regulatory complex; NA: not available data; Neg.: negative results; +: symptoms present in all patients; -: symptoms absent in all patients; +/-: symptoms present in some patients.

Thirty-five patients had normal distribution or presence of all IF antibodies. The clinical characteristics and results of PCD diagnostic tests for each patient with normal IF are presented in Table S2. We confirmed PCD in three of these patients because they presented likely pathogenic variants in *DNAH11* and hyperkinetic stiff cilia by HSVM (Tables 2 and S2). Another patient presented two variants in *SPAG1*, but there was no concordance with HSVM and IF results (Table S2). Another 11 patients presented normal IF, but abnormal HSVM results together with typical PCD symptoms, so they were considered highly likely PCD (Table S2). Thus far, we have not detected any likely pathogenic genetic variants in these patients. Finally, 20 out of the 33 patients with normal IF were considered highly unlikely to have PCD because of weak clinical history, normal or mild HSVM results and/or negative genetics (Table S2).

It should be mentioned that six (8.1%) samples were not technically evaluable by our IF panel: two cases lacked enough cells to analyze and were considered insufficient; two cases remained inconclusive for one or more antibodies; and two cases resulted in being insufficient for some markers and inconclusive for others (Table S3). Only one patient with insufficient and inconclusive IF sample was diagnosed with PCD because of presenting stiff cilia by HSVM and likely pathogenic variants in *CCDC39*. Among the other cases, four were finally regarded as having no PCD or unlikely to have PCD because of normal or mild HSVM results (Table S3).

Considering all the previous results, IF analysis as a diagnostic test for PCD had a sensitivity of 68.8% (CI 95% 53.7–81.3%) and a specificity of 100% (CI 95% 83.2–100%). In our laboratory, the PCD prevalence (confirmed or highly likely cases) of patients referred for clinical suspicion in the last 4 years was 27.4% (non-published data). Assuming this prevalence, IF positive predictive value would be 100% and the negative predictive value 89.4% (CI 95% 84.8–92.8%).

#### 4. Discussion

In this study, we have explored the diagnostic utility of an immunofluorescence panel of commercial antibodies in 74 patients with clinical suspicion of PCD. A technical evaluable result was possible in 91.9% of cases (Table 1). IF evidenced a protein defect in 44.6% of analyzed patients, all with confirmed or highly likely PCD (Table 1). A normal IF result (47.3% of cases) was seen not only in all non-PCD patients, but also in some patients with confirmed or highly likely PCD. This means that IF detected ciliary structural defects in 68.8% of confirmed or highly likely PCD patients. In our population, IF has shown the highest positive predictive value (a positive value is consistent with a PCD diagnosis) of 100% and a negative predictive value (a normal result may be seen not only in non-PCD patients but also in PCD patients) of 89.4%. Considering our low availability of TEM results, IF was a useful PCD diagnostic test, because it showed a sensitivity (68.8%) close to TEM studies, where 30% of all affected individuals had normal ciliary ultrastructure [16].

To our knowledge, only one previous study by Shoemark et al. [5] evaluated the accuracy of IF in PCD, concluding that IF and TEM have a similar diagnostic rate. Therefore, they proposed IF as a useful diagnostic tool when TEM equipment or expertise is not available, as IF is cheaper, easier to perform, requires more basic equipment and improves the turnaround time [5]. As TEM analysis was not available in most of our cases, we have confirmed that, under these circumstances, IF is a reliable test to study cilia structure. Furthermore, IF may be useful to confirm the results of other diagnostic tests like HSVM and genetics and guide new tests in those cases with absent or aberrant protein/s localization. In Shoemark's study, IF failed to identify 12% of PCD cases [5], which is lower than the 31.3% of normal IF results that we found in our confirmed or highly likely PCD cases. This difference could be related to genetic differences between both series.

*DNAH5* absence in ciliary axoneme correlated with immotile cilia by HSVM and variants in genes related to ODA defects concurring with other studies: *DNAH5* [17,18], *DNAI2* [19], *TTC25* [20] and *CCDC151* [21] (Table 2 and Table S1). Moreover, we found proximal axonemal *DNAH5* IF staining in three unrelated patients (Figure 2d) with mild clinical symptoms and subtle HSVM defects (mainly

stiff and disorganized ciliary beat). One of them presented likely pathogenic variants in *DNAH9*, in concordance with recently published data [22,23] (Tables 2 and S1).

Some of the patients showed absence of both *DNAH5* and *DNALI1* (Figure 2a) also with completely immotile cilia. We could not find any candidate variant in these patients (Tables 2 and S1). These IF and HSVM results could be explained by genetic alterations in proteins involved in the assembly of both ODA and IDA [24–35] and further studies are warranted.

The patients with absent *DNALI1* and abnormal localization (cytoplasmatic) of *GAS8* (Figure 2b) had mainly stiff (reduced amplitude) and immotile cilia and likely pathogenic variants in *CCDC39* and *CCDC40* (Tables 2 and S1). These results are consistent with previous description of *CCDC39* [36] and *CCDC40* [37] as assembling factors of the IDA and the nexin–dynein regulatory complex structures [36–38].

Only one patient presented an absence of *GAS8* in ciliary axoneme. This patient had hyperkinetic stiff cilia and respiratory symptoms beginning at neonatal age. These results could be explained by defects in the nexin–dynein regulatory complex (DRC) subunits, as previously described [39–41].

In our IF approach, radial spoke defects were first studied with the *RSPH4A* antibody and later with *RSPH9*. We decided to switch to *RSPH9* because it is more informative for detecting all radial spoke head defects, and it has been recommended due to its reported absence from ciliary axonemes in radial spoke mutant cells [5,42]. In fact, one of our patients had normal *RSPH4A*, but absent *RSPH9* (Figure 2c). Radial spoke defects in our patients were related to situs solitus and two different HSVM patterns: circular motion and stiff cilia, consistent with previously reported data (Tables 2 and S1) [42–44].

Our IF panel could not detect defects caused by *DNAH11* genetic variants in our patients, consistent with previously reported data [45]. For this reason, it would be interesting to include an anti-*DNAH11* antibody in the IF panel, considering that it is commercially available, but it has not been optimized. As it happens with *DNAH11*, other ciliary proteins have been described to cause none or subtle ultrastructural defects: *HYDIN* [46], *STK36* [47] and, most recently, *SPEF2* [48]. *STK36* has been described as a protein involved in the interaction between the central pair and the radial spoke [47]. *HYDIN* and *SPEF2* have been functionally described to cause central pair defects in humans, and mutants of both proteins can be detected using antibodies against *SPEF2* [48]. These ultrastructural defects could explain some of our normal IF results in highly likely PCD patients.

Some patients could not be resolved by IF as analysis was inconclusive and/or insufficient for some of the target proteins, requiring reevaluation of new brushing samples. Blood and mucus in the IF samples were found to be confounding factors in the analysis in a previous publication [5]. From our experience, we considered the slides with nasal brush sample prepared by dropping a better option than those by spreading. Slides with a dropped sample allowed a faster analysis due to having more cells in a smaller area. In addition, when the sample contained mucus, analysis was more complicated in spread samples, and usually there were not enough viable cells to complete the analysis.

The major limitation of the IF analysis is that, because of the use of primary antibodies directed to specific proteins, defects in unrelated proteins may be missed [5]. Moreover, patients with partial defects or missense mutations have been reported to have normal IF results [5], although we did not have any case with this particular observation in our cohort. As new genes and proteins related to PCD are discovered, the IF antibody panels may need to be revised and expanded in the future for an accurate diagnosis [49]. In fact, antibodies against a high number of ciliary proteins are already commercially available, although most of them have not yet been tested and/or validated for immunofluorescence or in human respiratory tissue [11]. For this reason, the optimization of antibodies in nasal brushing samples is difficult and time-consuming. Furthermore, from our experience, we have not even been able to properly optimize some commercially available antibodies, i.e., *DNAH11*. Further antibody optimization is necessary, and, as a matter of fact, Liu et al.'s extensive IF technical protocols may help with this [11]. Another pitfall is the lack of consensus regarding the performance of the IF technique and,

more importantly, the agreement in the IF considerations when the analysis is performed. Currently, a consensus statement on IF, initiated during the European BEAT-PCD 2019, is on the way.

One important limitation of measuring the accuracy of IF for PCD diagnosis is the lack of a gold standard reference against which to measure it. In our study, we use the ERS task force criteria [6] assuming as a standard for comparison confirmed and highly likely PCD cases, with the added limitation of low availability of TEM analysis.

Moreover, the positive rate of our series was quite high (25 confirmed and 25 highly likely of 74 cases). This is related to a previous pre-screening for IF study of cases with more suggestive clinical symptoms.

Taking all into account, we propose a two-step IF analysis: a first panel with DNAH5, DNALI1, GAS8 and RSPH9 and, in cases with normal IF and consistent PCD suspicion (clinical symptoms and other techniques), a second IF round with antibodies against ciliary components associated with none or subtle ultrastructural defects: DNAH11 [45], STK36 [47] and SPEF2 [48]. Shoemark et al. [5] also recommended a first antibody panel with DNAH5, GAS8 and RSPH9 and omitted DNALI1 because its absence always coexists with an absence of DNAH5 or GAS8 [5]. This recommendation is supported by our cohort results, but as TEM is mostly unavailable and we are using IF results to clarify the genetics, we considered to maintain anti-DNALI1 antibody in our IF studies. Therefore, our proposed two-step IF analysis may be used in cases with non-available TEM. Alternatively, centers with available TEM analysis might use a first step IF panel with DNAH11, SPEF2, GAS8 and RSPH9 antibodies, omitting DNAH5 and DNALI1. For the translation to clinical diagnosis, Liu et al. also proposed a restricted 10-antibody panel (instead of 21) based on proteins which are non-detectable by TEM or those indirectly detecting mislocalization of other proteins (DNAH5, DNAH11, DNALI1, GAS8, CCDC65, RSPH4A, RSPH9, RPGR, OFD1 and SPEF2) [11]. Although a quantitative super-resolution imaging tool, such as the one proposed by Liu et al. [11], gives much more information and may solve so-called difficult or unsolved cases, it would be hard to implement in our clinical setting due to its high costs in time and personnel.

To conclude, the presented results confirm that IF is a reliable diagnosis technique for PCD (with a sensitivity of 68.8% and a specificity of 100%), even when TEM analysis is unavailable, although it cannot be used as a standalone test. Considering our results, we propose IF as a cheap, easy and widely available test to include in PCD diagnosis.

**Supplementary Materials:** The following are available online at <http://www.mdpi.com/2077-0383/9/11/3603/s1>, Table S1: Patients with absence or aberrant distribution of target proteins by immunofluorescence and correlation with other PCD analysis techniques, Table S2: Patients with normal localization of target proteins by immunofluorescence and correlation with other PCD analysis techniques, Table S3: Patients with inconclusive and/or insufficient immunofluorescence results and correlation with other PCD analysis techniques.

**Author Contributions:** A.M.-G. and N.C.-T. were responsible for the conception and design of this study. N.B.-R., N.C.-T., M.F.-C., M.G.-P., S.R.-A., M.A.C.-R, F.D. and A.R. performed immunofluorescence studies and/or diagnostic PCD studies. S.R.-A., S.C.-C., M.C., M.A.C.-R., O.A., C.M.d.V., M.d.M.M.-C., A.T.-V., I.M.-M., S.G., I.I.-S., A.D.-I., E.P., E.A.-P., R.A.-R., M.V., M.M., M.T.P.-S., B.P.-D., A.R., A.E., F.D. and M.A.-C. recruited the patients and undertook the data collection. N.B.-R., N.C.-T. and A.M.-G. performed statistical analysis. N.B.-R., N.C.-T., S.R.-A. and A.M.-G. drafted the manuscript. All remaining authors revised and approved the manuscript before submission. All authors have read and agreed to the published version of the manuscript.

**Funding:** This research was funded by a grant from the Health Research and Development Strategy (AES) of Instituto de Salud Carlos III (ISCIII) (PI16/01233), co-financed by the European Regional Development Fund, Smart Growth Operational Programme 2014–2020, and with grants from the Spanish Society of Pediatric Pulmonology (SENP, 2016) and the Catalan Pneumology Foundation (FUCAP, 2016). N.C.-T. received a grant for a Short Term Scientific Mission from COST Action BM1407. It was also supported by the CIBER of Rare Diseases (CIBERER, ISCIII) U-712 to N.C.-T. and M.F.-C.

**Acknowledgments:** The authors have participated in COST Action BM1407 Translational research in primary ciliary dyskinesia: bench, bedside, and population perspectives (BEAT PCD). A.M.-G. and S.R.-A. participate at ERN-LUNG. This work has been carried out within the framework of the Doctorate Program of Pediatrics, Obstetrics and Gynecology of Universitat Autònoma de Barcelona.

**Conflicts of Interest:** The authors declare no conflict of interest.

## References

1. Lucas, J.S.; Burgess, A.; Mitchison, H.M.; Moya, E.; Williamson, M.; Hogg, C. Diagnosis and Management of Primary Ciliary Dyskinesia. *Arch. Dis. Child.* **2014**, *99*, 850–856. [[CrossRef](#)] [[PubMed](#)]
2. Reula, A.; Lucas, J.S.; Moreno-Galdó, A.; Romero, T.; Milara, X.; Carda, C.; Mata-Roig, M.; Escribano, A.; Dasi, F.; Armengot-Carceller, M. New Insights in Primary Ciliary Dyskinesia. *Expert Opin. Orphan Drugs* **2017**, *5*, 537–548. [[CrossRef](#)]
3. Wallmeier, J.; Nielsen, K.G.; Kuehni, C.E.; Lucas, J.S.; Leigh, M.W.; Zariwala, M.A.; Omran, H. Motile Ciliopathies. *Nat. Rev. Dis. Prim.* **2020**, *6*, 1–29. [[CrossRef](#)] [[PubMed](#)]
4. Shapiro, A.J.; Davis, S.D.; Ferkol, T.; Dell, S.D.; Rosenfeld, M.; Olivier, K.N.; Sagel, S.D.; Milla, C.; Zariwala, M.A.; Wolf, W.; et al. Laterality Defects Other Than Situs Inversus Totalis in Primary Ciliary Dyskinesia. *Chest* **2014**, *146*, 1176–1186. [[CrossRef](#)] [[PubMed](#)]
5. Shoemark, A.; Frost, E.; Dixon, M.; Ollosson, S.; Kilpin, K.; Patel, M.; Scully, J.; Rogers, A.V.; Mitchison, H.M.; Bush, A.; et al. Accuracy of Immunofluorescence in the Diagnosis of Primary Ciliary Dyskinesia. *Am. J. Respir. Crit. Care Med.* **2017**, *196*, 94–101. [[CrossRef](#)] [[PubMed](#)]
6. Lucas, J.S.; Barbato, A.; Collins, S.A.; Goutaki, M.; Behan, L.; Caudri, D.; Dell, S.; Eber, E.; Escudier, E.; Hirst, R.A.; et al. European Respiratory Society Guidelines for the Diagnosis of Primary Ciliary Dyskinesia. *Eur. Respir. J.* **2017**, *49*, 1601090. [[CrossRef](#)]
7. Shapiro, A.J.; Davis, S.D.; Polineni, D.; Manion, M.; Rosenfeld, M.; Dell, S.D.; Chilvers, M.; Ferkol, T.W.; Zariwala, M.A.; Sagel, S.D.; et al. Diagnosis of Primary Ciliary Dyskinesia. An Official American Thoracic Society Clinical Practice Guideline. *Am. J. Respir. Crit. Care Med.* **2018**, *197*, e24–e39. [[CrossRef](#)]
8. Ibañez-Tallon, I.; Heintz, N.; Omran, H. To Beat or Not to Beat: Roles of Cilia in Development and Disease. *Hum. Mol. Genet.* **2003**, *12*, R27–R35. [[CrossRef](#)]
9. Olm, M.A.K.; Caldini, E.G.; Mauad, T. Diagnosis of Primary Ciliary Dyskinesia. *J. Bras. Pneumol.* **2015**, *41*, 251–263. [[CrossRef](#)]
10. Omran, H.; Loges, N.T. Immunofluorescence Staining of Ciliated Respiratory Epithelial Cells. *Methods Cell Biol.* **2009**, *91*, 123–133. [[CrossRef](#)]
11. Liu, Z.; Nguyen, Q.P.H.; Guan, Q.; Albulescu, A.; Erdman, L.; Mahdaviyeh, Y.; Kang, J.; Ouyang, H.; Hegele, R.G.; Moraes, T.J.; et al. A Quantitative Super-Resolution Imaging Toolbox for Diagnosis of Motile Ciliopathies. *Sci. Transl. Med.* **2020**, *12*, eaay0071. [[CrossRef](#)]
12. Behan, L.; Dimitrov, B.D.; Kuehni, C.E.; Hogg, C.; Carroll, M.; Evans, H.J.; Goutaki, M.; Harris, A.; Packham, S.; Walker, W.T.; et al. PICADAR: A Diagnostic Predictive Tool for Primary Ciliary Dyskinesia. *Eur. Respir. J.* **2016**, *47*, 1103–1112. [[CrossRef](#)]
13. Horváth, I.; Barnes, P.J.; Loukides, S.; Sterk, P.J.; Högman, M.; Olin, A.-C.; Amann, A.; Antus, B.; Baraldi, E.; Bikov, A.; et al. A European Respiratory Society Technical Standard: Exhaled Biomarkers in Lung Disease. *Eur. Respir. J.* **2017**, *49*, 1600965. [[CrossRef](#)] [[PubMed](#)]
14. Baz-Redón, N.; Rovira-Amigo, S.; Paramonov, I.; Castillo-Corullón, S.; Roig, M.C.; Antolín, M.; Arumí, E.G.; Torrent-Vernetta, A.; Messa, I.D.M.; Gartner, S.; et al. Implementation of a Gene Panel for Genetic Diagnosis of Primary Ciliary Dyskinesia. *Arch. Bronconeumol.* **2020**, *20*, 30073–30079. [[CrossRef](#)]
15. Kempeneers, C.; Seaton, C.; Espinosa, B.G.; Chilvers, M.A. Ciliary Functional Analysis: Beating a Path towards Standardization. *Pediatric Pulmonol.* **2019**, *54*, 1627–1638. [[CrossRef](#)] [[PubMed](#)]
16. Kouis, P.; Yiallourous, P.; Middleton, N.; Evans, J.S.; Kyriacou, K.; Papatheodorou, S.I. Prevalence of Primary Ciliary Dyskinesia in Consecutive Referrals of Suspect Cases and the Transmission Electron Microscopy Detection Rate: A Systematic Review and Meta-Analysis. *Pediatric Res.* **2016**, *81*, 398–405. [[CrossRef](#)]
17. Fliegau, M.; Olbrich, H.; Horvath, J.; Wildhaber, J.H.; Zariwala, M.A.; Kennedy, M.; Knowles, M.R.; Omran, H. Mislocalization of DNAH5 and DNAH9 in Respiratory Cells from Patients with Primary Ciliary Dyskinesia. *Am. J. Respir. Crit. Care Med.* **2005**, *171*, 1343–1349. [[CrossRef](#)]



18. Baz-Redón, N.; Rovira-Amigo, S.; Camats-Tarruella, N.; Fernández-Cancio, M.; Garrido-Pontnou, M.; Antolín, M.; Reula, A.; Armengot-Carceller, M.; Carrascosa, A.; Moreno-Galdó, A. Role of Immunofluorescence and Molecular Diagnosis in the Characterization of Primary Ciliary Dyskinesia. *Arch. Bronconeumol.* **2019**, *55*, 439–441. [[CrossRef](#)]
19. Loges, N.T.; Olbrich, H.; Fenske, L.; Mussaffi, H.; Horvath, J.; Fliegau, M.; Kuhl, H.; Baktai, G.; Peterffy, E.; Chodhari, R.; et al. DNAI2 Mutations Cause Primary Ciliary Dyskinesia with Defects in the Outer Dynein Arm. *Am. J. Hum. Genet.* **2008**, *83*, 547–558. [[CrossRef](#)] [[PubMed](#)]
20. Wallmeier, J.; Shiratori, H.; Dougherty, G.W.; Edelbusch, C.; Hjeij, R.; Loges, N.T.; Menchen, T.; Olbrich, H.; Pennekamp, P.; Raidt, J.; et al. TTC25 Deficiency Results in Defects of the Outer Dynein Arm Docking Machinery and Primary Ciliary Dyskinesia with Left-Right Body Asymmetry Randomization. *Am. J. Hum. Genet.* **2016**, *99*, 460–469. [[CrossRef](#)]
21. Hjeij, R.; Onoufriadis, A.; Watson, C.M.; Slagle, C.E.; Klena, N.T.; Dougherty, G.W.; Kurkowiak, M.; Loges, N.T.; Diggle, C.P.; Morante, N.F.; et al. CCDC151 Mutations Cause Primary Ciliary Dyskinesia by Disruption of the Outer Dynein Arm Docking Complex Formation. *Am. J. Hum. Genet.* **2014**, *95*, 257–274. [[CrossRef](#)]
22. Loges, N.T.; Antony, D.; Maver, A.; Deardorff, M.A.; Güleç, E.Y.; Gezdirici, A.; Nöthe-Menchen, T.; Höben, I.M.; Jelten, L.; Frank, D.; et al. Recessive DNAH9 Loss-of-Function Mutations Cause Laterality Defects and Subtle Respiratory Ciliary-Beating Defects. *Am. J. Hum. Genet.* **2018**, *103*, 995–1008. [[CrossRef](#)]
23. Fassad, M.R.; Shoemark, A.; Legendre, M.; Hirst, R.A.; Koll, F.; Le Borgne, P.; Louis, B.; Daudvohra, F.; Patel, M.P.; Thomas, L.; et al. Mutations in Outer Dynein Arm Heavy Chain DNAH9 Cause Motile Cilia Defects and Situs Inversus. *Am. J. Hum. Genet.* **2018**, *103*, 984–994. [[CrossRef](#)]
24. Tarkar, A.; Loges, N.T.; Slagle, C.E.; Francis, R.; Dougherty, G.W.; Tamayo, J.V.; Shook, B.; Cantino, M.; Schwartz, D.; Jahnke, C.; et al. DYX1C1 is Required for Axonemal Dynein Assembly and Ciliary Motility. *Nat. Genet.* **2013**, *45*, 995–1003. [[CrossRef](#)]
25. Knowles, M.R.; Ostrowski, L.E.; Loges, N.T.; Hurd, T.; Leigh, M.W.; Huang, L.; Wolf, W.E.; Carson, J.L.; Hazucha, M.J.; Yin, W.; et al. Mutations in SPAG1 Cause Primary Ciliary Dyskinesia Associated with Defective Outer and Inner Dynein Arms. *Am. J. Hum. Genet.* **2013**, *93*, 711–720. [[CrossRef](#)]
26. Olcese, C.; UK10K Rare Group; Patel, M.P.; Shoemark, A.; Kiviluoto, S.; Legendre, M.; Williams, H.J.; Vaughan, C.K.; Hayward, J.; Goldenberg, A.; et al. X-Linked Primary Ciliary Dyskinesia Due to Mutations in the Cytoplasmic Axonemal Dynein Assembly Factor PIH1D3. *Nat. Commun.* **2017**, *8*, 14279. [[CrossRef](#)]
27. Paff, T.; Loges, N.T.; Aprea, I.; Wu, K.; Bakey, Z.; Haarman, E.G.; Daniels, J.M.; Sijm, E.A.; Bogunovic, N.; Dougherty, G.W.; et al. Mutations in PIH1D3 Cause X-Linked Primary Ciliary Dyskinesia with Outer and Inner Dynein Arm Defects. *Am. J. Hum. Genet.* **2017**, *100*, 160–168. [[CrossRef](#)]
28. Loges, N.T.; Olbrich, H.; Becker-Heck, A.; Häffner, K.; Heer, A.; Reinhard, C.; Schmidts, M.; Kispert, A.; Zariwala, M.A.; Leigh, M.W.; et al. Deletions and Point Mutations of LRRC50 Cause Primary Ciliary Dyskinesia Due to Dynein Arm Defects. *Am. J. Hum. Genet.* **2009**, *85*, 883–889. [[CrossRef](#)]
29. Austin-Tse, C.; Halbritter, J.; Zariwala, M.A.; Gilberti, R.M.; Gee, H.Y.; Hellman, N.; Pathak, N.; Liu, Y.; Panizzi, J.R.; Patel-King, R.S.; et al. Zebrafish Ciliopathy Screen Plus Human Mutational Analysis Identifies C21orf59 and CCDC65 Defects as Causing Primary Ciliary Dyskinesia. *Am. J. Hum. Genet.* **2013**, *93*, 672–686. [[CrossRef](#)] [[PubMed](#)]
30. Mitchison, H.; Schmidts, M.; Loges, N.T.; Freshour, J.; Dritsoula, A.; Hirst, R.A.; O’Callaghan, C.; Blau, H.; Al Dabbagh, M.; Olbrich, H.; et al. Mutations in Axonemal Dynein Assembly Factor DNAAF3 Cause Primary Ciliary Dyskinesia. *Nat. Genet.* **2012**, *44*, 381–389. [[CrossRef](#)] [[PubMed](#)]
31. Zariwala, M.A.; Gee, H.Y.; Kurkowiak, M.; Al-Mutairi, D.A.; Leigh, M.W.; Hurd, T.W.; Hjeij, R.; Dell, S.D.; Chaki, M.; Dougherty, G.W.; et al. ZMYND10 Is Mutated in Primary Ciliary Dyskinesia and Interacts with LRRC6. *Am. J. Hum. Genet.* **2013**, *93*, 336–345. [[CrossRef](#)] [[PubMed](#)]
32. Diggle, C.P.; Toddie-Moore, D.; Mali, G.; Lage, P.Z.; Ait-Lounis, A.; Schmidts, M.; Shoemark, A.; Munoz, A.G.; Halachev, M.R.; Gautier, P.; et al. HEATR2 Plays a Conserved Role in Assembly of the Ciliary Motile Apparatus. *PLoS Genet.* **2014**, *10*, e1004577. [[CrossRef](#)]

33. Horani, A.; Druley, T.E.; Zariwala, M.A.; Patel, A.C.; Levinson, B.T.; Van Arendonk, L.G.; Thornton, K.C.; Giacalone, J.C.; Albee, A.J.; Wilson, K.S.; et al. Whole-Exome Capture and Sequencing Identifies HEATR2 Mutation as a Cause of Primary Ciliary Dyskinesia. *Am. J. Hum. Genet.* **2012**, *91*, 685–693. [[CrossRef](#)] [[PubMed](#)]
34. Fassad, M.R.; Shoemark, A.; Le Borgne, P.; Koll, F.; Patel, M.; Dixon, M.; Hayward, J.; Richardson, C.; Frost, E.; Jenkins, L.; et al. C11orf70 Mutations Disrupting the Intraflagellar Transport-Dependent Assembly of Multiple Axonemal Dyneins Cause Primary Ciliary Dyskinesia. *Am. J. Hum. Genet.* **2018**, *102*, 956–972. [[CrossRef](#)]
35. Höben, I.M.; Hjeij, R.; Olbrich, H.; Dougherty, G.W.; Nöthe-Menchen, T.; Aprea, I.; Frank, D.; Pennekamp, P.; Dworniczak, B.; Wallmeier, J.; et al. Mutations in C11orf70 Cause Primary Ciliary Dyskinesia with Randomization of Left/Right Body Asymmetry Due to Defects of Outer and Inner Dynein Arms. *Am. J. Hum. Genet.* **2018**, *102*, 973–984. [[CrossRef](#)]
36. Merveille, A.-C.; Davis, E.E.; Becker-Heck, A.; Legendre, M.; Amirav, I.; Bataille, G.; Belmont, J.W.; Beydon, N.; Billen, F.; Clément, A.; et al. CCDC39 is Required for Assembly of Inner Dynein Arms and the Dynein Regulatory Complex and for Normal Ciliary Motility in Humans and Dogs. *Nat. Genet.* **2011**, *43*, 72–78. [[CrossRef](#)]
37. Becker-Heck, A.; Zohn, I.E.; Okabe, N.; Pollock, A.; Lenhart, K.B.; Sullivan-Brown, J.; McSheene, J.; Loges, N.T.; Olbrich, H.; Haefner, K.; et al. The Coiled-Coil Domain Containing Protein CCDC40 Is Essential for Motile Cilia Function and Left-Right Axis Formation. *Nat. Genet.* **2011**, *43*, 79–84. [[CrossRef](#)]
38. Antony, D.; Becker-Heck, A.; Zariwala, M.A.; Schmidts, M.; Onoufriadis, A.; Forouhan, M.; Wilson, R.; Taylor-Cox, T.; Dewar, A.; Jackson, C.; et al. Mutations in CCDC39 and CCDC40 are the Major Cause of Primary Ciliary Dyskinesia with Axonemal Disorganization and Absent Inner Dynein Arms. *Hum. Mutat.* **2013**, *34*, 462–472. [[CrossRef](#)]
39. Olbrich, H.; Cremers, C.; Loges, N.T.; Werner, C.; Nielsen, K.G.; Marthin, J.K.; Philipsen, M.; Wallmeier, J.; Pennekamp, P.; Menchen, T.; et al. Loss-of-Function GAS8 Mutations Cause Primary Ciliary Dyskinesia and Disrupt the Nexin-Dynein Regulatory Complex. *Am. J. Hum. Genet.* **2015**, *97*, 546–554. [[CrossRef](#)] [[PubMed](#)]
40. Wirschell, M.; Olbrich, H.; Werner, C.; Tritschler, D.; Bower, R.; Sale, W.S.; Loges, N.T.; Pennekamp, P.; Lindberg, S.; Stenram, U.; et al. The Nexin-Dynein Regulatory Complex Subunit DRC1 Is Essential for Motile Cilia Function in Algae and Humans. *Nat. Genet.* **2013**, *45*, 262–268. [[CrossRef](#)] [[PubMed](#)]
41. Horani, A.; Brody, S.L.; Ferkol, T.W.; Shoseyov, D.; Wasserman, M.G.; Ta-Shma, A.; Wilson, K.S.; Bayly, P.V.; Amirav, I.; Cohen-Cymbberknoh, M.; et al. CCDC65 Mutation Causes Primary Ciliary Dyskinesia with Normal Ultrastructure and Hyperkinetic Cilia. *PLoS ONE* **2013**, *8*, e72299. [[CrossRef](#)] [[PubMed](#)]
42. Frommer, A.; Hjeij, R.; Loges, N.T.; Edelbusch, C.; Jahnke, C.; Raidt, J.; Werner, C.; Wallmeier, J.; Große-Onnebrink, J.; Olbrich, H.; et al. Immunofluorescence Analysis and Diagnosis of Primary Ciliary Dyskinesia with Radial Spoke Defects. *Am. J. Respir. Cell Mol. Biol.* **2015**, *53*, 563–573. [[CrossRef](#)]
43. Kott, E.; Legendre, M.; Copin, B.; Papon, J.-F.; Moal, F.D.-L.; Montantin, G.; Duquesnoy, P.; Piterboth, W.; Amram, D.; Bassinet, L.; et al. Loss-of-Function Mutations in RSPH1 Cause Primary Ciliary Dyskinesia with Central-Complex and Radial-Spoke Defects. *Am. J. Hum. Genet.* **2013**, *93*, 561–570. [[CrossRef](#)]
44. Castleman, V.H.; Romio, L.; Chodhari, R.; Hirst, R.A.; De Castro, S.C.; Parker, K.A.; Ybot-Gonzalez, P.; Emes, R.D.; Wilson, S.W.; Wallis, C.; et al. Mutations in Radial Spoke Head Protein Genes RSPH9 and RSPH4A Cause Primary Ciliary Dyskinesia with Central-Microtubular-Pair Abnormalities. *Am. J. Hum. Genet.* **2009**, *84*, 197–209. [[CrossRef](#)]
45. Dougherty, G.W.; Loges, N.T.; Klinkenbusch, J.A.; Olbrich, H.; Pennekamp, P.; Menchen, T.; Raidt, J.; Wallmeier, J.; Werner, C.; Westermann, C.; et al. DNAH11 Localization in the Proximal Region of Respiratory Cilia Defines Distinct Outer Dynein Arm Complexes. *Am. J. Respir. Cell Mol. Biol.* **2016**, *55*, 213–224. [[CrossRef](#)]
46. Olbrich, H.; Schmidts, M.; Werner, C.; Onoufriadis, A.; Loges, N.T.; Raidt, J.; Banki, N.F.; Shoemark, A.; Burgoyne, T.; Al Turki, S.; et al. Recessive HYDIN Mutations Cause Primary Ciliary Dyskinesia without Randomization of Left-Right Body Asymmetry. *Am. J. Hum. Genet.* **2012**, *91*, 672–684. [[CrossRef](#)]
47. Edelbusch, C.; Cindrić, S.; Dougherty, G.W.; Loges, N.T.; Olbrich, H.; Rivlin, J.; Wallmeier, J.; Pennekamp, P.; Amirav, I.; Omran, H. Mutation of Serine/Threonine Protein Kinase 36 (STK36) Causes Primary Ciliary Dyskinesia with a Central Pair Defect. *Hum. Mutat.* **2017**, *38*, 964–969. [[CrossRef](#)]

48. Cindrić, S.; Dougherty, G.W.; Olbrich, H.; Hjejij, R.; Loges, N.T.; Amirav, I.; Philipsen, M.C.; Marthin, J.K.; Nielsen, K.G.; Sutharsan, S.; et al. SPEF2-and HYDIN-Mutant Cilia Lack the Central Pair-associated Protein SPEF2, Aiding Primary Ciliary Dyskinesia Diagnostics. *Am. J. Respir. Cell Mol. Biol.* **2020**, *62*, 382–396. [[CrossRef](#)]
49. Knowles, M.R.; Leigh, M.W. Primary Ciliary Dyskinesia Diagnosis. Is Color Better Than Black and White? *Am. J. Respir. Crit. Care Med.* **2017**, *196*, 9–10. [[CrossRef](#)]

**Publisher’s Note:** MDPI stays neutral with regard to jurisdictional claims in published maps and institutional affiliations.



© 2020 by the authors. Licensee MDPI, Basel, Switzerland. This article is an open access article distributed under the terms and conditions of the Creative Commons Attribution (CC BY) license (<http://creativecommons.org/licenses/by/4.0/>).

# **Immunofluorescence analysis as a diagnostic tool in a Spanish cohort of patients with primary ciliary dyskinesia**

**Supplementary Materials**

**Table S1: Patients with absence or aberrant distribution of target proteins by immunofluorescence and correlation with other PCD-analysis techniques.**

Patient#	YOB/Gender/Origin/Consanguinity/Family	PICADAR score [1]/PCD symptoms	nNO (nl/min)	Affected IF markers	HSVM	TEM	Genetics	Diagnosis [2] - Next step	Patient# in Baz-Redón et al. 2020 [3]
IF-009	2002/M/Caucasian/N	6/Neonatal distress. Chronic rhinitis and wet cough. Sinusitis. Recurrent otitis and hearing loss. Repeated bronchitis and pneumonia. Bronchiectasis. Persistent atelectasis.	5.1	DNAH5-, DNALI1-	Completely immotile	NA	Negative	Highly likely PCD - WES	53
IF-013	2016/M/Caucasian/N	8/Chronic rhinitis and wet cough. Repeated bronchitis. <i>Situs inversus</i> .	NA	DNAH5-	Completely immotile	NA	<i>DNAI2</i> (c.184-14G>A het. + c.740G>A/p.Arg247Gln het.)	Confirmed PCD <i>DNAI2</i>	31
IF-015	2006/M/Caucasian/N	8/Chronic rhinitis and wet cough. Bronchiectasis. <i>Situs inversus</i> .	67.7	DNALI1-, GAS8-	Mainly stiff	NA	<i>CCDC39</i> (c.610-2A>G hom.)	Confirmed PCD <i>CCDC39</i>	6
IF-021	2007/M/Pakistan/Y/sib. of IF-056, IF-057	8/Chronic rhinitis and wet cough. Recurrent otitis. Hearing loss. Repeated bronchitis and pneumonia. Heterotaxy.	6.4	DNALI1-, GAS8-	Mainly stiff	NA	<i>CCDC40</i> (c.1416delG/p.Ile473PhefsTer 2 hom.)	Confirmed PCD <i>CCDC40</i>	11
IF-024	1991/M/Caucasian/N	6/Neonatal distress. Chronic rhinitis and wet cough. Recurrent otitis and hearing loss. Repeated bronchitis. Bronchiectasis.	14.6	DNAH5-, DNALI1-	Completely immotile	Loss 30% ODA and 70% IDA	Negative	Highly likely PCD - WES	52

IF-025	1964/M/Caucasian/NA	?/Wet cough. Bronchiectasis. Infertility.	112.8	RSPH9-	Stiff	NA	NA	Highly likely PCD - Genetics	
IF-031	1992/F/Caucasian/N	5/Neonatal distress. Chronic rhinitis and wet cough. Repeated pneumonia. Bronchiectasis.	10	RSPH9-	Stiff	Loss 40% ODA and 80% IDA	<i>RSPH1</i> (c.85G>T/p.Glu29Ter het. + c.275-2A>C het.)	Confirmed PCD <i>RSPH1</i>	36
IF-040	2006/F/Moroccan/N	?/Chronic rhinitis and wet cough. Bronchiectasis. <i>Situs inversus</i> .	2.3	DNAH5-	Completely immotile	NA	<i>TTC25</i> (c.655_659delCTGAC/p.Leu219CysfsTer62 hom.)	Confirmed PCD <i>TTC25</i>	43
IF-041	2015/M/Moroccan/Y	3/Chronic rhinitis and wet cough.	NA	RSPH4A-	Circular	NA	<i>RSPH4A</i> (c.1453C>T/p.Arg486STer hom.)	Confirmed PCD <i>RSPH4A</i>	38
IF-043	2013/F/Pakistan/Y/sib. of IF-044	4/Chronic rhinitis and wet cough. Repeated pneumonia. Persistent atelectasis.	NA	DNAH5-	Completely immotile	ODA defect	<i>DNAI2</i> (c.546C>A/p.Tyr182Ter hom.)	Confirmed PCD <i>DNAI2</i>	28
IF-044	2006/M/Pakistan/Y/sib. of IF-043	6/Neonatal distress. Chronic rhinitis and cough. Bronchiectasis.	14.2	DNAH5-	Completely immotile	Partial ODA defect	<i>DNAI2</i> (c.546C>A/p.Tyr182Ter hom.)	Confirmed PCD <i>DNAI2</i>	29
IF-045	2005/F/Caucasian/N	4/Chronic rhinitis and cough. Bronchiectasis. Recurrent otitis. Hearing loss.	17.2	DNAH5-	Completely immotile	Loss 30% ODA and 70% IDA	<i>DNAH5</i> (c.4625_4628delGAGA/p.Arg1542ThrfsTer6 het. + c.12706-2A>T het.)	Confirmed PCD <i>DNAH5</i>	14
IF-046	2004/F/Caucasian/N	4/Chronic rhinitis and wet cough.	NA	Proximal DNAH5	Subtle defects (disorganized ciliary beat)	NA	<i>DNAH9</i> (c.7822-1G>A het. + c.8992C>T/p.Gln2998Ter het.)	Confirmed PCD <i>DNAH9</i>	23

IF-047	1970/M/Caucasian/N	?/Chronic rhinitis and wet cough. Sinusitis. Recurrent otitis and hearing loss. <i>Situs inversus</i> .	188.1	Proximal DNAH5	Subtle defects (stiff and disorganized ciliary beat)	NA	Negative	Highly likely PCD - WES	
IF-050	2010/F/Moroccan/Y	4/Chronic rhinitis and cough. Bronchiectasis. Recurrent otitis. Lobectomy.	5.4	RSPH4A+, RSPH9-	Stiff and circular	NA	<i>RSPH9</i> (c.293_294delTG/p.Val98Glyfs Ter14 hom.)	Confirmed PCD <i>RSPH9</i>	40
IF-053	1984/M/Caucasian/N/father of IF-067	10/Neonatal distress. Chronic rhinitis and wet cough. Sinusitis. Recurrent otitis and hearing loss. Repeated bronchitis and pneumonia. Bronchiectasis. <i>Situs inversus</i> .	4.7	DNAH5-	Completely immotile	NA	<i>DNAH5</i> (c.2575A>T/p.Lys859Ter het. + c.9730G>T/p.Glu3244Ter het.)	Confirmed PCD <i>DNAH5</i>	21
IF-055	2011/F/Caucasian/Y	6/Neonatal distress. Chronic rhinitis and wet cough. Recurrent otitis and hearing loss. Repeated bronchitis and pneumoniae. Bronchiectasis.	NA	DNAH5-	Completely immotile	NA	<i>DNAH5</i> (3.3kb inc. ex.29 and ex.30 del het.)	Confirmed PCD <i>DNAH5</i>	22
IF-056	2018/F/Pakistan/Y/sib. of IF-021, IF-057	7/Neonatal distress. Chronic rhinitis and cough. Recurrent atelectasis.	NA	DNALI1-, GAS8-	Stiff and immotile	NA	<i>CCDC40</i> (c.1416delG/p.Ile473PhefsTer 2 hom.)	Confirmed PCD <i>CCDC40</i>	12
IF-060	2003/F/Caucasian/N	8/Chronic rhinitis and wet cough. <i>Situs inversus</i> .	44.5	DNALI1-, GAS8-	Mainly stiff	ODA and IDA defects	<i>CCDC40</i> (c.2T>G/p.Met1Arg het. + 526pb inc. ex.8 and ex.9 del het.)	Confirmed PCD <i>CCDC40</i>	13
IF-061	2011/M/Caucasian/N	8/Neonatal distress. Chronic rhinitis and wet cough. Bronchiectasis. <i>Situs inversus</i> .	5.5	DNAH5-	Immotile, residual motility	NA	<i>DNAH5</i> (3.2kb inc. ex.2 and ex.3 del het. + c.10813G>A/p.Asp3605Asn het.)	Confirmed PCD <i>DNAH5</i>	19

IF-062	2002/M/Caucasian/N	8/Chronic rhinitis and wet cough. Sinusitis. Recurrent otitis and hearing loss. Repeated bronchitis. Bronchiectasis. <i>Situs inversus</i> .	NA	DNAH5-	Completely immotile	NA	<i>DNAI2</i> (c.346-3T>G hom.)	Confirmed PCD <i>DNAI2</i>	30
IF-071	1957/F/Caucasian/N	6/Neonatal distress. Chronic rhinitis and sinusitis. Hearing loss. Bronchiectasis.	5.6	GAS8-	Hyperkinetic stiff cilia	NA	NA	Highly likely PCD	
IF-072	2001/M/Caucasian/N	6/Neonatal distress. Chronic rhinosinusitis and wet cough. Bronchiectasis.	NA	DNALI1-, GAS8-	Immotile	NA	<i>CCDC39</i> (c.2250delT/p.Gln751LysfsTer11 hom.)	Confirmed PCD <i>CCDC39</i>	5
IF-073	2014/M/Caucasian/N	9/Neonatal distress. Wet cough. Recurrent otitis. <i>Situs inversus</i> .	NA	DNAH5-	Immotile	NA	<i>DNAH5</i> (c.2283_2284del/p.Arg761SerfsTer10 het. + c.3861T>G/p.Tyr1287Ter het.)	Confirmed PCD <i>DNAH5</i>	17
IF-076	2004/M/Caucasian/N	3/Chronic rhinitis. Repeated bronchitis. Bronchiectasis.	193.3	Proximal DNAH5	Subtle defects (stiff and immotile)	NA	Negative	Highly likely PCD - WES	
IF-089	2004/M/Caucasian/N	8/Chronic rhinitis. Recurrent otitis. Repeated bronchitis. Bronchiectasis. <i>Situs inversus</i> .	27.4	DNAH5-	Completely immotile	NA	NA	Highly likely PCD	
IF-091	2016/F/NA/NA	?/Neonatal distress. Chronic rhinitis and wet cough. Repeated pneumonia. <i>Situs inversus</i> .	NA	DNAH5-	Immotile, residual motility	NA	NA	Highly likely PCD - Genetics	
IF-092	2016/M/Caucasian/N	7/Neonatal distress. Chronic rhinitis and wet cough.	NA	DNALI1-, GAS8-	Immotile	NA	<i>CCDC39</i> (c.357+1G>C het. + c.2505_2506delCA/p.His835GlnfsTer4 het.)	Confirmed PCD <i>CCDC39</i>	4



IF-093	2002/M/NA/NA	?/Neonatal distress. Chronic rhinitis and wet cough. Rhinosinusitis. Recurrent otitis. Repeated pneumonia. Bronchiectasis.	NA	DNAH5-	Immotile, residual motility	NA	NA	Highly likely PCD - Genetics	
IF-094	2011/F/NA/NA	?/Neonatal distress. Chronic rhinitis and wet cough. Recurrent otitis. Bronchiectasis. Persistent atelectasis. <i>Situs inversus</i> .	NA	DNAH5-, DNALI1-	Completely immotile	NA	NA	Highly likely PCD - Genetics	
IF-095	2004/F/Caucasian/NA	9/Neonatal distress. Hearing loss. Repeated pneumonia. <i>Situs inversus</i> .	NA	DNAH5-	NA	ODA hypoplasia	<i>CCDC151</i> (c.410G>A/p.Trp137Ter hom.)	Confirmed PCD <i>CCDC151</i>	3
IF-096	1972/M/NA/NA	?/Neonatal distress. Chronic rhinitis and wet cough. Rhinosinusitis. Recurrent otitis. Repeated pneumonia. Fertility problems.	NA	DNAH5-	Immotile	NA	NA	Highly likely PCD - Genetics	
IF-098	2014/M/NA/NA	?/Neonatal distress. Chronic rhinitis and wet cough. <i>Situs inversus</i> .	NA	DNALI1-, GAS8-	Immotile and stiff	NA	NA	Highly likely PCD - Genetics	

Patient#: patient identification number; YOB: year of birth; PCD: primary ciliary dyskinesia; nNO: nasal nitric oxide; IF: immunofluorescence; HSVM: high-speed video-microscopy; TEM: transmission electron microscopy; M: male; F: female; N: no; Y: yes; Sib.: sibling; NA: not available data; ?: PICADAR was not calculated due to missing data; +: present in ciliary axoneme; -: absent in ciliary axoneme; ODA: outer dynein arms; IDA: inner dynein arms; het.: heterozygous variant; hom.: homozygous variant; inc.: including; ex.: exon; WES: whole-exome sequencing

**Table S2: Patients with normal localization of target proteins by immunofluorescence and correlation with other PCD-analysis techniques.**

Patient#	YOB/Gender/Origin/Consanguinity/Family	PICADAR score [1]/PCD symptoms	nNO (nl/min)	Affected IF markers	HSVM	TEM	Genetics	Diagnosis [2] - Next step	Patient# in Baz-Redón <i>et al.</i> 2020 [3]
IF-002	2016/M/Caucasian/N	11/Neonatal distress. Chronic rhinitis and cough. <i>Situs inversus totalis</i> .	15.01	All markers +	Hyperkinetic stiff cilia	NA	<i>DNAH11</i> (c.12507+1G>C het. + c.13415_13416insCAAA/p.Thr4472fs het.)	Confirmed PCD <i>DNAH11</i>	24
IF-003	2001/F/Caucasian/N	4/Chronic rhinitis and wet cough. Sinusitis. Recurrent otitis and hearing loss. Repeated pneumonia. Bronchiectasis.	3.5	All markers +	Immotile	NA	Negative	Highly likely PCD - WES	48
IF-005	2004/F/South-American/N	?/Chronic rhinitis and wet cough. Sinusitis. Recurrent otitis and hearing loss. Repeated bronchitis and pneumonia. Bronchiectasis.	50.2	All markers +	Disorganized ciliary beat	NA	Negative	Highly likely PCD - WES	47
IF-010	2002/M/Moroccan/NA	?/Chronic rhinitis and wet cough. Recurrent otitis and hearing loss. Bronchiectasis.	13.8	All markers +	Normal	NA	Negative	Highly unlikely PCD	
IF-011	1999/M/Caucasian/N	?/Chronic rhinitis and wet cough. Recurrent otitis and hearing loss. <i>Situs inversus</i> .	14.3	All markers +	Stiff	NA	<i>SPAG1</i> (c.583delA/p.Ile195Ter het. + c.1855G>C/p.Asp619His het.)	Highly likely PCD – Re-evaluation of variants and/or IF with new sample.	41
IF-016	2013/M/Caucasian/N	2/Chronic wet cough. Bronchiectasis.	NA	All markers +	Normal	NA	Negative	Highly unlikely PCD	
IF-017	2016/M/Moroccan/N	8/Neonatal distress. <i>Situs inversus</i> .	NA	All markers +	Normal	NA	Negative	Highly unlikely PCD	

IF-018	1994/M/Caucasian/N	4/Chronic rhinitis and wet cough. Nasal polyps. Sinusitis. Recurrent otitis and hearing loss. Repeated bronchitis and pneumoniae. Bronchiectasis.	14.8	All markers +	Immotile and disorganized ciliary beat	Loss 10% ODA and 40% IDA	Negative	Highly likely PCD - WES	46
IF-022	2003/F/Caucasian/N	2/Chronic rhinitis. Recurrent otitis.	100	All markers +	Normal	NA	Negative	Highly unlikely PCD	
IF-023	2013/F/Caucasian/N	?/Wet cough	NA	All markers +	Normal	NA	Negative	Highly unlikely PCD	
IF-028	2010/F/Caucasian/N	2/Bronchiectasis	NA	All markers +	Normal	NA	Negative	Highly unlikely PCD	
IF-029	2012/F/Caucasian/N	4/Neonatal distress. Repeated bronchitis and pneumonia.	NA	All markers +	Normal	NA	Negative	Highly unlikely PCD	
IF-030	2006/M/Caucasian/N	?/Chronic rhinitis and wet cough. Bronchiectasis.	196.8	All markers +	Normal	NA	Negative	Highly unlikely PCD	
IF-032	1985/M/Caucasian/NA	?/Wet cough. Repeated pneumonia. Bronchiectasis. Infertility.	103.2	All markers +	Reduced CBF	NA	NA	Highly likely PCD - Genetics	
IF-034	2007/F/Caucasian/N	6/Neonatal distress. Chronic rhinitis and wet cough. Recurrent otitis and hearing loss. Repeated bronchitis. Bronchiectasis.	128.7	All markers +	Completely immotile	NA	Negative	Highly likely PCD - WES	44
IF-035	2007/M/Caucasian/NA	?/Wet cough. Bronchiectasis.	NA	All markers +	Normal	NA	Negative	Highly unlikely PCD	
IF-036	2004/M/Caucasian/N	2/Bronchiectasis. Repeated bronchitis and pneumonia.	NA	All markers +	Normal	NA	Negative	Highly unlikely PCD	
IF-037	1987/M/Caucasian/N	?/Chronic rhinitis and wet cough. Nasal polyps. Sinusitis. Repeated pneumonia. Bronchiectasis. Lobectomy.	24.3	All markers +	Immotile	NA	Negative	Highly likely PCD - WES	50

IF-039	2010/F/Caucasian/N	4/Chronic rhinitis and wet cough. Nasal polyps. Recurrent otitis and hearing loss. Bronchiectasis.	15.8	All markers +	Stiff and disorganized ciliary beat	NA	Negative	Highly likely PCD - WES	45
IF-042	2011/F/Caucasian/NA	3/Chronic rhinitis. Bronchiectasis.	NA	All markers +	Normal	NA	NA	Highly unlikely PCD	
IF-048	2005/F/Caucasian/N	7/Neonatal distress. Chronic rhinitis and cough. Recurrent atelectasis.	44.5	All markers +	Normal	NA	Negative	Highly unlikely PCD	
IF-049	2017/M/Arabian/Y	7/Neonatal distress. Chronic rhinitis and wet cough. Repeated bronchitis. Cardiopathy.	NA	All markers +	Hyperkinetic stiff cilia	NA	<i>DNAH11</i> (c.983-1G>T het. + c.3439C>T/p.Gln1147Ter het.)	Confirmed PCD <i>DNAH11</i>	26
IF-051	2004/M/Caucasian/N	4/Chronic rhinitis and cough. Bronchiectasis. Recurrent otitis. Hearing loss.	NA	All markers +	Normal	NA	NA	Highly unlikely PCD	
IF-052	1963/M/Caucasian/N	3/Chronic rhinitis and cough. Bronchiectasis. Infertility	12.8	All markers +	Mainly stiff	NA	NA	Highly likely PCD - Genetics	
IF-057	2016/M/Pakistan/Y/sib. of IF-021, IF-056	2/Recurrent bronchitis and pneumonias.	NA	All markers +	Normal	NA	Negative	Highly unlikely PCD	
IF-058	1964/F/Caucasian/N	2/Bronchiectasis. Recurrent pneumonias.	218.7	All markers +	Normal	NA	Negative	Highly unlikely PCD	
IF-059	2002/F/Caucasian/N	2/Recurrent pneumonias	300	All markers +	Normal	NA	Negative	Highly unlikely PCD	
IF-063	1967/F/Caucasian/NA	?/Chronic rhinitis and wet cough. Sinusitis. Recurrent otitis and hearing loss. Repeated bronchitis. Bronchiectasis. <i>Situs inversus</i> .	11.4	All markers +	Stiff and immotile	NA	Negative	Highly likely PCD - WES	49

IF-064	2016/F/Caucasian/N	3/Chronic rhinitis. Persistent atelectasis.	NA	All markers +	Normal	NA	NA	Highly unlikely PCD	
IF-066	1983/F/Caucasian/N	8/Chronic rhinitis and cough. Recurrent otitis. Hearing loss. Neonatal distress and intensive care	154.7	All markers +	Normal	NA	NA	Highly unlikely PCD	
IF-067	2018/M/Caucasian/N/sib of IF-053	2/Recurrent bronchitis	NA	All markers +	Normal	NA	Negative	Highly unlikely PCD	
IF-068	2000/M/Caucasian/N	4/Chronic rhinitis and wet cough. Sinusitis. Recurrent otitis and hearing loss. Repeated bronchitis. Bronchiectasis.	4.3	All markers +	Hyperkinetic stiff cilia	NA	<i>DNAH11</i> (c.3898C>T/p.Gln1300Ter het. + c.6983+1G>A het.)	Confirmed PCD <i>DNAH11</i>	27
IF-077	2011/F/Moroccan/NA	2/Bronchiectasis	145	All markers +	Normal	NA	NA	Highly unlikely PCD	
IF-097	1973/F/NA/NA	?/Chronic rhinitis and wet cough. Recurrent otitis and hearing loss. Bronchiectasis. Fertility problems.	NA	All markers +	Immotile and stiff	NA	NA	Highly likely PCD - Genetics	
IF-102	2016/M/Pakistan/Y	2/Recurrent bronchitis	44.2	All markers +	Disorganized ciliary beat and stiff	NA	NA	Highly likely PCD - Genetics	

Patient#: patient identification number; YOB: year of birth; PCD: primary ciliary dyskinesia; nNO: nasal nitric oxide; IF: immunofluorescence; HSVM: high-speed video-microscopy; TEM: transmission electron microscopy; M: male; F: female; N: no; Y: yes; Sib.: sibling; NA: not available data; ?: PICADAR was not calculated due to missing data; +: present in ciliary axoneme; -: absent in ciliary axoneme; CBF: ciliary beat frequency; ODA: outer dynein arms; IDA: inner dynein arms; het.: heterozygous variant; WES: whole-exome sequencing

**Table S3: Patients with inconclusive and/or insufficient immunofluorescence results and correlation with other PCD-analysis techniques.**

Patient#	YOB/Gender/Origin/ Consanguinity/Family	PICADAR score [1]/PCD symptoms	nNO (nl/min)	Affected IF markers	HSVM	TEM	Genetics	Diagnosis [2] – Next step	Patient# in Baz- Redón <i>et</i> <i>al.</i> 2020 [3]
IF-006	2004/M/Caucasian/N	8/Chronic rhinitis and wet cough. Bronchiectasis. <i>Situs</i> <i>inversus</i> .	14.6	Insufficient and inconclusive	Stiff and immotile	NA	<i>CCDC39</i> (c.216_217delTT/p.Cys73GlnfsTer6 het. + c.357+1G>C het.)	Confirmed PCD <i>CCDC39</i>	8
IF-012	1977/F/Caucasian/NA	?/Chronic rhinitis and wet cough. Sinusitis. Recurrent otitis. Bronchiectasis.	155.9	Insufficient	Normal	NA	NA	Highly unlikely PCD	
IF-014	2008/M/Caucasian/N	8/Neonatal distress. Repeated bronchitis. <i>Situs inversus</i> .	115.8	Inconclusive	Normal	NA	NA	Highly unlikely PCD	
IF-019	2006/M/Caucasian/NA	2/Chronic wet cough. Nasal polyps.	NA	Insufficient and inconclusive	Normal	NA	NA	Highly unlikely PCD	
IF-074	2019/F/Pakistan/Y	9/Neonatal distress. Chronic rhinitis. <i>Situs inversus</i> .	9	Inconclusive	Completely immotile	NA	NA	Highly likely PCD - Genetics	
IF-100	2004/M/Caucasian/N	?/Repeated bronchitis.	NA	Insufficient	Normal	NA	NA	Highly unlikely PCD	

Patient#: patient identification number; YOB: year of birth; PCD: primary ciliary dyskinesia; nNO: nasal nitric oxide; IF: immunofluorescence; HSVM: high-speed video-microscopy; TEM: transmission electron microscopy; M: male; F: female; N: no; Y: yes; Sib.: sibling; NA: not available data; ?: PICADAR was not calculated due to missing data; +: present in ciliary axoneme; -: absent in ciliary axoneme; het.: heterozygous variant

## References:

1. Behan, L.; Dimitrov, B.D.; Kuehni, C.E.; Hogg, C.; Carroll, M.; Evans, H.J.; Goutaki, M.; Harris, A.; Packham, S.; Walker, W.T.; et al. PICADAR : a diagnostic predictive tool for primary ciliary dyskinesia. *Eur. Respir. J.* **2016**, *47*, 1103–1112, doi:10.1183/13993003.01551-2015.
2. Lucas, J.S.; Barbato, A.; Collins, S.A.; Goutaki, M.; Behan, L.; Caudri, D.; Dell, S.; Eber, E.; Escudier, E.; Hirst, R.A.; et al. European Respiratory Society guidelines for the diagnosis of primary ciliary dyskinesia. *Eur. Respir. J.* **2017**, *49*, doi:10.1183/13993003.01090-2016.
3. Baz-Redón, N.; Rovira-Amigo, S.; Paramonov, I.; Castillo-Corullón, S.; Cols Roig, M.; Antolín, M.; García Arumí, E.; Torrent-Vernetta, A.; de Mir Messa, I.; Gartner, S.; et al. Implementation of a Gene Panel for Genetic Diagnosis of Primary Ciliary Dyskinesia. *Arch. Bronconeumol.* **2020**, *20*, 30073–9, doi:10.1016/j.arbres.2020.02.010.









